ULTRASTRUCTURE, CYTOCHEMISTRY AND IMMUNOCYTOCHEMISTRY OF THE INTERACTION BETWEEN WHEAT (*TRITICUM AESTIVUM*) AND LEAF RUST (*PUCCINIA RECONDITA* F.SP. *TRITICI*)

GUANGGAN HU
(M.Sc. Beijing Agricultural University)

Submitted in fulfilment of the
requirements for the Ph.D. degree
in the
Department of Microbiology and Plant Pathology
University of Natal

Pietermaritzburg

1996

To my wife Feihua
my daughter Xiaozhou

ABSTRACT

Hu, Guanggan. (1996). Ultrastructure, cytochemistry and immunocytochemistry of the interaction between wheat (*Triticum aestivum*) and leaf rust (*Puccinia recondita* f.sp. *tritici*). Ph.D. thesis, University of Natal, South Africa. 167pp

The development of infection structures, derived from urediospores of *Puccinia recondita* f.sp. *tritici* in near-isogenic lines of susceptible and resistant wheat, and in non-hosts, viz. maize, oat, sorghum and barley, was examined by fluorescence microscopy and scanning electron microscopy (SEM). The infection structure formation on and in five cereal species follows a similar pattern. In sorghum, fungal development is arrested at the stage of substomatal vesicle formation, while, in maize, most fungal structures collapse during the stage of primary hypha development. On the other hand, in wheat, barley and oat, the fungus forms many branched infection hyphae and haustorial mother cells. There were no significant structural and numerical differences in infection structure development between susceptible and resistant wheat lines.

The ultrastructure of intercellular hyphae and D-haustoria of *P. recondita* f.sp. *tritici*, and the host response to haustorial invasion, was investigated. The intercellular hyphae share common characteristics with other uredial stage

rust fungi. Anastomosis was observed between intercellular hyphae. Two nucleoli were frequently observed in a single nucleus in the haustorium, indicating possible nuclear fusion between the two nuclei in D-haustoria of this fungus. The close association of host organelles, such as the nucleus, Golgi bodies, endoplasmic reticulum, vesicles and mitochondria, with the developing haustorium, was described.

The investigation of urediospore formation of *P. recondita* f.sp. *tritici* on wheat leaves by SEM and transmission electron microscopy (TEM) showed that one or more protuberances arise sympodially from several different loci on the distal surface of a basal cell, each protuberance developing into a urediospore. At the same site at which one urediospore formed previously, at least one other urediospore initial can form subsequently.

A study of the cytochemistry of the interaction between wheat and *P. recondita* f.sp. *tritici*, using various enzyme- and lectin-conjugated gold probes, was conducted. This research provided additional information on the nature and composition of the walls of fungal hyphae, the haustorial mother cell, the haustorial neck, the haustorial body and the extrahaustorial matrix. Cellulose, the major component of the host cell wall, was not detected in the extrahaustorial matrix and in the host tubules associated with the invaded haustorium. The composition of walls of the haustorial body of *P. recondita* f.sp. *tritici* appears to change as the haustorium matures. The study identified

the existence of mannose/glucose, galactose, *N*-acetylgalactosamine and fucose residues in the extrahaustorial matrix.

An antiserum raised against the purified 33 kDa wheat ß-1,3-glucanase was used to investigate the subcellular localization of the enzyme in *P. recondita* f.sp. *tritici*-infected wheat leaves by means of a post-embedding immunogold labelling technique. In the compatible interaction, ß-1,3-glucanase was demonstrated to accumulate predominantly in the haustorial wall and extrahaustorial matrix. In the incompatible interaction, strong labelling for ß-1,3-glucanase was found in host cell wall appositions, extracellular matrix in the intercellular space, and in electron-dense structures of host origin which only occurred in the incompatible interaction.

Using anti-zeatin riboside and anti-isopentenyladenosine antibodies in post-embedding immunocytochemical procedures, cytokinins were localized at the ultrastructural level in *P. recondita* f.sp. *tritici*-infected wheat leaves. The sites where cytokinins accumulate were not significantly different between the compatible and incompatible interactions. The cytokinins are mainly present in the fungal cytoplasm of the intercellular hyphal cell, the haustorial mother cell, the haustorial body and extrahaustorial matrix, indicating that cytokinins, primarily of fungal origin, are associated with the nutrient translocation in this host-fungus interaction.

ACKNOWLEDGEMENTS

I would like to thank the following for their contributions to the work presented in this thesis.

Professor F.H.J. Rijkenberg for his guidance, encouragement and constructive criticism throughout the course of this study. I am especially grateful to him for his kind care during my stay in South Africa and for supporting me to attend the 9th Rusts & Powdery Mildew Conference in the Netherlands.

The Foundation for Research Development for financial assistance in the form of a doctoral bursary and for their financial support in the form of an overseas conference supplement.

The University of Natal for financial support in the form of a graduate assistantship.

Professor Z.A. Pretorius, Department of Plant Pathology, University of the Orange Free State, South Africa, for supplying the rust races and wheat cultivars used in this study, and his helpful advice during this study.

Dr. B. Sotta, INRA, France, for kindly supplying the polyclonal antibodies against the cytokinin derivatives.

Dr. R.P. Baayen and Ms. M.G. Förch, DLO Research Institute for Plant Protection (IPO-DLO), the Netherlands, for supplying the cellulase-conjugated gold probes.

Dr. X.M. Qian, Department of Botany and Genetics, University of the Orange Free state, South Africa, for supplying the polyclonal antibody against wheat ß-1,3-glucanase.

Drs. D.E. Harder and J. Chong, Winnipeg, Agriculture Canada, for discussions on some transmission electron micrographs presented in this study.

The staff and students, especially Mrs. Petro Nortje, Mrs. Kathy Milford, Mrs. C. Christianson, Ms. D. Fowlds and Ms. Ingrid Schlösser, of the Department of Microbiology and Plant Pathology, University of Natal, for their support.

Mr. Vijay Bandu, Mrs. Belinda White, Mrs. Priscilla Donnelly and Mr. Tony Bruton of the Centre for Electron Microscopy in Pietermaritzburg, for technical assistance with the electron microscopy and for the preparation of electron micrographs.

My parents, parents-in-law and family for their endless support and encouragement.

Finally, I wish to express my deepest gratitude towards my wife Feihua and my daughter Xiaozhou for their love, sacrifice, patience and encouragement.

DECLARATION

I hereby declare that these studies represent original work by the author and have not been submitted in any form to another university. Where use was made of the work of others, it has been duly acknowledged in the text.

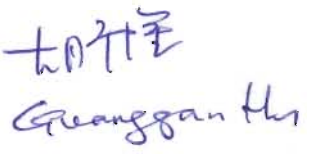

GUANGGAN HU

PREFACE

The experimental work described in this thesis was conducted in the Department of Microbiology and Plant Pathology, University of Natal, Pietermaritzburg, South Africa, under the supervision of Professor F.H.J. Rijkenberg.

This thesis consists of seven manuscripts. Each chapter has been prepared as an individual manuscript with the aim of publication in a scientific journal. Therefore some repetition was unavoidable. Since some manuscripts have been submitted to different journals and had to comply with different requirements, the reader will notice some inconsistencies in author citation and referencing in the chapters of this thesis.

TABLE OF CONTENTS

CHAPTER 1

SCANNING ELECTRON MICROSCOPY STUDIES OF EARLY INFECTION STRUCTURE FORMATION BY *PUCCINIA RECONDITA* F.SP. *TRITICI* ON AND IN SUSCEPTIBLE AND RESISTANT WHEAT LINES[1]

INTRODUCTION

Infection structure morphology may provide an additional criterion valuable for the identification and classification of rust fungi on grasses and cereals (Niks, 1986; Niks *et al.*, 1991; Swertz, 1994). A number of studies have been done on infection structure formation of rust fungi with the transmission electron microscope and the light microscope. However, until fairly recently, investigations using scanning electron microscopy, a technique extremely useful to mycological research in recent years, were confined to those describing infection structure differentiation from the urediospores of rust fungi on artificial, host and non-host surfaces. Little information is available on the initiation and formation of the substomatal vesicle and its subsequent development. Hughes and Rijkenberg (1985) developed a leaf-fracture technique in their studies on the early infection stages of *Puccinia sorghi* Schw. in *Zea mays* L. This technique enables the investigation of early infection structures in both host and non-host tissues. In recent years, this technique has been applied in studies on several other rust-plant (host and non-host) interactions including those of *Uromyces transversalis* (Thum.) Winter in *Gladiolus* L. and *Zea mays* L. (Ferreira & Rijkenberg, 1989), *P.*

[1]This Chapter has been submitted to *Mycological Research*. Therefore the conventions of this journal have been followed

graminis f.sp. *tritici* Erikss. & E. Henn. in *Triticum aestivum* L. and several cereal species (Lennox & Rijkenberg, 1989) and *Hemileia vastatrix* Berk. & Br. in *Coffea* spp. and *Phaseolus vulgaris* L. (Coutinho, Rijkenberg & Van Asch, 1993a). Davies & Butler (1986) used a very similar method to describe infection structure formation by *P. porri* (Sow.) Wint. in leaves of leek (*Allium porrum* L.).

Puccinia recondita Rob. ex Desm. f.sp. *tritici* Eriks. & Henn. (syn. *P. triticina*), is the pathogen of leaf rust of wheat. Its infection process has been investigated with light microscopy by several researchers (Allen, 1926; Romig & Caldwell, 1964; Niks, 1983, 1987; Staples & Macko, 1984; Lee & Shanner, 1984; Southerton & Deverall, 1989; Jacobs, 1989, 1990; Kloppers, 1994; Swertz, 1994). Published details of early morphological development within the host, however, are few.

The objective of the present research was to describe the ontogeny and morphology of infection structure formation of *P. recondita* f.sp. *tritici* within susceptible and resistant near-isogenic lines of wheat (*Triticum aestivum* L.) with the aid of scanning electron microscopy. The leaf fracture method of Hughes & Rijkenberg (1985) was adopted in the present investigation.

MATERIALS AND METHODS

Plant materials, rust propagation and inoculation

The near-isogenic wheat lines used were RL 6040 and RL 6043 which have leaf rust resistance genes *Lr19* and *Lr21*, respectively, and Thatcher which is

susceptible (kindly provided by Prof. Z. A. Pretorius, Department of Plant Pathology, University of the Orange Free State, South Africa). RL 6040 is Thatcher*7/translocation 4 (derived from *Agropyron elongatum*) and shows a high resistance reaction to UVPrt 8 while RL 6043 is Thatcher*6/RL 5406 (Tetra Canthatch)/*Ae. squarrosa* var. Meyeri-RL 5289 and is intermediately resistant UVPrt 8 at a temperature of 20°C. All seedlings were grown singly in 10 cm pots and maintained at 20°C in a leaf-rust free constant environment chamber with a 12-hour photoperiod.

The South African pathotype UV Prt 8 of *P. recondita* f.sp. *tritici* (obtained from Professor Z.A. Pretorius, University of the Orange Free State, South Africa) was employed in this study. Race UV Prt 8 has an avirulence/virulence formula of *3a,3bg,3ka,11,16,20,26,30/1,2a,2b,2c,10,14a,15,17,24*. To this race, RL 6040 shows a 0; reaction while RL 6043 shows a 2 infection type and Thatcher shows a 4 reaction.

Freshly harvested urediospores of *P. recondita* f.sp. *tritici* produced on 15-day-old plants of susceptible wheat cultivar Agent in a greenhouse (20-26°C) were used to inoculate the adaxial surface of the first leaf of 10-day-old plants of the above-mentioned wheat lines at an inoculum dose of 50 mg urediospores per ml of Soltrol 130 (Phillips Chemical Co.). A modified Andres & Wilcoxson (1984) inoculator was used to inoculate the plants. To prevent Soltrol damage to leaves, inoculated seedlings were allowed to dry for approximately 1 hour before placement in the dark in a dew chamber at 20°C and 100% R.H. for 24 hours. The inoculated leaves of 10 seedlings of each wheat line were harvested at 6, 12, 24, 48, 72, 96, and 144 hours post-inoculation (hpi). At 24 hpi, the remaining seedlings in the dew chamber were removed and placed in a constant environment chamber at 18-20°C.

Specimen preparation for SEM

The harvested leaves were cut into about 3 × 3 mm squares and fixed in 3% glutaraldehyde in 0.05 M sodium cacodylate buffer, pH 6.8-7.2, for 24 hours, washed twice in the buffer, postfixed for 2 hour in 2% osmium tetroxide in the buffer, washed twice in the buffer, and dehydrated in a graded ethanol series. The specimens were then critical-point dried with carbon dioxide as a transition fluid and were mounted on copper stubs. The leaf-fracture method of Hughes & Rijkenberg (1985) was used on specimens harvested at 12 to 96 hpi. Both stubs used in fracturing were then processed for observation. Samples harvested at 6 and 144 hpi were left unfractured. All stripped epidermis and the tissue remaining on the stubs was gold/palladium-coated in a Polaron Sputter coater. Samples were examined with a Hitachi S-570 Scanning Electron Microscope (SEM) operating at 8.0 or 10.0 kV. The specimens harvested at 6 hpi and 144 hpi were scanned only exteriorly. In some instances, after freeze-fracturing in an EM Scope SP 2000 cryo unit, or without such fracturing, freshly harvested materials were viewed with the SEM at 8.0 kV. Counts of infection structures were made directly from the screen and micrographs were made of both typical and atypical infection structures observed.

RESULTS

At germination, a germ tube protrudes from a germ pore in the urediospore wall and then elongates closely appressed to the cuticular surface of the leaf. Along the germ tube's length, several exploratory branches are formed at the anticlinal wall depressions (Fig. 1). Normally, the germ tubes extend

perpendicularly to the long axis of the leaf (Fig. 1).

When a stoma is encountered by the germ tube, an appressorium is formed terminally (Fig. 1). Occasionally, germ tubes fail to recognize the stoma, do not form an appressorium and pass the stomatal aperture. Initially, the appressorium is approximately spherical. As the appressorium matures, it enlarges and becomes oval- or oblong-shaped, the long axis of the appressorium being orientated parallel to the stomatal slit (Fig. 3). A mature appressorium is delimited from the germ tube by a septum (Figs. 2 and 3). In many instances, two (Fig. 2), or even three appressoria are seen on a single stoma. Moreover, often, a urediospore on or near a stoma produces either a short germ tube or a germ tube appears to be absent from the spore/appressorium combination (Fig. 3). Some urediospores with long germ tubes do not develop appressoria by 12 hpi.

An appressorium at its periphery produces 4-6 (mostly 4) near-symmetrically orientated lobes which appear to adhere closely to the surface of the guard cells (Fig. 3). The appressorium appears to secrete some mucilaginous substance bonding the appressorium to the host cuticle (Fig. 4). At 6 hpi, mature appressoria are typically observed on leaves of all susceptible and resistant wheat lines.

The lower surface of the appressorium, observable after it has been stripped from the stoma, has a rugose texture and carries an imprint of the parts of stoma to which it was attached (Fig. 5). Particles of host cuticle and/or wax appear to adhere to the surface of the appressorial wall (Fig. 5). The appressorium, albeit in collapsed form, remains on the leaf surface even 144 hpi. No significant difference was observed between the appearance of the appressorium on susceptible and that on resistant wheat near-isogenic lines.

Originating from the lower surface of the appressorium, a single infection peg swells into a substomatal vesicle (SSV) in the substomatal chamber after penetration into this chamber. The blade-like connection between the appressorium and the SSV has been termed the interconnective tube by Hughes & Rijkenberg (1985) and Lennox & Rijkenberg (1989) (Fig. 6). A septum delimits the SSV from the interconnective tube (Fig. 6). When the SSV is mature and the transfer of cytoplasm to this structure has taken place, the appressorium and the germ tube on the exterior surface of the plant collapse.

The SSV initial emerges from the stomatal slit as a round or near-spherical structure (approximately $8.4 \times 6.3\ \mu m$) and then increases in both dimensions to about $11 \times 7\ \mu m$. A subsequent increase in length is not associated with a further increase in width. The mature SSV is oblong or ellipsoid (Figs. 7, 8, 9). At 12 hpi, the most mature SSVs measure about $22\text{-}25 \times 7\text{-}8\ \mu m$. In most cases, elongated SSVs lie parallel to the long axis of stomatal slit (Fig. 7). However, other orientation of SSVs has also been observed (Figs. 8 and 9), Some are orientated perpendicularly (or nearly so) to the stomatal opening, and develop further in this direction (Fig. 8). Few SSVs are orientated at right angles to the stomatal slit (Fig. 9). A statistical comparison between the types of SSV orientation (parallel, perpendicular, and at right angles) indicates that there is a nearly equal tendency for the SSVs to position their long axes perpendicularly to the stomatal slit or parallel to it (Table 1). Occasionally, an amorphous material is associated with the collapsed SSV (Fig. 11). At 12 hpi, many mature SSVs are found in both susceptible and resistant wheat lines. A number of stomatal chambers were seen in which two SSVs had formed (Fig. 10). The near-spherical or stub-like SSVs (Fig. 12), often collapsed, observed at the later sampling stages, are considered to be aborted structures.

Table 1. Frequencies of long axis orientation of the stomatal vesicles of *Puccinia recondita* f.sp. *tritici* to the stomatal slits of the hosts (Wheat)

Orientation	Observed	Expected
Parallel	56	38
Perpendicular	48	38
Others	10	38

Note: The following X^2 tests were performed: $X^{2(2)}$ (parallel vs. perpendicular vs. others) = 31.78, $P < 0.001$; $X^{2(1)}$ (parallel vs. perpendicular) = 11.15, $P = 0.001$; $X^{2(1)}$ (perpendicular vs. others) = 23.26, $P < 0.001$; $X^{2(1)}$ (parallel vs. others) = 29.16, $P < 0.001$.

PLATE 1

Fig. 1. Urediospore germ tube (G) of *Puccinia recondita* f.sp. *tritici* on RL 6043 (intermediately resistant) leaf at 6 h post-inoculation (hpi). Orientation of germ tube is perpendicular to long axis of leaf and germ tube has formed short exploratory lateral branches (B). Appressorium (A) formed on stoma. U: Urediospore. (Bar = 40 μm)

Fig. 2. Two appressoria (A) over stoma. Note septum (S) which delimits appressorium from germ tube. 6 hpi on RL 6040 (resistant). (Bar = 10 μm)

Fig. 3. Appressorium (A) formed over stoma. Note septum (S) which delimits appressorium from germ tube. Note appressorial lobes (L) on periphery of appressorium. 6 hpi on RL 6043. (Bar = 8 μm)

Fig. 4. Mucilage (Mu) produced by appressorium (A) (Cryo-SEM). 24 hpi, Thatcher. (Bar = 12 μm)

Fig. 5. A young appressorium detached from RL 6040 (resistant) leaf showing rugose texture of lower surface of appressorium on which imprint (Gi) of guard cells appears. (Bar = 8 μm)

Fig. 6. Interconnective tube (IT) is visible after epidermis is stripped off. A septum (S) delimits the substomatal vesicle (SSV) from the interconnective tube. 24 hpi in Thatcher. (Bar = 2.4 μm)

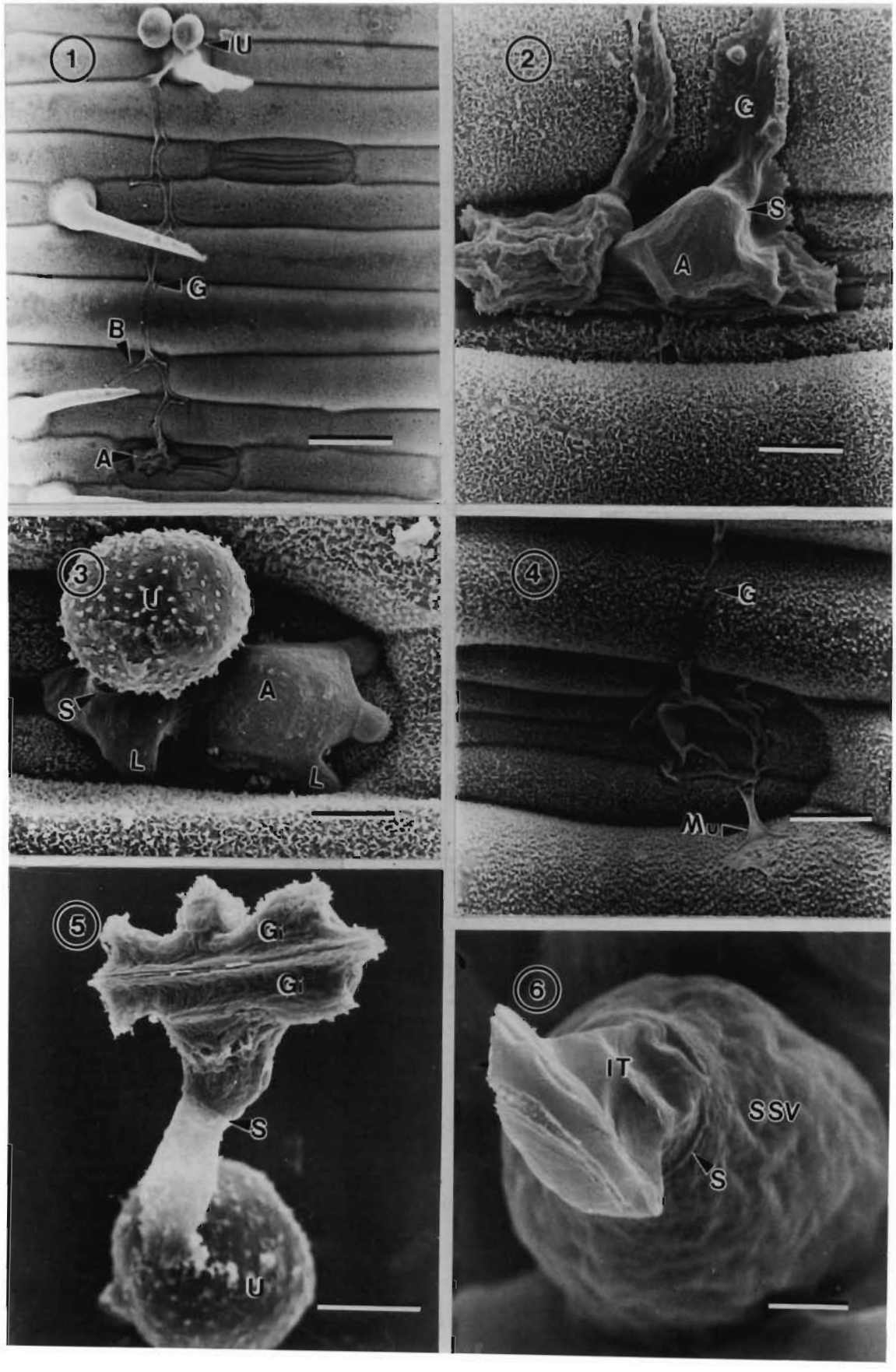
1
U
G
B
A
2
G
S
A
3
U
S
A
L
L
4
G
MU
5
Gi
Gi
S
U
6
IT
SSV
S

PLATE 2

Fig. 7. Mature ellipsoid substomatal vesicle (SSV) parallel to stomatal slit. 12 hpi in Thatcher. (Bar = 10 μm)

Fig. 8. Substomatal vesicle (SSV) perpendicularly arranged to leaf surface. 24 hpi in RL 6040. (Bar = 10 μm)

Fig. 9. Substomatal vesicle (SSV) positioned at right angles to stomatal opening. 12 hpi in RL 6043. (Bar = 10 μm)

Fig. 10. Two substomatal vesicles situated on same stomatal slit. 12 hpi in RL 6040. (Bar = 17 μm)

Fig. 11. Amorphous material (arrow) on surface of substomatal vesicle (SSV). 24 hpi in RL 6040. (Bar = 7 μm)

Fig. 12. Collapsed stub-shaped substomatal vesicle (SSV), orientated parallel to stomatal slit. 24 hpi in RL 6040. (Bar = 6 μm)

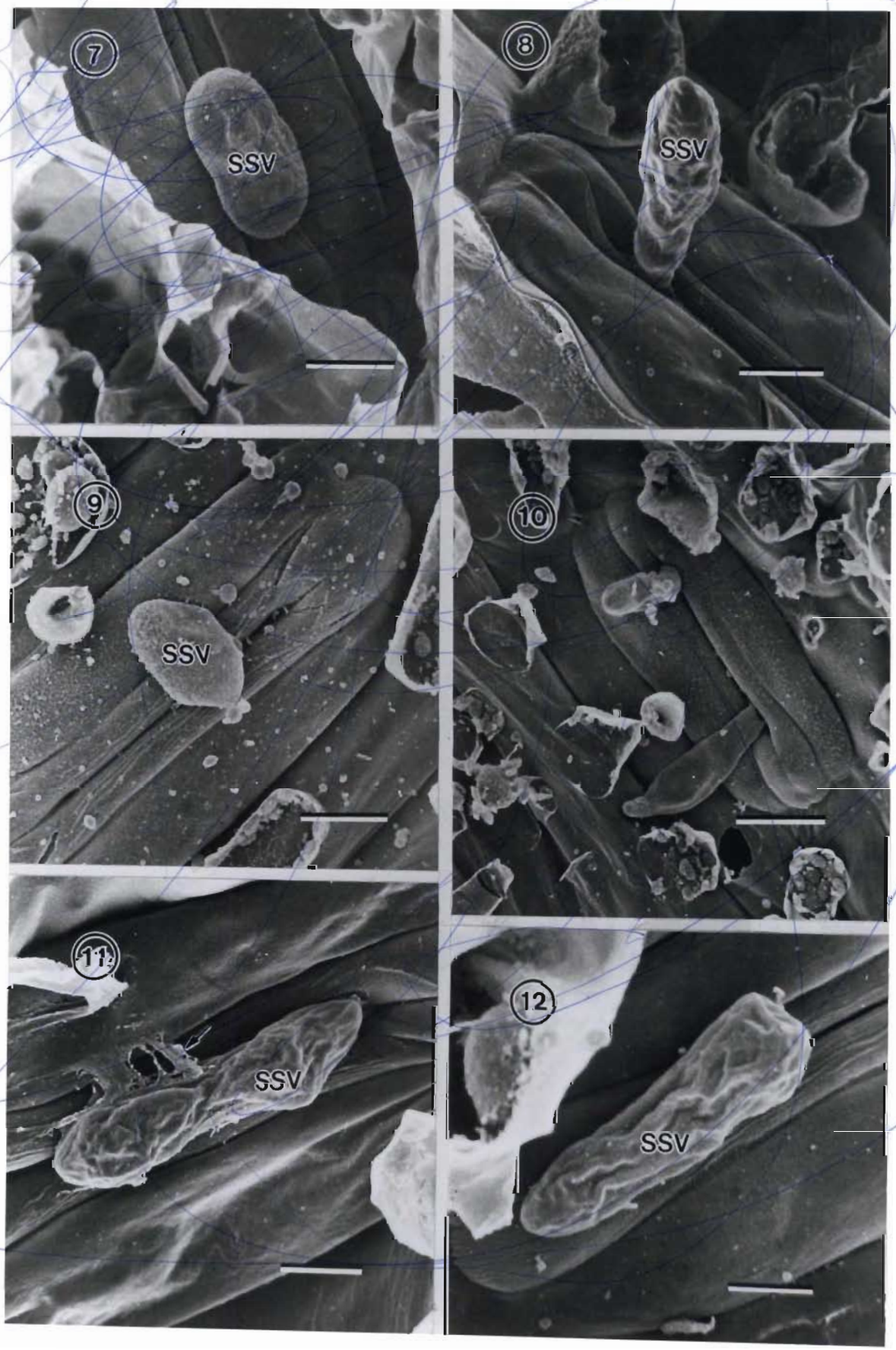
7
SSV
8
SSV
9
SSV
10
11
SSV
12
SSV

PLATE 3

Fig. 13. Substomatal vesicle (SSV) elongates in a direction parallel to leaf vein forming a primary infection hypha initial (PHi). 24 hpi in Thatcher. (Bar = 3 μm)

Fig. 14. Primary infection hypha initial (PHi) located perpendicularly on the chamber side of substomatal vesicle (SSV) which has formed at the right angles to stomatal opening. 24 hpi in Thatcher. (Bar = 5 μm)

Fig. 15. Primary hypha (PH) has elongated between mesophyll cells (M). 24 hpi in Thatcher. (Bar = 5 μm)

Fig. 16. Substomatal vesicle (SSV) orientated perpendicularly to long axis of stomatal opening. Primary infection hypha (PH) arises from terminal end. Septum (S) delimits haustorial mother cell (HMC) from primary hypha. 48 hpi in RL 6043. (Bar = 3 μm)

Fig. 17. Primary infection hypha (PH) formed from the SSV surface away from the stomatal slit and in contact with mesophyll cell (M). Haustorial mother cell (HMC) has formed on contact with host cell. Secondary infection hypha (SH) arises on the substomatal vesicle side of HMC septum. 48 hpi in RL 6040. (Bar = 7 μm)

Fig. 18. Primary infection hypha (PH) formed from the lower surface of SSV and has extended between mesophyll cells (M) in a direction approximately parallel to the stomatal slit. One HMC has formed where primary hypha has become attached to mesophyll cell and secondary hypha (SH) initial has formed in proximity of HMC. 48 hpi in Thatcher. (Bar = 7 μm)

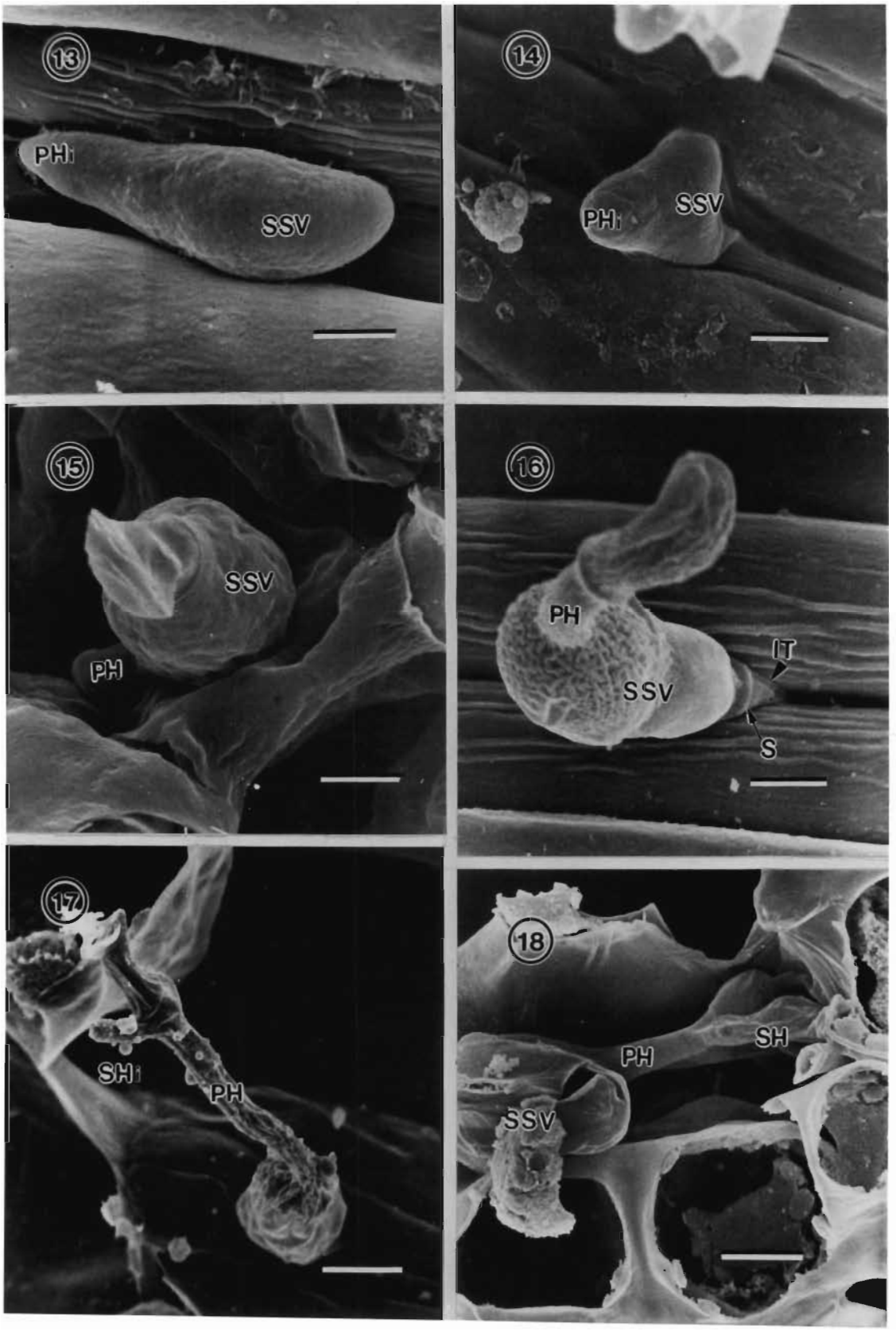
13
PH
SSV
14
PH
SSV
15
SSV
PH
16
PH
IT
SSV
S
17
SH
PH
18
SH
PH
SSV

PLATE 4

Fig. 19. Abnormal formation of infection hyphae. SSV is perpendicular to stomatal slit. One primary hypha (arrow) has arisen from a location on SSV close to stomatal slit, while another (arrowhead) is located terminally at the end of the same SSV. HMCs and secondary hyphae (SH) have formed. 48 hpi in RL 6040. (Bar = 10 μm)

Fig. 20. Possibly collapsed mature haustorial mother cell (HMC). 48 hpi in RL 6040. M: Mesophyll cell; S: Septum. (Bar = 2.4 μm)

Fig. 21. Cryo-fractured leaf tissue. Haustorium in mesophyll cell. Note haustorial neck (HN). 48 hpi in Thatcher. HB: Haustorial body; IH: Intercellular hypha. (Bar = 7 μm)

Fig. 22. Overview of the infection by *Puccinia recondita* f.sp. *tritici*. Appressorium (A) on leaf surface has collapsed and intercellular hyphae ramify in the leaf tissue. 72 hpi in RL 6043. (Bar = 24 μm)

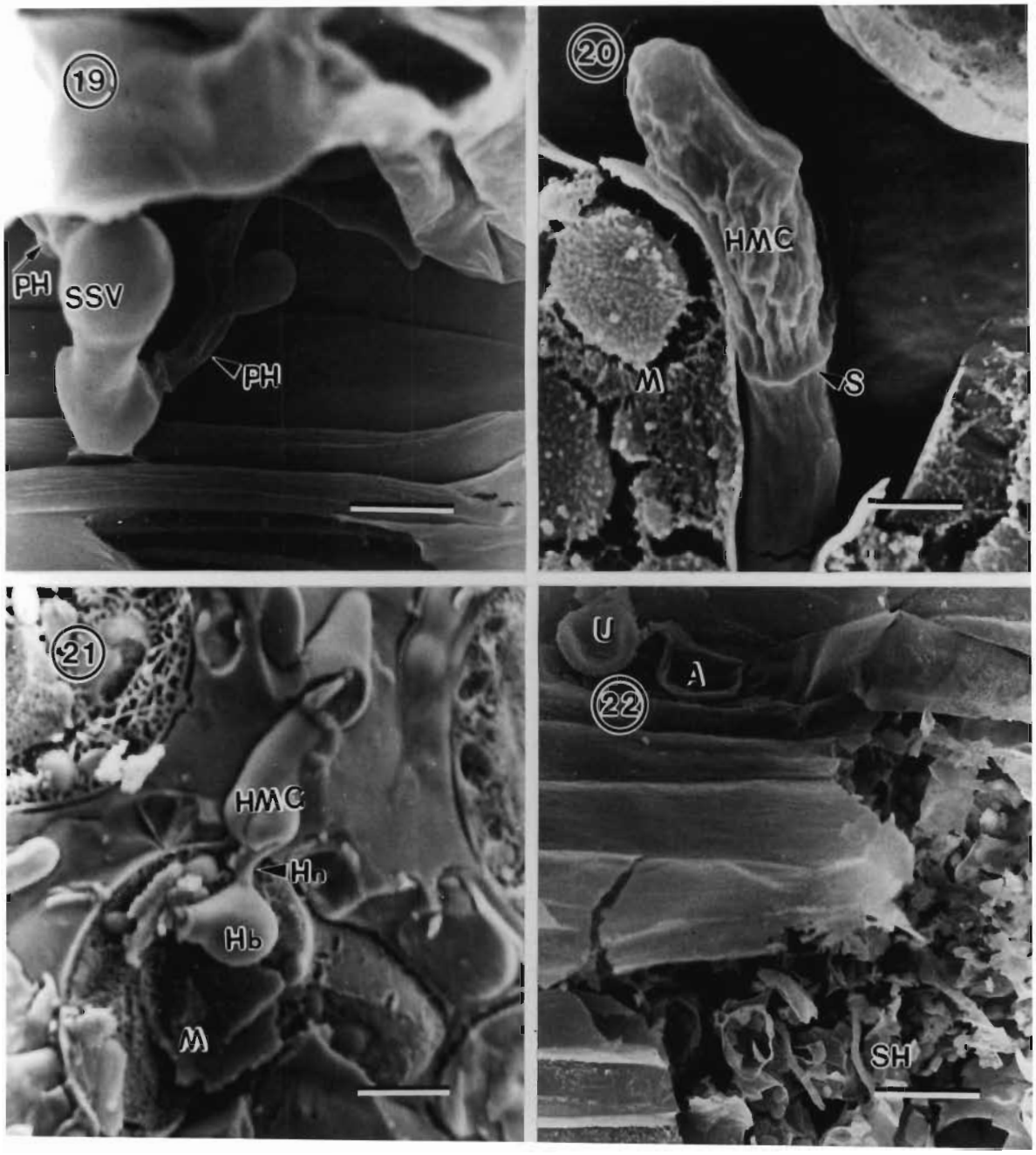
19
PH
SSV
PH
20
HMC
M
S
21
HMC
Hb
Hb
M
U
A
22
SH

In instances where the SSV is parallel to the stomatal slit, the SSV progressively develops and elongates unilaterally, while remaining closely attached to the inner epidermal surface, in a direction parallel to the long axis of stomatal slit, to form a primary hypha (Fig. 13). In instances where the SSV develops in a direction perpendicular to the long axis of the leaf, a primary hypha forms from one end of the SSV, generally in the proximity of a mesophyll cell, and extends further (Figs. 14, 15, 16, 17). In a few cases, the primary hypha arises from the surface of the SSV, away from the host epidermis, rather than from the end, in a direction perpendicular to the stomatal opening, and extends further into the mesophyll (Fig. 18). Primary infection hyphae were about 4.2 μm in diameter in Thatcher (susceptible), approximately 3.9 μm in *Lr21* (intermediately resistant), and 3.8 μm in *Lr19* (resistant).

At 12 hpi, many early stages of SSV development were observed and the primary infection hypha begins to form. A small number of collapsed SSVs was also found at this stage in all wheat lines investigated. More collapsed SSVs were counted at 24, 48, 72 and 96 hpi. Some SSVs (often of the near-spherical type) had formed a very elongate and slender primary infection hypha which apparently does not develop beyond this stage. Hence these are regarded as abortive primary hyphae and SSVs. Generally, relatively low numbers of the atypical primary hyphae were recorded at 48 hpi and the subsequent stages of harvest (Table 2).

Once the primary infection hypha has expanded fully and/or has become attached to a mesophyll cell or epidermal cell, a septum is produced which delimits a haustorial mother cell (HMC) from the primary hypha at the hyphal tip (Fig. 16). This septum was seen at 24 hpi and thereafter.

Table 1. Counts (%) of infection structures at specific time intervals post-inoculation

Infection structures	Hours post-inoculation											
	RL 6040				RL 6043				Thatcher			
	12	24	48	96	12	24	48	96	12	24	48	96
Substomatal vesicle	80	81	81	72	86	88	84	90	89	88	92	90
Collapsed SSVs	20	19	19	28	14	12	16	10	11	12	8	10
Primary hypha	18	58	55	62	20	62	61	77	22	60	65	85
Collapsed primary hypha	7	14	9	15	9	13	4	10	11	11	9	5
Primary hypha with HMC	10	46	52	55	12	47	53	70	9	41	53	75
Secondary hypha		26	42	44		23	42	56		19	41	59
Intercellular mycelium and HMCs		2	24	32		3	27	40		4	23	36
Total sites	102	170	170	279	116	203	178	125	89	185	211	168

NB: based on the cumulative totals

When the SSV and the primary infection hypha have developed, a secondary infection hyphal initial may emerge at several sites on the primary hypha (Fig. 17). A secondary infection hypha mostly arises at a position adjacent to, or in the proximity of, the HMC on the SSV side of the HMC septum of the primary infection hypha (Figs. 17 and 18). By 48 hpi, many HMCs have formed from the secondary hyphae which form in this manner (Table 2). Abnormal patterns of secondary hypha formation were occasionally observed in leaves of both susceptible (Fig. 19) and resistant wheat lines. Some haustorial mother cells are collapsed (Fig. 20). The mature haustorial mother cell produces a penetration peg which penetrates the host cell and a haustorium is formed (Fig. 21).

More intercellular hyphae originate from the secondary infection hyphae with HMCs, and form the fungal thallus (Fig. 22).

Relatively more collapsed SSVs, collapsed primary infection hyphae, collapsed secondary infection hyphae and collapsed HMCs were observed in the tissues of the resistant line, i.e. RL 6040 (*Lr19*), than in the intermediately resistant RL6043 (*Lr21*) and susceptible Thatcher lines (Table 2). However, there were no significant structural and numerical differences in infection structure development between the wheat lines.

At 144 hpi, uredia with a number of immature urediospores were found in Thatcher while fewer urediospores were found in RL 6043 and no sporulation was observed in RL 6040.

DISCUSSION

In general terms, the process of infection structure formation of *Puccinia recondita* f.sp. *tritici* on and in susceptible and resistant wheat lines in the present investigation was similar to that observed for other rust fungi (Hughes & Rijkenberg, 1985; Ferreira and Rijkenberg, 1989; Lennox & Rijkenberg, 1989; Coutinho *et al.*, 1993a).

P. recondita f.sp. *tritici* germ tubes were observed to grow and elongate perpendicularly to the long axis of the leaf on susceptible, intermediately resistant and resistant wheat lines. Dickinson (1969) noted the directional growth of germ tubes of *P. recondita* f.sp. *tritici* along the transverse axis of the plant surface. Dickinson (1970) suggested that the elongation toward the stoma was a curved thigmotropic stimulus. The directional growth of germ tubes has also been observed to occur in other rust fungi, such as *P. graminis* f.sp. *tritici* (Johnson, 1934; Lewis & Day, 1972; Lennox & Rijkenberg, 1989), and *Uromyces phaseoli* var. *typica* (Wynn, 1976). Several investigators have proposed that the physical or chemical features of the leaf surface may influence the direction of growth. These may include cuticular ridges (Wynn, 1976) and patterns of epicuticular wax crystals (Lewis & Day, 1972), or pH gradients at the leaf surface (Edwards & Bowling, 1986). However, Hughes & Rijkenberg (1985) reported that *P. sorghi* germ tubes grow towards maize stomata randomly as they traverse both axes of the leaf surface. Coutinho *et al.* (1993) also noted that *Hemileia vastatrix* germ tubes appeared to lack directional growth on both host and non-host leaf surfaces. Wynn (1976) proposed that random growth of germ tubes may be due to the lack of close adhesion between the germ tubes and the leaf surface.

In the present investigation, some urediospores which landed on the stomatal pore directly or near the stoma developed appressoria without the apparent formation of germ tubes, or form short germ tubes, while a few urediospores with long germ tubes failed to produce appressoria. Niks (1990) observed a negative correlation between the germ tube length of *P. hordei* Otth. on *Hordeum vulgare* L. and establishment of a colony, and was of the opinion that the formation of a long germ tube and exploratory branches reduce the amount of energy available to infect the plant. Ferreira & Rijkenberg (1989) showed that germ tubes of *Uromyces transversalis* (Thum.) Winter which failed to locate stomata often attained considerable length.

A septum which separates the mature appressorium from the germ tube was observed in the present study. Such a septum was also reported to form in *P. graminis* f.sp. *tritici* (Allen, 1923) but not reported by Lennox & Rijkenberg (1985).

The appressorium of *P. recondita* f.sp. *tritici* develops four to six lobes. The lobes appear to play a role in the adherence of the appressorium to the stomatal apparatus. A putatively mucilaginous substance, apparently formed by the appressorium of *P. recondita* f.sp. *tritici*, has also been reported in numerous direct-penetrating rusts and non-rust fungi (Gold & Mendgen, 1984). Gold & Mendgen (1984) suggested that the mucilaginous substance produced by the fungi be a non-specific contact response and that the substance might have multiple roles in the penetration process, eg. attachment to the plant surface and sealing up of the penetration site; protection of the appressorium against desiccation and other unfavourable conditions; and the reservoir for "penetration enzymes".

More than one appressorium over a stoma have been reported in other host-

pathogen interactions (Niks, 1981; Falahati-Rastegar, Manners & Smart, 1983; Ferreira & Rijkenberg, 1988; Lennox & Rijkenberg, 1989; Coutinho *et al.*, 1993b). In the present investigation, *P. recondita* f.sp. *tritici* urediospore germ tubes occasionally form two or even three appressoria on one stoma which resulted in more than one functional substomatal vesicle occupying the same stoma. Torabi & Manners (1989) proposed that the proportion of appressoria of *P. recondita* resulting in successful penetration was greater when two or more appressoria occurred over a stoma.

Pole-Evans (1907), Niks (1983, 1986), Helfer (1987) and Swertz (1994) noted that the SSV of *P. recondita* f.sp. *tritici* tended to be orientated mostly parallel to the stomatal slit with the primary infection hypha then becoming orientated perpendicularly to the leaf surface. In the present investigation, however, the orientation of SSVs of *P. recondita* f.sp. *tritici* in the substomatal chamber was found to be mainly either parallel or perpendicular to the stomatal opening. Swertz (1994) also observed that the SSVs were orientated perpendicularly to the leaf surface and orientation of the primary hyphae was parallel to the long axis of the leaf. She proposed that the orientation of SSVs is highly influenced by temperature. Our experiment was carried out at a temperature of 20^{0}C to enable *Lr19* and *Lr21* to express their resistance properly (Pretorius, personal communication). Perpendicular orientation of the SSVs has also been described for *P. porri* on *Allium porrum* (Davies & Butler, 1986) and *U. transversalis* on *Gladiolus* (Ferreira & Rijkenberg, 1988). Ferreira & Rijkenberg (1988) postulated that SSV orientation has co-evolved with, or adapted to, substomatal chamber orientation. In the present study, there was no significant difference in SSV orientation between the susceptible, intermediately resistant and susceptible wheat lines.

The considerable number of collapsed SSVs in both susceptible and resistant wheat lines at early stage in the interaction, persisting at later sampling stages, indicates their inability to establish compatible host-pathogen interaction, and supports the postulation of Hughes & Rijkenberg (1985) that urediospores differ in inherent aggressiveness, or that some form of host resistance is expressed even in the susceptible tissues.

The growth and extension of the primary infection hypha occurs at one side of SSV. Similar to those of *P. sorghi* (Hughes & Rijkenberg, 1985) and *P. porri* (Davies & Butler, 1986), the primary hypha of *P. recondita* f.sp. *tritici* is two-celled. The terminal cell of the primary hypha is a haustorial mother cell (HMC). In most cases, the secondary infection hypha of *P. recondita* f.sp. *tritici*, similarly to those in *P. sorghi* (Hughes & Rijkenberg, 1985), *U. transversalis* (Ferreira & Rijkenberg, 1988), *P. graminis* f.sp. *tritici* (Lennox & Rijkenberg, 1989) and *H. vastatrix* (Coutinho *et al.*, 1993a), arises mainly on the SSV side of the septum separating the primary hypha from the HMC.

The time course for infection structure formation and development of *P. recondita* f.sp. *tritici* within susceptible and resistant wheat lines is more or less similar to that of *P. sorghi* (Hughes & Rijkenberg, 1985) and *P. graminis* f.sp. *tritici* (Lennox & Rijkenberg, 1989).

The present study indicates that there are more SSVs, primary hyphae, secondary hyphae and HMCs that are collapsed in resistant than in susceptible wheat lines. However, no significant difference between the wheat lines was observed in the timing and morphology of early infection structure development. The resistant wheat line RL 6040 does not support sporulation by 144 hpi. It appears that the expression of resistance is initiated at some stage after the formation of the first haustorial mother cells.

The leaf-fracture technique developed by Hughes & Rijkenberg (1985) is very simple and useful in the investigation of early infection structure morphology in plant tissue. Our observations confirmed that wheat leaves can be fractured particularly well (Lennox & Rijkenberg, 1985).

REFERENCES

Allen, R. F. (1923). A cytological study of infection of Baart and Kanred wheats by *Puccinia graminis tritici*. *Journal of Agricultural Research* **23,** 131-152.

Allen, R. F. (1926). A cytological study of *Puccinia triticina* physiologic form 11 on Little Club wheat. *Journal of Agricultural Research* **33**: 201-222

Andres, M. W. & Wilcoxson, R. D. (1984). A device for uniform deposition of liquid-suspended urediospores on seedling and adult cereal plants. *Phytopathology* **74,** 550-552.

Coutinho, T. A., Rijkenberg, F. H. J. & Van Asch, M. A. J. (1993a). Development of infection structures by *Hemileia vastatrix* in resistant and susceptible selections of *Coffea* and in *Phaseolus vulgaris*. *Canadian Journal of Botany* **71,** 1001-1008

Coutinho, T. A., Rijkenberg, F. H. J. & Van Asch, M. A. J. (1993b). Appressorium formation by *Hemileia vastatrix*. *Mycological Research* **97,** 951-956.

Davies, M. E. & Butler, M. G. (1986). Development of infection structures of the rust *Puccinia porri* on leek leaves. *Transactions of the British Mycological Society* **86,** 475-479

Dickinson, S. (1969). Studies on the physiology of obligate parasitism. VI. directed growth. *Phytopathologische Zeitschrift* **66,** 38-49

Dickinson, S. (1970). Studies on the physiology of obligate parasitism. VII. The effect of a curved thigmotropic stimulus. *Phytopathologische Zeitschrift* **69,** 115-124

Edwards, M. C. & Bowling, D. J. F. (1986). The growth of rust germ tubes towards stomata in relation to pH gradients. *Physiological and Molecular Plant Pathology* **29,** 185-196

Falahati-Rastegar, M., Manners, J. G. & Smart, J. (1983). Factors determining results of competition between physiologic races of *Puccinia hordei. Transactions of the British Mycological Society* **81,** 233-239.

Ferreira, J. F. & Rijkenberg, F. H. J. (1989). Development of infection structures of *Uromyces transversalis* in leaves of the host and a non-host. *Canadian Journal of Botany* **67,** 429-433

Gold, R. E. & Mendgen, K. (1984). Cytology of basidiospore germination, penetration, and early colonization of *Phaseolus vulgaris* by *Uromyces appendiculatus* var. *appendiculatus*. *Canadian Journal of Botany* **62,** 1989-2002.

Helfer, S. (1987). Development of cereal rusts on host and non-host plants. *Cereal Rust Bulletin* **15,** 44-52

Hughes, F. L. & Rijkenberg, F. H. J. (1985). Scanning electron microscopy of early infection in the uredial stage of *Puccinia sorghi* in *Zea mays*. *Plant Pathology* **34,** 61-68

Jacobs, Th. (1989). Germination and appressorium formation of wheat leaf rust on susceptible, partially resistant and resistant wheat seedling and on seedlings of other Gramineae. *Netherlands Journal of Plant Pathology* **95,** 65-71

Jacobs, Th. (1990). Abortion of infection structures of wheat leaf rust in susceptible and partially resistant wheat genotypes. *Euphytica* **45,** 81-86

Johnson, T. (1934). A tropic response in germ tubes of urediospores of *Puccinia recondita* f.sp. *tritici*. *Phytopathology* **24,** 80-82.

Kloppers, F. J. (1994). Characterisation of resistance conferred by selected *Lr* genes with emphasis on histopathology, leaf rust development and associated quality attributes in wheat. Ph.D. Dissertation, University of the Orange Free State, 187pp.

Lee, T. S. & Shanner, G. (1984). Infection processes of *Puccinia recondita* in slow- and fast-rusting wheat cultivars. *Phytopathology* **74,** 1419-1423.

Lennox, C. L. & Rijkenberg, F. H. J. (1989). Scanning electron microscopy study of infection structure formation of *Puccinia graminis* f.sp. *tritici* in host and non-host cereal species. *Plant Pathology* **38,** 547-556.

Lewis, B. G. & Day, J. R. (1972). Behaviour of urediospore germ-tubes of *Puccinia graminis tritici* in relation to the fine structure of wheat leaf surfaces. *Transactions of the British Mycological Society* **58,** 139-145

Niks, R. E. (1981). Appressorium formation of *Puccinia hordei* on partially resistant barley and two non-host species. *Netherlands Journal of Plant Pathology* **87,** 201-207.

Niks, R. E. (1983). Comparative histology of partial resistance and the non-host reaction to leaf pathogens in barley and wheat seedlings. *Phytopathology* **73,** 60-64.

Niks, R. E. (1986). Variation of mycelial morphology between species and formae speciales of rust fungi of cereals and grasses. *Canadian Journal of Botany* **64,** 2976-2983

Niks, R. E. (1990). Effect of germ tube length on the fate of sporelings of *Puccinia hordei* in susceptible and resistant barley. *Phytopathology* **80,** 57-60.

Niks, R. E. & Dekens, R. G. (1991). Prehaustorial and posthaustorial resistance to wheat leaf rust in diploid wheat seedlings. *Phytopathology* **81,** 847-851.

Pole-Evans, B. (1907). The cereal rusts. I. The development of their Uredo mycelia. *Annals of Botany* **21,** 441-466.

Romig, R. W. & Caldwell, R. M. (1964). Stomatal exclusion of *Puccinia recondita* by wheat peduncles and sheaths. *Phytopathology* **54,** 214-218.

Southerton, S. G. & Deverall, B. J. (1989). Histological studies of the expression of the *Lr9, Lr20* and *Lr28* alleles for resistance to leaf rust in wheat. *Plant Pathology* **38,** 190-199.

Staples, R. C. & Macko, V. (1984). Germination of urediospores and differentiation of infection structures. In: *The Cereal Rusts. Vol. 1. Origins,*

specificity, structure, and physiology (Eds. Bushnell, W. R. & Roelfs, A. P.), pp. 255-289. Academic Press, Orlando.

Swertz, C. A. (1994). Morphology of germlings of urediospores and its value for the identification and classification of grass rust fungi. *Studies in Mycology* **36,** 1-80.

Torabi, M. & Manners, J. G. (1989). Appressorium formation of *Puccinia recondita* on susceptible and resistant wheat cultivars. *Mycological Research* **92,** 440-444.

Wynn, W. K. (1976). Appressorium formation over stomata by the bean rust fungus: response to a surface contact stimulus. *Phytopathology* **66,** 136-146

CHAPTER 2

DEVELOPMENT OF EARLY INFECTION STRUCTURES OF *PUCCINIA RECONDITA* F.SP. *TRITICI* IN HOST AND NON-HOST CEREAL SPECIES

INTRODUCTION

Non-host resistance, the most common and the most effective form of naturally occurring disease resistance, initiated by the attempted invasion of organisms which are normally pathogenic on other plant species or genera, has received much attention in rust diseases in the past few decades (Fernandez and Heath, 1985; Heath, 1972; 1974; 1977; 1981; 1982; 1983; Heath and Stumpf, 1986; Jacobs, 1989; Leath and Rowell, 1966; 1969; 1970; Niks, 1983; 1987; Niks and Dekens, 1991; Sellam and Wilcoxson, 1976; Stumpf and Heath, 1985; Wood and Heath, 1986). The elucidation of the resistance mechanisms expressed by non-hosts could provide more understanding of the plant-parasite interaction (Heath, 1985). Previous investigations suggested that non-host resistance is durable and difficult to overcome by rust fungi (Heath, 1985). Non-host plants of plant pathogens are thought to be a potential source of resistance genes for host plants of a pathogen (Niks, 1987).

Histological investigation showed that *Puccinia graminis* infection of a non-host, corn, was hampered after appressorium development or before haustorial mother cell formation (Leath and Rowell, 1966). Quantitative

studies of infection structures by Niks (1983a, 1983b) showed the early arrest of *Puccinia hordei* Otth. and *Puccinia recondita* Rob. ex Desm. f.sp. *tritici* Eriks. & Henn. infection of wheat and barley immediately after the development of the first haustorial mother cells. It has been postulated that prehaustorial resistance, which implies that sporeling development is arrested before the formation of haustoria, is very common in non-host interactions (Elmhirst and Heath, 1989; Heath, 1977; 1981; 1982, Mendgen, 1978; Niks and Dekens, 1991).

Most descriptions of non-host resistance in rusts were made with the aid of light microscopy and transmission electron microscopy until the publication of a leaf-fracturing technique which facilitates the observation of the infection structures within plants by scanning electron microscopy (Hughes and Rijkenberg, 1985). Using the leaf-fracturing technique, Ferreira and Rijkenberg (1989) recorded the development of infection structures of *Uromyces transversalis* (Thum.) Winter in leaves of the host (*Gladiolus* L.) and a non-host (*Zea mays* L.), Lennox and Rijkenberg (1989) described the development of infection structures of *Puccinia graminis* f.sp. *tritici* Eriks. & Henn. in the host (*Triticum aestivum* L.) and non-hosts (*Sorghum caffrorum* L., *Hordeum vulgare* L., and *Zea mays* L.) and Coutinho, Rijkenberg and Van Asch (1993) observed the development of infection structures by *Hemileia vastatrix* Berk. & Br. in the host (*Coffea arabica* L.) and a non-host (*Phaseolus vulgaris* L.). These investigations have provided more insight into non-host resistance mechanisms.

The purpose of the present study was to describe infection structure formation and development of *Puccinia recondita* Rob. ex Desm. f.sp. *tritici* Eriks. & Henn. (syn. *P. triticina* Eriks.), the pathogen of wheat leaf rust, in

non-host plant species and to compare such development with that in the host plant (*Triticum aestivum* L.) described previously (Hu and Rijkenberg, 1996; Chapter 1).

MATERIALS AND METHODS

Plant Materials

Inappropriate (non-host) hosts of *Puccinia recondita* f.sp. *tritici*, sorghum (*Sorghum caffrorum* L.) cultivar Tx01, an unnamed cultivar of maize (*Zea mays* L.), barley (*Hordeum vulgare* L.) cultivar Clipper and Oat (*Avena sativa* L.) cultivar Heros were used in this study. For fluorescence microscopy, the host, near-isogenic wheat (*Triticum aestivum* L.) lines, Thatcher (susceptible), RL 6043 which is Thatcher*6/RL 5406 (Tetra Canthatch)/*Ae. squarrosa* var. Meyeri-RL 5289 (with resistance gene *Lr21*, intermediately resistant to UVPrt 8) and RL 6040 which is Thatcher*7/translocation 4 (derived from *Agropyron elongatum*) (with resistant gene *Lr19*, highly resistant to UVPrt 8) were included in the present study. All seedlings were grown singly in 10 cm pots and maintained at 20^{0}C in a leaf-rust free constant environment chamber with a 12-hour photoperiod.

Rust propagation and inoculation

The South African pathotype UV Prt 8 of *Puccinia recondita* f.sp. *tritici* was used in the present investigation (obtained from Professor Z. A. Pretorius, University of the Orange Free State, South Africa). The South African pathotype UV Prt 8 has an avirulence/virulence formula of

3a,3bg,3ka,11,16,20,26,30/1,2a,2b,2c,10,14a,15,17,24.

Freshly harvested urediospores of *P. recondita* f.sp. *tritici* produced on 15-day-old plants of susceptible wheat cultivar Agent in a greenhouse (20-26^{0}C) were used to inoculate the adaxial surface of the first leaf of 10-day-old plants of oat, the second leaf of 8-day-old plants of barley, the third leaf of 8-day-old plants of sorghum and the third leaf of 15-day-old maize at an inoculum dose of 40 mg urediospores per ml of Soltrol 130 (Phillips Chemical Co.). A modified Andres & Wilcoxson (1984) inoculator was used to inoculate the plants. To prevent damage to leaves covered with Soltrol oil, inoculated seedlings were allowed to dry for approximately 1 hour before placement in the dark in a dew chamber at 20^{0}C and 100% R.H. for 24 hours.

Observation by fluorescence microscopy

For fluorescence microscopy, the methods described by Rubiales and Niks (1991) were employed. A segment from the central part of each leaf, 48 hours post-inoculation, was harvested, fixed and stained. The segments were laid, adaxial surface up, on filter paper, one end of which was dipped in fixative (3:1, absolute ethanol/glacial acetic acid, V/V), while keeping the specimen moist in a petri dish. About 48 hours later, the bleached specimens were transferred to filter paper moistened with lactophenol-ethanol (1:2, V/V) for 24 hours and then were put onto filter paper soaked in Trypan blue stain (0.1% in lactophenol-ethanol) for 24 to 48 hours. The surface of the stained leaf segments was examined under ×100 magnification using a Zeiss Axiophot research microscope fitted with epifluorescence equipment (exciter filter 330-380 nm; barrier filter 420 nm). Colour photographs were taken using Kodak Ektachrome 160 Professional 35-mm film.

Six leaves of each species or cultivar were used in a single replication. About 100 urediospores per leaf segment were counted. The experiment was repeated three times.

The following four pre-penetration stages were recorded: (1) non-germinated urediospores; (2) germinated urediospores that did not form appressoria; (3) germinated urediospores that formed appressoria over stomata; and (4) germinated urediospores that formed appressoria not over stomata. The mean percentage of the total counts recorded on each segment from each replicate was calculated for all pre-penetration stages. Differences between the means were examined for significance by the LSD statistical test.

Specimen preparation for scanning electron microscopy

For each of the three experiments, the inoculated leaves of 10 seedlings of each species were harvested at 6, 12, 24, 48, 72, 96 and 144 hours post-inoculation (hpi). At 24 hpi, the remaining seedings in the dew chamber were removed and placed in a constant environment chamber at 18-20 C.

The harvested leaves were cut into about 3 × 3 mm squares and fixed in 3% glutaraldehyde in 0.05 M sodium cacodylate buffer, pH 6.8-7.2, for 24 hours, washed twice in the buffer, postfixed for 2 hours in 2% osmium tetroxide in the buffer at the room temperature, washed twice in the buffer, and dehydrated in a graded ethanol series. The specimens were then critical point dried with carbon dioxide as a transition fluid and were mounted on copper stubs. The leaf fracture method of Hughes and Rijkenberg (1985) was used on specimens harvested from 12 to 96 hpi. Both stubs used in fracturing were then processed for observation. Samples harvested at 6 and 144 hpi were left unfractured. All stripped epidermis and that of the tissue remaining on the

stubs was gold/palladium-coated in a Polaron Sputter coater. Both stripped-epidermis and stripped-leaf materials were examined with a Jeol S-350 Scanning Electron Microscopy (SEM) operating at 8.0 or 10.0 kV. The specimens harvested at 6 hpi were scanned only exteriorly. In some instances, after freezing in an EM Scope SP 2000 cryo unit, freshly harvested materials (6 hpi) were viewed with the SEM at 8.0 kV. Counts of infection structures were made directly from the screen and micrographs were made of both typical and atypical infection structures observed. Three leaf piece per leaf sample per plant were examined.

An investigation of infection structure formation and development of *Puccinia recondita* f.sp. *tritici* on and in susceptible and resistant wheat lines, with the aid of scanning electron microscopy, was conducted. The results, described in Chapter 1, were used for comparative purposes.

RESULTS

Fluorescence microscopy

Percentages of infection structures observed, by fluorescence microscopy, on and in the leaf piece of the wheat lines and four other Gramineae species are presented in Table 1. The data indicate that there is no significant difference between the proportions of germinated urediospores and appressoria formed on the wheat lines and those on the other four Gramineae species. In general, the percentages of the four categories noted between wheat lines and four other species were similar.

Table 1. Germination and appressorium formation by *Puccinia recondita* f.sp. *tritici* on host and non-host leaf surfaces*

Plant species	Germinated urediospores			
	germination (%) **	germ tubes (%)	appressorium over stoma (%)	appressorium not over stoma (%)
Wheat line RL 6040 (*Lr19*)	81 a	28 a	61 a	11 a
Wheat line RL6043 (*Lr21*)	84 a	32 a	58 a	10 a
Wheat line Thatcher	78 a	28 a	62 a	10 a
Barley cv. Clipper	69 a	28 a	63 a	8 a
Oat cv. Heros	84 a	28 a	64 a	8 a
Maize cv. unnamed	80 a	38 a	49 a	13 a
Sorghum cv. TX01	72 a	24 a	68 a	8 a

*: Mean values calculated from counts obtained from 6 leaves in three replicates and examined 48 hours post-inoculation.

**: Values across rows with different letters differed significantly at the P = 0.01 level.

Scanning electron microscopy

The morphology of infection structures and the pattern of formation and

development of infection structures of *Puccinia recondita* f.sp. *tritici* on and in four cereal plants, namely, sorghum, maize, oat and barley is similar to those described in susceptible and resistant wheat lines (Hu and Rijkenberg, 1996; Chapter 1).

At 6 hpi, urediospores on the leaves of all four plant species germinate and the germ tubes grow and extend in a direction perpendicular to the long axis of the leaf (Fig. 1). Several short branches, along the germ tube's length, are produced in some cases (Fig. 1). A terminal appressorium differentiates when the germ tube locates a plant stoma (Fig. 2). Some germ tubes, especially on the surface of sorghum and maize plants, had failed to locate a stoma and had collapsed without forming an appressorium. On all plant species, four to six lobes are produced along the periphery of the appressorium (Fig. 3). The appearance of appressoria on oat and barley leaves was found to resemble closely that on wheat leaves. However, some appressoria on maize and sorghum were collapsed (Fig. 4). On all four species, two or even three appressoria could form over a single stoma (Fig. 5).

On the lower surface of the appressorium, an infection peg arises and penetrates into the stomatal opening. The tip of infection peg swells into a substomatal vesicle (SSV) initial in the stomatal chamber (Figs. 6-8). In some instances, the infection peg from the appressorium produces the SSV on the outer surface of the guard cells and fails to penetrate into the stomatal chamber (Fig. 9). The infection peg is visible after the plant epidermal layer was stripped off (Fig. 6). The orientation of infection peg is confined to the stomatal slit (Fig. 6).

Substomatal vesicle (SSV) initials and SSVs were observed at 6 hpi and subsequent sampling stages. SSV initials firstly appear as a bulbous or

globose structure (Fig. 7) and then swell (Fig. 8), extending in both length and width, becoming more elongate. Further increase in length is associated with slight increase in breadth and the mature SSV becomes torpedo-shaped (Figs. 10-13). In some cases, two SSVs were observed protruding into a single substomatal chamber (Fig. 13). As that in wheat leaves, the orientation of SSVs in the non-hosts varied, viz. either parallel to the long axis of the stomatal slit (Fig. 10), thus parallel to the long axis of the leaf, or perpendicular to the long axis of stomatal slit and developing further into the substomatal cavity (Fig. 11). In a few cases, the SSV was orientated at right angles to the stomatal slit (Fig. 12). Occasionally, in oat, maize and sorghum, amorphous materials had adhered to the infection structures, especially the SSVs (Figs. 14, 15). Infection structures in sorghum do not develop beyond the initiation stage of primary hyphae, and then collapse (Fig. 16). By 48 hpi, most infection structures in sorghum have collapsed. On a few occasions, a bulbous structure was evident terminally on the SSV (Fig. 17) and this structure does develop further (Fig. 18). Primary hypha initials form unilaterally from the end of the SSVs or form from a position beneath the SSV (Fig. 19). In maize at 12 hpi and subsequent sampling times, the primary hypha have developed further (Fig. 19), but most primary hyphae collapse, only a few forming a septum delimiting a haustorial mother cell (HMC) from the primary hypha as it attaches to a plant cell. In such instances, a secondary hypha had occasionally emerged from a position on the SSV side of the HMC septum, only to have apparently collapsed at that juncture. It appears that the first HMC collapsed before the abortion of the secondary hypha (Fig. 20). By 72 hpi, most infection structures in maize had collapsed. In most cases, however, infection structures in barley and oat had developed further (Fig. 21) although many collapsed structures were found in these species at 72 hpi. When the extending primary hypha abuts a plant cell in barley or oat, a septum is formed which cuts off a terminal haustorial mother

PLATE 1

Fig. 1. Urediospore (U) and germ tube (G) of *Puccinia recondita* f.sp. *tritici* on maize leaf at 6 hour post-inoculation (hpi). Orientation of germ tube (G) is perpendicular to the long axis of the leaf and the germ tube has produced several short exploratory branches (B). (Bar = 24 μm)

Fig. 2. Appressorium (A) on the oat leaf at 6 hpi. (Bar = 17 μm)

Fig. 3. Appressorium (A) over a stoma on the barley leaf at 6 hpi (cryo-SEM photograph). Several lobes (L), closely adherent to the guard cell, are seen around the periphery of appressorium. A germ tube appears to be absent. (Bar = 9 μm)

Fig. 4. Collapsed appressorium over a stoma on the sorghum leaf at 6 hpi. (Bar = 9.5 μm)

Fig. 5. Three appressoria (A) over a single stoma on the oat leaf at 6 hpi. (Bar = 15 μm)

Fig. 6. Substomatal vesicle (SSV) in stomatal chamber in the oat leaf at 12 hpi, after stripping off of the epidermis, showing the penetration wedge. The SSV carries the imprints of guard cells (arrows) and subsidiary cells. The lumen of the interconnective tube is to one side of the stomatal imprint (arrowheads). (Bar = 4 μm)

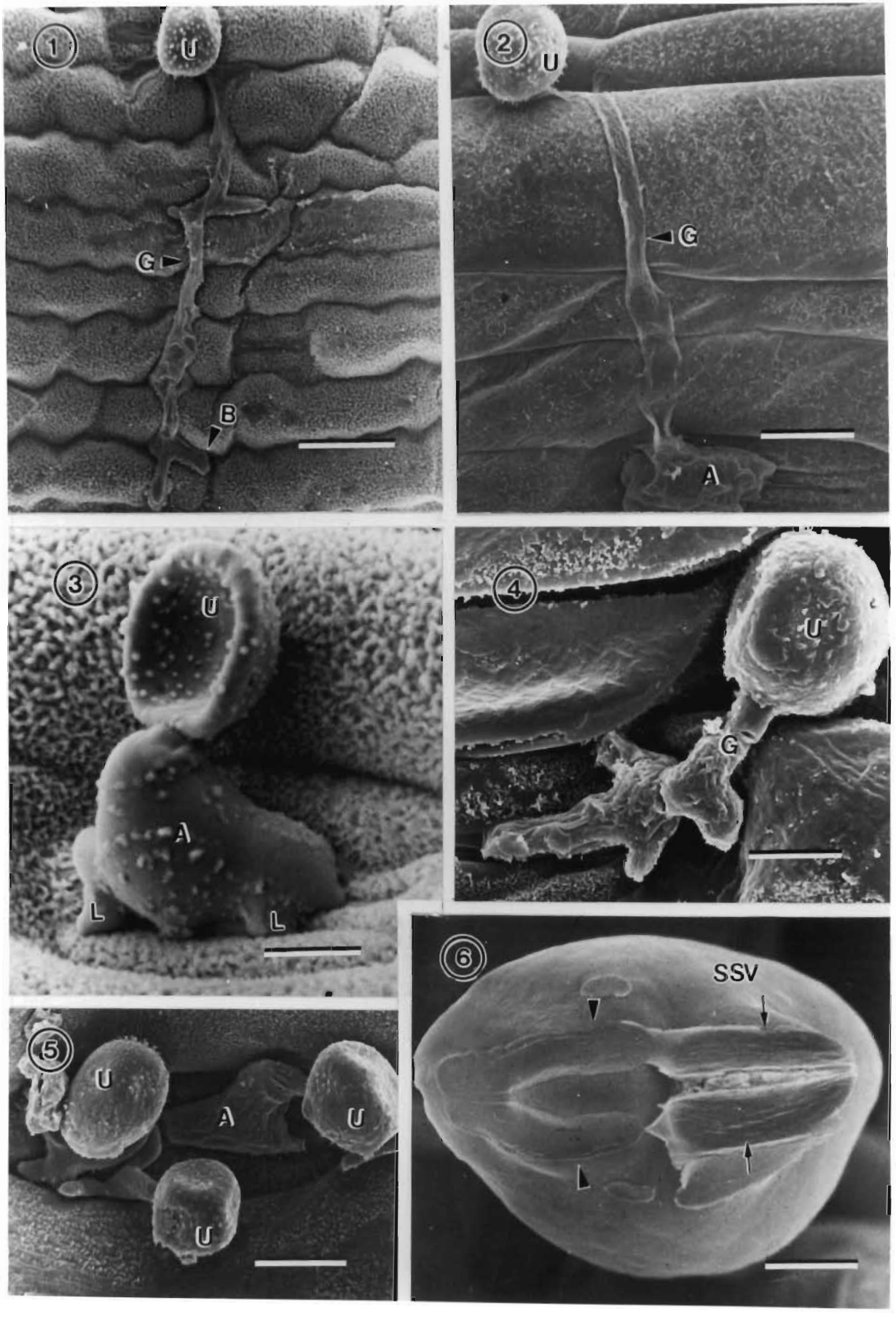
1
U
G
B
2
U
G
A
3
U
A
L
L
4
U
G
5
U
A
U
U
6
SSV

PLATE 2

Fig. 7. Near-spherical substomatal vesicle initial in the barley leaf at 12 hpi. (Bar = 8 μm)

Fig. 8. Spherical substomatal vesicle in the maize leaf at 12 hpi. (Bar = 7 μm)

Fig. 9. The penetration wedge fails to penetrate into stomatal chamber and forms a substomatal vesicle on the surface of the sorghum leaf at 12 hpi. (Bar = 10 μm)

Fig. 10. Ovoid-shaped substomatal vesicle orientated parallel to the stomatal slit in the maize leaf at 12 hpi. (Bar = 5 μm)

Fig. 11. Substomatal vesicle orientated perpendicularly to the stomatal opening in the maize leaf at 12 hpi. The interconnective tube (IT) protrudes through the stoma into the substomatal chamber and a septum (S) delimiting the interconnective tube from the substomatal vesicle is visible. (Bar = 5.5 μm)

Fig. 12. Substomatal vesicle orientated at right angle to the stomatal slit in the barley leaf at 12 hpi. (Bar = 6 μm)

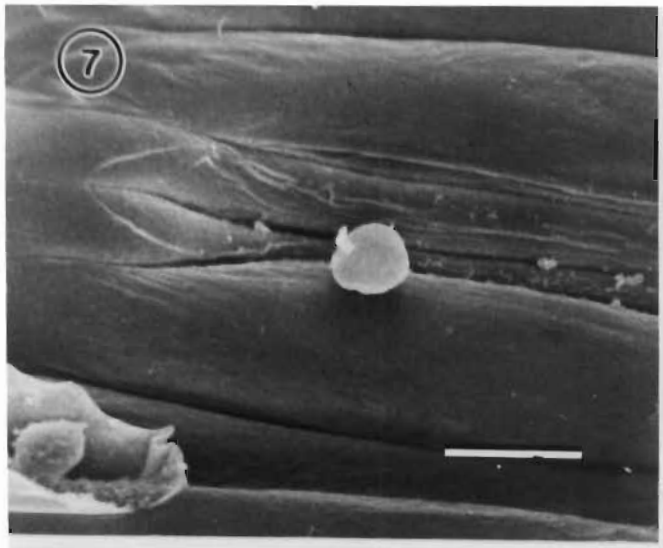
7

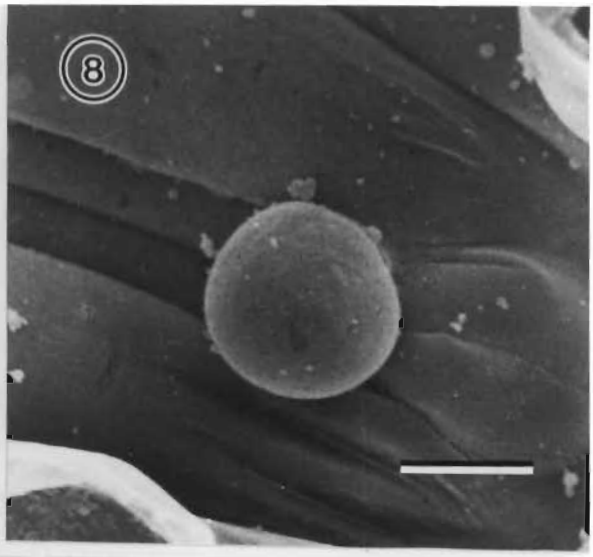
8

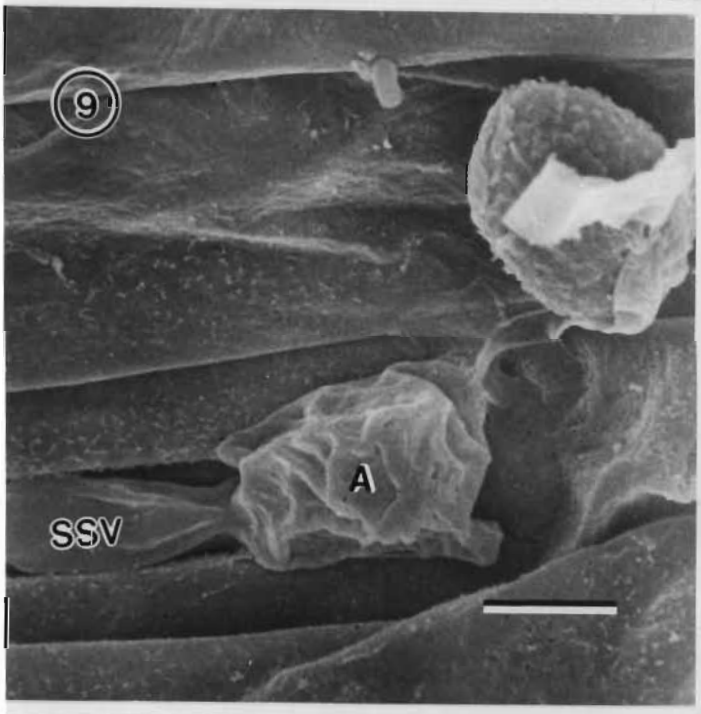
9
A
SSV

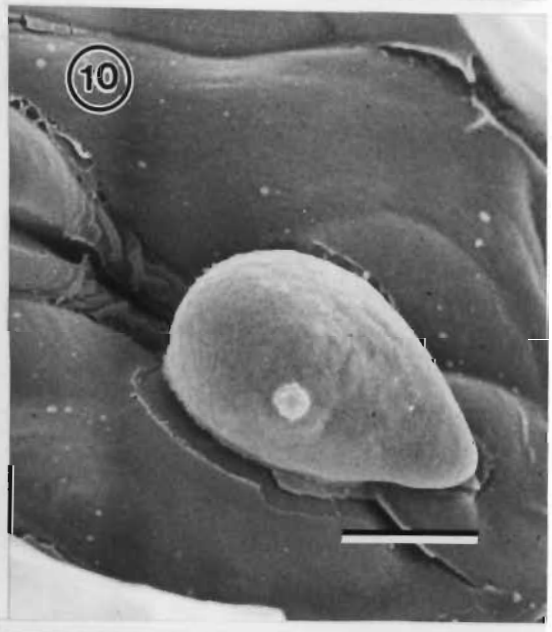
10

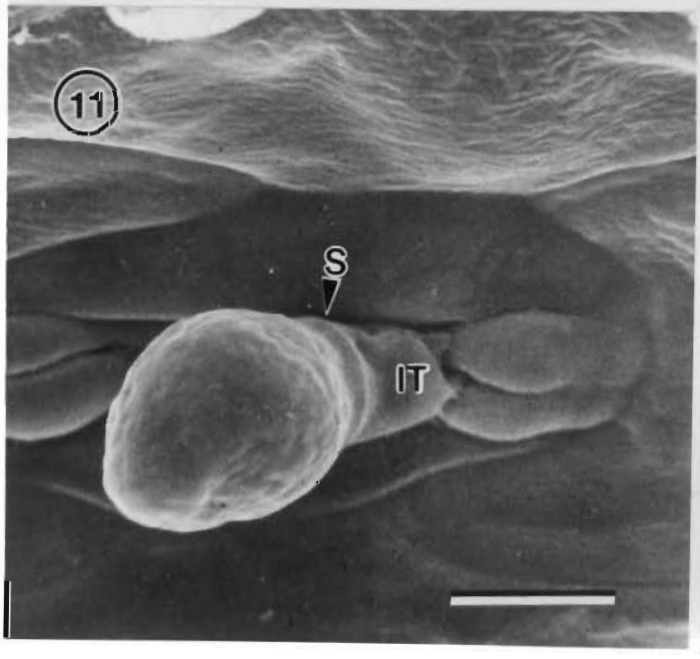
11
S
IT

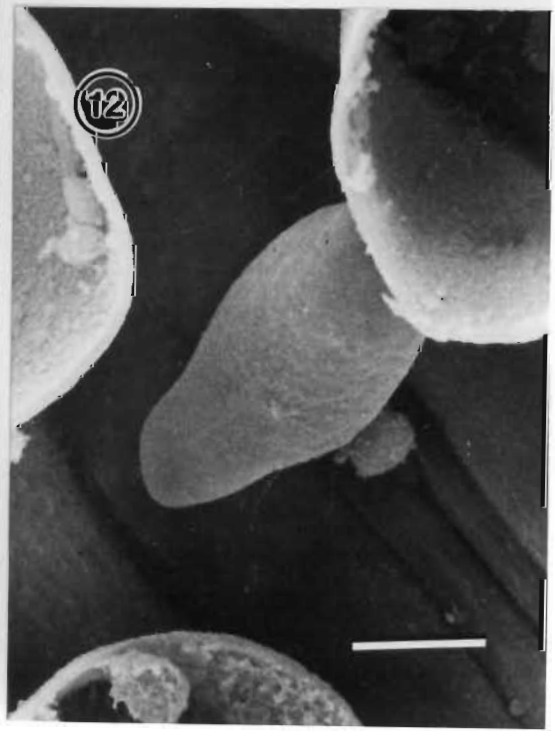
12

PLATE 3

Fig. 13. Two substomatal vesicles are seen in a substomatal chamber in the oat leaf at 12 hpi. (Bar = 5 μm)

Fig. 14. Collapsed substomatal vesicle, in the sorghum leaf at 24 hpi. An amorphous material (arrow) is associated with the substomatal vesicle. (Bar = 5 μm)

Fig. 15. Collapsed substomatal vesicle, orientated perpendicularly to the stomatal opening, in the oat leaf at 24 hpi. An amorphous material (arrow) is associated with the substomatal vesicle. (Bar = 5 μm)

Fig. 16. Collapsed substomatal vesicle in the maize leaf at 24 hpi. The interconnective tube protrudes into the substomatal chamber. (Bar = 5.5 μm)

Fig. 17. A bulbous structure (arrow), is noticeable at one end of the substomatal vesicle in the maize leaf 24 hpi. (Bar = 3.5 μm)

Fig. 18. Primary hypha initial emerging from the end of substomatal vesicle in the oat leaf at 24 hpi. (Bar = 4 μm)

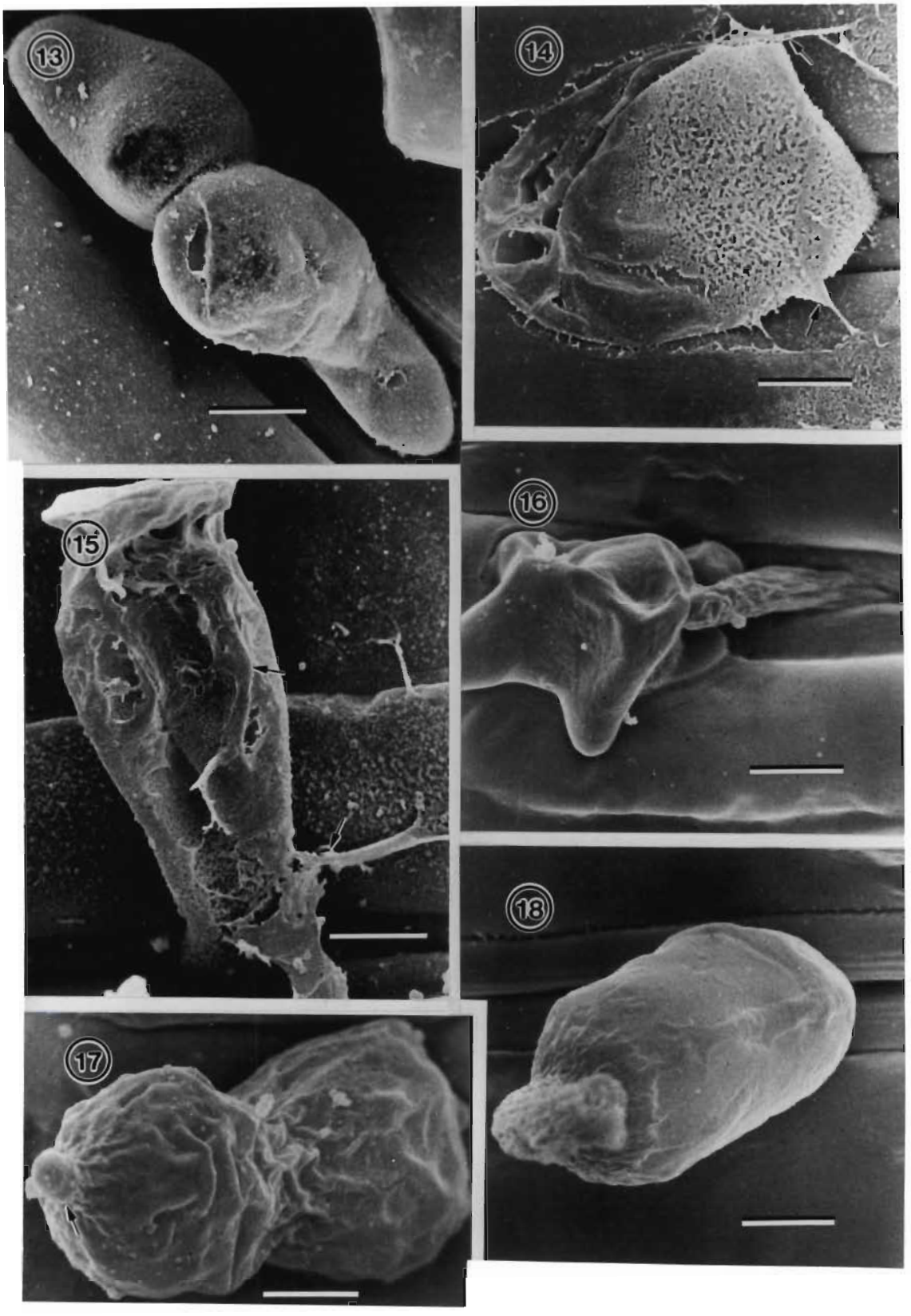
13
14
15
16
17
18

PLATE 4

Fig. 19. Primary hypha (PH) extending into the intercellular space between the mesophyll cells in the maize leaf at 24 hpi. (Bar = 6 μm)

Fig. 20. At 48 hpi in the maize leaf, a septum has cut off the haustorial mother cell (HMC) from the primary hypha (PH). A secondary hypha (SH) has arisen on SSV side of the HMC septum. The HMC has subsequently collapsed. (Bar = 10 μm)

Fig. 21. Primary hypha (PH) extending into the intercellular space between the mesophyll cells in the barley leaf at 24 hpi. (Bar = 6 μm)

Fig. 22. A septum (S) cutting off the haustorial mother cell (HMC) from the primary hypha (PH) where the hypha attaches to the host cell. A secondary hypha (SH) has emerged on the SSV side of the HMC septum and has elongated further into the mesophyll cells. Oat leaf, 48 hpi. (Bar = 4 μm)

Fig. 23. More secondary hyphae (SH) with HMCs have ramified in the barley leaf at 72 hpi. (Bar = 17 μm)

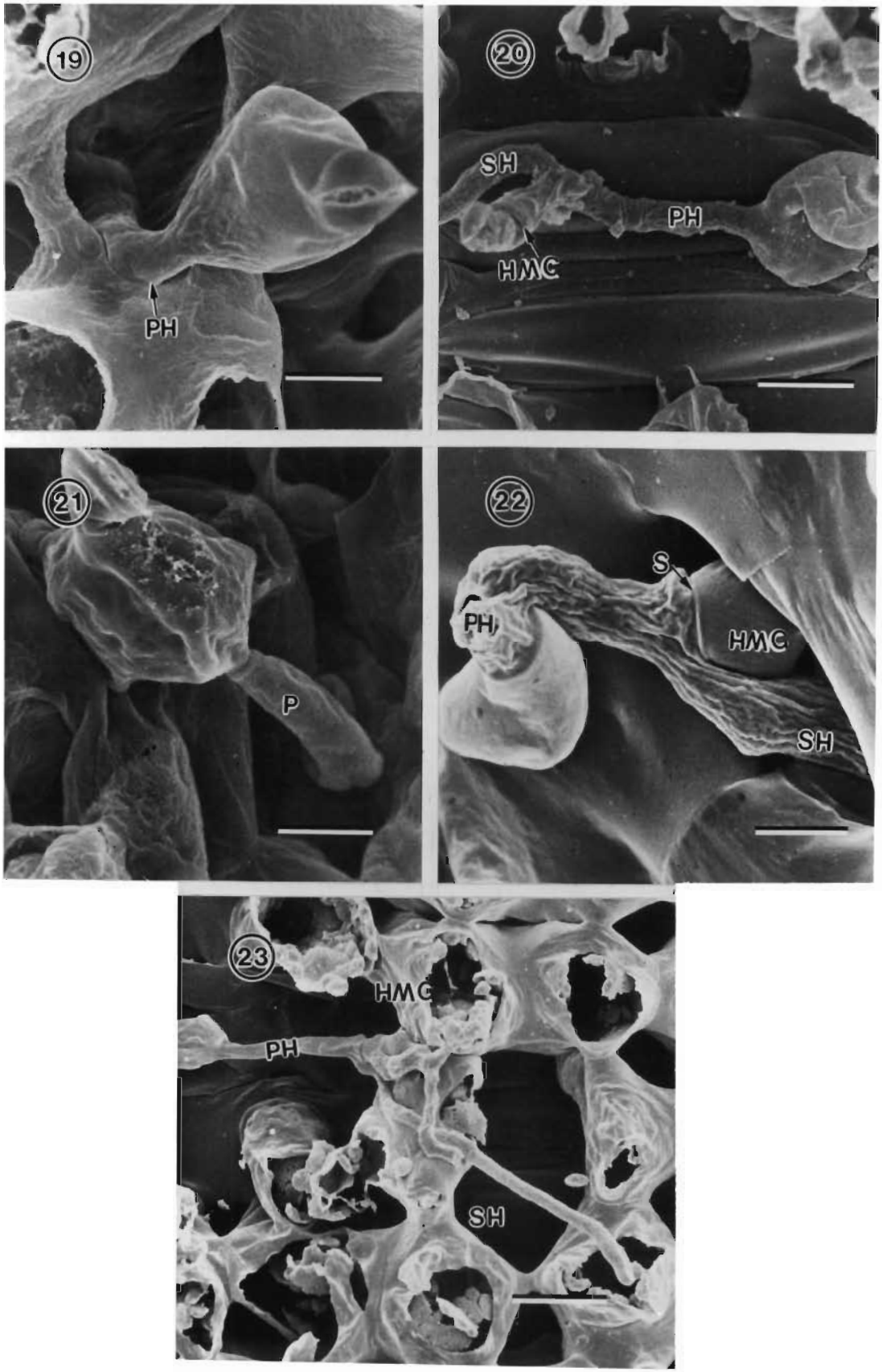
19
PH
20
SH
PH
HMC
21
P
22
S
PH
HMC
SH
23
HMC
PH
SH

Table 2. Counts (%) of infection structures at specific time intervals post-inoculation

Infection structures	Hours post-inoculation															
	Sorghum				Maize				Barley				Oat			
	12	24	48	96	12	24	48	96	12	24	48	96	12	24	48	96
SSV	54	63	68	45	63	54	71	78	59	69	71	84	85	73	82	85
Collapsed SSVs	46	37	32	55	37	46	29	22	41	31	29	16	15	27	18	15
Primary hypha	4	7	5	10	25	18	29	32	23	40	62	69	19	51	56	75
Collapsed PH	4	10	3	7	14	29	29	40	9	13	9	15	13	16	15	10
PH with HMCs					4	7	26	30	14	38	42	56	8	35	46	49
Secondary hypha						4	5	15		17	36	38		12	32	27
IH and HMCs										4	18	25		2	15	15
Total sites	28	41	37	29	52	28	42	65	80	72	45	68	89	49	54	68

NB: Columns are based on the cumulative totals
Abbreviations: SSV, substomatal vesicle; PH, primary hypha; HMC, haustorial mother cell
SH, secondary hypha; IH, intercellular mycelium.

cell from the primary hypha (Fig. 22). A secondary hypha emerges from the primary hypha at a position on the SSV side of the septum cutting off the terminal HMC from the primary hypha and extends further (Fig. 22). At most infection sites in barley and oat tissues at 24 hpi and at all later sampling times, secondary infection hyphae have developed and have cut off many HMCs. Further branching from the secondary hyphae occurs behind the HMCs and by 72 hpi, a much-branched mycelium ramifies through the intercellular spaces of the oat and barley mesophyll tissues (Fig. 23). No differences in the appearance of these infection structures were recorded between barley, oat and wheat. Collapsed infection structures were also noted in barley and oat tissues from 24 hpi onwards.

A few small colonies were observed on barley leaves at 144 hpi and some sporulated.

Counts of infection structures of *P. recondita* f.sp. *tritici* observed on sorghum, maize, barley and oat at 12, 24, 48, and 96 hpi are recorded in Table 2.

DISCUSSION

Infection processes by rust fungi in plants can be grouped into several phases (Niks, 1982). In principle, defense mechanisms may occur at any phase during infection.

This investigation revealed that urediospores of *P. recondita* f.sp. *tritici* are capable of germinating equally well on the different susceptible and resistant

near-isogenic wheat lines and the non-host species. Heath (1974; 1977) suggested that the surface characteristics of non-host plants, such as hirsuteness and waxiness, could significantly reduce the number of urediospores which encountered favourable conditions for germination, thus playing an important practical part in non-host resistance.

It is believed that the directional growth of the germ tube towards a stoma and the subsequent differentiation of the appressorium, is a response to the particular topographical features of the leaf surface (Wynn, 1976). In non-host resistance, Heath (1977) proposed that whether the pre-penetration behaviour of a rust can play a significant role essentially depends on whether such behaviour leads to fewer attempts at penetration into the leaf. The present study indicates that the germ tube of *P. recondita* f.sp. *tritici* grows in a direction perpendicular to the long axis of leaf on all plant species tested. The size and shape of the subsequently induced appressorium is similar on all plant species although a small number of abnormal appressoria was observed in maize and sorghum. It appears that there is no marked difference in appressorium formation between different genotypes. Similar observations have also been reported for wheat stem rust *(Puccinia graminis tritici)* on corn (Leath and Rowell, 1966). Niks and Dekens (1987) also reported that stomatal penetration by *P. recondita* f.sp. *tritici* and *Puccinia recondita* f.sp. *recondita* on an inappropriate host species is not impeded significantly. In an investigation on the germination and appressorium formation by *P. recondita* f.sp. *tritici* on different genotypes of host and non-hosts, Jacobs (1989a) indicated no measurable differences between hosts and non-hosts. However, a reduction in attempts at leaf penetration was found for cowpea rust on some non-host plants examined (Heath, 1974; 1977) and was also reported for bean rust on cowpea and soybean (Wynn, 1976). Reduced percentages of appressoria over stomata, due to apparent stomatal nonrecognition by the

rusts, were also recorded when *Phaseolus vulgaris* L. and *Camellia sinensis* L. were inoculated with *Hemileia vastatrix* (Coutinho *et al.*, 1992). Similarly, Ferreira and Rijkenberg (1989) observed that many of the germ tubes of gladiolus rust (*Uromyces transversalis*) aborted on maize (non-host) leaves, and of those that successfully formed appressoria on maize, many failed to penetrate the stomatal opening. However, the molecular events that allow the germ tube to recognize and respond to physical features of the plant surface and induce appressorium formation remain unknown.

The morphology of the appressorial complex and the lobes of appressorium in *P. recondita* f.sp. *tritici* are unique. The observations in this study confirm those structures described on hosts of *P. recondita* (Hu and Rijkenberg, 1996; Chapter 1). The appressorial lobes, around the periphery of the appressorium, had also been observed to have a sucker-like nature on the lower surface after being stripped off from the leaf surface (Crooks & Rijkenberg, unpublished), thus suggesting an attachment role.

In the present investigation, it was common that there were two, even three appressoria over a singly stoma on the non-hosts. This is contrast to the report on *Hemileia vastatrix* appressorium formation by Coutinho *et al.* (1993), who observed that more than one appressorium were occasionally seen over a host stoma, but never on a non-host stoma. This may reflect the difference in response to stimuli among the rust species (Wynn, 1976). Dickinson (1970) revealed that a topographical stimulus is sufficient to induce appressorium formation in *Puccinia recondita*. More than one appressorium over a stoma have been reported in many host-pathogen combinations (Niks, 1981; Lennox and Rijkenberg, 1989; Torabi and Manners, 1989; Hu and Rijkenberg, 1996; Chapter 1) but in few non-host-pathogen interactions. It has been reported that the proportion of appressoria of *P. recondita* f.sp. *tritici* resulting in

successful penetration was greater when two or more appressoria occurred over the same stoma (Torabi and Manners, 1989).

Another unique feature of *P. recondita* f.sp. *tritici* infection structures on non-hosts is the presence of amorphous material on the SSVs observed occasionally within maize, oat and sorghum leaves. A similar substance has also been observed occasionally in the resistant wheat line, RL 6040 (*Lr19*) (Hu and Rijkenberg, 1996; Chapter 1). Similar amorphous material has been observed in the interaction between *Puccinia coronata* f.sp. *avenae* Erikss. and susceptible oat tissue (Onoe *et al.,* 1987) and is thought to contribute to the establishment of susceptibility. Coutinho *et al.* (1993) also described a similar amorphous material on SSVs of *Hemileia vastatrix* within a susceptible cultivar.

The orientation of SSVs of *P. recondita* f.sp. *tritici* within non-host leaves is similar to that within the hosts, viz, either parallel to the long axis of the stomatal slit, or at right angles to the stomatal slit, or perpendicular to the stomatal opening. It was proposed that such alignment has co-evolved with, or adapted to, stomatal chamber orientation (Ferreira and Rijkenberg, 1989), but this does not appear to be the case for *P. recondita* f.sp. *tritici*.

The results presented in this study suggest that the resistance within plants expresses itself at different stages in each non-host species. In sorghum, fungal development is arrested at the stage of SSV formation and the fungus does not develop beyond this. Similar observations were reported for *Puccinia graminis* f.sp. *tritici* in sorghum as a non-host (Lennox and Rijkenberg, 1989). It is unknown at this stage whether the cessation of SSV development in sorghum is due to growth inhibition or lack of stimulation. Heath (1977; 1979) suggested that the poor growth of fungal structures within the non-

hosts may result from an inhibitor. The presence of a growth inhibitor has been postulated to account for the resistance of corn leaves to wheat stem rust (Leath and Rowell, 1966; 1969; 1970).

In contrast to the sorghum-*Puccinia recondita* f.sp. *tritici* interaction, the primary hypha in maize can develop beyond the 12 hpi substomatal vesicle stage, although most collapsed during the stage of primary hypha development. On a few occasions, a septum formed to cut off a terminal haustorial mother cell from the primary hypha, and a secondary hypha initial emerged which collapsed soon. These results are consistent with the observations by Heath (1977) on non-host interactions of maize, sunflower and cowpea rusts. Her study revealed that whether a haustorium formed or not, secondary hyphae sometimes started to develop but remained short and never developed haustorial mother cells or haustoria of their own. In maize infected by *Puccinia graminis* f.sp. *tritici*, Lennox and Rijkenberg (1989) showed that secondary hyphae were present. By means of light microscopy Leath and Rowell (1969) established that no HMCs were formed in maize leaves infected with wheat stem rust.

Heath (1977) proposed that the common cessation of growth before the formation of a haustorial mother cell in non-hosts may result from the absence of the septum delimiting the haustorial mother cell rather than any reduction in the linear growth of the mycelium. Furthermore, many studies have indicated that fungal growth in non-host plants is characterized by the common absence of haustoria (Heath, 1977). Three mechanisms have been suggested to be responsible for the prevention of haustorium formation; the presence of osmiophilic material deposited on and within the adjacent non-host cell wall; loss of contact between the haustorial mother cell and the non-host wall; and fungal death occurring before the haustorium could be initiated

(Heath, 1977). It has also been suggested that the molecules on the outer layer of haustorial mother cells may play a role in rust fungus-host cell contact and in the process of recognition or nonrecognition between host cells and fungal infection hyphae (Ferreira and Rijkenberg, 1991).

On the other hand, in both oat and barley, the secondary hyphae are well developed, many with an HMC. It was also observed that there is sporulation by *P. recondita* f.sp. *tritici* on the barley cultivar Clipper after seven to ten days post-inoculation, but not on oat cultivar Heros, indicating that this cultivar Heros is resistant. In a light microscopy study of the development of *P. recondita* f.sp. *tritici* on susceptible and resistant barley cultivars (Jacobs, 1989b), the barley genotype L94, which is highly susceptible to barley leaf rust, developed sporulating wheat leaf rust colonies. Sporulation of rust pathogens on non-host cereals has also been reported in other interactions (Helfer, 1987; Niks and Dekens, 1987). In an extensive study, Niks (1983a, b) demonstrated that *P. recondita* f.sp. *tritici* and *Puccinia hordei* infection of barley and wheat cultivars were arrested early, immediately after the formation of the first haustorial mother cell. Jacobs (1989b) also showed that most of the wheat leaf rust infection structures in barley aborted although some developed few small haustoria. Such growth inhibition was associated with the presence of the cell wall appositions. Jacobs (1989) postulated that barley shows a non-host reaction in which most of the non-pathogen infection structures are prevented from entering the cell by cell wall appositions, a minority of infection structures being arrested after a haustorium had formed.

Heath (1974; 1977; 1982) suggested that defence reaction to rust fungi in non-host tissue usually commences before the first haustorium is formed. Our observation for sorghum and maize is in accordance with this view, thus suggesting that maize and sorghum are typical non-hosts of *P.recondita* f.sp.

tritici. However, from the description for oat and barley presented in this report, it may be deduced that they appear to express an intermediate form of compatibility/incompatibility to *P. recondita* f.sp. *tritici*. *P. recondita* f.sp. *tritici* has been noted to attack *Hordeum* spp. (Anikster and Wahl, 1979; Niks, 1983a, b; Swertz, 1994), and accordingly, whether barley is to be considered a host or non-host remains questionable. The present investigation has demonstrated that each non-host interaction may have its own unique properties.

LITERATURE CITED

Andres, M.W. and Wilcoxson, R.D. (1984). A device for uniform deposition of liquid-suspended urediospores on seedling and adult cereal plants. *Phytopathology* **74**, 550-552.

Anikster, Y. and Wahl, I. (1979). Coevolution of the rust fungi on Gramineae and Liliaceae and their hosts. *Annual Review of Phytopathology* **17**, 367-403.

Coutinho, T.A., Rijkenberg, F.H.J. and Van Asch, M.A.J. (1992). The preinvasion behaviour of *Hemileia vastatrix* on host and nonhost leaf surfaces. *Journal of Phytopathology* **135**, 274-280.

Coutinho, T.A., Rijkenberg, F.H.J. and Van Asch, M.A.J. (1993). Development of infection structures by *Hemileia vastatrix* in resistant and susceptible selections of *Coffea* and in *Phaseolus vulgaris*. *Canadian Journal of Botany* **71**, 1001-1008.

Dickinson, S. (1970). Studies in the physiology of obligate parasitism. VII. The effect of a curved thigmotropic stimulus. *Phytopathologische Zeitschrift*

69, 115-124.

Elmhirst, J.F. and Heath, M.C. (1989). Interactions of the bean rust and cowpea rust fungi with species of the *Phaseolus-Vigna* plant complex. II. Histological responses to infection in heat-treated and untreated leaves. *Canadian Journal of Botany* **67,** 58-72.

Fernandez, M.R. and Heath, M.C. (1985). Cytological responses induced by five phytopathogenic fungi in a non-host plant, *Phaseolus vulgaris. Canadian Journal of Botany* **64,** 648-657.

Ferreira, J. and Rijkenberg, F.H.J. (1989). Development of infection structures of *Uromyces transversalis* in leaves of the host and a nonhost. *Canadian Journal of Botany* **67,** 429-433.

Ferreira, J. and Rijkenberg, F.H.J. (1991). Ultrastructural morphology of *Uromyces transversalis* infection of resistant and susceptible gladiolus hosts and a nonhost, *Zea mays. Phytopathology* **81,** 596-602.

Heath, M.C. (1972). Ultrastructure of host and non-host reactions to cowpea rust. *Phytopathology* **62,** 27-38.

Heath, M.C. (1974). Light and electron microscope studies of the interactions of host and non-host plants with cowpea rust-*Uromyces phaseoli* var. *vignae. Physiological Plant Pathology* **4,** 403-414.

Heath, M.C. (1977). A comparative study of non-host interactions with rust fungi. *Physiological Plant Pathology* **10,** 73-88.

Heath, M.C. (1981). Non-host resistance. In: *Plant disease control: Resistance and susceptibility* (Eds. R.C. Staples and G.H. Toennieseen), pp. 201-217.

John Wiley, New York.

Heath, M.C. (1982). Host defense mechanisms against infection by rust fungi. In: *The Rust Fungi.* (Eds. K.J. Scott and A.K. Chakravorty), pp. 223-235. Academic Press, Orlando.

Heath, M.C. (1983). Relationship between developmental stage of the bean rust fungus and increased susceptibility of surrounding bean tissue to the cowpea rust fungus. *Physiological Plant Pathology* **22,** 45-50.

Heath, M.C. (1985). Implications of nonhost resistance for understanding host-parasite interactions. In: *Genetic Basis of Biochemical Mechanisms of Plant Disease*. (Eds. J.V. Groth and W.R. Bushnell), pp. 25-42. APS, St. Paul, MN.

Heath, M.C. and Stumpf, M.A. (1986). Ultrastructural observations of penetration sites of the cowpea rust fungus in untreated and silicon-depleted French bean cells. *Physiological and Molecular Plant Pathology* **29,** 27-39.

Helfer, S. (1987). Development of cereal rusts on host and non-host plants. *Cereal Rusts Bulletin* **15,** 44-52.

Hu, G.G. and Rijkenberg, F.H.J. (1996). Scanning electron microscopy studies of early infection structure formation of *Puccinia recondita* on and in susceptible and resistant wheat lines (Abstract). *Proceedings of the 9th European and Mediterranean Cereal Rusts & Powdery Mildews Conference, 2-6 September, 1996, Lunteren, The Netherlands* p225.

Hughes, F.L. and Rijkenberg, F.H.J. (1985). Scanning electron microscopy of early infection in the uredial stage of *Puccinia sorghi* in *Zea mays. Plant Pathology* **34,** 61-68.

Jacobs, Th. (1989a). Germination and appressorium formation of wheat leaf rust on susceptible, partially resistant and resistant wheat seedlings and on seedlings of other Gramineae. *Netherlands Journal of Plant Pathology* **95,** 65-71.

Jacobs, Th. (1989b). Haustorium formation and cell wall appositions in susceptible and partially resistant wheat and barley seedlings infected with wheat leaf rust. *Journal of Phytopathology* **127,** 250-261.

Leath, K.T. and Rowell, J.B. (1966). Histological study of the resistance of *Zea mays* to *Puccinia graminis. Phytopathology* **56,** 1305-1309.

Leath, K.T. and Rowell, J.B. (1969). Thickening of corn mesophyll cell walls in response of *Zea mays* to *Puccinia graminis. Phytopathology* **59,** 1654-1656.

Leath, K.T. and Rowell, J.B. (1970). Nutritional and inhibitory factors in the resistance of *Zea mays* to *Puccinia graminis*. *Phytopathology* **60,** 1097-1100.

Lennox, C.L. and Rijkenberg, F.H.J. (1989). Scanning electron microscopy study of infection structure formation of *Puccinia graminis* f.sp. *tritici* in host and non-host cereal species. *Plant Pathology* **38,** 547-556.

Mendgen, K. (1978). Attachment of bean rust cell wall material to host and non-host plant tissue. *Archives of Microbiology* **199,** 113-117.

Niks, R.E. (1981). Appressorium formation of *Puccinia hordei* on partially resistant barley and two non-host species. *Netherlands Journal of Plant Pathology* **87,** 201-207.

Niks, R.E. (1982). Early abortion of colonies of leaf rust, *Puccinia hordei*, in

partially resistant barley seedlings. *Canadian Journal of Botany* **60,** 714-723.

Niks, R.E. (1983a). Comparative history of partially resistance and the nonhost reaction to leaf rust pathogens in barley and wheat seedlings. *Phytopathology* **73,** 60-64.

Niks, R.E. (1983b). Haustorium formation by *Puccinia hordei* in leaves of hypersensitive, partially resistant, and nonhost plant genotypes. *Phytopathology* **73,** 64-66.

Niks, R.E. (1987). Nonhost plant species as donors for resistance to pathogens with narrow host range. I. Determination of nonhost status. *Euphytica* **36,** 841-852.

Niks, R.E. and Dekens, R.G. (1987). Histological studies on the infection of triticale, wheat and rye by *Puccinia recondita* f.sp. *tritici* and *P. recondita* f.sp. *recondita*. *Euphytica* **36,** 275-285.

Niks, R.E. and Dekens, R.G. (1991). Prehaustorial and posthaustorial resistance to wheat leaf rust in diploid wheat seedlings. *Phytopathology* **81,** 847-851.

Onoe, T., Tani, T., Minagawa, S. and Sagawa, H. (1987). Ultrastructural changes of stomata in relation to specificity to rust fungi. In: *Molecular determinants of plant diseases.* (Eds. S. Nishimura, C.P. Vance and N. Doke. Japan Scientific Societies Press, Tokyo, and Springer-Verlag, Berlin.

Rubiales, D. and Niks, R.E. (1992). Low appressorium formation by rust fungi on *Hordeum chilense* lines. *Phytopathology* **82,** 1007-1012.

Sellam, M.A. and Wilcoxson, R.D. (1976). Development of *Puccinia graminis*

f.sp. *tritici* on resistant and susceptible barley cultivars. *Phytopathology* **66,** 667-668.

Stumpf, M.A. and Heath, M.C. (1985). Cytological studies of the interactions between the cowpea rust fungus and silicon-depleted French bean plants. *Physiological Plant Pathology* **27,** 369-385.

Swertz, C.A. (1994). Morphology of germlings of urediniospores and its value for the identification and classification of grass rust fungi. *Studies in Mycology* **36,** 1-152.

Torabi, M. and Manners, J.G. (1989). Appressorium formation of *Puccinia recondita* on susceptible and resistant wheat cultivars. *Mycological Research* **92,** 440-444.

Wood, L.A. and Heath, M.C. (1986). Light and electron microscopy of the interaction between the sunflower rust fungus (*Puccinia helianthi*) and leaves of the non-host plant, French bean (*Phaseolus vulgaris*). *Canadian Journal of Botany* **64,** 2476-2486.

Wynn, W.K. (1976). Appressorium formation over stomata by the bean rust fungus: response to a surface contact stimulus. *Phytopathology* **66,** 136-146.

CHAPTER 3

ULTRASTRUCTURAL STUDIES OF THE INTERCELLULAR HYPHA AND HAUSTORIUM OF *PUCCINIA RECONDITA* F.SP. *TRITICII*

INTRODUCTION

The development and structure of the uredial stage of many rust fungi in hosts have been extensively investigated at the cellular and subcellular levels using light and electron microscopy. Al-Khesraji and Lösel (1981) described the fine structure of *Puccinia poarum* Nielsen in *Poa pratensis* L., Heath and Bonde (1983) recorded the ultrastructure of *Physopella zeae* (Mains) Cumm. & Ram. in *Zea mays* L.. Chong *et al.* (1985) gave a detailed description of intercellular hyphae of *Puccinia graminis* f.sp. *tritici* Eriks. & Henn. in wheat (*Triticum aestivum* L.). Mims *et al.* (1989) investigated the fine structure of *Puccinia arachidis* Speg. within its groundnut host, *Arachis hypogaea* L.. Reviews by Littlefield and Heath (1979) and Harder and Chong (1984) have appeared. More recently, Kang *et al.* (1993a, b) described the intercellular hyphal anastomosis and the haustorial mother cell invasion of its own intercellular hyphae in *Puccinia striiformis* West., which have not been reported to occur in other uredial stages of the rust fungi, indicating that there may be considerable variation between the rust fungi.

The haustorium, a specialized structure formed by biotrophic fungal

pathogens, such as powdery mildew and rust fungi, in the living cells of host plants, has been well documented and described, since the first description of the *Hemileia vastatrix* Berk. & Br. haustorium (Ward, 1882). By means of haustoria, rust fungi associate closely with their host plants. The possible roles of haustoria in establishing nutrient absorption and transportation have long been proposed and discussed. Although the structure of uredial stage haustoria and their relationship with the hosts have been well characterized in many rust fungi, little is known about the haustorial development of *Puccinia recondita* Rob. ex Desm. f.sp. *tritici* Eriks. and Henn, (syn. *Puccinia triticina*), the pathogen of wheat leaf rust which is one of the most serious diseases worldwide, and its relationship with the wheat host. This interaction was the subject of the present study, since it was thought that further elucidation of haustorial development and the relationship of the haustorium with the host plant, could provide more insights into understanding the rust-plant interaction.

Uredial stage haustoria, often termed as D-haustoria, have generally been described from host mesophyll and epidermal cells. However, in an extensive investigation by Andreev *et al.* (1982), the D-haustoria of *Puccinia graminis* f.sp. *tritici* were found to occur in xylem and phloem cells of leaves and in stem cells of older plants of susceptible cultivars, even though this occurred at low frequencies. Thus, it appears that the occurrence of D-haustoria is not always restricted to leaf mesophyll and epidermal cells.

A wide range of cytochemical and immunocytochemical procedures has been effectively used to analyze the structure and composition of fungi (Harder, 1989; Harder and Chong, 1991). To permit further cytochemical and immunocytochemical analysis of the interaction between *P. recondita* f.sp. *tritici* and the wheat host, the current study was conducted to describe the

fine structure of intercellular hyphae and haustoria of *P. recondita* f.sp. *tritici*, and the wheat host reaction to the haustorial invasion.

MATERIALS AND METHODS

Plant materials and inoculation

The wheat line Thatcher, susceptible to *P. recondita* f.sp. *tritici*, was used in this study. Freshly harvested urediospores of *P. recondita* f.sp. *tritici* (the South African pathotype UVPrt 8, obtained through the courtesy of Professor Z.A. Pretorius, Department of Plant Pathology, University of the Orange Free State, South Africa), were used to inoculate the adaxial surface of the first leaf of 10-day-old plants at an inoculum dose of 40 mg urediospores per ml of Soltrol 130 (Phillips Chemical Co.) using a modified Andres and Wilcoxson (1984) inoculator. Inoculated plants were allowed to dry for about 1 hour before placement in a dark dew chamber at 20°C for 20 hours. The inoculated leaves were sampled 4, 5, 6 days after inoculation.

Specimen preparation

The harvested leaves were cut into 3×3 mm^2 pieces which were fixed in 3% glutaraldehyde in a 0.05 M sodium cacodylate buffer (pH 7.2) overnight, washed twice in that buffer, and post-fixed for 2 hours in 2% osmium tetroxide in the buffer at room temperature. Samples were dehydrated in a graded ethanol series and embedded in Spurr's resin (Spurr, 1969). Ultrathin sections were prepared using a glass or diamond knife and stained with 2% uranyl acetate for 15 minutes, washed in double-distilled water and post-

stained in lead citrate for 15 minutes, washed in double-distilled water and viewed with a Jeol 100 CX transmission electron microscope at 80 kV.

RESULTS

Intercellular Hyphae

In the uredial stage, intercellular hyphae of *P. recondita* f.sp. *tritici* develop in the intercellular space between the mesophyll cells. The wall of the intercellular hypha consists of four layers (Fig. 1). Organelles in the intercellular hyphae include nuclei, mitochondria, endoplasmic reticulum, lipid bodies and vacuoles. There are generally two, occasionally three, nuclei in each hyphal cell.

The typical pulley-wheel septal pore in the Uredinales, which has been described by Littlefield and Heath (1979), is present (Fig. 2). The septal pore apparatus has diaphragms covering the pore, which is surrounded by several microbodies associated with the endoplasmic reticulum. Some variant septal pores were also observed. Fig. 3 shows a septal pore lacking a typical pore apparatus: an electron-opaque substance is seen plugging the pore and several microbodies which are associated with the endoplasmic reticulum, surround the pore on both sides.

Another type of septum in the intercellular hypha is the "partial septum" or "infolded septum" (Müller *et al.*, 1974) (Fig. 4). Fig 4 shows a mature partial septum (in serial section) in a hypha. The pore has a large diameter and several organelles, eg. mitochondria, are seen apparently in the process of

passing. Through it, abundant mitochondria, microbodies and endoplasmic reticulum aggregate in the area around the septum. The septum at the pore (Fig. 4) appears to be closely associated with a membranous structure.

Occasionally, intercellular hyphal anastomosis was observed (Fig. 5), fusion occurring between two hyphae when they lie contiguously in the intercellular space.

Haustorial Mother Cells (HMCs) and Haustoria

Similarly to those in other rust fungi, the mature haustorium of *P. recondita* f.sp. *tritici* consists of a generally round highly specialized body, connected to a well-defined haustorial mother cell (HMC) by a tubular neck with a neck band (Fig. 6).

An HMC is formed and differentiated when an infection hypha of *P. recondita* f.sp. *tritici* contacts a host cell (epidermal or mesophyll cell). Fungal nuclei move into the tip of the hypha, a septum then cutting off the terminal HMC from the remaining of the hypha (Figs. 7, 8). Of 130 HMCs examined in this observation, about 90% are binucleate (Fig. 7). Occassionally, three nuclei (Fig. 8) were observed in the HMC.

The cytoplasm in nascent HMCs is dense and the organelles in HMCs are similar to those in intercellular hyphal cells, including nuclei, mitochondria, endoplasmic reticulum, lipid bodies, small vacuoles (Figs. 7, 8) and occasionally, lomasomes. Mitochondria were frequently observed to lie in a pattern around the periphery of HMC cells, near the hyphal plasmalemma, especially near the site of the penetration tube (Fig. 7), while in other instances, they are distributed randomly in the HMC cytoplasm (Fig. 8). The

peripheral type of orientation of mitochondria was not observed in the cytoplasm of intercellular hyphae. Membranous structures and small vesicles, which seem to associate with the HMC nucleus, were often observed in the cytoplasm of HMCs (Fig. 9)

The HMC wall is thicker than that of the intercellular hypha. Six layers could be distinguished in the cell wall of the HMC (Fig. 10). On the hyphal side of the HMC septum, mitochondria appear to aggregate near the septum (Fig. 11). As the HMC differentiates, numerous membranous structures, termed protrusions (Chong and Harder, 1982; Fig. 11), appear and develop on the hyphal side of, and against, the HMC septum, in association with the mitochondrion aggregation. When fully developed, some protrusions extend 3-5 μm into the cytoplasm of the hypha. The protrusions are composed of a substance more electron-opaque than the material comprising the septal wall.

In some sections, a septal pore is occasionally observed in the HMC septum in some sections (Fig. 12). Fig. 12 shows a HMC septal pore with a Woronin body in the cytoplasm on the HMC side, while there are several mitochondria around the pore on the hyphal side. No septal pore apparatus is visible in the HMC septal pore is observed. A Woronin body is plugging the pore.

The HMC is appressed to the host cell wall (Figs. 6, 13). At the interface between the HMC and host cells, an extracellular substance was frequently observed (Fig. 13), although the substance is not clearly evident on other occasions (Fig. 6). The inner wall of the HMC is thickened significantly in a localized manner around the penetration site, the swollen inner layer of this swollen wall being electron-opaque (Figs. 6, 10, 13).

At the penetration site, the haustorium and its penetration tube invaginate the

host plasmalemma. Cytoplasm and two nuclei move into the haustorial body. After much of the HMC cytoplasm has moved into the haustorium, the electron-dense wall protrusions become short, and finally only a trace is left (Fig. 14). The HMC becomes highly vacuolated. Although haustoria are often spherical or oval in shape, elongated haustoria were also observed (Fig. 15).

There is an extrahaustorial membrane that surrounds the haustorial complex. The width of the extrahaustorial matrix, which is between the extrahaustorial membrane and the haustorial wall, varies with the haustorial age and the host cells.

Haustoria were observed mainly in mesophyll cells, but also in epidermal cells (Fig. 13), guard cells (Fig. 16), and bundle sheath cells (Fig. 17). There is no difference in the appearance of haustoria between these cells. The vascular tissue remains free from infection by *P. recondita* f.sp. *tritici*.

One or two nuclei are generally present in each haustorial body (Fig. 18). Serial sectioning of approximately 25 sites revealed that two nucleoli appear to present in one nucleus in the haustorium (Fig. 19). When two nucleoli were observed in one nucleus, only one nucleus was found in the haustorium.

As is the case in other rusts, especially in the case of young haustorium, the mitochondria in haustoria are usually orientated peripherally (Chong *et al.*, 1981) (Figs. 13, 16, 18, 19).

PLATE 1

Fig. 1. Septum delimiting haustorial mother cell (HMC) from the intercellular hypha (IH). Four wall layers (L_1-L_4) in intercellular hypha are discernable. (Bar = 0.3 μm)

Fig. 2. Hyphal septum and typical pulley wheel-type septal pore apparatus (PA) in *Puccinia recondita* f.sp. *tritici*. Diaphragms cover the pore, and microbodies (MB) occur in the surrounding cytoplasm. The presence of vacuoles (V) on both sides of the septum, indicates that the hypha is senescing. (Bar = 0.2 μm)

Fig. 3. Plugged septal pore in hypha. The typical septal pore apparatus is absent. Microbodies (MB) have aggregated in the surrounding hyphal cytoplasm. Note endoplasm reticulum (ER) membrane associated with some microbodies. (Bar = 0.5 μm)

Fig. 4. Partial septum in hypha. Septal pore is large in size, one side of septum is continuous with all layers of the wall. A number of mitochondria (M) and endoplasmic reticulum (ER) accumulate in the cytoplasm near the septum. Some mitochondria (M) and a lomasome (L) are in the pore area. Note membrane vesicle (Ve) projecting into the pore from the septum. (Bar = 0.5 μm)

Fig. 5. Anastomosis (arrow) of *Puccinia recondita* f.sp. *tritici* between two adjoining intercellular hyphae. Note the vacuole (V) extending from one hypha into the other. (Bar = 0.2 μm)

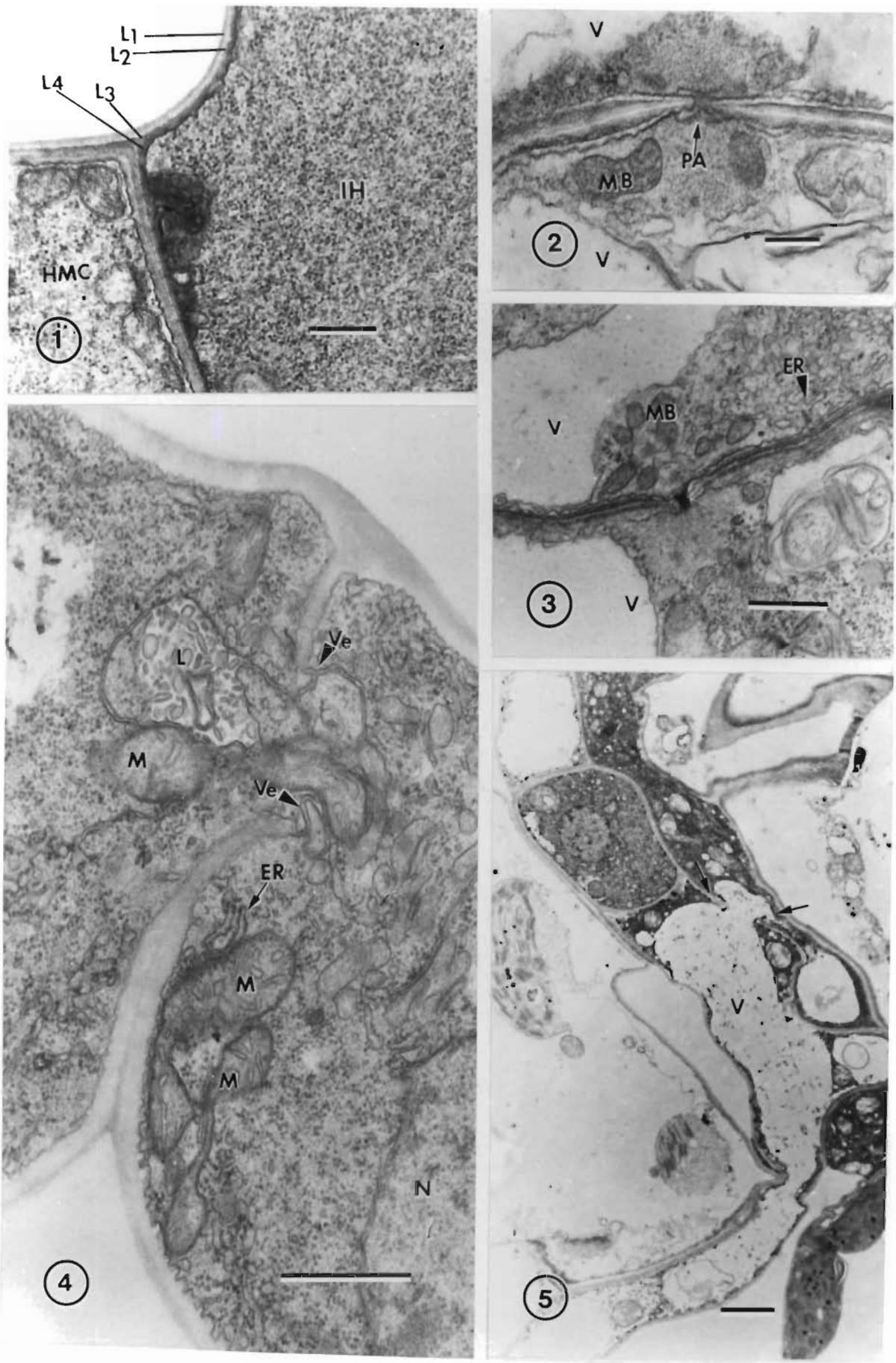
L1
L2
L4
L3
IH
HMC
1
V
PA
MB
2
V
V
ER
MB
V
3
V
L
Ve
M
Ve
ER
M
M
N
4
V
5

PLATE 2

Fig. 6. A mature haustorium, consisting of a tubular haustorial neck (HN) with a darkly stained neck band (Nb), and a near-spherical haustorial body (HB), attached to a highly vacuolated haustorium mother cell (HMC). CH: Chloroplast. (Bar = 1 μm)

Fig. 7. An HMC, with two nuclei (N), attached to an epidermal cell (Ec). Note the mitochondria (M) are distributed at the periphery of the HMC. Mc: Mesophyll cell. (Bar = 2 μm)

Fig. 8. An HMC, with three nuclei (N) in the plane of section, attached to a mesophyll cell (Mc). (Bar = 2 μm)

Fig. 9. Membrane structures and a vesicle complex (arrows), associated with the HMC nucleus (N). IH: Intercellular hypha. (Bar = 0.3 μm)

Fig. 10. Multilayered HMC wall near the penetration site. Six layers (labelled L_1, L_2, L_3, L_4, L_5 and L_6) of HMC wall may be distinguished. (Bar = 0.3 μm)

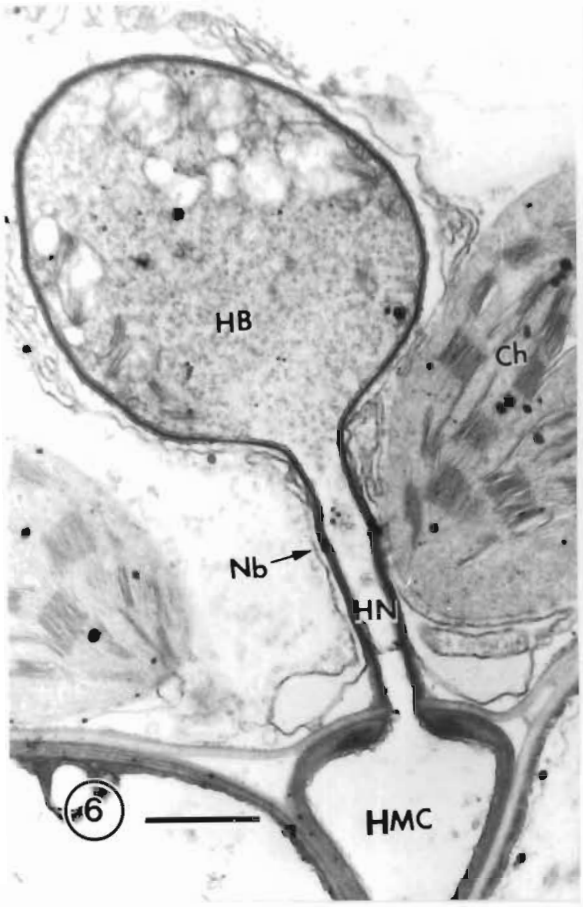
HB
Ch
Nb
HN
HMC
6

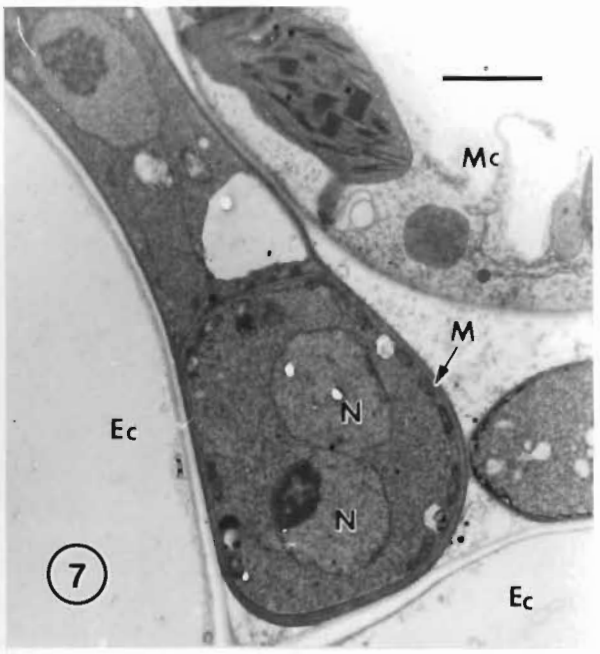
Mc
M
N
N
Ec
Ec
7


N
N
N
Mc
8

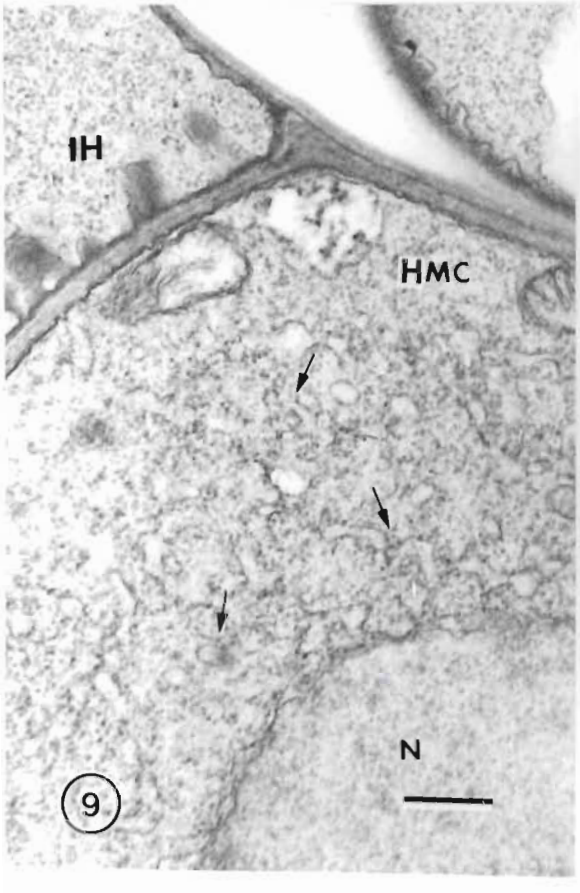
IH
HMC
N
9

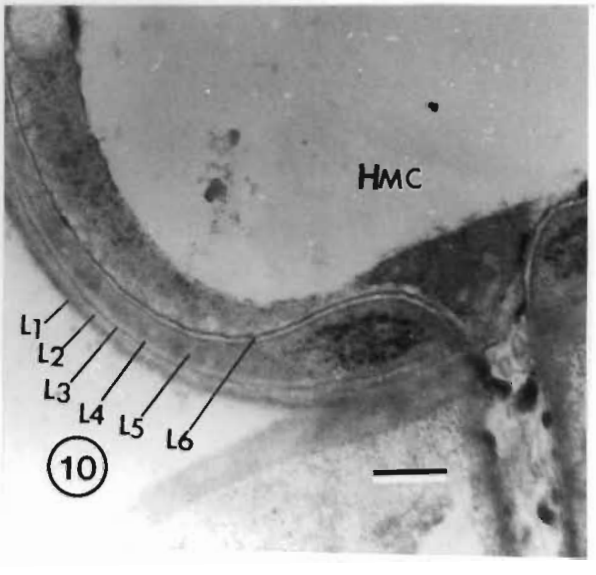
HMC
L1
L2
L3
L4
L5
L6
10

PLATE 3

Fig. 11. Tubular membrane protrusions (P) on the hyphal side of HMC septum at an early stage of HMC differentiation. Note the mitochondria in close association with the protrusions. A lomasome (L) is present in the HMC cytoplasm. (Bar = 0.5 μm)

Fig. 12. A septal pore between the HMC and its subtending hyphal cell. A number of microbodies in the cytoplasm surround the septal pore. A Woronin body (arrowhead) is evident near the septal pore. Note the lack of a septal pore apparatus and the plugging of the pore by a microbody. IH: Intercellular hypha. (Bar = 0.5 μm)

Fig. 13. HMC is appressed to an epidermal cell. Note an electron-opaque extracellular matrix (arrow) between the HMC and host cell wall. (Bar = 1 μm)

Fig. 14. A vacuolate HMC. Protrusions (P) on the hyphal side of HMC septum have become round with age. (Bar = 0.5 μm)

Fig. 15. Haustorial body (HB) in mesophyll cell with a more unusual elongate/oblate shape. (Bar = 2 μm)

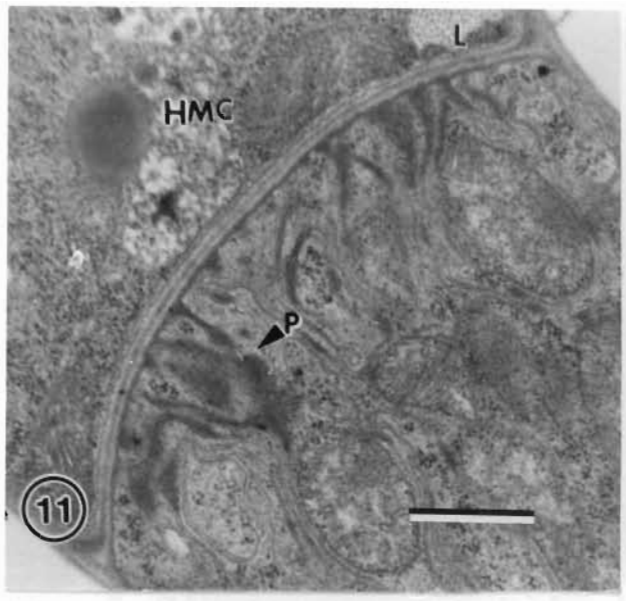
L
HMC
P
11

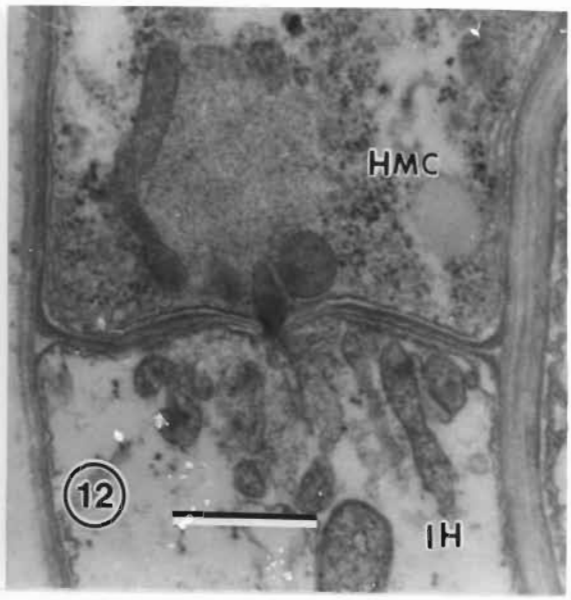
HMC
12
IH

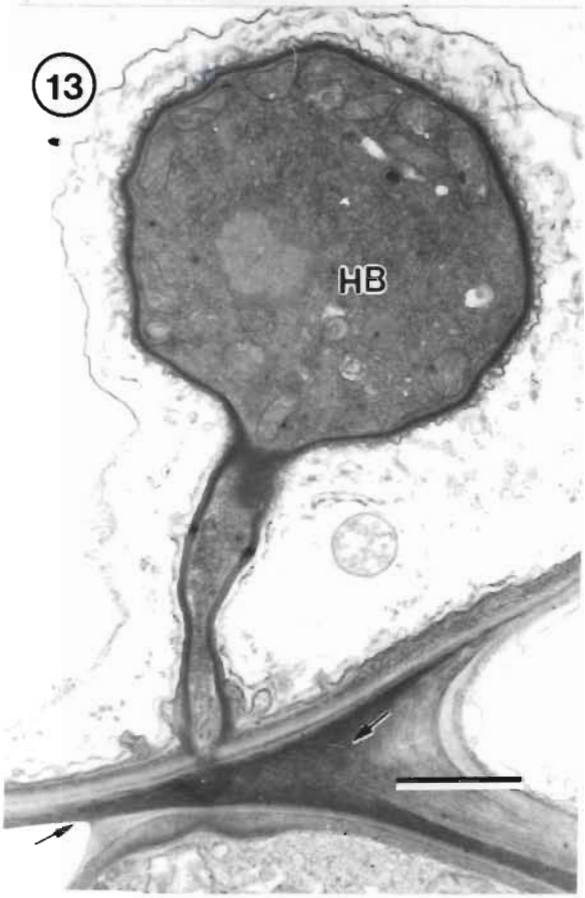
13
HB

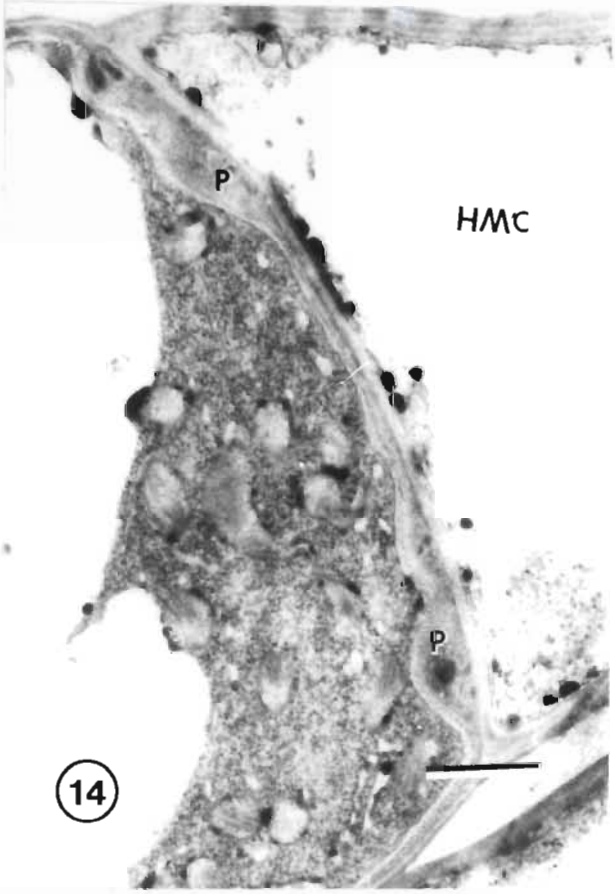
P
HMC
P
14

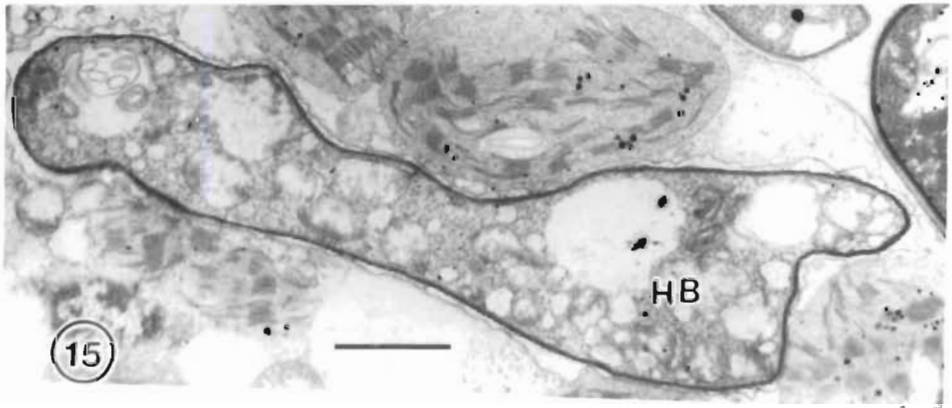
HB
15

Host Reaction to the Haustorial Invasion

The invasion of the host cell by the haustorium seems to initiate several host responses, viz. the attraction of, and association between, the host organelles and the haustorium, host cell wall apposition, and collar formation.

The host endoplasmic reticulum was often seen in association with the haustorial neck (Fig. 20) and the haustorial body (Figs. 13, 21). Some smooth (ribosome-free) endoplasmic reticulum occasionally appears to be attached to the extrahaustorial membrane (Fig. 21). The cisternae of endoplasmic reticulum in the host cytoplasm near the haustorium usually appear to be rough (Figs. 20, 25), however, smooth endoplasmic reticulum was also observed (Fig. 21). In many instances, the host cytoplasm surrounding the haustorium contains some membrane-bound vesicles, with electron-transparent contents, which appear to originate from the host endoplasmic reticulum (Fig. 22).

There are also a large number of tubular complexes found in close proximity to the haustorium (Fig. 23). Occasionally, a close association of the host tubule with the extrahaustorial membrane was found (Fig. 24). These tubular structures, appear to be closely associated with, or derived from, the host endoplasmic reticulum.

Golgi bodies are frequently present in the vicinity of the haustorial neck and the haustorium (Fig. 25). Fig. 26 shows one a structure, possibly a swollen Golgi body, in the host cytoplasm near a haustorium.

A type of small smooth-membraned vesicle, several of which were aggregated and bound by a membrane, occasionally appears in the vicinity of haustorium

(Fig. 27). Vesicles of this type were easily distinguished, on a basis of their size, from Golgi-secreted vesicles shown in the same micrograph (Fig. 27).

Mitochondria in the host cytoplasm, were often observed to be closely associated with the haustorium (Figs. 28, 29). Generally, they appear to be present in larger numbers in the host cytoplasm near the haustorium (Fig. 28). In some instances, the mitochondria aggregated to almost surround the haustorium (Fig. 29).

In the present investigation, the host nuclei showed a frequent association with the haustorium. The host nucleus was frequently found appressed to one side of haustorium (Fig. 31), and in some instances, the nucleus enveloped, or deeply invaginated, by the haustorium (Fig. 30).

In a few instances, electron-dense, granular cell wall apposition between the host cell wall and the plasmalemma was observed in the mesophyll cell and/or epidermis cell contact with a haustorial mother cell (Fig. 32). The cell wall apposition usually extends beyond the direct contact area of mesophyll cell and the haustorial mother cell.

In the region where the haustorium penetrates the host cell, deposition of material against host cell wall leads to the formation of collar around the haustorial neck (Fig. 33). Material in the collar is of uniform electron-density and is bound by the host plasmalemma. The collar was usually associated with the older haustoria. At an early stage of collar development, the collar was seen to contain electron-transparent material, while mature collars were electron-opaque.

PLATE 4

Fig. 16. Haustorial body (HB) in a host guard cell. Note the haustorial mitochondria are at the periphery. (Bar = 1 μm)

Fig. 17. Haustorial body in a bundle sheath cell. Xylem and phloem cells are free from haustoria. (Bar = 5 μm)

Fig. 18. Two nuclei (N) are frequently found in the haustorium. Note the mitochondria peripherally positioned in the haustorium. (Bar = 1 μm)

Fig. 19. Serial sectioning confirms that one nucleus (N) with two nucleoli (arrows) frequently occurs in the haustorium. (Bar = 2 μm)

Fig. 20. Rough endoplasmic reticulum (ER) in association with the haustorial neck. (Bar = 0.5 μm)

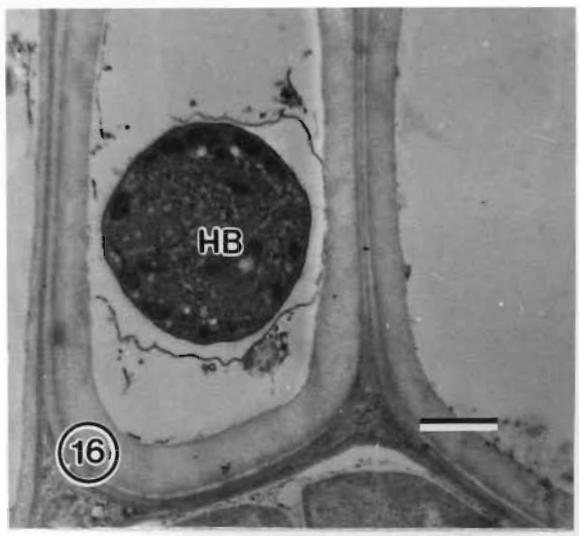
HB
16


17

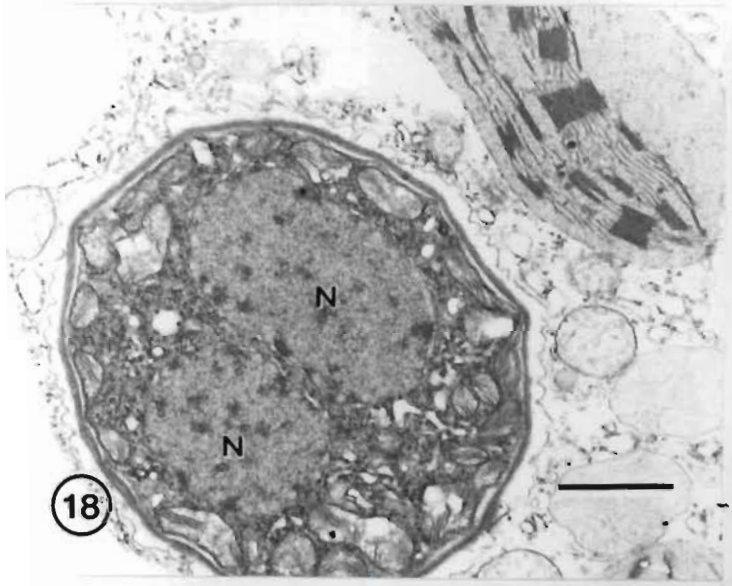
N
N
18

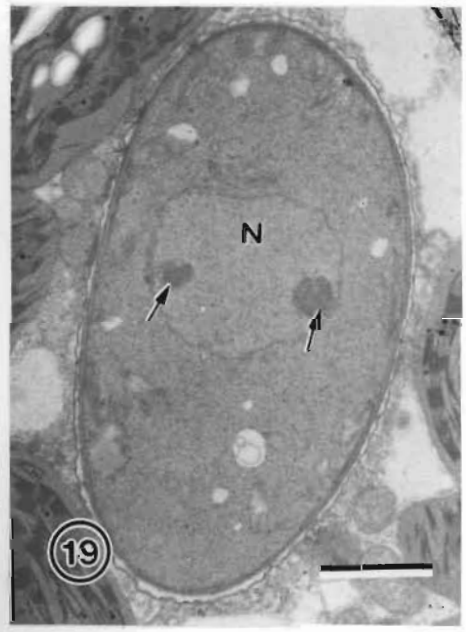
N
19

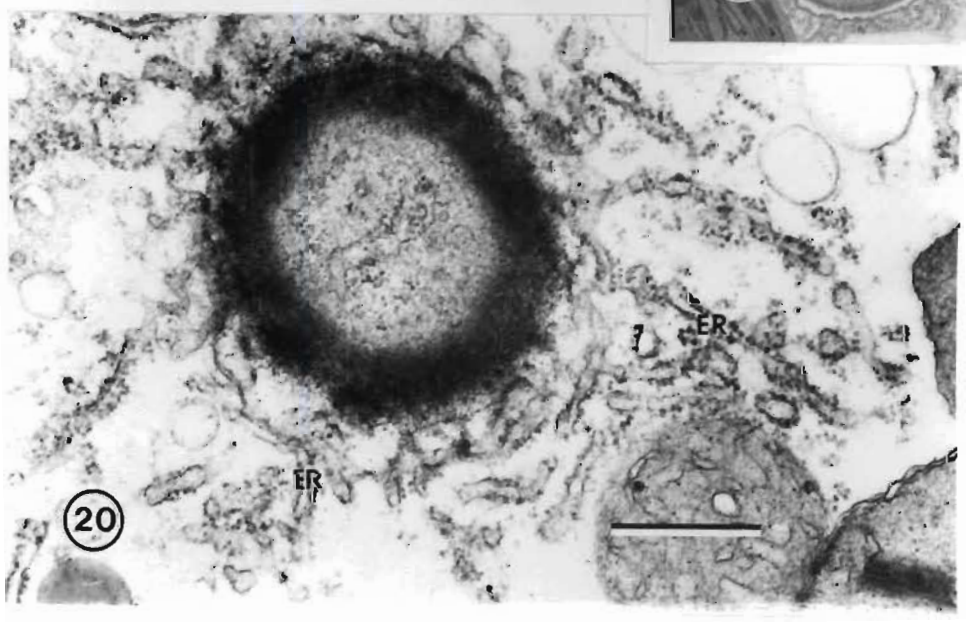
ER
ER
20

PLATE 5

Fig. 21. Endoplasmic reticulum (ER), mostly smooth, associated with two haustorial bodies (HB). Note that some smooth ER appears to be attached to the extrahaustorial membrane (EM). (Bar = 0.5 μm)

Fig. 22. Membrane-bound, large vesicles, possibly having originated from the endoplasmic reticulum, in the vicinity of the haustorial body (HB). (Bar = 1 μm)

Fig. 23. Tubular complex is present in the host cytoplasm near the haustorial body (HB). (Bar = 0.5 μm)

Fig. 24. A tubular structure is closely associated with the extrahaustorial membrane (arrow). (Bar = 0.2 μm)

Fig. 25. Golgi bodies (arrows) are frequently found in the proximity of the haustorial body. (Bar = 1 μm)

Fig. 26. A structure which may be a swollen Golgi body (arrowhead) is occasionally observed near the haustorial body. (Bar = 0.5 μm)

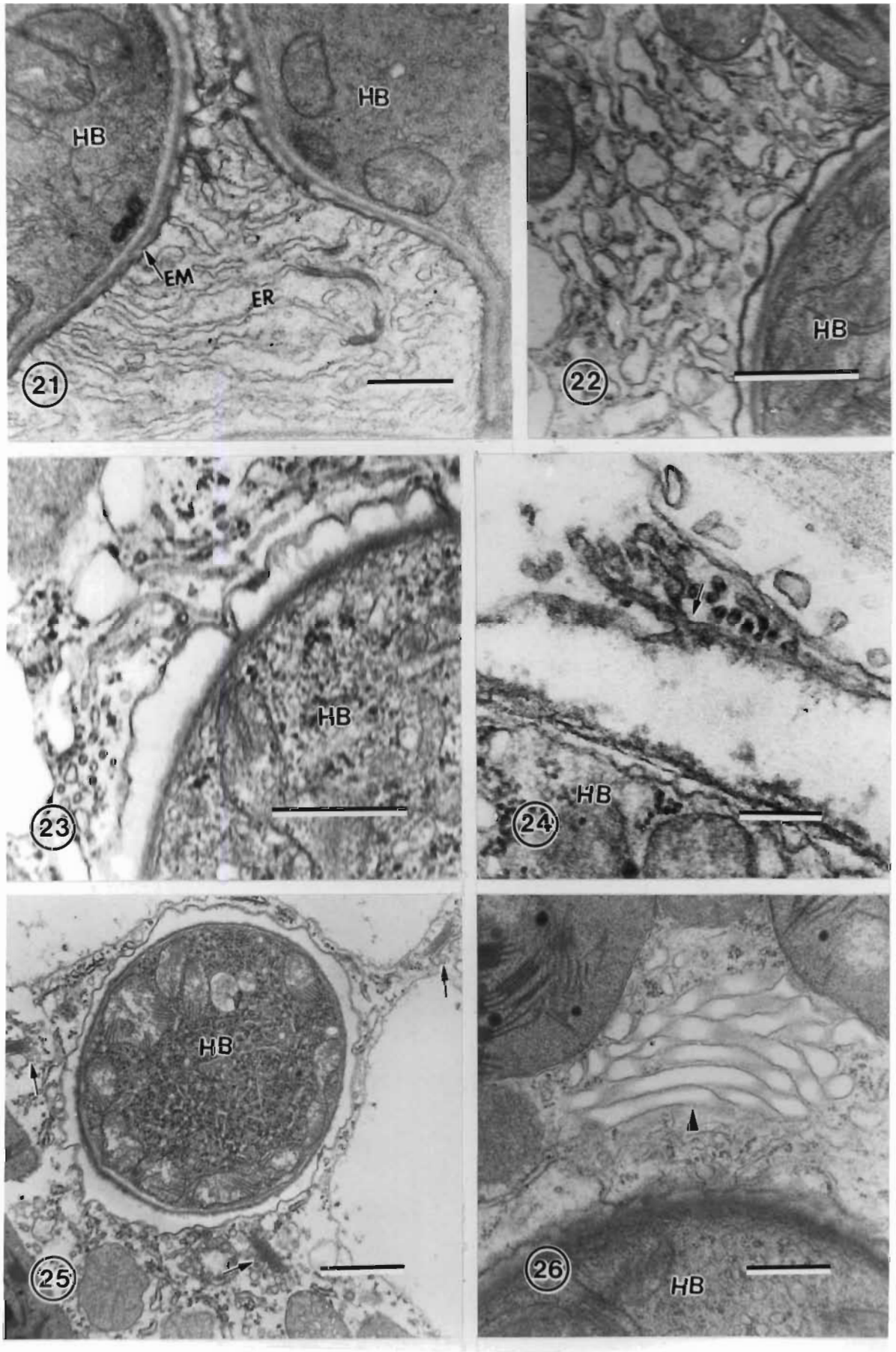
HB
HB
EM
ER
21
HB
22
HB
23
HB
24
HB
25
HB
26

PLATE 6

Fig. 27. A large number of small vesicles aggregate, bound by a membrane structure (arrow), presenting near the haustorium. (Bar = 0.2 μm)

Fig. 28. Host mitochondria are often associated with the haustorium. (Bar = 1 μm)

Fig. 29. Host mitochondria often surround the haustorial body. (Bar = 1 μm)

Fig. 30. A host nucleus (N) is invaginated by a haustorial body (HB). Note no other host organelles and cytoplasm is discernable in the invaginated region. (Bar = 1 μm)

Fig. 31. The host nucleus (N) is attracted to the haustorium and is bent by the invading haustorial lobe (HB). A mitochondrion (arrowhead) and some host cytoplasm is trapped in the region between the haustorial body and the host nucleus. (Bar = 1 μm)

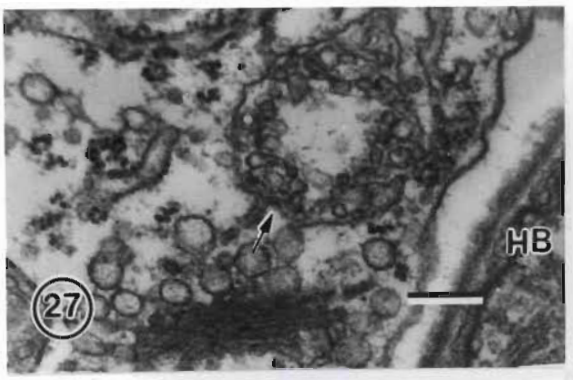
HB
27


28

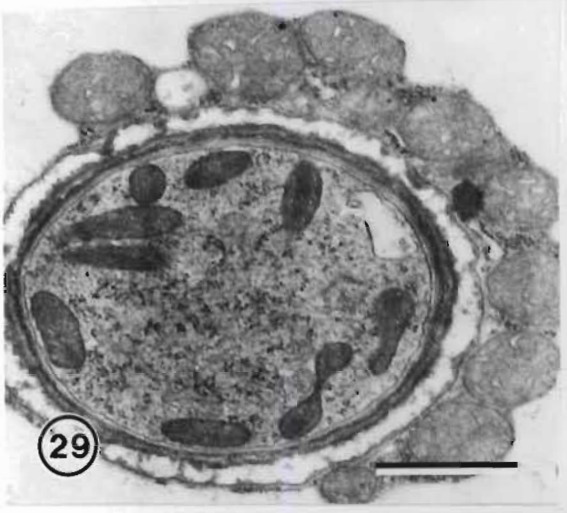
29

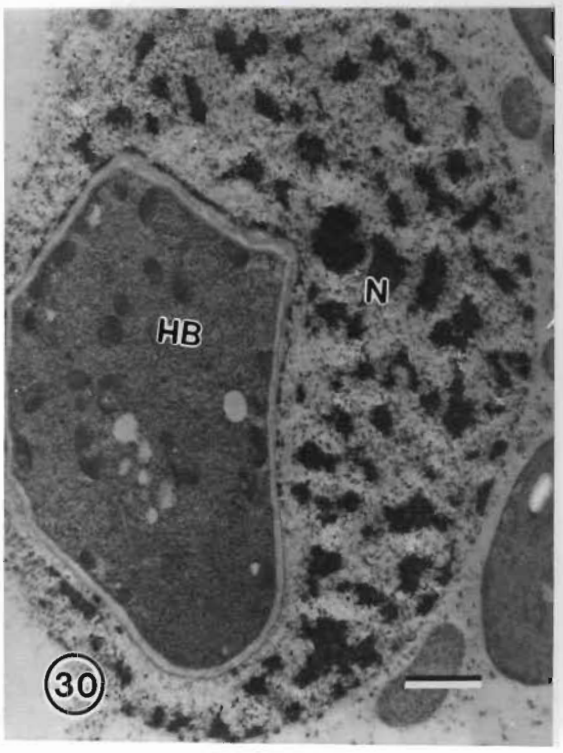
HB
N
30

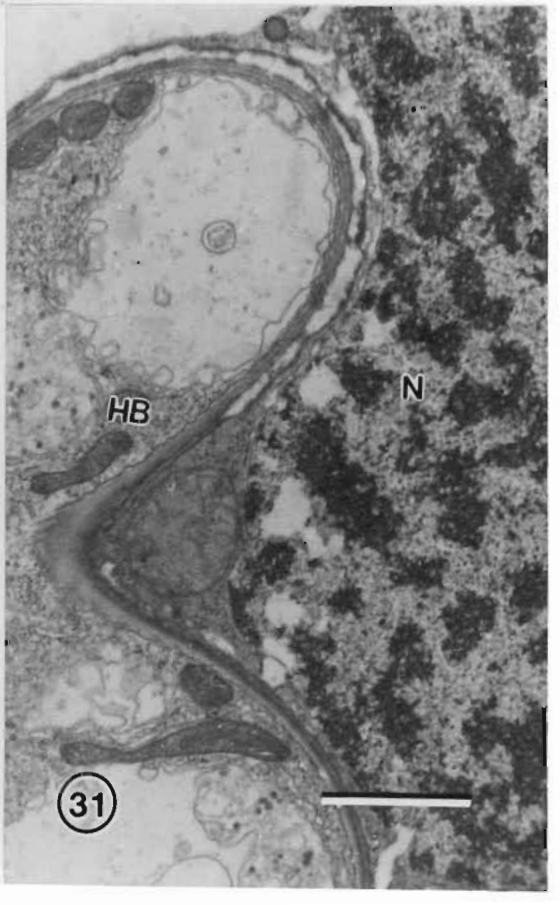
HB
N
31

PLATE 7

Fig. 32. Wall apposition (arrowhead) is occasionally found between the host cell wall and the plasmalemma at the point where the HMC is attached to the host cell. (Bar = 0.5 μm)

Fig. 33. A collar (arrow) is often observed around the haustorial neck. (Bar = 0.5 μm)

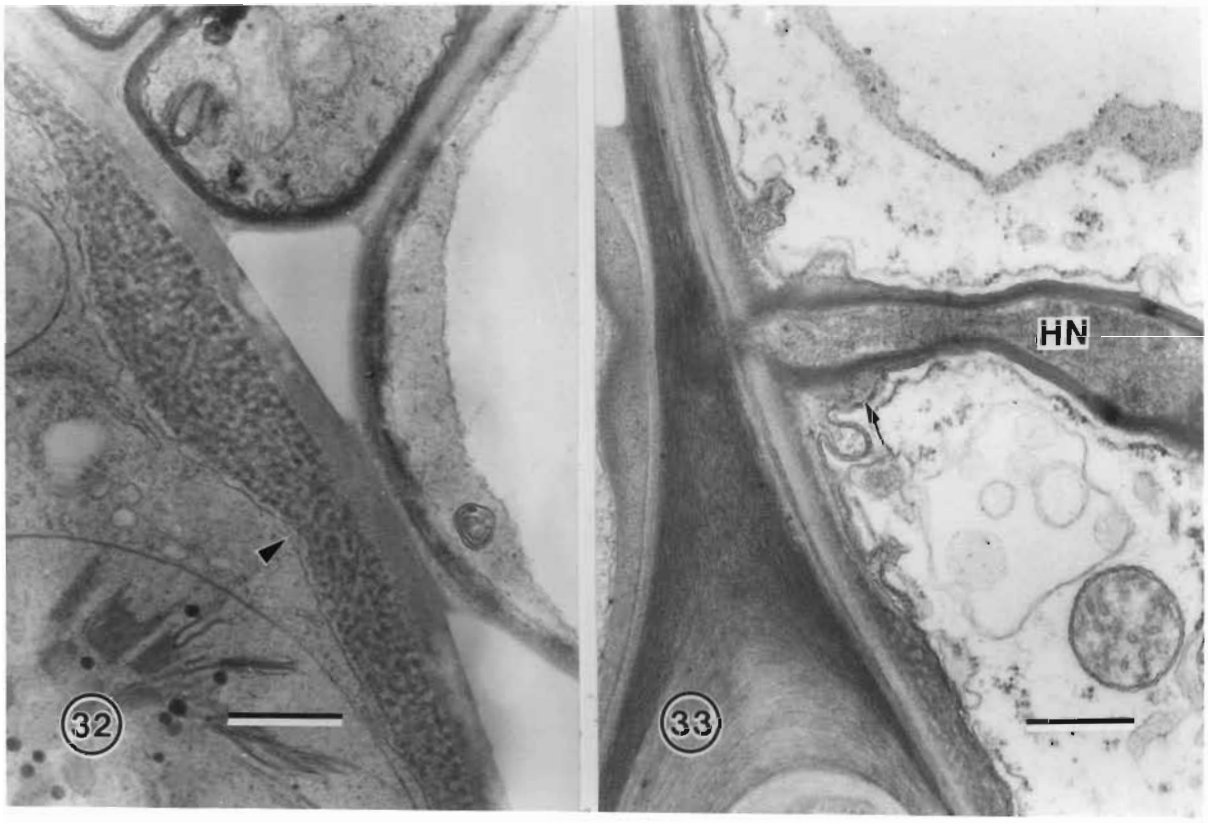
32
33
HN

DISCUSSION

The ultrastructure of intercellular hyphae and HMCs of *P. recondita* f.sp. *tritici* resembles that of most other rust fungi, eg. *Uromyces phaseoli* var. *vignae* (Pers.) Wint. (Heath and Heath, 1975), *Puccinia graminis* f.sp. *tritici* (Chong *et al.*, 1985, 1986) and *Puccinia arachidis* (Mims *et al.*, 1989). The hypha is septate and usually binucleate, although three nuclei in one hyphal cell were also occasionally observed. The pulley-wheel shape septal pore apparatus, commonly considered to be typical to the rusts, had been reported in uredial stages, eg. *Melampsora lini* (Ehrenb.) Desm. (Littlefield and Bracker, 1972), *Puccinia coronata* f.sp. *avenae* Eriks. (Harder, 1976), *Puccinia helianthi* (Coffey *et al.*, 1972), *Uromyces phaseoli* var. *typica* (Müller *et al.*, 1974), *Uromyces phaseoli* var. *vignae* (Littlefield and Heath, 1979). Other septal pore types, viz. the perforate septum which lacks a typical septal pore apparatus and the "partial septum" (Littlefield and Heath, 1979), have also been observed in the present study.

Intercellular hyphal anastomosis of the type described here for *P. recondita* f.sp. *tritici*, has been reported infrequently for the uredial stage of other rust fungi. Kang *et al.* (1993a) reported that anastomosis was frequently observed in intercellular hyphae of *Puccinia striiformis* and they proposed that the commonly observed multinucleate hyphae of *Puccinia striiformis* result from this process. In this study, more than two nuclei in one hyphal cell were occasionally observed, possibly as a result of the occurrence of hyphal anastomosis in *P. recondita* f.sp. *tritici*.

As is the case in other rust fungi, the HMC of *P. recondita* f.sp. *tritici* shows some features not observed in intercellular hyphae. Such features include

membrane protrusions which develop against the septum on the hyphal side of HMC at an early stage of HMC differentiation, a thicker cell wall and the peripheral distribution of mitochondria in HMCs. Such characteristics have also been found to be accurate indicators of HMCs in other rusts (Heath and Heath, 1975; Littlefield and Heath, 1979; Chong and Harder, 1982; Chong *et al.*, 1985; Mims *et al.*, 1989).

The extracellular matrix at the interface between the HMC and host cells, observed here in *P. recondita* f.sp. *tritici*, has been found in many rust fungi. Using complimentary fractures and low-temperature SEM, Beckett and Porter (1988) indicated a stronger adhesion between HMC walls of *Uromyces viciae-fabae* (Pers.) Schroet. and host cell walls than between like walls. The material responsible for this adhesion is appears to be the matrix at the interface between the HMC and the host cell (Chong *et al.*, 1985, Mims *et al.*, 1989).

Haustoria of *P. recondita* f.sp. *tritici* are found not only in mesophyll cells, but also in epidermal cells, guard cells and bundle sheath cells. In these cell types, they are of similar appearance. Haustoria in epidermal cells were also reported to occur in wheat infected with *Puccinia graminis* f.sp. *tritici* (Harder *et al.*, 1979). However, as in most rust fungi investigated so far, this study indicates that the vascular tissues of wheat leaves are free from the infection by the uredial stage of *P. recondita* f.sp. *tritici*. The report by Andreev *et al.* (1982) appears to be the only record of invasion in vascular tissues by D-haustoria thus far. Their observations revealed a low incidence of D-haustoria of *Puccinia graminis* f.sp. *tritici* in the xylem and phloem of wheat leaves.

In this investigation, haustoria of *P. recondita* f.sp. *tritici* were usually found to have two nuclei at maturity. This conforms to the general description of D-

haustoria. Serial sectioning from different directions indicated that the nucleoli in the nuclei of the haustorial bodies, are usually round or near-round in shape. However, on many occasions, serial sections confirmed that only one nucleus was present in the haustorial body. In these instances, two nucleoli were present in the single nucleus. This leads us to propose the likelihood of nuclear fusion between the two nuclei in D-haustoria of this uredial stage. It would be of interest to determine whether this phenomenon exists in other rust fungi and what biological function it could have. To our knowledge, this phenomenon of two nucleoli in a single nucleus in D-haustoria has not been reported before in the uredial stage of rusts and is reminiscent of nuclear fusion in the young teliospore. Is nuclear fusion induced by the small amount of cytoplasm in, and the round shape of, the haustorial body? In the literature, the single haustorial nucleus in D-haustoria has been described in several rust fungi. By light microscopy, the mature haustoria of *P. recondita* (Allen, 1926) and *P. coronata* (Ruttle and Fraser, 1927) were observed to contain only one nucleus. By electron microscopy, Al-Khestraji and Lösel (1981) found only one nucleus for *P. poarum*. Mendgen and Dressler (1983) and Harder and Chong (1984) also indicated that there is only one nucleus per haustorium of *P. coronata*. Mendgen and Dressler (1981) also suggested the possibility of nuclear fusion in haustoria.

The association of host organelles with the developing haustorium observed in this investigation, eg. the close proximity of the host nucleus to the haustorium, modification of the endoplasmic reticulum, the presence of vesicles, and the increased occurrence of Golgi bodies in the host cytoplasm in the vicinity of the haustorium, has been widely recorded in the uredial stage of many rust fungi (Littlefield and Heath, 1979; Harder and Chong, 1984).

In the uredial stage of many rust infections, the attraction between the

haustorium and the host nucleus has been recorded at both the light microscopy level (Allen, 1923; Al-Khesraji and Lösel, 1980) and the electron microscopy level (Al-Khesraji and Lösel, 1981; Littlefield and Heath, 1979; Chong and Harder, 1982). In the present study, host nucleus is consistently associated with the invading haustorium and the nucleus of the infected cell frequently bends around or is deeply invaginated by the haustorium. Al-Khesraji and Lösel (1980) indicated that the host nucleus shows striking alterations in form and size when associated with the haustorium of *Puccinia poarum*, which they interpreted as being due to changes in nuclear contents or in the properties of the nuclear membrane, and intimating a direct involvement of nucleic acid metabolism of the host during the interaction. Chong and Harder (1982) observed pronounced proliferation of a tubular complex in the indented region of host nuclei, where a haustorial lobe of *Puccinia coronata* f. sp. *avenae* was located. They suggested that the tubular complex between the haustorium and invaginated region of host nucleus may provide additional membrane area and present a high level of exchange between the host and the fungus, which include elevated levels of nuclear metabolism. Thus these structural component may play a synthetic-transport-intermediary role to meet the requirements of the fungus. In *P. recondita* f.sp. *tritici*, however, such a tubular complex is absent in the invaginated region of host nuclei, though occasionally a little cytoplasm or organelles eg. mitochondria were observed in this region. Since the close association between the host nucleus and the haustorium occurs in many rust infections, Littlefield and Heath (1979) and Chong and Harder (1982) concluded that a close association of haustoria and host nuclei is a characteristic response of the host to the invasion of haustoria. However, the exact nature of the interaction between the host nucleus and the haustorium awaits further elucidation (Al-Khesraji and Lösel, 1981).

It is generally accepted that, in the rusts, there is proliferation of the endoplasmic reticulum near the haustorial neck and around the haustorial body (Littlefield and Heath, 1979; Harder and Chong, 1984; 1991). The smooth endoplasmic reticulum appears to attach to the extrahaustorial membrane, while much rough endoplasmic reticulum is present in the proximity of the haustorium of *P. recondita* f.sp. *tritici*. In the host cytoplasm near the developing haustorium, vesicles and tubular membrane structures were observed in this investigation. Vesicles, several of which aggregate in a membrane-bound complex, were observed here. Such complexes have not been observed in other rust fungi. The larger vesicular formations in *P. recondita* f.sp. *tritici* observed in the present investigation are reminiscent of those in *P. graminis* f.sp. *tritici* in wheat (Harder *et al.*, 1978), but they appeared to be less organised. In *P. graminis* f.sp. *tritici* infections, there is a highly organized complex of small and large tubules derived from the host endoplasmic reticulum near the haustoria (Harder *et al.*, 1978). The small and large tubules in *P. graminis* f.sp. *tritici* infections are interconnected (Harder and Chong, 1984), but the tubular structures in the *P. recondita* f.sp. *tritici* infection in the present study do not appear to be regularly interspersed with the large vesicles. This may indicate that the form of the membranous complexes induced in wheat by rust fungi is also dependent on the fungal species as are those in oat (Harder and Chong, 1984). The latter authors found that the type of complex induced in oats by *P. graminis* f.sp. *avenae* is similar to that induced in wheat by *P. graminis* f.sp. *tritici*, but distinct from the type induced in oat by *P. coronata* (Harder and Chong, 1984). Modifications of the host plasmalemma, as previously described by Littlefield and Heath (1979), triggered by the invasion of the haustorium, are common in rusts (Ehrlich and Ehrlich, 1963; 1971; Rijkenberg, 1975; Harder, 1978; Littlefield and Heath, 1979; Chong *et al.*, 1981; Harder and Chong, 1984). The effect of such modifications on changes in metabolic activity needs

further study.

On a few occasions, a cell wall apposition between the host cell wall and the host plasmalemma was observed at the site where the HMC contacts the host cell wall. Jacobs *et al.* (1993) also described similar cell wall apposition in a genotype, Morocco, highly susceptible to *P. recondita* f.sp. *tritici*. Jacobs *et al.* (1993) indicated that the appearance and composition of cell wall apposition in the susceptible host differ from those in a partially resistant host.

A collar, which results from the material deposited onto the host cell wall, occurs around the haustorial neck. Collars are not present in every invaded cell. More detailed description of the collar and its formation has been presented by Heath and Heath (1971), Littlefield and Heath (1979), Harder (1978), and Harder and Chong (1984).

LITERATURE CITED

Al-Khesraji, T.O. and Lösel, D.M. (1980). Intracellular structures of *Puccinia poarum* on its alternate hosts. *Transactions of the British Mycological Society* **75,** 397-411.

Al-Khesraji, T.O. and Lösel, D.M. (1981). The fine structure of haustoria, intracellular hyphae and intercellular hyphae of *Puccinia poarum*. *Physiological Plant Pathology* **19,** 301-311.

Allen, R.F. (1923). A cytological study of infection of Baart and Kanred wheats by *Puccinia graminis tritici*. *Journal of Agricultural Research* **23,** 131-152.

Allen, R.F. (1926). A cytological study of *Puccinia triticina* physiologic form II on Little Club wheat. *Journal of Agricultural Research* **33,** 201-222.

Andreev, L.N., Plotnikova, Y.M. and Serezhkina, G.V. (1982). Haustoria of *Puccinia graminis* Pers. f.sp. *tritici* Eriks. & Henn. in the vascular system of wheat. *Mikologia I Fitopatologiya* **16,** 335-338.

Andres, M.W. and Wilcoxson, R.D. (1984). A device for uniform deposition of liquid-suspended urediospores on seedling and adult cereal plants. *Phytopathology* **74,** 550-552.

Beckett, A. and Porter, R. (1988).The use of complementary fractures and low-temperature scanning electron microscopy to study hyphal - host cell surface adhesion between *Uromyces viciae-fabae* and *Vicia faba*. *Canadian Journal of Botany* **66,** 645-652.

Chong, J. and Harder, D.E. (1982). Ultrastructure of haustorium development in *Puccinia coronata avenae*: some host responses. *Phytopathology* **72,** 1527-1533.

Chong, J., Harder, D.E. and Rohringer, R. (1981). Ontogeny of mono- and dikaryotic rust haustoria: Cytochemistry and ultrastructural studies. *Phytopathology* **71,** 975-983.

Chong, J., Harder, D.E. and Rohringer, R. (1985). Cytochemistry studies on *Puccinia graminis* f.sp. *tritici* in a compatible wheat host. I. Walls of intercellular hyphal cells and haustorium mother cells. *Canadian Journal of*

Botany **63,** 1713-1724.

Chong, J., Harder, D.E. and Rohringer, R. (1986). Cytochemistry studies on *Puccinia graminis* f.sp. *tritici* in a compatible wheat host. II. Haustorial mother cell walls at the host cell penetration site, haustorial walls, and the extrahaustorial matrix. *Canadian Journal of Botany* **64,** 2561-2575.

Coffey, M.D., Palevitz, B.A. and Allen, P.J. (1972). The fine structure of two rust fungi: *Puccinia helianthi* and *Melampsora lini*. *Canadian Journal of Botany* **50,** 231-240.

Ehrlich, H.G. and Ehrlich, M.A. (1963). Electron microscopy of the host-parasite relationships in stem rust of wheat. *American Journal of Botany* **50,** 123-130.

Ehrlich, H.G. and Ehrlich, M.A. (1971). Fine structures of the host-parasite interfaces in mycoparasitism. *Annual Review of Phytopathology* **9,** 155-184.

Harder, D.E. (1976). Mitosis and cell division in some cereal rust fungi. II. The process of mitosis and cytokinesis. *Canadian Journal of Botany* **54,** 995-1009.

Harder, D.E. (1978). Comparative ultrastructure of the haustoria in uredial and pycnial infections of *Puccinia coronata avenae*. *Canadian Journal of Botany* **56,** 214-224.

Harder, D.E. (1989). Rust fungal haustoria - past, present, future. *Canadian Journal of Plant Pathology* **11,** 91-99.

Harder, D.E. and Chong, J. (1984). Structure and physiology of haustoria. in: *The Cereal Rusts. I. Origins, Specificity, Structure, and Physiology* (Eds.

Bushnell, W.R. and Roelfs, A.P.). pp.431-476. Academic Press, Florida.

Harder, D.E. and Chong, J. (1991). Rust haustoria. in: *Electron Microscopy of Plant Pathogens* (Eds. by K. Mendgen and D.E. Lesemann), pp.235-250. Springer-Verlag. Berlin.

Harder, D.E., Rohringer, R., Samborski, D.J., Kim, W.K. and Chong, J. (1978). Electron microscopy of susceptible and resistant near isogenic (*sr6/Sr6*) lines of wheat infected by *Puccinia graminis tritici*. I. The host pathogeninterface in the compatible (*sr6/Sr6*) interaction. *Canadian Journal of Botany* **56,** 2955-2966.

Harder, D.E., Rohringer, R., Samborski, D.J., Rimmer, S.R., Kim, W.K. and Chong, J. (1979). Electron microscopy of susceptible and resistant near-isogenic (*sr6/Sr6*) lines of wheat infected by *Puccinia graminis tritici*. II. Expression of incompatibility in mesophyll and epidermis cells and the effect of temperature on host-parasite interactions in these cells. *Canadian Journal of Botany* **57,** 2617-2625.

Heath, M.C. and Bonde, M.R. (1983). Ultrastructural observations of the rust fungus *Physopella zeae* in *Zea mays*. *Canadian Journal of Botany* **61,** 2231-2242.

Heath, M.C. and Heath, I.B. (1971). Ultrastructure of an immune and a susceptible reaction of cowpea leaves to rust infection. *Physiological Plant Pathology* **1,** 277-287.

Heath, M.C. and Heath, I.B. (1975). Ultrastructural changes associated with the haustorial mother cell during haustorium formation in *Uromyces phaseoli* var. *vignae*. *Protoplasma* **84,** 297-314.

Jacobs, Th., Van Hee, F.P. and Engels, F.M. (1993) The ultrastructure of the interface between susceptible, partially resistant spring wheat genotypes and wheat leaf rust. *Med. Fac. Landbouww. Univ. Gent.* **58,** 1-10.

Kang, Z.S., Li, Z.Q., Shang, H.S., Chong, J. and Rohringer, R. (1993a). Ultrastructure and cytochemistry of intercellular hyphae of wheat stripe rust. *Acta Mycologica Sinica* **12,** 208-213.

Kang, Z.S., Li, Z.Q., Shang, H.S., Chong, J. and Rohringer, R. (1993b). Further studies on the invasion of the haustorial mother cell of *Puccinia striiformis* West. to its own intercellular hyphae. *Acta Mycologica Sinica* **12,** 313-317.

Littlefield, L.J. and Bracker, C.E. (1972). Ultrastructural specialization of the host-pathogen interface in rust-infected flax. *Protoplasma* **74,** 271-305.

Littlefield, L.J. and Heath, M.C. (1979). Ultrastructure of rust fungi. pp. 1-277. Academic Press, New York

Mendgen, K. and Dressler, E. (1983). Culturing *Puccinia coronata* on a cell monolayer of the *Avena sativa* coleoptile. *Phytopathologische Zeitschrift* **108,** 226-234.

Mims, C.W., Taylor, J. and Richardson, E.A. (1989). Ultrastructure of the early stages of infection of peanut leaves by the rust fungus *Puccinia arachidis*. *Canadian Journal of Botany* **67,** 3570-3579.

Müller, L.Y., Rijkenberg, F.H.J. and Truter, S.J. (1974). Ultrastructure of the uredial stage of *Uromyces appendiculatus*. *Phytophylactica* **6,** 73-104.

Rijkenberg, F.H.J. (1975). The uredial stage of maize rust. *Proceedings of the*

Electron Microscopy Society of Southern Africa **5,** 35-36.

Ruttle, M.L. and Fraser, W.P. (1927). A cytological study of *Puccinia coronata* Cda. on Banner and Cowra 35 oats. *University of California, Berkeley, Publication Botany* **14,** 21-72.

Spurr, A.R. (1969). A low-viscosity epoxy resin embedding medium for electron microscopy. *Journal of Ultrastructural Research* **26,** 31-43.

Ward, H.M. (1882). On the morphology of *Hemileia vastatrix* Berk. & Br. *Quarterly Journal of Microscopy Science* **22,** 1-11.

CHAPTER 4

ULTRASTRUCTURAL MORPHOLOGY OF UREDIOSPORE FORMATION OF *PUCCINIA RECONDITA* F.SP. *TRITICI* ON WHEAT LEAVES[1]

INTRODUCTION

There are several electron microscopic investigations of urediospore formation and development, e.g. of *Melampsora lini* (Ehrenb.) Lev. (Hassan and Littlefield 1979), *M. larici-populina* Thüem., *M. medusae* Thüem. and *M. coleosporioides* Dietel (Spiers and Hopcroft 1985), *Puccinia coronata* Cda. f.sp. *avenae* Eriks. and *P. graminis* Pers. f.sp. *avenae* Eriks. and Henn. (Harder 1976), *P. digitariae* (Rey and Garnett 1983), *P. sorghi* Schw. (Rijkenberg 1975), *Physopella zeae* (Mains) Cumm. and Ramachar (Heath and Bonde 1983), *Uromyces appendiculatus* (Pers.) Unger (Müller *et al.* 1974), and *U. transversalis* (Thüm.) Winter (Ferreira and Rijkenberg 1990). These studies have provided considerable insight into the fine ultrastructural features of urediospore development in the rusts.

The formation of collars in urediosporogenesis "provides an exceptionally interesting object for ultrastructural study" (Littlefield and Heath 1979).

---

[1]This Chapter has been submitted to *International Journal of Plant Sciences*. Therefore the conventions of this journal have been followed

Electron microscopical observations by Rey and Garnett (1983), Heath and Bonde (1983) and Ferreira and Rijkenberg (1990) illustrated collar formation in urediosporogenesis. When light microscopical studies are also considered, collar formation has so far been reported in at least five genera/species of the Uredinales, viz. *Kernkampella breyniae-patentis* Munk. and Thirum. (Rajendren 1970), *Intrapes* spp. (Hennen and Figueiredo 1979), *Puccinia digitariae* (Rey and Garnett 1983), *Physopella zeae* (Heath and Bonde 1983) and *Uromyces transversalis* (Ferreira and Rijkenberg 1990). Moreover, Ferreira and Rijkenberg (1990) presented detailed diagrammatic representations of collar formation during urediosporogenesis in *U. transversalis*, *K. breyniae-patentis*, *I. paliformis* and *P. digitariae*. It is interesting to note that so far no collar formation in the urediosporogenesis of cereal rusts has been reported (Harder 1976; Littlefield and Heath 1979).

Wheat leaf rust caused by *Puccinia recondita* Rob. ex Desm. f.sp. *tritici* Eriks. and Henn. is a widespread disease. Gold *et al.* (1979) described the ultrastructure of the pycnial and aecial stages of *P. recondita*. Salako (1981) undertook an investigation of the ultrastructure of the urediospore of *P. recondita* f.sp. *tritici*. Thus far, however, there is no ultrastructural information available on the urediospore development of *P. recondita* f.sp. *tritici*. In the present study, the author describe uredium morphology, urediospore formation and subsequent collar formation of the uredial stage of *P. recondita* f.sp. *tritici*.

MATERIALS AND METHODS

Plants and inoculation

Ten-day-old wheat plants cv. Thatcher, susceptible to *P. recondita* f.sp. *tritici* the South African pathotype UV Prt8 (kindly supplied by Prof. Z.A. Pretorius, Department of Plant Pathology, University of the Orange Free State, South Africa), were used in this experiment. Freshly harvested urediospores of *P. recondita* f.sp. *tritici* were used to inoculate the adaxial surface of the plants at an inoculum dose of 50 mg urediospores per ml of Soltrol 130 (Phillips Chemical Co.) using a modified Andres and Wilcoxson (1984) inoculator. The inoculated plants were then allowed to dry for 1 hour before placement in a dark dew chamber at 20°C for 24 hours and transferred to a constant environment chamber at 18-20°C. Samples were taken at 10-15 days post-inoculation.

Scanning electron microscopy

Leaf pieces were cut into 3 × 3 mm squares and fixed in 3% glutaraldehyde in 0.05 M sodium cacodylate buffer, pH 6.8-7.2, for 24 hours, washed twice in the buffer, post-fixed for 2 hours in 2% osmium tetroxide in the buffer, washed twice in the buffer, and dehydrated in a graded ethanol series. The specimens were then critical point dried with carbon dioxide as a transition fluid and were mounted on copper stubs. Specimens were coated with gold-palladium in a Polaron sputter coater and examined with a S-570 Scanning Electron Microscope at 8.0 or 10 kV. After freeze-fracturing in an EM Scope SP 2000 cryo unit, freshly harvested materials was viewed with the SEM at 8.0 kV.

Transmission electron microscopy

Pieces of wheat leaves were cut into 3 × 3 mm squares with the uredium in the centre and were fixed for 24 hours in 3% glutaraldehyde in a 0.05 M sodium cacodylate buffer (pH 7.2), washed twice in that buffer, and post-fixed for 3 hours in 2% osmium tetroxide in the buffer at room temperature. Samples were dehydrated in an ethanol series and embedded in Spurr's resin (Spurr, 1969). Ultrathin sections were cut using glass knives and stained with 2% uranyl acetate in double-distilled water for 15 minutes, washed in double-distilled water, and post-stained in lead citrate for 15 minutes, washed in double-distilled water, and viewed with a Jeol 100 CX transmission electron microscope.

Terminology

Terms that are used in this article follow the Ferreira and Rijkenberg (1990) paper.

RESULTS AND DISCUSSION

On wheat leaves, the uredia are characterized as brown, scattered, aparaphysate sori and lack a periderm. The scanning and transmission electron microscopy observations revealed that the uredium morphology (Fig. 1) of *P. recondita* f.sp. *tritici* is similar to that of other rusts which have pedicellate urediospores.

The basal cells of developing urediosori are variable in size and shape (Fig. 2)

and usually closely packed in the intercellular space underneath the host epidermis. Each basal cell is generally swollen at one end with dense cytoplasm and numerous vacuoles and lipid bodies. Two nuclei are usually observed in a basal cell. The wall of a basal cell is thicker than that of a cell of the intercellular mycelium and an electron-opaque substance between the basal cells is noticeable which appears to bind the basal cells (Fig. 2). This cementing substance between basal cells in the uredium is also observed in uredia of *P. graminis* f.sp. *tritici* and *P. coronata* f.sp. *avenae* (Harder 1976) and *M. lini* (Hassan and Littlefield 1979).

Urediospore formation is initiated by the holoblastic development of a protuberance from a sporogenous locus on the distal surface of the basal cell (Fig. 3). The protuberance receives two nuclei from the basal cell. A septum forms near the base of protuberance, delimiting a urediospore initial from the basal cell. The urediospore initial elongates further and a new septum forms that delimits the initial into an immature urediospore and pedicel (Figs. 4, 5). Nuclear division and migration associated with the formation of the urediospore were not observed, but a young, uncompleted septum at the base of a urediospore initial suggests that the nuclear division had recently occurred in the urediospore initial (Fig. 4). Each basal cell (Figs. 2, 3), urediospore initial (Fig. 7), pedicel (Fig. 4) and urediospore (Fig. 6) is dikaryotic.

At the same locus at which the first urediospore is produced, at least one urediospore initial is able to form subsequently (Fig. 7). The initial develops as a protuberance which grows out, bulging the septum which separates the pedicel of the previously formed spore from the basal cell, displacing it laterally. Thus the pedicel wall of a previously formed spore remains attached to the basal cell and becomes a collar around the new protuberance (Figs. 7-

11). A new septum is produced to delimit the subsequent urediospore initial from the basal cell (Figs. 7, 8). Collars are first identified (Figs. 7-11) in uredia after the formation of the second urediospore initial, the first urediospore, for obvious reasons, lacking a collar. The protuberance on the basal cell of *P. recondita* f.sp. *tritici* develops in a manner similar to that of *Physopella zeae* on leaves of *Zea mays* (Heath and Bonde 1983) and that of *Uromyces transversalis* (Ferreira and Rijkenberg 1990) in *Gladiolus*. In Fig. 7. an immature septum indicates that the urediospore initial has recently developed and a collar which is the remnant of the pedicel of the previously formed urediospore is visible. The collar is continuous with the outer wall of the basal cell, and the pedicel wall of the newly formed urediospore initial is continuous with the inner wall of the basal cell (Fig. 8). After the septum, which delimits the newly formed pedicel from a locus that produced a urediospore previously, has formed (Figs. 10, 11), the collar is attached to the new pedicel. The ultrastructure of the collar has been investigated by other authors who report that several are often produced at one locus (Rajendren 1970; Hennen and Figueiredo 1983; Ferreira and Rijkenberg 1990). However, only one collar was usually observed at a locus in *P. recondita* f.sp. *tritici*. It has been suggested that the collars are possibly involved in protecting the urediospore initial against the spines of adjacent urediospores and against the desiccation of the septum between the basal cell and the initial (Ferreira and Rijkenberg 1990).

Sympodially, on the distal surface of a basal cell, one or more protuberances arise progressively from several different loci, each protuberance developing into a urediospore (Fig. 12). This observation supports the conclusion by Hughes (1970), based on light microscopy observations, that urediospores develop sympodially. In most studies on urediospore formation in the Uredinales, the urediospore is generally described as borne on a pedicel that

arises from a new growing site on a basal cell (Harder 1976; Hassan and Littlefield 1979). The present investigation on the urediospore formation of *P. recondita* f.sp. *tritici*, shows that many urediospores of this fungus are also formed progressively on the pedicels at the new growing loci on the basal cells in a sympodial fashion, whereas at least one new protuberance may be borne at the locus that has produced a previous urediospore, and thus a collar is observed at such a locus.

A septal pore is observed in the septum which separates the pedicel from the basal cell. The pore lacks a septal pore apparatus which is often found in the intercellular hyphae (Hu and Rijkenberg, unpublished) of this fungus, but is plugged with an electron-opaque substance (Fig. 13).

The urediospore initial length is determined by the number of urediospores and/or pedicels and urediospores in its proximity (Figs. 14, 15). Urediospore initials develop to different lengths to accommodate the expansion of neighbouring urediospores (urediospore initials) during maturation (Fig. 14). The urediospore grows rapidly to full size, accompanied by the accumulation of lipids, an increased density of the cytoplasm, a thickening of the spore wall and spine formation (Fig. 6). These features are similar to those described for *P. graminis* f.sp. *tritici*, *P. coronata* f.sp. *avenae* (Harder 1976) and *M. lini* (Hassan and Littlefield 1979). The urediospore, such as that of other rusts, contains organelles and cytoplasmic structures, such as: nuclei, mitochondria, vesicles, lipid bodies, endoplasmic reticulum and ribosomes. Glycogen, which was reported to occur in urediospores of *P. recondita* f.sp. *tritici* by Salako (1981), was also observed in the present study. Nucleoli were observed in the nuclei in all stages of spore development.

The development of spines on urediospores of *P. recondita* f.sp. *tritici* appears

PLATE 1

Fig. 1. Freeze-fractured section across long axis of uredium erupting through the epidermis (E). Note the mass of hyphae in the layer of mesophyll cells (M) which produce pedicels on each of which is borne a urediospore (U)

Fig. 2. Section through part of a young urediosorus under epidermis. The basal cell (BC) is packed closely with dense cytoplasm and numerous lipid bodies and vacuoles. Note an electron-opaque substance between the basal cells. The basal cell is dikaryotic. N: Nucleus.

Fig. 3. Section through basal cell (BC) and urediospore initial (Ui). N: Nucleus; U: Urediospore.

Fig. 4. Longitudinal section of elongating urediospore initial (Ui). A septum (arrows) is forming to delimit the urediospore initial from the pedicel (P). Two nuclei (N) are evident in the pedicel. Bc: Basal cell.

Fig. 5. Enlargement of part of Fig. 4 showing developing septum (S) delimiting the urediospore initial from the pedicel.

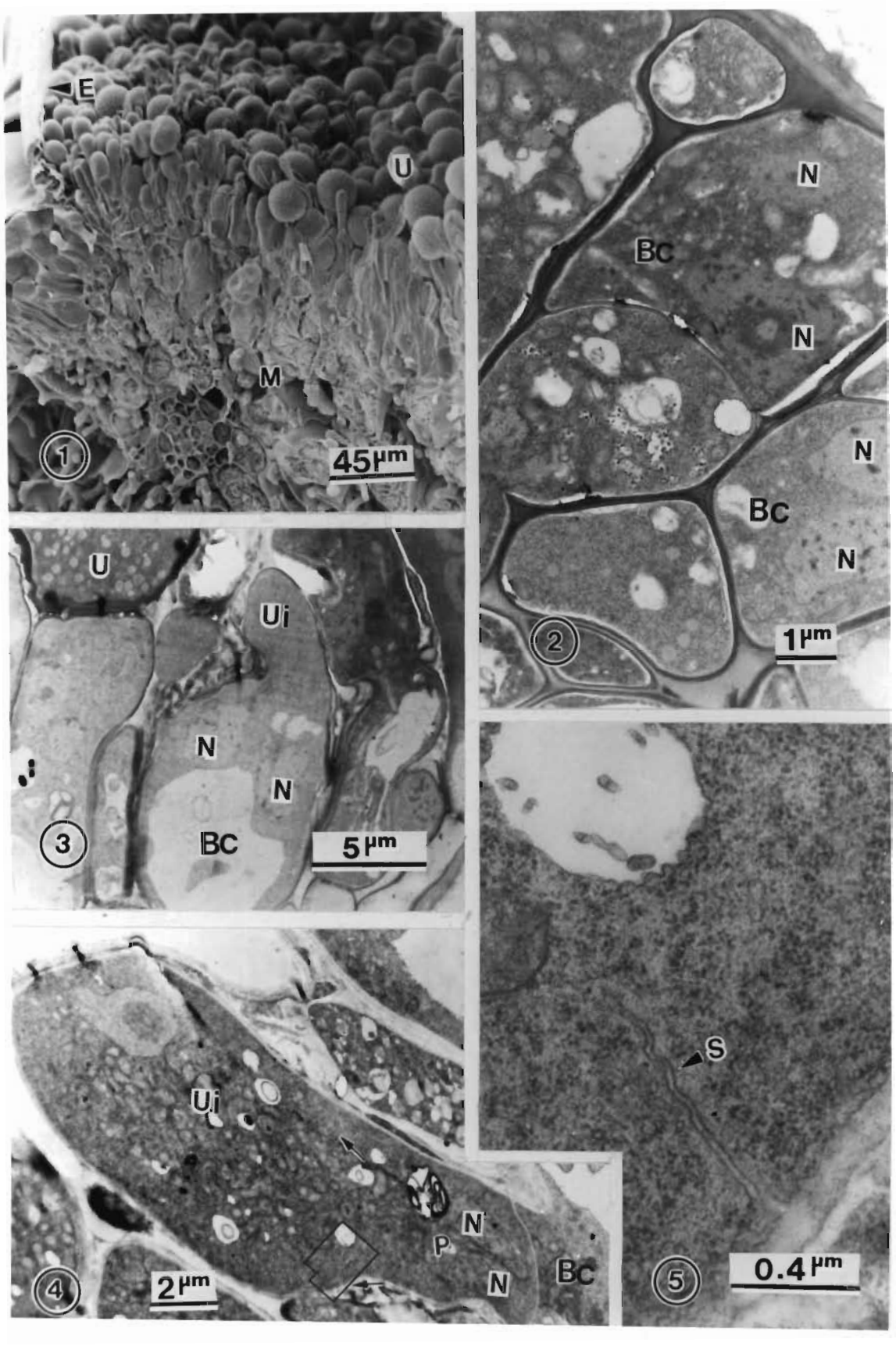
E
U
M
45µm
1
N
Bc
N
N
Bc
N
1µm
2
U
Ui
N
N
Bc
5µm
3
S
0.4µm
5
Ui
N
P
N
Bc
2µm
4

PLATE 2

Fig. 6. Longitudinal section of basal cell (BC), pedicel (P) and attached urediospore (U) with dense cytoplasm. Note urediospore is dikaryotic and nucleolus is evident in the urediospore on the left.

Fig. 7. Section of a new urediospore initial (Ui) forming inside the collar (C) left behind by the first pedicel. A septum (arrow) is forming to separate the urediospore initial (Ui) and basal cell (BC).

Fig. 8. Enlargement of part of Fig. 7. Note the collar (C) is continuous with the outer wall of the basal cell and the pedicel wall of newly formed urediospore initial is continuous with the inner wall of basal cell. S: Septum.

Fig. 9. Lateral view of a collar around the urediospore initial. Ui: Urediospore initial; C: Collar.

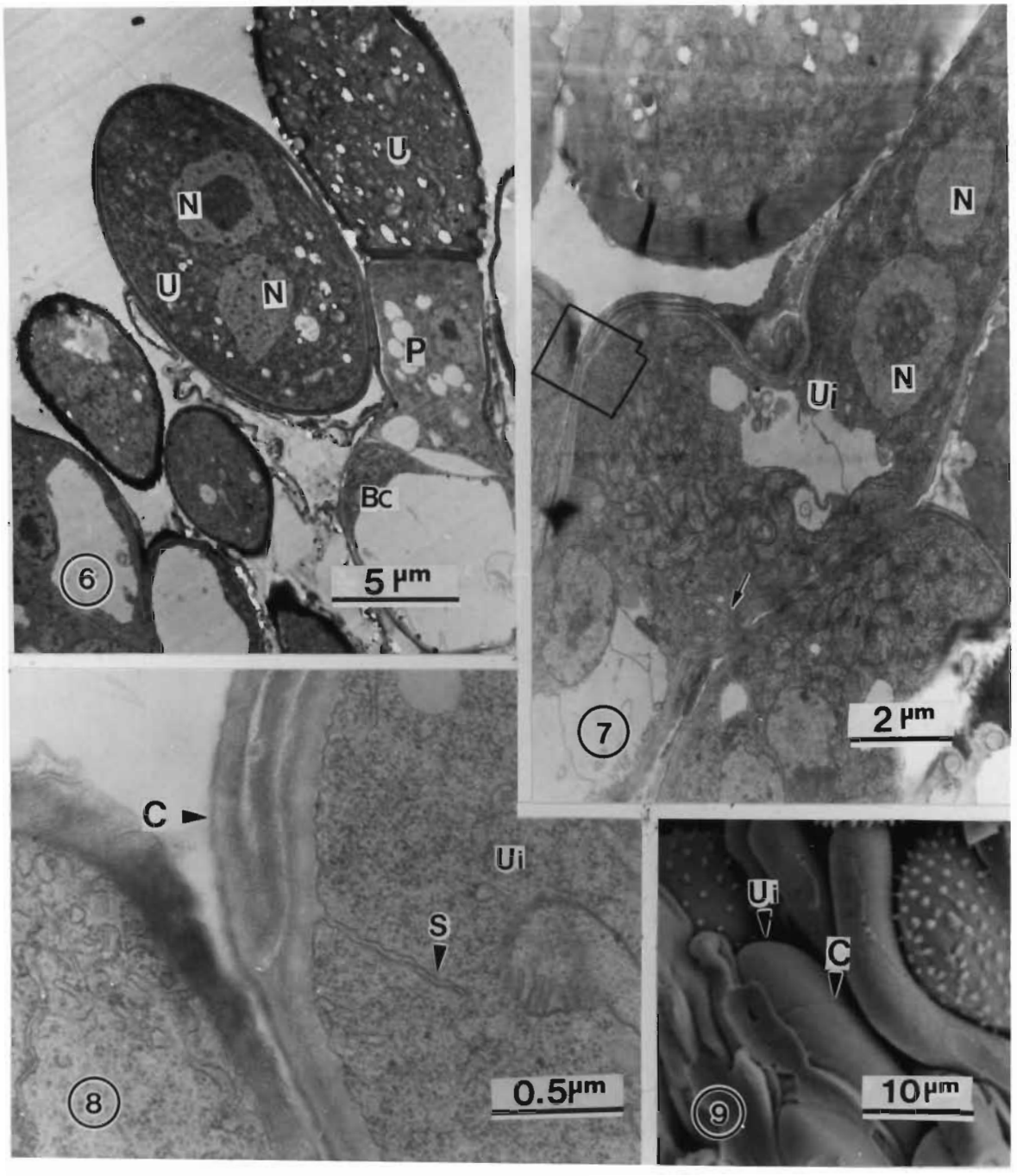
U
N
U
N
P
Bc
5 µm
6
N
N
Ui
2 µm
7
C
Ui
S
0.5µm
8
Ui
C
10µm
9

PLATE 3

Fig. 10. Section of enlongated second urediospore (U) containing intact collar (C) of previous urediospore. A septum separates the pedicel (P) and basal cell (BC). N: Nucleus.

Fig. 11. Close-up of longitudinal section of part of collar (C) and pedicel (P).

Fig. 12. Longitudinal section of pedicel (P), urediospore initial (Ui) from same basal cell (BC).

Fig. 13. Section of part of septum delimiting the pedicel (P) from basal cell (BC). Note the septal pore lacks a septal pore appratus (arrow).

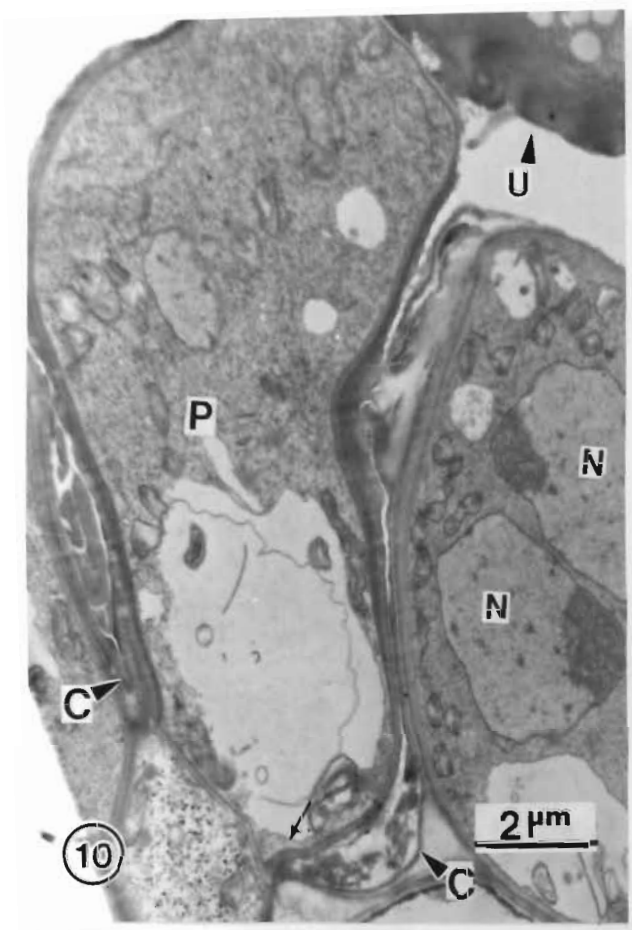

10

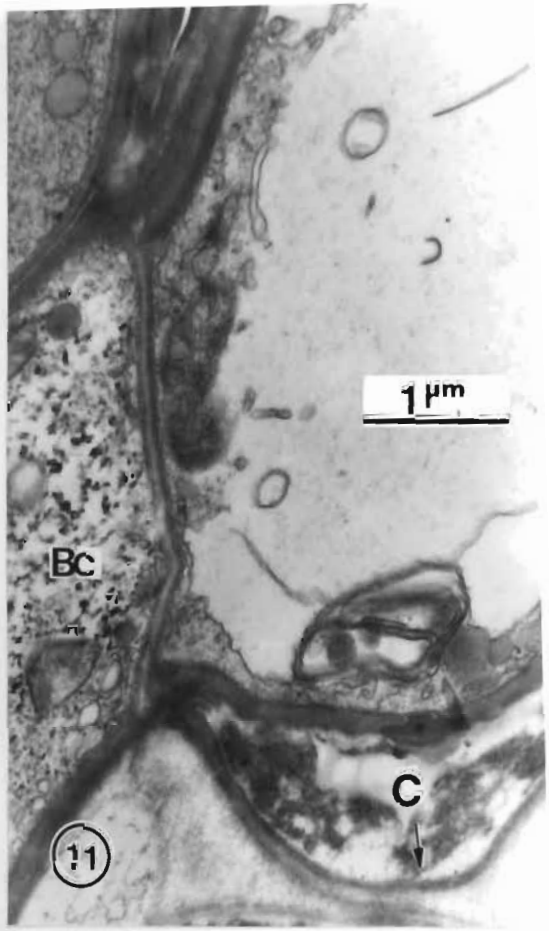

11

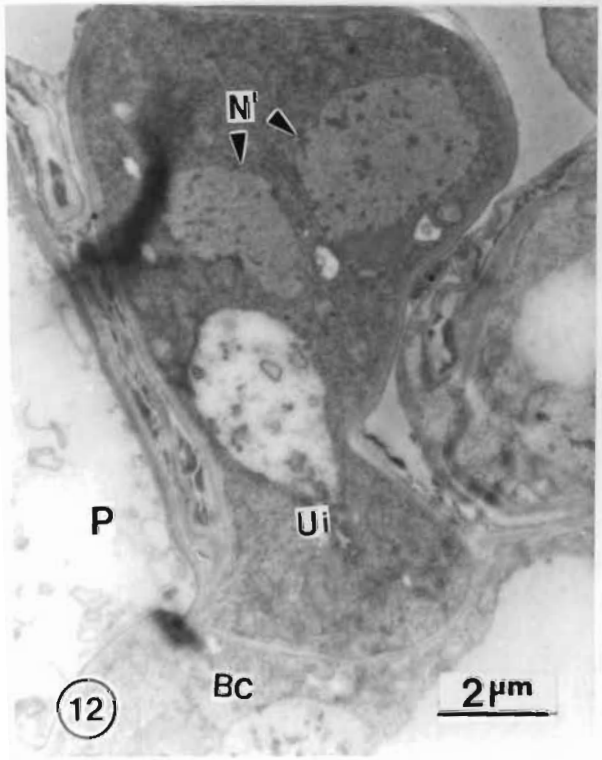

12

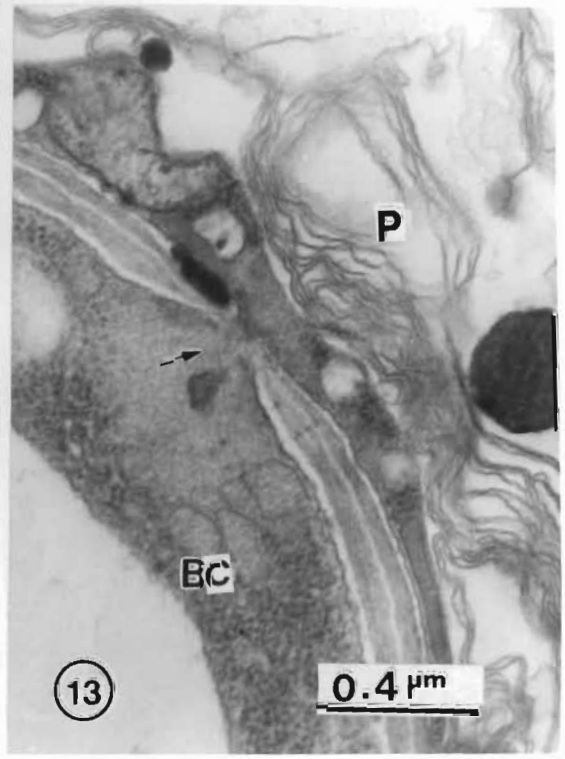

13

PLATE 4

Fig. 14. View of urediospores at different stages of maturity. Note fully elongated spines on urediospore (U). The pedicels of urediospore initials (Ui) develop to different lengths to accommodate the expansion of neighbouring urediospores (urediospore initials) during maturation. M: Mesophyll.

Fig. 15. View of urediospore ornamentation at different stages of development. Letters a, b, c and d indicate consecutive developmental stages of urediospore ornamentation.

Fig. 16. Lateral view of spine ornamentation. A layer of endoplasmic reticulum (ER) under the base of spine embedded in the wall is visible. Note many lipid bodies (L) in the dense cytoplasm of urediospore (U).

Fig. 17. Cross section of spine. Note a layer of endoplasmic reticulum (ER) around the periphery of spine. The spine consists of three layers (L1-L3).

Fig. 18. View of urediospore surface. Fully developed spine (Sp) extends beyond the urediospore wall and situated in a depression (D) surround by an annulus (A).

Fig. 19. Section of part of urediospore (U) and pedicel (P). Note a funnel-shaped indentation (arrow) in the urediospore wall.

Fig. 20. Mature urediospore (U) (arrow) separating from the pedicel (P).

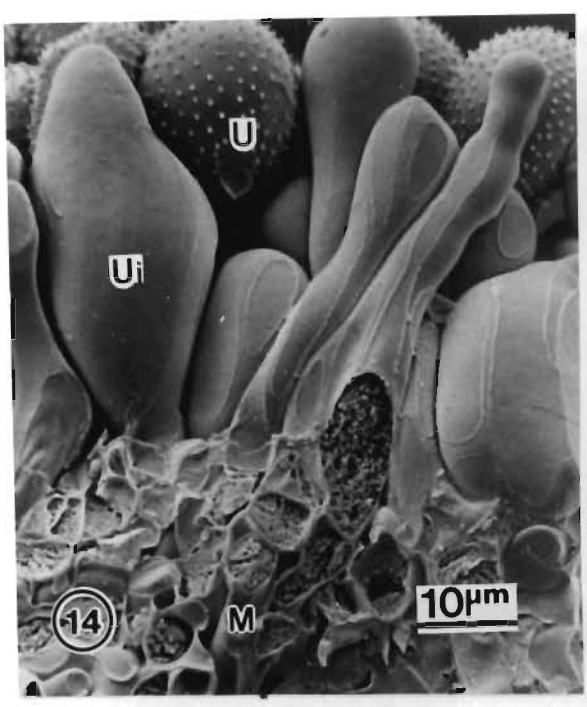
U
Ui
M
14
10μm

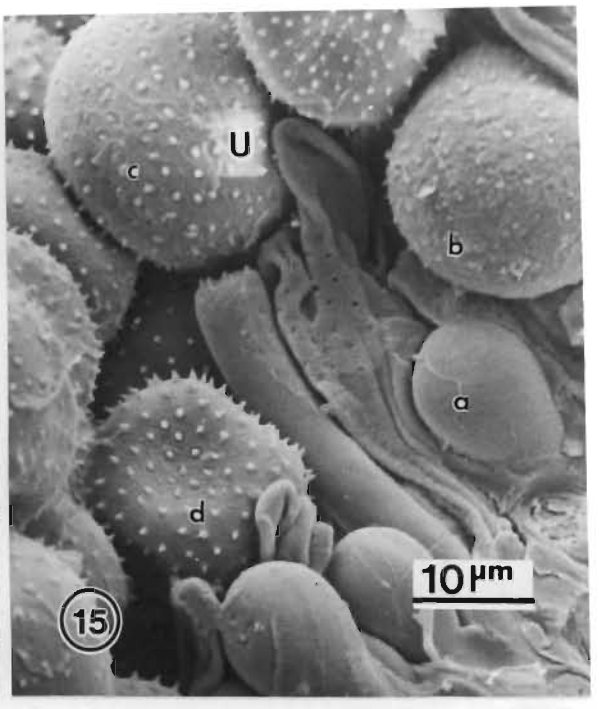
U
c
b
a
d
15
10μm

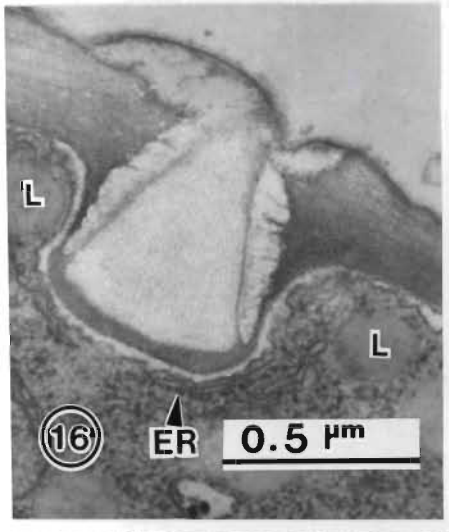
L
L
16
ER
0.5 μm

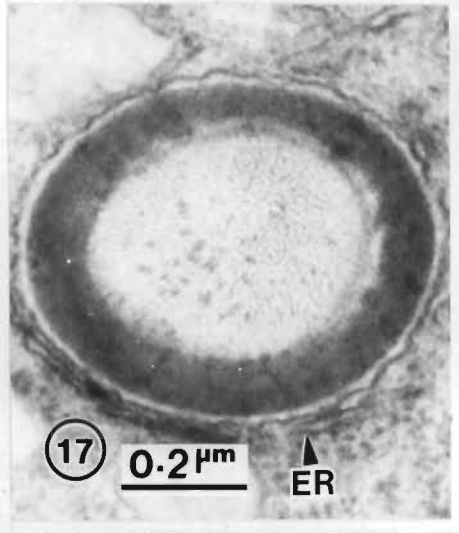
17
0·2μm
ER

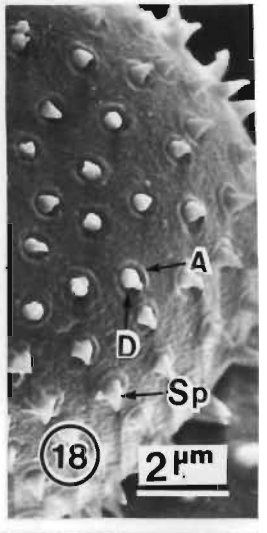
A
D
Sp
18
2μm

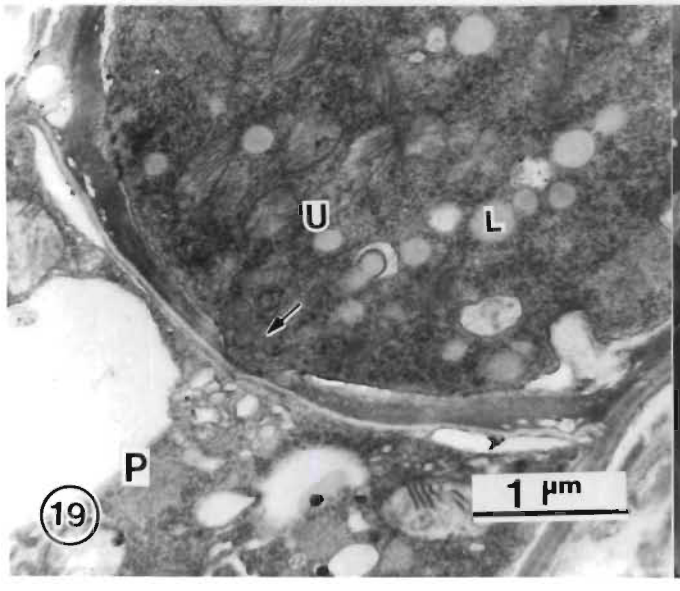
U
L
P
19
1 μm

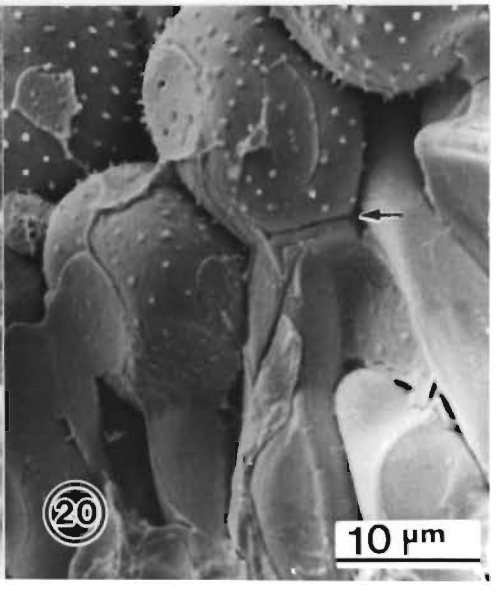
20
10 μm

substantially similar to that of other rusts. Several phases of urediospore development are illustrated in Fig. 15.

In the cytoplasm, a short distance underneath the base of the spine, and to the sides of spines, there is a layer of endoplasmic reticulum (Figs. 16, 17). This layer of endoplasmic reticulum associated with the spines is also described by Amerson and van Dyke (1978), Ehrlich and Ehrlich (1969), Harder (1984), Littlefield and Bracker (1971), Müller *et al.* (1974) and Ferreira and Rijkenberg (1990). Spines are comprised of three layers: an outer layers that is thin at the bottom of the spine while thicker at the spine tip, a middle layer that is thick and electron-opaque and an inner that contains longitudinally orientated, fibrillar materials (Figs. 16, 17). The spine is situated in a small, circular depression on the spore surface, which is encircled by a slightly raised annulus (Fig. 18). Spines are normally curved near the tip (Fig. 18).

There is funnel-shaped indentation in the spore wall that links the spore to the pedicel (Fig. 19). The urediospore separates itself from the pedicel by schizolysis in the middle lamella of the septum which delimits the spore from the pedicel (Figs. 19, 20).

Literature cited

Andres MW, RD Wilcoxson 1984 A device for uniform deposition of liquid-suspended urediniospores on seedling and adult cereal plants. Phytopathology 74: 550-552.

Amerson HV, CG van Dyke 1978 The ontogeny of echinulation (spines) in urediospores of *Puccinia sparganioides*. Exp Mycol 2: 41-50.

Ehrlich MA, HG Ehrlich 1969 Urediospore development in *Puccinia graminis*. Can J Bot 47: 2061-2064.

Ferreira JF, FHJ Rijkenberg 1990 Ultrastructural morphology of the uredium and collar formation during urediosporogenesis of *Uromyces transversalis* on gladiolus. Can J Bot 68: 605-612.

Gold RE, LJ Littlefield, GD Statler 1979 Ultrastructure of the pycnial and aecial stages of *Puccinia recondita*. Can J Bot 57: 74-86.

Harder DE 1976 Electron microscopy of urediospore formation in *Puccinia coronata avenae* and *P. graminis avenae*. Can J Bot 54: 1010-1019.

Harder DE 1984 Developmental ultrastructure of hyphae and spores. Pages 333-369 *in* WR Bushnell, AP Roelfs, eds. The Cereal Rusts I: Origins, Specificity, Structure, and Physiology, Academic Press, Inc. New York.

Hassan ZM, LJ Littlefield 1979 Ontogeny of the uredium of *Melampsora lini*. Can J Bot 57: 639-649.

Heath MC, MR Bonde 1983 Ultrastructural observations of the rust fungus *Physopella zeae* in *Zea mays*. Can J Bot 61: 2231-2242.

Hennen JF, MB Figueiredo 1979 *Intrapes*, a new genus of fungi imperfecti (Uredinales) from Brazilian cerrado. Mycologia 71:836-840.

Hughes SJ 1970 Ontogeny of spore forms in Uredinales. Can J Bot 48: 2147-2157.

Littlefield LJ, CE Bracker 1971 Ultrastructure and development of urediospore ornamentation in *Melampsora lini*. Can J Bot 49: 2067-2073.

Littlefield LJ, MC Heath 1979 Ultrastructure of rust fungi. Academic Press, New York.

Müller LY, FHJ Rijkenberg, SJ Truter 1974 Ultrastructure of the uredial stage of *Uromyces appendiculatus*. Phytophylactica 6: 73-104.

Rajendren RB 1970 Cytology and developmental morphology of *Hernkampella breyniae-patentis* and *Ravenelia hobsoni*. Mycologia 62: 1112-1121.

Rey MEC, HM Garnett 1983 Sporogenesis in the uredial stage of *Puccinia digitariae*. Trans Br Mycol Soc 80: 521-526.

Rijkenberg FHJ 1975 The uredial stage of maize rust. Proc Electron Microsc Soc South Afr 5: 35-36.

Salako EA 1981 The ultrastructure of the uredospore of *Puccinia recondita*. Mycopathologia 76: 3-12.

Spiers AG, DH Hopcroft 1985 Ultrastructural studies of pathogenesis and uredinal development of *Melampsora larici-populina* and *M. medusae* on poplar and *M. coleosporioides* and *M. epitea* on willow. NZ J Bot 23: 117-133.

Spurr AR 1969 A low-viscosity epoxy resin embedding medium for electron microscopy. J Ultrastruct Res 26: 31-43.

CHAPTER 5

CYTOCHEMISTRY OF THE INTERACTION BETWEEN WHEAT(*TRITICUM AESTIVUM* AND *PUCCINIA RECONDITA* F.SP. *TRITICI*: LOCALIZATION OF CELLULOSE, CHITIN, GLUCOSE/MANNOSE, GALACTOSE AND FUCOSE [1]

INTRODUCTION

Light microscopy, scanning electron microscopy and transmission electron microscopy have provided a good understanding of the cytological events occurring during the interaction between plants and rust fungi. However, limited information is available on the specific molecular processes of the host-fungus interaction. In recent years, cytological, biochemical, as well as molecular biological investigations, have provided increasing evidence that the interaction involves a series of molecular and cellular recognition and information exchange processes between the two partners. The cell surface composition, in the interaction between rust fungus and host, is considered to be of likely importance in explaining plant-rust specificity and in determining compatibility or incompatibility (Harder et al. 1989). Both the cytochemical approach using lectin and enzyme probes and the

---

[1]This Chapter has been submitted to *Protoplasma*. Therefore the conventions of this journal have been followed

immunocytochemical approach using antibody probes have been successfully used to elucidate the nature and the composition of the cell surface.

Previous studies using lectin probes have indicated that the differentiation of specific infection structures, by rust fungi, is associated with changes in their cell wall composition (Chong et al. 1981, 1986, Mendgen et al. 1985). In *Puccinia graminis* f.sp. *tritici*-infected wheat leaves, for instance, Chong et al. (1985) described the occurrence of concanavalin A- and wheat germ lectin-binding material in cell walls of the stem rust fungus. In conjunction with other tests, they showed the remarkable complexity of the infection structures, such as haustorial walls and the wall of the haustorial neck, including an age-dependent deposition of chitin in the wall of the haustorial body. Cytochemical tests have also shown that substances, such as cellulose, ß-glycosyl and galactosyl residues, α-linked glucans or mannans, occur in the extrahaustorial matrix, the interface between rust fungus and host, in the wheat-*P. graminis* f.sp. *tritici* interaction (Chong et al. 1986, Rohringer et al. 1989).

What determines the recognition and host specificity of *Puccinia recondita* Rob. ex Desm. f.sp. *tritici* Eriks. and Henn. is not yet known. In a study to isolate the haustoria from wheat leaves infected by *P. recondita* f.sp. *tritici*, the pathogen of wheat leaf rust, which is a serious disease of wheat worldwide, Cantrill and Deverall (1993) found that the concanavalin A- and wheat germ lectin-binding properties of the host-free haustoria of *P. recondita* f.sp. *tritici* were different from those of the haustoria of wheat stem rust described by Chong et al. (1986). This raises the possibility that the lectin-binding properties may vary in different rust species. To obtain more insights in the cellular and molecular events of the interaction between wheat and *P. recondita* f.sp. *tritici*, the present study was conducted using the various

sugar-specific lectins and enzyme as probes to localize the different molecules on the cell surfaces of *P. recondita* f.sp. *tritici* and wheat (*Triticum aestivum* L.).

MATERIALS AND METHODS

Chemicals and probes

Most chemicals including haptens and lectin probes, and bovine serum albumin (BSA), were purchased from Sigma Chemical Co., St. Louis, MO, U.S.A.

The cellulase-gold complex (10 nm in diameter) for detection of cellulose (ß-1,4-glucans polymers) was a kind gift of Drs R.P. Baayen and M.G. Förch, Institute of Plant Protection, Wageningen, The Netherlands. This enzyme-gold complex was in 0.01 M PBS, 0.02% PEG, 0.5% BSA, pH 7.4. The inhibitor used was 0.5 M carboxymethylcellulose.

The lectins, conjugated with 10 nm diameter colloidal gold particles, used in this study, were the following: Wheat germ agglutinin (WGA), from *Triticum vulgaris*, in 0.01 M sodium phosphate-buffered saline with 0.15 M NaCl (PBS), pH 7.2, containing 0.02% (W/V) BSA and 0.02 % (W/V) Tween 20. Inhibitor: 0.2 M *N,N',N''-triacetylchitotriose*. *Concanavalia ensiformis* agglutinin (ConA), in 0.15 M NaCl, 0.01 M phosphate buffer, 0.1 mM Ca^{+2}, 0.1 mM Mn^{+2}, 0.02% polyethylene glycol 20 000 (PEG 20 000), pH 6.8. Inhibitor: 0.2 M α-methyl-D-mannopyranoside. Peanut agglutinin (PNA), from *Arachis hypogaea*, in 0.01 M PBS, 0.5% albumin, 0.05% Tween-20, pH 7.2.

Inhibitor: 0.2 M ß-D-galactose. Lentil agglutinin (LCA), from *Lens culinaris*, in 0.15 M NaCl, 0.01 M sodium phosphate, pH 7.2, 0.1 mM Ca^{+2}, 0.1 mM Mn^{+2}, 0.02% PEG 20. Inhibitor: 0.2 M *α*-methyl-D-mannopyranoside. Soybean agglutinin (SBA), from *Glycine max*, in 0.01 M PBS, 0.02 % Tween 20, 0.5% BSA, pH 7.0. Inhibitor: 0.2 M *N*-acetylgalactosamine. *Helix pomatia* agglutinin (HPA)2, in 0.01 M PBS, 0.1 mM Ca^{+2}, 0.1 mM Mn^{+2}, 0.5% BSA, 0.05% Tween 20, pH 7.2. Inhibitor: 0.2 M *N*-acetylgalactosamine. *Ulex europeaus* agglutinin (UEA I), in 0.01 M PBS, 0.5% BSA, 0.05% Tween 20, pH 7.2. Inhibitor: 0.5 M *α*-L-fucose.

Plant materials and inoculation

Wheat line Thatcher, susceptible to *P. recondita* f.sp. *tritici*, the pathogen of leaf rust, was used in this study. Freshly harvested urediospores of *P. recondita* f.sp. *tritici* (the South African pathotype UVPrt 8) (both wheat seeds and the rust race were kindly supplied by Prof. Z.A. Pretorius, Department of Plant Pathology, University of the Orange Free State, South Africa), were used to inoculate the adaxial surface of the first leaf of 10-day-old plants at an inoculum dose of 45 mg urediospores per ml of Soltrol 130 (Phillips Chemical Co.) using a modified Andres and Wilcoxson (1984) inoculator. Inoculated plants were allowed to dry for about 1 hour before placement in a dark dew chamber at 20°C for 20 hours. The inoculated leaves were sampled 4, 5 and 6 days after inoculation.

Specimen processing for electron microscopy

The harvested leaves were cut into squares (3×3 mm^2) which were fixed in 3% glutaraldehyde in 0.05 M sodium cacodylate buffer (pH 7.2) overnight and washed twice in that buffer. Samples were then dehydrated in an ethanol

series and embedded in Epon 812. Some samples were post-fixed in 2% osmium tetroxide in 0.05 M sodium cacodylate buffer (pH 7.2) at room temperature for 1 hour before dehydration and embedding. Ultrathin sections were cut using glass knives or a diamond knife and collected on 200 or 300 mesh nickel grids for cytochemical processing.

Cytochemical labelling

Ultrathin sections on grids were first floated for 15 min on a drop of 0.01 M sodium phosphate-buffered saline (PBS) containing 0.02% of polyethylene glycol 20 000 (PEG 20 000) at the pH corresponding to the optimal activity of the protein to be tested, according to the instructions provided by the producer. They were then transferred to a drop of 20 μl of the gold-conjugated probe for 2 hours at room temperature in a moist chamber. The grids with sections were then washed with a series of drops of 0.01 M PBS, containing 0.5% BSA (PBS-BSA), rinsed with double-distilled water, stained with 2% uranyl acetate for 15 minutes, washed in double-distilled water, post-stained in lead citrate for 15 minutes, washed in double-distilled water and viewed with a Jeol 100 CX transmission electron microscope at 80 kV.

Cytochemical controls

Specificity of the different labellings was assessed by the following cytochemical controls: (1) incubation for 30 min with each gold-conjugated complex to which was added the corresponding sugar inhibitor; (2) incubation with bovine serum albumin (BSA)-gold complex, a nonenzymic protein-gold complex.

RESULTS

In the present investigation, it was found that the labelling patterns observed in tissues post-fixed with osmium tetroxide were similar to those in tissues fixed with glutaraldehyde only, indicating that postfixation did not affect markedly the accessibility of the gold-conjugated lectins or enzyme toward to the sugar-specific sites. This is consistent with other reports indicating that postfixation with osmium tetroxide did not alter accessibility of both the lectins and the enzymes to their corresponding receptors (Benhamou et al. 1987, 1996, Benhamou 1995).

Localization of cellulose (ß-1,4-glucan polymers)

After incubation of the ultrathin sections of infected wheat leaf tissue with the cellulase-gold complex, numerous gold particles were observed on the cell walls of host cells, such as epidermal cells, mesophyll cells, guard cells and vascular cells. Gold particles were usually numerous and regularly distributed on the walls, while no labelling was found on the cell walls of the intercellular hyphae of *P. recondita* f.sp. *tritici* (Fig. 1). Regions of thickened cell wall in mesophyll cells, to which fungal hyphae are appressed, are also labelled with the enzyme-gold complex (Fig. 1). The host cytoplasm and organelles, such as mitochondria, chloroplasts, nuclei, vacuoles, Golgi bodies and endoplasmic reticulum are free of gold particles. The walls of haustorial mother cells, hyphal cytoplasm and hyphal organelles are unlabelled. At the penetration site (Figs. 2, 3), the labelling of the host cell wall is interrupted by the penetrated fungal haustorial neck. Some slight cell wall modifications are observed at the penetration site. The modified host cell wall, at the penetration site, is pushed

somewhat into the host cytoplasm (Fig. 4). Regardless of the age of the haustorium, no cellulose labelling is shown of the haustorial neck wall, the haustorial body wall or the extrahaustorial matrix, c.f. young (Fig. 2) and mature haustorium (Figs. 5, 6). The cytochemical control test (gold-conjugated enzyme pre-absorbed with carboxymethylcellulose) showed very few scattered gold particles on the host cell walls. The sections incubated with the BSA-gold complex, showed no labelling anywhere. Thus, the reaction specificity was clearly indicated.

Localization of chitin (N-acetylglucosamine residues)

Application of the wheat germ agglutinin (WGA)-gold complex to the sections of infected wheat leaf tissue led to an even deposition of gold particles over cell walls of intercellular hyphae. Four layers of cell wall are discernible in the fungal intercellular hypha, while the labelling occurred mainly over the two inner layers (Fig. 7). Six layers of cell wall can be distinguished in the haustorial mother cell. The gold particles were predominantly restricted to the four inner layers of HMC walls (Fig. 8) and the two outer layers appeared unlabelled. The extracellular matrix, observed at the contact region between the HMC and host cell wall, was free of labelling (Fig. 9). The thickened region in the HMC wall, termed the annulus of the intrawall penetration torus (IPT) by Chong et al. (1986), was strongly labelled with the WGA probe (Fig. 9). As that in the wheat-*P. graminis* f.sp. *tritici* interaction (Chong et al. 1986), the stem of IPT was not bound by the WGA probe. Also, there was no labelling of the haustorial neck, regardless of its age (Fig. 9). After penetration, the protrusions on the haustorial mother cell septum on the hyphal side become short and electron-opaque, the septum was also bound by WGA but the protrusions were free of gold particles (Fig. 10). WGA labelling was observed to occur in walls of the haustorial body at an older age

(Fig. 11). The extrahaustorial matrix was free of gold particles.

Host cell walls, cytoplasm, and organelles were unlabelled.

Localization of mannose and/or glucose residues

Sections of wheat leaf tissue infected by the leaf rust fungus, harvested at 4 or 6 days post-inoculation (dpi), after treatment with the Concanavalin A (ConA)-gold complex, showed heavy gold particle deposition in the starch granules of host chloroplasts (Fig. 13) and the glycogen-like granules in fungal cytoplasm, but no labelling of the host cell walls was detected. ConA labelled the walls of the intercellular hyphae and haustorial mother cells (Fig. 12). The septum was heavily bound by the ConA (Fig. 12) and the haustorial neck was also labelled (Fig. 14). ConA labelling was pronounced on the walls of younger haustorial bodies and the extrahaustorial matrix (Fig. 15) while in the case of older haustoria, only the extrahaustorial matrix was labelled (Fig. 16).

Incubation with the Lentil agglutinin-gold complex (LCA) resulted in a similar pattern of binding but the labelling was much weaker than that by the ConA-gold complex. Fig. 17 shows LCA labelling on the wall of the haustorial body and the extrahaustorial matrix.

Localization of galactose and N-acetylgalactosamine residues

Two lectins used in this study, peanut agglutinin (PNA) and soybean agglutinin (SBA) could detect galactose residues, whereas SBA and *Helix pomatia* agglutinin (HPA) could recognize *N*-acetylgalactosamine residues. PNA and SBA were found to bind to the same regions in both host and fungal walls, although the labelling with PNA was always stronger than that with

PLATE 1

Figs. 1-5. Labelling with the cellulase-gold complex of ultrathin sections of wheat leaf tissues infected by *Puccinia recondita* f.sp *tritici*.

Fig. 1. Host mesophyll cell walls (MCW) are densely labelled. Some thickened regions of host cell wall, contiguous with fungal cells, are also labelled, but the hyphal walls (FW) are free of gold particles. (Bar = 1 μm)

Fig. 2. Young haustorium in which a fungal nucleus (N) is in the process of migration from the haustorial mother cell (HMC) to the haustorial body (HB). The neckband on the haustorial neck (HN) is not fully developed. Gold particles are only deposited over the host cell wall. EHM: Extrahaustorial matrix. (Bar = 0.5 μm)

Fig. 3. High magnification of the penetration site in Fig. 2. Labelling of the host cell wall, at the site of penetration, is locally interrupted. (Bar = 0.2 μm)

Fig. 4. An oblique section of the point of cell wall penetration. Only the host cell wall is labelled and some wall component, labelled with the cellulase-gold complex, is pushed into the host cytoplasm (arrows). (Bar = 0.5 μm)

Fig. 5. A mature haustorium from which most fungal cytoplasm and nuclei (N) have moved into the haustorium. Dark-stained neck band (arrow) is visiable on the haustorial neck. Gold particles are only bound to the host cell wall. The walls of hyphae haustorial mother cells (HMC), haustorial necks, and haustorial bodies, and the extrahaustorial matrix (EHM) are unlabelled. (Bar = 2 μm)

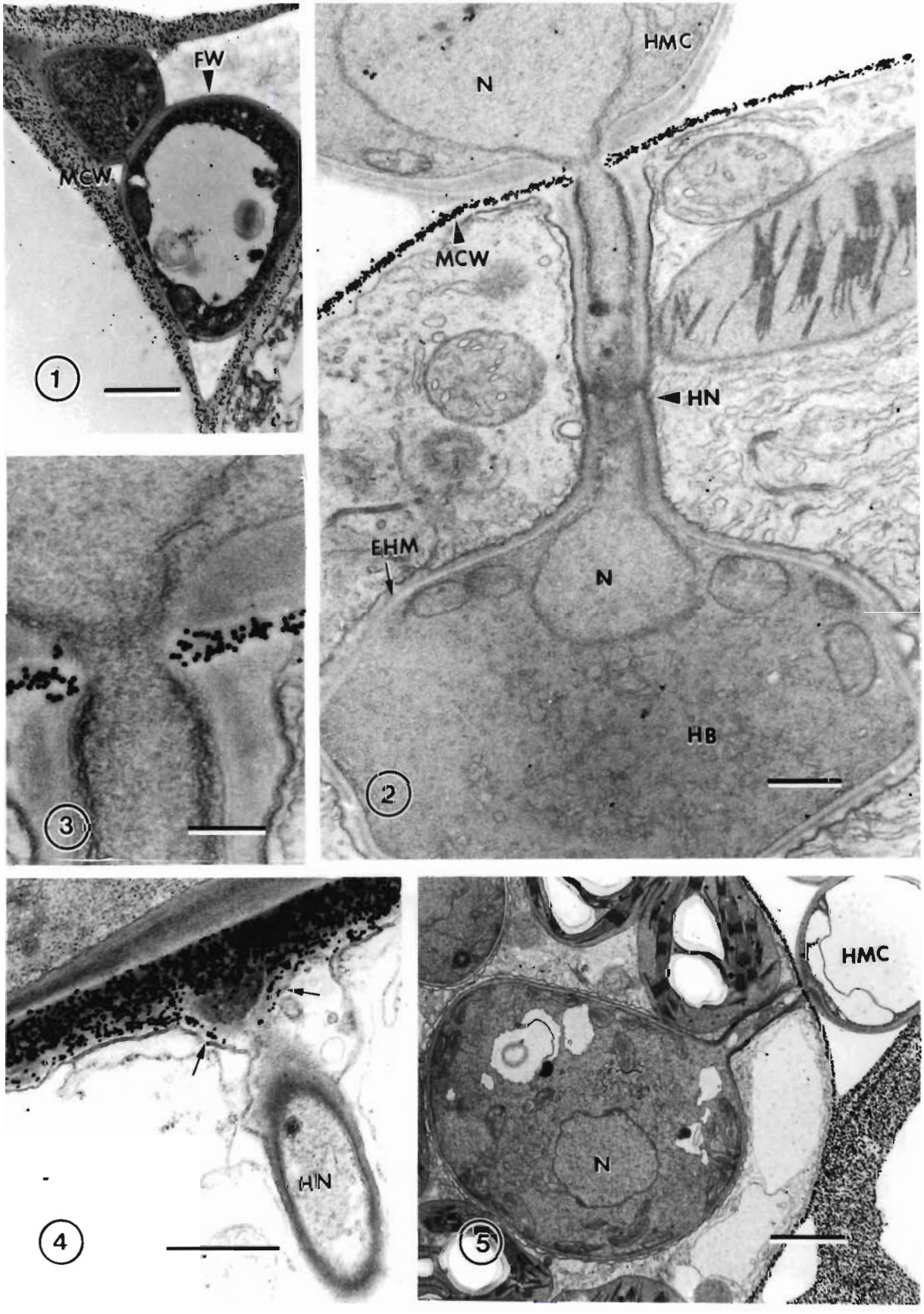
FW
MCW
1
HMC
N
MCW
HN
EHM
N
HB
2
3
HN
4
HMC
N
5

PLATE 2

Fig. 6. Labelling with the cellulase-gold complex of ultrathin sections of wheat leaf tissues infected by *Puccinia recondita* f.sp *tritici*. A mature haustorium in a host guard cell. The walls of the guard cell are strongly labelled, whereas no gold particles are found in the extrahaustorial matrix or at any other site. (Bar = 1 μm)

Figs. 7-9. Ultrathin sections of wheat leaf tissues infected by *P. recondita* f.sp. *tritici*, labelled with wheat germ agglutinin (WGA)-gold conjugates which labels *N*-acetylglucosamine residues.

Fig. 7. Intercellular hypha (IH). The inner layers of the hyphal cell wall are labelled regularly. (Bar = 0.2 μm)

Fig. 8. Haustorial mother cell (HMC). The inner layers of the HMC are evenly labelled with the WGA-gold probe while the two outer layers (arrows) of HMC are free of labelling. (Bar = 0.1 μm)

Fig. 9. The site of penetration. The extracellular matrix (MX) at the interface between the haustorial mother cell (HMC) and host cell wall (MCW) is not labelled with the probe. The thickened region of the HMC at the penetration site had been named as the intrawall penetration torus (IPT) which consists of two parts: an annulus (A) around the penetration site (which causes the thickening of the HMC wall) and a stem (arrows) that extend from inside the annulus through the host wall (Chong *et al.* 1986). The annulus (A) of the intrawall penetration torus (IPT) in the haustorial mother cell is bound by gold particles. The stem (arrow) of the intrawall penetration torus and the haustorial neck (HN) are free of labelling. (Bar = 0.2 μm)

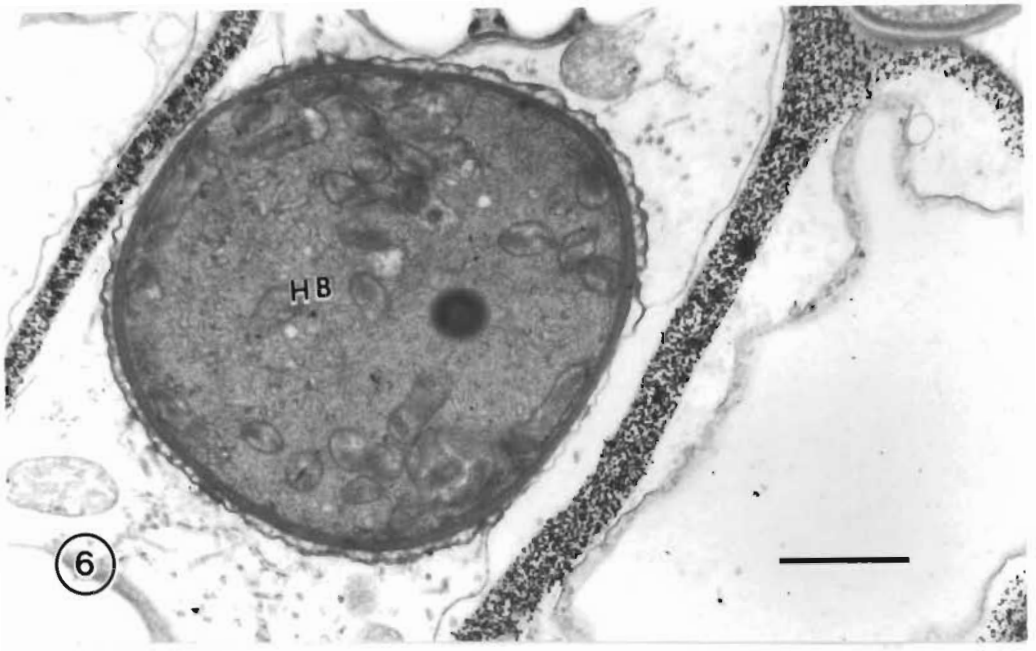
HB
6

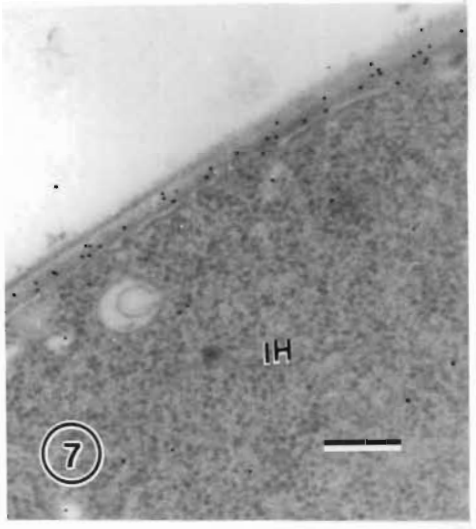
IH
7

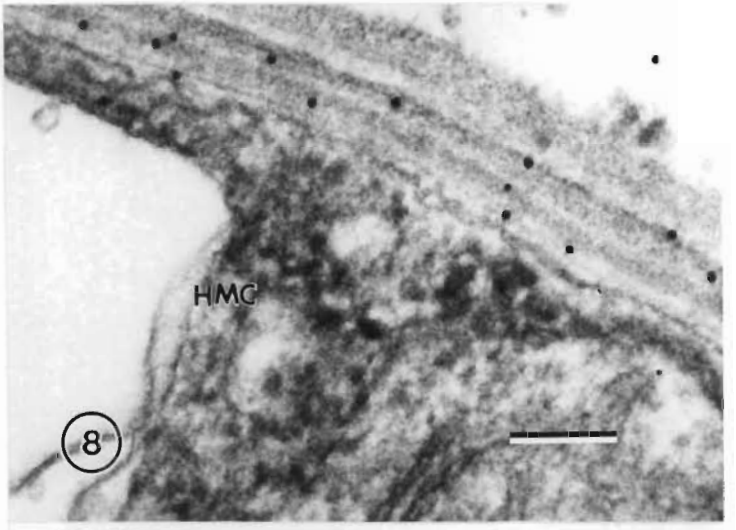
HMC
8

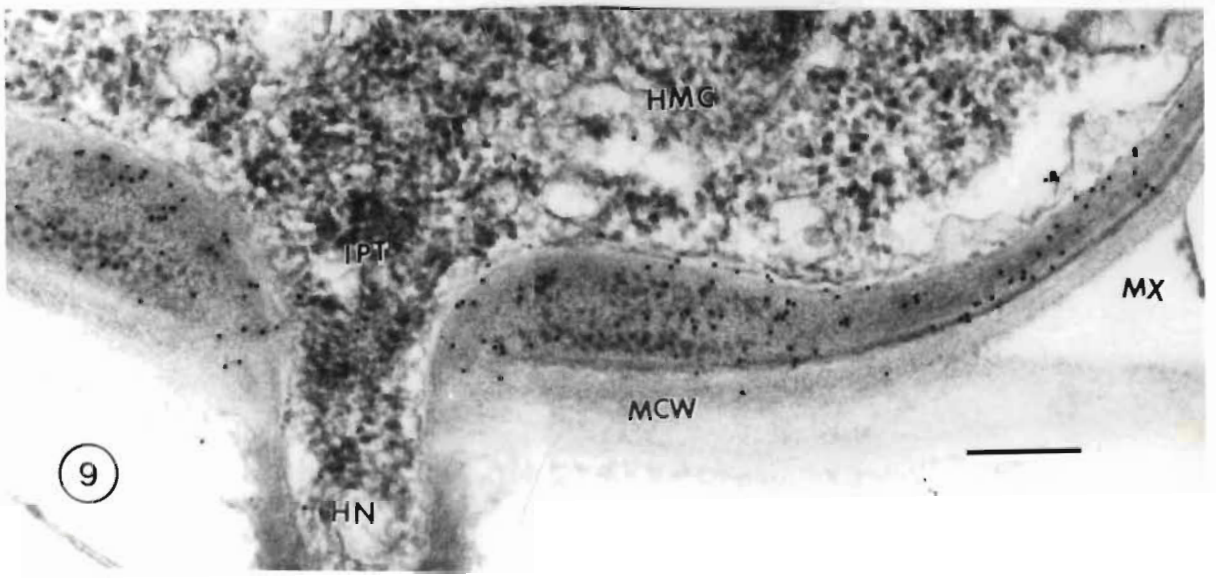
HMC
IPT
MX
MCW
9
HN

PLATE 3

Figs. 10-11. Ultrathin sections of wheat leaf tissues infected by *P. recondita* f.sp. *tritici*, labelled with wheat germ agglutinin (WGA)-gold conjugates which labels *N*-acetylglucosamine residues.

Fig. 10. Septum delimiting the haustorial mother cell (HMC) from the intercellular hypha, is labelled. The protrusions (arrowhead) on the HMC septum are unlabelled. (Bar = 0.2 μm)

Fig. 11. Mature haustorium. Labelling is limited to the wall of haustorial body. (Bar = 0.1 μm)

Figs. 12-14. Ultrathin sections of wheat leaf tissue infected by *P. recondita* f.sp. *tritici* labelled with the Concanavalin A (ConA)-gold complex which identifies glucose/mannose residues.

Fig. 12. Septum separating the haustorial mother cell from the hyphal cell (IH). Walls of hypha and haustorial mother cell, and some glycogen-like granules in fungal cytoplasm are labelled. (Bar = 0.3 μm)

Fig. 13. Labelling is of the starch granules (S) of host chloroplasts (CH). (Bar = 0.2 μm)

Fig. 14. The walls of the haustorial neck (HN) are evenly labelled. (Bar = 0.2 μm)

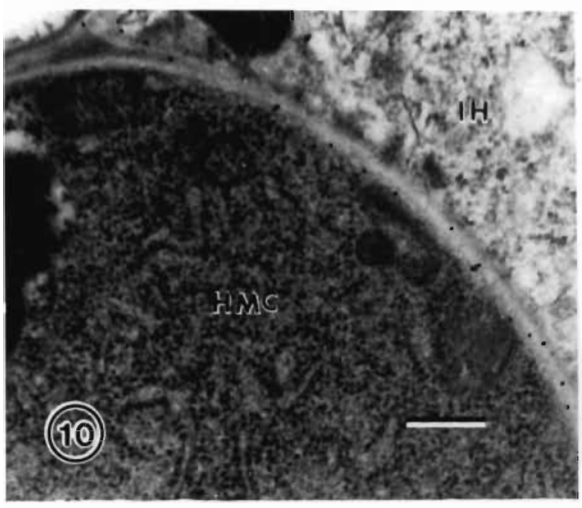
IH
HMC
10

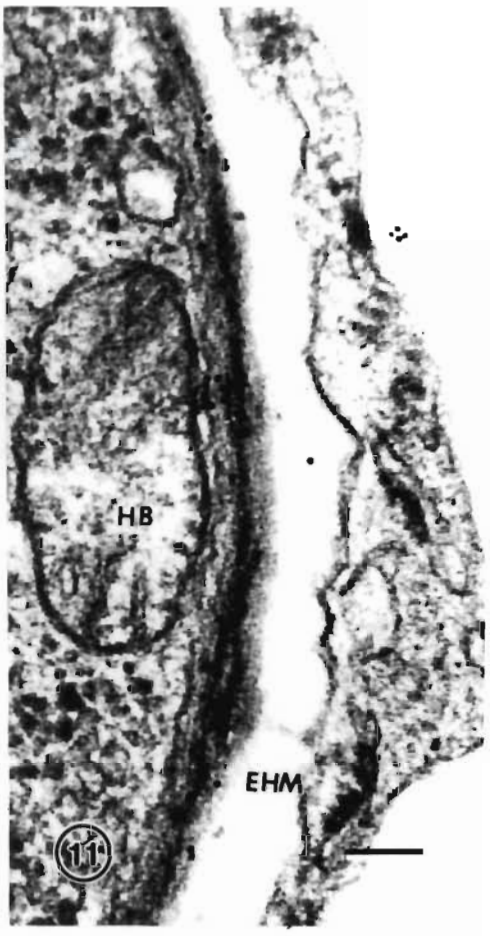
HB
EHM
11

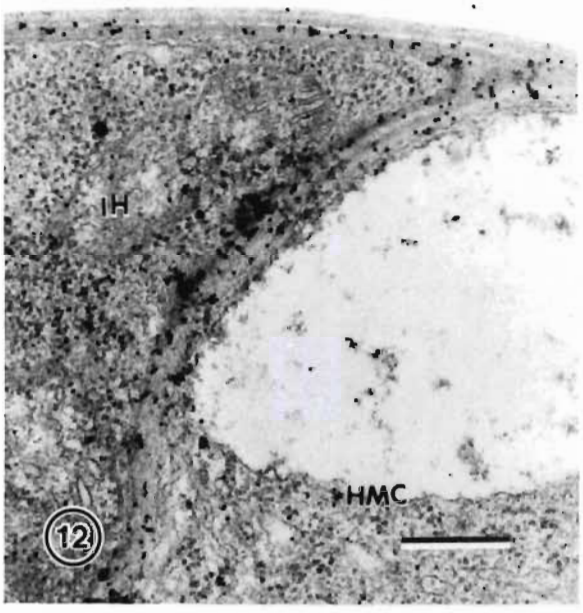
IH
HMC
12

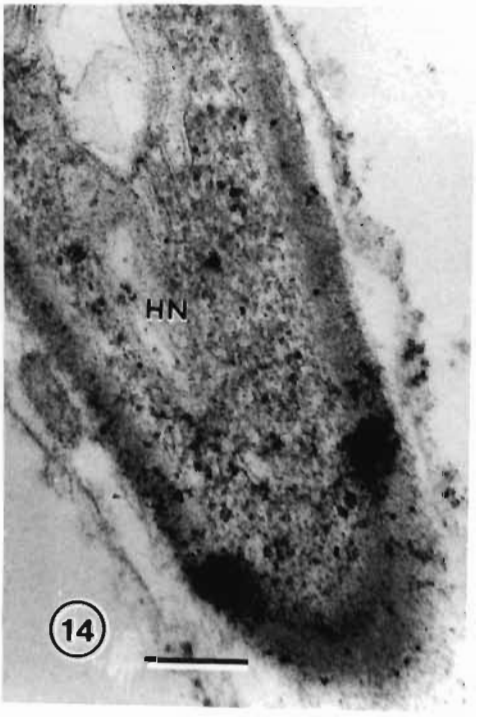
HN
14

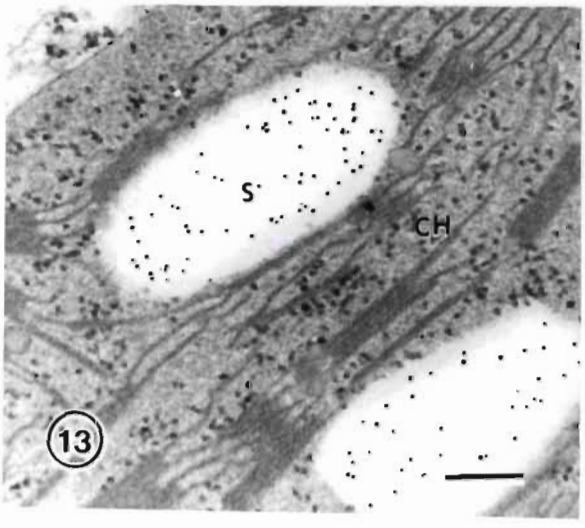
S
CH
13

SBA. Moreover, labelling achieved with SBA was quite variable in this experiment.

After incubation of the sections of wheat leaf tissue infected by the leaf rust with PNA-gold complex, labelling was observed on the cell walls of intercellular hyphae and of host cells (Figs. 18, 19), and the extracellular matrix between the host cells (Fig. 19). At the penetration site, both lectins bound to the intrawall penetration torus (IPT), the annulus and the stem (Fig. 20). They also bound to the haustorial neck wall (Fig. 20). The HMC septum was bound by the PNA-gold complex and a few particles were present over the protrusions (Fig. 21). Similar to the labelling with the ConA-gold complex, PNA and SBA bound to the walls of younger haustorial bodies and the extrahaustorial matrix (Fig. 22), while only to the extrahaustorial matrix in the older haustoria (Fig. 23).

The labelling pattern of the SBA-gold complex was similar to that of PNA-gold complex, but more weakly expressed. SBA lectin bound to fungal hyphal walls (Fig. 24), host cell walls, and walls of the haustorial neck (Fig. 25). In the young haustorium, SBA-gold complex binding occurred over both the haustorial wall and the extrahaustorial matrix (Fig. 26), whereas on the older haustorium, labelling was only present in the extrahaustorial matrix (Fig. 27).

Application of the *Helix pomatia* agglutinin (HPA)-gold complex to sections of infected wheat leaf tissues resulted in a very light labelling over the glycogen-like granules in fungal cytoplasm and no or very few gold particles over the fungal walls and the septum (Fig. 28). No labelling of the walls of haustorial neck was found. However, few gold particles were observed on the walls of the haustorial body and the extrahaustorial matrix (Fig. 30). No labelling was found over host cell walls, host cytoplasm and host organelles.

PLATE 4

Figs. 15-16. Ultrathin sections of wheat leaf tissue infected by *P. recondita* f.sp. *tritici* labelled with the Concanavalin A (ConA)-gold complex which identifies glucose/mannose residues.

Fig. 15. In the younger haustorium, gold particles are deposited over the walls of the haustorial body (HB) and the extrahaustorial matrix (EHM). (Bar = 0.2 μm)

Fig. 16. In the older haustorium, labelling mainly occurs in the extrahaustorial matrix. (Bar = 0.2 μm)

Fig. 17. Ultrathin sections of wheat leaf tissues infected by *P. recondita* f.sp. *tritici* labelled with Lentil agglutinin (LCA)-gold complex which identifies glucose/mannose residues. In the young haustorium, labelling is evident on the walls of the haustorial body (HB), and on the extrahaustorial matrix. (Bar = 0.3 μm)

Fig. 18-20. Ultrathin sections of wheat leaf tissues infected by *P. recondita* f.sp. *tritici*, subjected to incubation with the Peanut agglutinin (PNA)-gold complex which detect galactose residues.

Fig. 18. Labelling occurs on both host cell walls and the walls of the intercellular hypha. (Bar = 0.5 μm)

Fig. 19. The extracellular matrix in the intercellular space between mesophyll cells, is heavily bound by the PNA-gold complex. (Bar = 0.3 μm)

Fig. 20. An oblique section of the haustorial neck at the point of penetration. The intrawall penetration torus (both annulus and stem), the walls of haustorial mother cell (HMC) and the haustorial neck (HN) are strongly labelled. The host cell walls are also heavily labelled. (Bar = 0.5 μm)

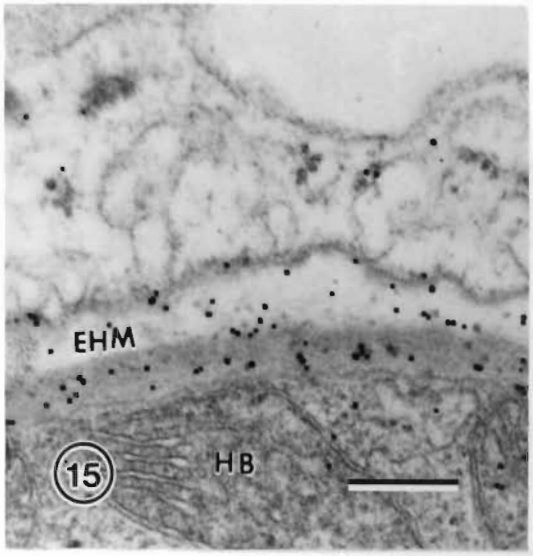
EHM
HB
15

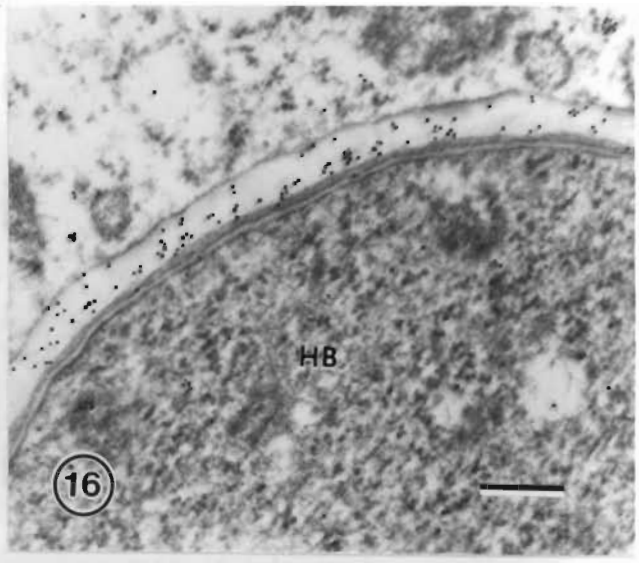
HB
16

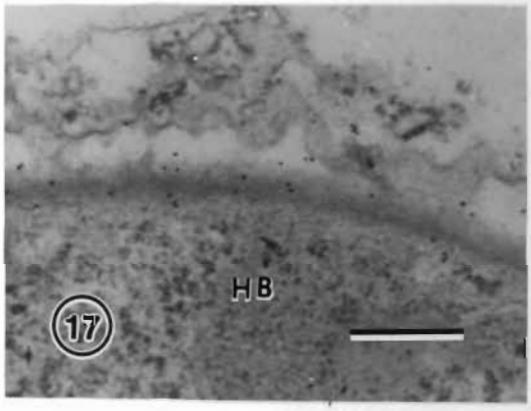
HB
17

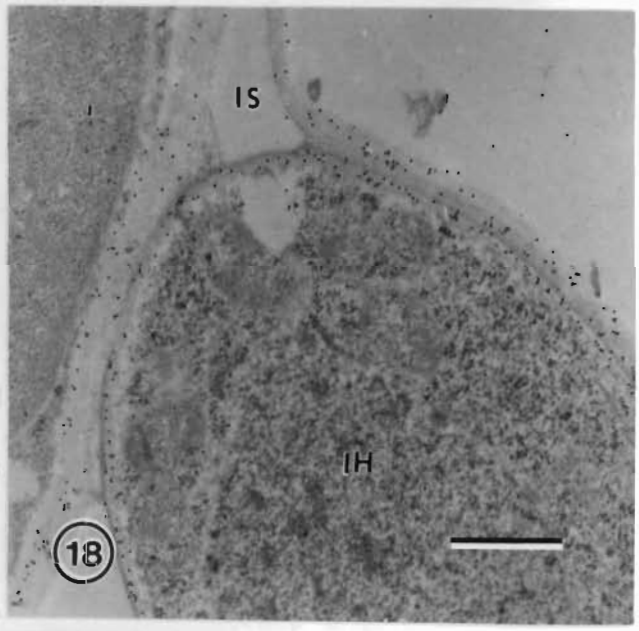
IS
IH
18

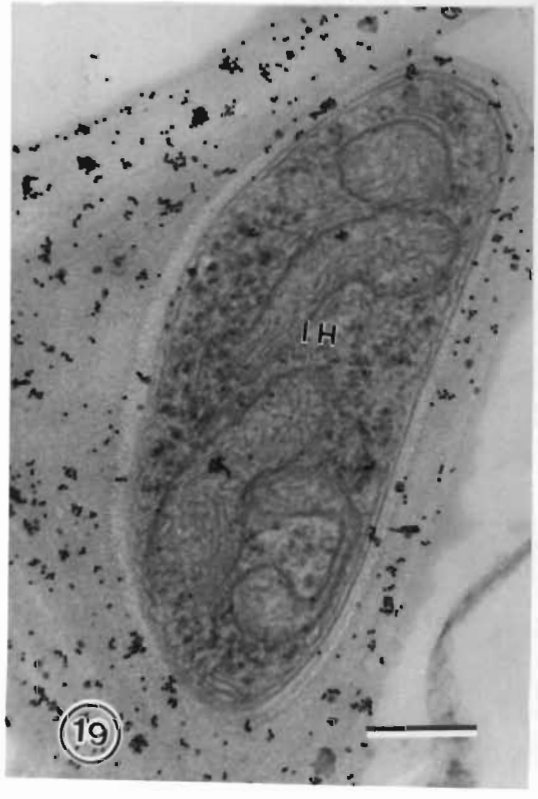
IH
19

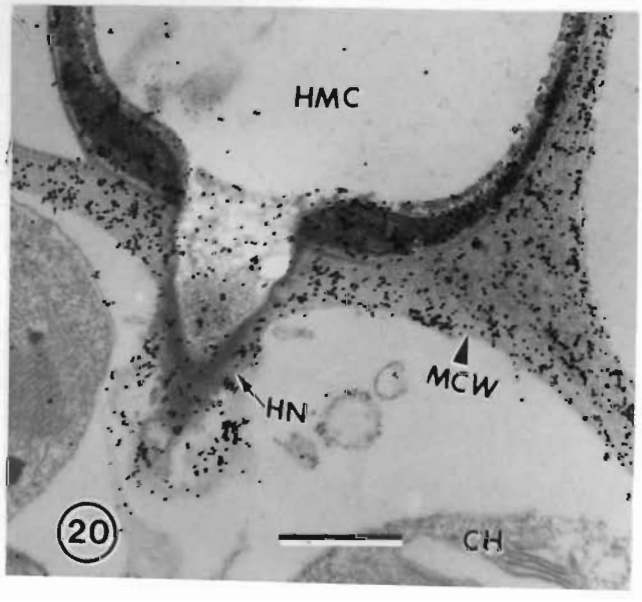
HMC
MCW
HN
20
CH

PLATE 5

Fig. 21-23. Ultrathin sections of wheat leaf tissues infected by *P. recondita* f.sp. *tritici*, subjected to incubation with the Peanut agglutinin (PNA)-gold complex which detect galactose residues.

Fig. 21. The septum between the haustorial mother cell and the hypha, is labelled with the PNA-gold complex. (Bar = 0.3 μm)

Fig. 22. Gold particles are evident on both the wall of haustorial body and the extrahaustorial matrix of a the younger haustorium. (Bar = 0.2 μm)

Fig. 23. In the older haustorium, labelling appears in the extrahaustorial matrix only. (Bar = 0.2 μm)

Figs. 24-27. Ultrathin sections of wheat leaf tissues infected by *P. recondita* f.sp. *tritici* labelled with soybean agglutinin (SBA)-gold complex, which identifies galactose residues.

Fig. 24. A few particles are distributed over the wall of the hyphal cell (IH). (Bar = 0.2 μm)

Fig. 25. A cross-section of haustorial neck. Gold particles are regularly deposited on the walls of haustorial neck. (Bar = 0.2 μm)

Fig. 26. SBA-gold complex binds mainly to the wall of the haustorial body. A few particles are found in the extrahaustorial matrix. (Bar = 0.2 μm)

Fig. 27. A mature haustorium. Gold particles are predominantly present in the extrahaustorial matrix. (Bar = 0.2 μm)

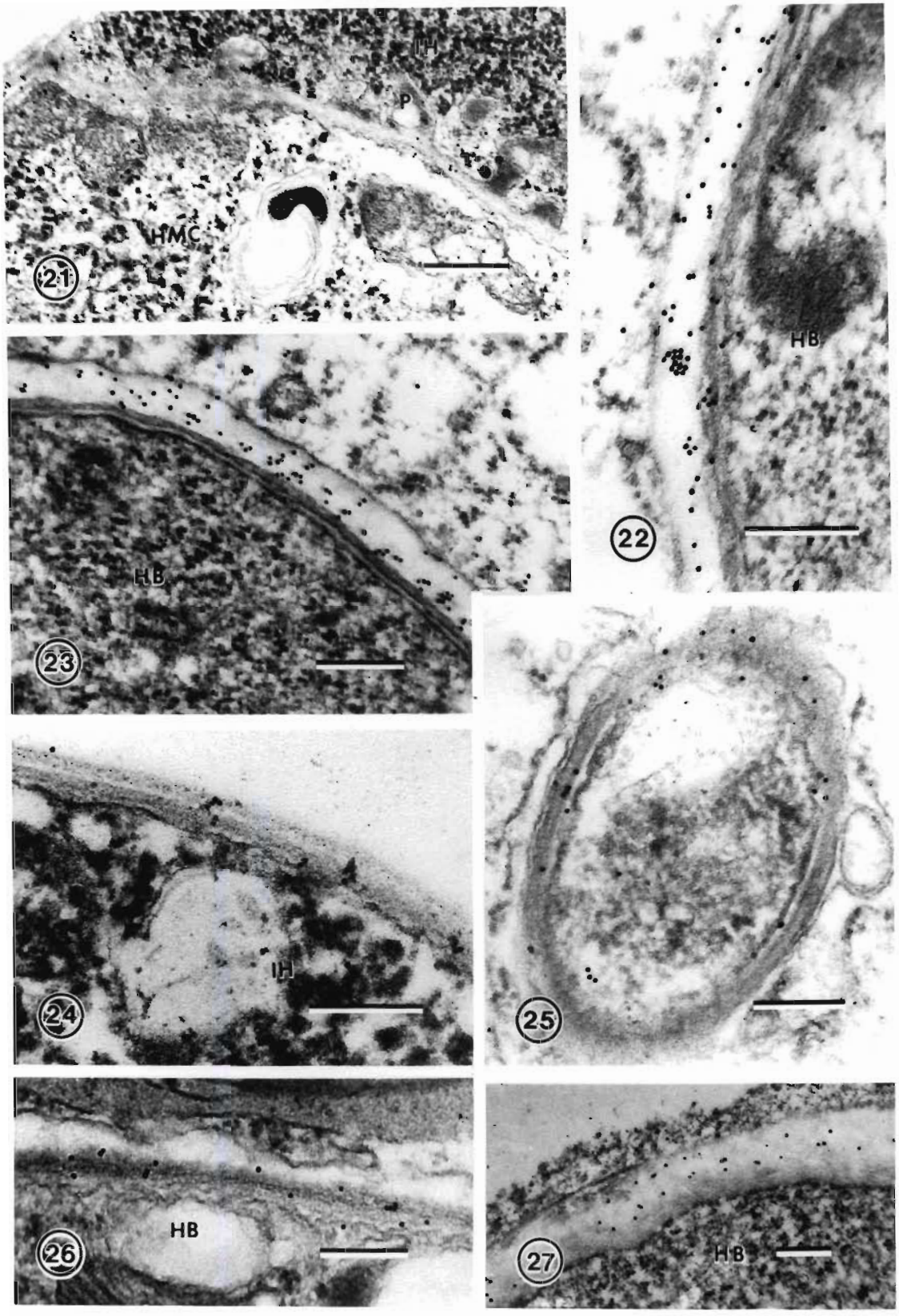
IH
P
HMC
21
HB
22
HB
23
IH
24
25
HB
26
HB
27

PLATE 6

Figs. 28-30. Ultrathin sections of the wheat leaf tissues infected by *P. recondita* f.sp. *tritici* labelled with *Helix pomatia* agglutinin (HPA)-gold complex which identifies *N*-acetylgalactosamine residues.

Fig. 28. The HPA probe only slightly binds to the glycogen-like granules (arrowheads) in the fungal cytoplasm. (Bar = 0.3 μm)

Fig. 29. The starch granules of host chloroplasts (CH) are heavily labelled with the HPA-gold complex. (Bar = 0.3 μm)

Fig. 30. Labelling is present over the wall of haustorial body (HB) and in the extrahaustorial matrix (EHM). (Bar = 0.2 μm)

Figs. 31-33. Ultrathin sections of the wheat leaf tissues infected by *P. recondita* f.sp. *tritici* labelled with the *Ulex europeaus* agglutinin I (UEA I)-gold complex which recognises α-fucose residues.

Fig. 31. Labelling in intercellular hyphae (IH) is predominantly present over the inner walls. (Bar = 0.2 μm)

Fig. 32. Labelling of the walls of the haustorial mother cell (HMC). (Bar = 0.5 μm)

Fig. 33. A section of a haustorium. Gold particles occur mainly on the extrahaustorial matrix. (Bar = 0.2 μm)

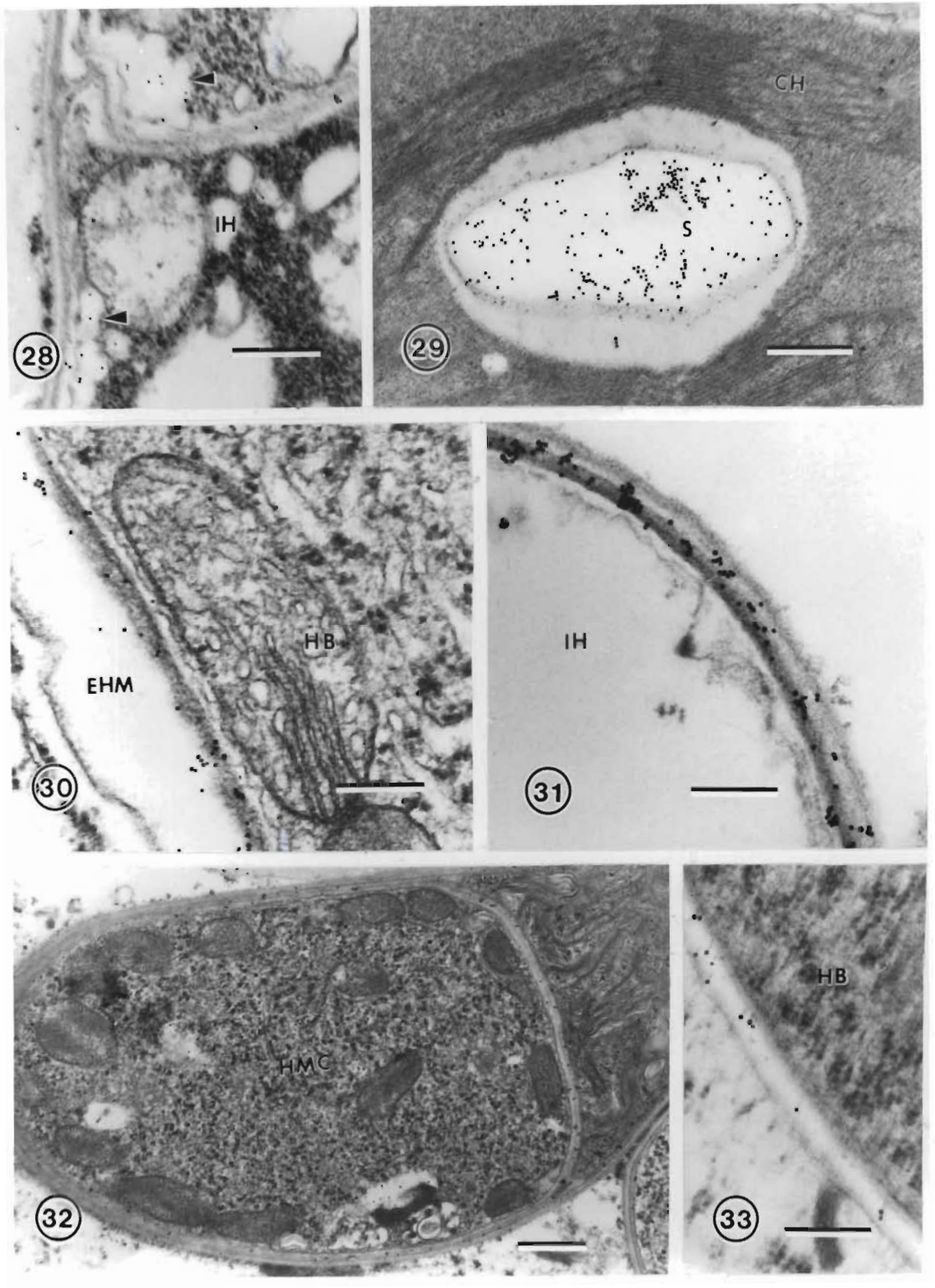
IH
28
CH
S
29
EHM
HB
30
IH
31
HMC
32
HB
33

All three lectins which have an affinity for galactose and/or *N*-acetylgalactosamine residues in this study were found to be able to bind to starch granules in the chloroplasts of the host (Fig. 29).

Localization of α-fucose residues

Using the *Ulex europeaus* agglutinin (UEA I)-gold complex as a probe, gold particles were found to be distributed over the inner walls of the intercellular hyphae (Fig. 31) and the inner walls of haustorial mother cells (Fig. 32). No labelling was demonstrable over the walls of the haustorial neck and the haustorial body, however, gold particles were observed to occur sparsely on the extrahaustorial matrix (Fig. 33). UEA I-gold complex did not bind to the host cell wall, cytoplasm and organelles, but, starch granules in the host chloroplasts were labelled.

Specificity of the labelling patterns obtained with the lectin probes was assessed by the negative results obtained with all control tests. The appropriate sugar inhibitor used for each lectin probe was effective in either greatly reducing the gold labelling (ConA, ULE, SBA) or in completely inhibiting it (WGA, PNA, HPA, LCA).

DISCUSSION

It is universally accepted that the outcome of a host-pathogen interaction involves a series of molecular and cellular recognition processes and constant information exchange between the plant and the pathogen (Lamb et al. 1989). There is increasing evidence that the cell surface carbohydrates of the host

cells and fungal infection structures could be important in the interaction, e.g. in attachment of fungal spores, germ-tubes and appressoria to the plant surface (Nicholson and Epstein 1991), and in the determination of cell-cell recognition (Callow 1977, Hahn et al. 1989; Mazau et al., 1988). Moreover, degradation of the plant cell wall by fungal enzymes, or by hydrolytic enzymes of the plants, may lead to the release of potential elicitors of the plant defense system (Esquerré-Tugayé et al. 1979). Undoubtedly, an understanding of the localization and distribution of these molecules in the infected tissues, is a prerequisite to a more comprehensive knowledge of the host-fungus interaction. Results of this study illustrate the location of some of these molecules on and in plant and fungal structures during the interaction between wheat and *P. recondita* f.sp. *tritici*.

Plant cell walls contain cellulose as the major structural component (McNeil et al. 1984), while the presence of cellulose has been confirmed in the walls of a few fungi as well (Benhamou et al. 1987, Benhamou 1988). Several cytochemical techniques have been developed to demonstrate the localization and distribution of cellulose. Among them, the method based on the use of an enzyme, e.g. cellulase, as an extractive agent, has led to the discovery of the occurrence of cellulose in the extrahaustorial matrix and in the host tubules in host cytoplasm which are associated with the haustorium in the oat-*P. coronata* f.sp. *avenae* interaction (Chong et al. 1981, 1986, Harder and Chong 1991). With similar enzyme preparations, Gil and Gay (1977), Scannerini and Bonfante-Fasolo (1979) and Hickey and Coffey (1978) also reported that cellulose is a component of the extrahaustorial matrix in other plant-fungal interactions. In rusts, the nature of extrahaustorial matrix has received considerable attention (see reviews in Littlefield and Heath 1979, Harder 1989). Since the cellulose is not detected elsewhere in the rust fungus, Chong et al.(1981, 1986) and Harder and Chong (1991) proposed

that the presence of cellulose is evidence that the extrahaustorial matrix is of host origin. However, in the present investigation, using the cellulase-gold conjugated probe which could specifically detect cellulose, the author can only localize the cellulose of the host cell wall, while no labelling was observed elsewhere in the wheat-*P. recondita* f.sp. *tritici* interaction. The host tubules associated with the invaded haustorium and the extrahaustorial matrix, regardless of the age of haustorium development remained unlabelled. Under the conditions of the protocol used here, the present observations reveal that cellulose does not appear to occur in the extrahaustorial matrix of wheat leaf tissues infected by *P. recondita* f.sp. *tritici*. This finding may reflect differences in the components of the extracellular matrix between oat crown rust and wheat leaf rust, or differences between the methods that were used and/or, but less likely, the possibility that the cellulose in this tissue was not available for binding to the probe. Findings presented here agree with the observations of Coffey and Allen (1983), that in flax tissue infected by *Melampsora lini* the extrahaustorial matrix was not affected by treatment with a cellulase preparation.

Conventional electron microscopy has revealed that the host cell wall is seldomly distorted at the site of penetration and that the dissolution of the host cell wall by rust fungi is restricted to the site of penetration (Chong et al. 1981, Taylor and Mims 1991) thus indicating that the penetration of the host cell wall appears to be enzymatic. The present study, using the labelling probe for cellulose, showed that, at most penetration sites, no distortion of the host cell wall is observed, supporting the view that cellulose around the infection peg is enzymatically degraded. However, in a few instances, cellulose labelling showed that the host cell wall is pushed into the cytoplasm. This may indicate that, while the penetration by *P. recondita* f.sp. *tritici* mainly occurs as a result of the localized dissolution of host cell wall by cellulolytic

enzymes, mechanical forces possibly facilitate penetration. The other evidence for mechanical force is the extra wall layers in the HMC, which may help to contain the turgor pressure of mechanical force. The activity of cellulolytic enzymes has been investigated in *Uromyces viciae-fabae* (Deising and Mendgen 1992, Heiler et al. 1993). These authors found that cellulases are formed in the rust fungus after the perception of a thigmotropic stimulus, and continue to be produced during the later stage of infection structure differentiation, suggesting that the cellulolytic enzymes, especially those formed at a later stage of development, might be involved in localized dissolution of the host cell wall.

Chitin, a ß-1,4-linked homopolymer of *N*-acetyl-D-glucosamine, is an important structural component in cell walls of many fungal pathogens (Wessels and Sietsma 1981, O'Connell and Ride 1990), including rust fungi (Chong et al. 1981, 1986, Ebrahim-Nesbat et al. 1985, Heath 1989, Kapooria and Mendgen 1985, Mendgen et al. 1985). It is also believed to be a potent elicitor of host lignification and other defense mechanisms (Barber et al. 1989, Kurosaki et al. 1988, Roby et al. 1988). Chitin is a target of plant chitinases, which are able to inhibit hyphal growth and cause the lysis of hyphal tips *in vitro* (Broekaert et al. 1988, Mauch et al. 1988, Schlumbaum et al. 1986). In the present investigation, the labelling pattern of chitin in the interaction between wheat and *P. recondita* f.sp. *tritici*, using the WGA-gold complex, was similar to that in the interaction between wheat and *P. graminis* f.sp. *tritici* (Chong et al. 1986). Chitin was detected on the inner layers of hyphal cell walls and HMC walls. It was also demonstrated in the walls of haustorial bodies, but neither in the walls of the haustorial neck nor in the extrahaustorial matrix. The extrahaustorial matrix of obligately biotrophic fungi, such as other rusts (Chong et al. 1981, 1986) and powdery mildews (Ebrahim-Nesbat et al. 1985) also lacks *N*-acetyl-D-glucosamine residues.

Freytag and Mendgen (1991) suggested that a thick chitin layer in haustorial mother cells might reflect the requirement to resist the high turgor pressure during penetration. It has been proposed that the chitin in cell walls may be mixed with some glycoproteins and/or sugar residues (Freytag and Mendgen 1991).

Similar to that in *P. graminis* f.sp. *tritici*, the composition of walls of the haustorial body of *P. recondita* f.sp. *recondita* appears to change as the haustorium matures. In the present study, the walls of younger haustoria contained binding sites for ConA, LCA, PNA and SBA, indicating the presence of glucose/mannose and galactose residues, whereas in older haustoria, the walls of the haustorial body seemed to have lost their binding sites for these lectins but only bind to WGA which labels *N*-acetylglucosamine residues. The reason remains unknown. The appearance of PNA- and SBA-labelling in this study was somewhat different from that in *P. graminis* f.sp. *tritici* (Rohringer et al. 1989). Both lectins were found not to have affinities for the walls of the haustorial body of *P. graminis* f.sp. *tritici*, whereas in the present study, PNA and SBA appeared to bind to the walls of younger haustoria, while the haustoria, as they matured, lost their binding affinities. This may reflect a composition difference between the different rust species. The author's suggestion could be supported by the reports that there are no galactose residues (as demonstrated by PNA and another lectin, *Ricinus communis* agglutinin I, RCA I) on the surfaces of the infection structures of two rust fungi, *P. coronata* f.sp. *avenae* and *Uromyces appendiculatus* f.sp. *appendiculatus* (Mendgen et al. 1985).

In an attempt to isolate haustoria from wheat leaves infected by *P. recondita* f.sp. *tritici*, Cantrill and Deverall (1993) described that WGA and ConA were observed to bind to host-free haustoria in a similar pattern. Our result for the

same fungus is contrary to this report. This may, although the authors (Cantrill and Deverall 1993) doubted this, reflect the difference between fresh and fixed materials and the relative preservation and availability of active binding sites.

Labelling with HPA-gold conjugate results in the localization of *N*-acetylgalactosamine residues. In this study, HPA labelling is only found in the glycogen-like granules in fungal cytoplasm and in the extrahaustorial matrix, but not in other infection structures. The presence of *N*-acetylgalactosamine residues was also demonstrated on the substomatal vesicle of *Uromyces appendiculatus* (rust of bean), using a lectin *Phaseolus vulgaris* agglutinin (PHA) probe (Mendgen et al. 1985). Substomatal vesicles may possess specific sites for the interaction between the fungus and its host (Mendgen et al. 1985). These structures were, however, not studied by the present author.

Ulex europeaus agglutinin (UEA I) has specific affinity for α-L-fucose. In the present study, UEA I binding sites were found in the walls of both the fungal hyphae and the haustorial mother cells, and more interestingly, in the extrahaustorial matrix. α-L-fucose may be involved in the recognition processes in the interaction between wheat and *P. recondita* f.sp. *tritici*. This is in contrast to the report concerning *P. graminis* f.sp. *tritici,* using lectin, *Lotus tetragonolobus* agglutinin (LTA) as the probe (Rohringer et al. 1989). The binding of fucose-specific LTA was only found on outer layers of the hyphal cell of *P. graminis* f.sp. *tritici* and was not inhibitable with the haptens. These differences may be explained by the fact that we used a different lectin in this study or because of the different disease system. α-L-fucose-specific LTA binding was also demonstrated in the dikaryotic infection hyphae of *Uromyces rumicis* (Freytag and Mendgen 1991a, b), indicating that α-L-fucose

might be involved in the regulation of host compatibility. Besides, fucose has been reported to be a component of the germ tube walls of *P. graminis* f.sp. *tritici* (Kim et al. 1982).

Summarizing the observations, the present study provides additional information on the nature and composition of the walls of the fungal hyphae, the haustorial mother cell, the haustorial neck, the haustorial body and the extrahaustorial matrix. Especially the new information about the extrahaustorial matrix as the interface between the fungus and the host tissue, is significant, this study confirming the existence of mannose/glucose and galactose residues in the extrahaustorial matrix. *N*-acetylgalactosamine and fucose residues as components of the extrahaustorial matrix has not hitherto been reported. It however needs to be stressed that there may be significant differences between the surface characteristics of different disease system.

ConA, LCA, PNA, SBA, HPA and ULE I were found to bind to the starch granules in the host chloroplasts. It is reasonable to assume that granules, besides starch, may contain other glycosubstances, such as galactans.

REFERENCES

Andres MW, Wilcoxson RD (1984) A device for uniform deposition of liquid-suspended urediospores on seedling and adult cereal plants. Phytopathology 74: 550-552

Barber MS, Bertram RE, Ride JP (1989) Chitin oligosaccharides elicit lignification in wounded wheat leaves. Physiol Mol Plant Pathol 34: 3-12

Benhamou N (1988) Ultrastructural localization of carbohydrates in the cell walls of two pathogenic fungi: A comparative study. Mycologia 80: 324-337

- (1995) Elicitor-induced resistance in tomato plants against fungal pathogens: ultrastructure and cytochemistry of the induced response. Scan Microsc 9: 861-880

- Bélanger RR, Paulitz TC (1996) Pre-inoculation of Ri T-DNA-transformed pea roots with *Pseudomonas fluorescens* inhibits colonization by *Pythium ultimum* Trow: an ultrastructural and cytochemical study. Planta 199: 105-117

- Chamberland H, Ouellette GB, Pauzé FJ (1987) Ultrastructural localization of cellulosic ß-(1→4)-D-glucans in two pathogenic fungi and in their host tissues by means of an exoglucanase-gold complex. Can J Microbiol 5: 405-417

Broekaert WF, Van Parijs J, Allen AK, Peumans WJ (1988) Comparison of some molecular, enzymatic and antifungal properties of chitinases from thorne-apple, tobacco and wheat. Physiol Mol Plant Pathol 33: 319-331.

Callow JA (1977) Recognition, resistance and the role of plant lectins in host-parasite interactions. Adv Bot Res 4: 1-49

Cantrill LC, Deverall BJ (1993) Isolation of haustoria from wheat leaves infected by the leaf rust fungus. Physiol Mol Plant Pathol 422: 337-343

Chong J, Harder DE, Rohringer R (1981) Ontogeny of mono- and dikaryptic rust haustoria: Cytochemistry and ultrastructural studies. Phytopathology 71:

975-983

- - - (1985) Cytochemistry studies on *Puccinia graminis* f.sp. *tritici* in a compatible wheat host. I. Walls of intercellular hyphal cells and haustorium mother cells. Can J Bot 63: 1713-1724

- - - (1986) Cytochemistry studies on *Puccinia graminis* f.sp. *tritici* in a compatible wheat host. II. Haustorial mother cell walls at the host cell penetration site, haustorial walls, and the extrahaustorial matrix. Can J Bot 64: 2561-2575

Coffey MD, Allen FHE (1983) A quantitative histological and ultrastructural analysis of interactions between the flax rust and near-isogenic host lines varying in their degree of incompatibility. Can J Bot 61: 1831-1850

Deising H, Mendgen K (1992) Developmental control of enzyme production and cell wall modification in rust fungi, and defence reactions of the host plant. In: Stahl, UT (ed.) Molecular Biology of Filamentous Fungi. Weinheim, New York, pp 27-44

Ebrahim-Nesbat F, Hoppe HH, Rohringer R (1985) Lectin binding studies on the cell walls of soybean rust (*Phakopsora pachyrhizi* Syd.). Phytopathol Z 114: 97-107

Esquerré-Tugayé MT, Lafitte C, Mazau D, Toppan A, Touzé A (1979) Cell surfaces in plant-microorganism interaction. II. Evidence for the accumulation of hydroxyproline-rich glycoproteins in the cell wall of diseased plants as a defense mechanism. Plant Physiol 64: 320-326

Freytag S, Mendgen K (1991a) Carbohydrates on the surface of urediniospore- and basidiospore-derived infection structures of heteroecious

and autoecious rust fungi. New Phytol 119: 527-534

- - (1991b) Surface carbohydrates and cell wall structure of *in vitro* induced uredospore infection structures of *Uromyces viciae-fabae* before annd after treatment with enzymes and alkali. Protoplasma 161: 94-103.

Gil F, Gay JL (1977) Ultrastructural and physiological properties of the host interfacial components of haustoria of *Erysiphe pisi in vivo* and *in vitro*. Physiol Plant Pathol 10: 1-12

Hahn MG, Buchell PP, Gervone F, Doares SH, O'Neill RA, Darvill A, Albersheim P (1989) The roles of cell wall constituents in plant-pathogen interactions. Mol Plant-Microbe Interact 3: 131-181

Harder DE (1989) Rust fungal haustoria - past, present and future. Can J Plant Pathol 11: 91-99

- Chong J (1991) Rust haustoria. In: Mendgen, K, Lesemann, DE (eds) Electron microscopy of Plant Pathogens. Springer-Verlag. Berlin, pp 235-250

- - Rohringer R, Mendgen K, Schneider A, Welter K, Knauf G (1989) Ultrastructure and cytochemistry of extramural substances associated with intercellular hyphae of several rust fungi. Can J Bot 76: 2043-2051

Heath MC (1989) *In vitro* formation of haustoria of the cowpea rust fungus, *Uromyces vignae*, in the absence of a living plant cell. I. Light microscopy. Physiol Mol Plant Pathol 35: 357-366

Heiler S, Mendgen K, Deising H (1993) Cellulolytic enzymes of the obligately biotrophic rust fungus *Uromyces viciae-fabae* are regulated differentiation-specifically. Mycol Res 97: 45-52

Hickey EL, Coffey MD (1978) A cytochemical investigation of the host-parasite interface in *Pisum sativum* infected by the downy mildew fungus *Peronospora pisi*. Protoplasma 97: 201-220

Kapooria RG, Mendgen K (1985) Infection structures and their surface changes during differentiation in *Uromyces fabae*. Phytopathol Z 113: 317-323

Kim WK, Rohringer R, Chong J (1982) Sugar and amino acid composition of macromolecular constituents released from walls of uredosporelings of *Puccinia graminis tritici*. Can J Plant Pathol 4: 317-327

Kurosaki F, Tashiro N, Nishi A (1988) Role of chitinase and chitin oligosaccharides in lignification response of cultured carrot cells treated with mycelial walls. Plant Cell Physiol 29: 527-531

Lamb CJ, Lawton MA, Dron M, Dixon RA (1989) Signals and transduction mechanisms for activation of plant defense against microbial attack. Cell 56: 215-224

Littlefield LJ, Heath MC (1979) Ultrastructure of Rust Fungi. Academic Press. New York

Mauch F, Mauch-Mani B, Boller T (1988) Antifungal hydrolases in pea tissue II. Inhibition of fungal growth by combinations of chitinase and ß-1,3-glucanase. Plant Physiol 88: 936-942.

Mazau D, Rumeau D, Esquerré-Tugayé MT (1988) Molecular approaches to understanding cell surface interactions between plants and fungal pathogens. Plant Physiol Biochem 25: 337-343

McNeil M, Darvill AG, Fry SC, Albersheim P (1984) Structure and function of the primary cells of plants. Ann Rev Biochem 53: 625-663

Mendgen K, Lange M, Bretschneider K (1985) Quantitative estimation of the surface carbohydrates on the infection structures of rust fungi with enzymes and lectins. Arch Microbiol 140: 307-311

Nicholson RL, Epstein L (1991) Adhesion of fungi to the plant surface: Prerequisite for pathogenesis. In: Cole GT, Hoch HC (Eds.) The fungal spore and disease initiation in plants and animals. Plenum Press, New York. pp. 3-23.

- Yoshioka H, Yamaoka N, Kunoh H (1988) Preparation of the infection court by *Erysiphe graminis*. II. Release of esterase enzyme from conidia in response to a contact stimulus. Exp Mycol 12: 336-349

O'Connell RJ, Ride JP (1990) Chemical detection and ultrastructural localization of chitin in cell walls of *Colletotrichum lindemuthianum*. Physiol Mol Plant Pathol 37: 39-53

Roby D, Gadelle A, Toppan A (1987) Chitin oligosaccharides as elicitors of chitinase activity in melon plants. Biochem Biophys Res Comm 143: 885-892

Rohringer R, Chong J, Gillespie R, Harder DE (1989) Gold-conjugated arabinogalactan-protein and other lectins as ultrastructural probes for the wheat/stem rust complex. Histochemistry 91: 383-393

Scannerini S, Bonfante-Fasolo P (1979) Ultrastructural cytochemical demonstration of polysaccharides and proteins within the host-arbuscule interfacial matrix in an endomycorrhiza. New Phytol 83: 87-94

Schlumbaum A, Mauch F, Vögeli U, Boller T (1986) Plant chitinases are potent inhibitors of fungal growth. Nature 324: 365-367

Taylor J, Mims CW (1991) Fungal development and host cell responses to the rust fungus *Puccinia substriata* var. *indica* in seedling and mature leaves of susceptible and resistant pearl millet. Can J Bot 69: 1207-1219

Wessels JGH, Sietsma JH (1981) Fungal cell walls: a survey. In: Tanner W, Loewus FA (eds) Plant Carbohydrates. II. Extracellular Carbohydrates, Encyclopedia of Plant Physiology (New Series). Vol. 13B. Springer-Verlag, Berlin, pp 352-394

CHAPTER 6

SUBCELLULAR LOCALIZATION OF ß-1,3-GLUCANASE IN *PUCCINIA RECONDITA* F.SP. *TRITICI*-INFECTED WHEAT LEAVES

INTRODUCTION

Plants have developed a wide range of mechanisms to defend themselves against the attack of plant fungal pathogens, for instance, the accumulation of antifungal phytoalexins, lignification, the deposition of callose and phenolic compounds, the increase of wall-bound hydroxyproline-rich glycoproteins (HRGPs) and toxic proteins (thionins), and the synthesis of proteinase inhibitors and hydrolytic enzymes (Benhamou *et al.*, 1990). The possible implication of plant hydrolytic enzymes, such as ß-1,3-glucanase and chitinase, in the defense against fungal infection, has received much attention in recent years (Boller, 1987; Graham and Graham, 1991; Linthorst, 1991; Van Loon, 1989; Young and Pegg, 1982). Since many fungi contain ß-1,3-glucan and chitin as the main structural components of their cell walls (Wessels and Sietsma, 1981; Young and Pegg, 1982), it seems reasonable to assume that the enhancement of ß-1,3-glucanase and chitinase after fungal infection, might play an important role in plant defense against invasion by the pathogen. It has been established that hydrolytic enzymes can degrade fungal cell wall components and cause growth inhibition of fungi *in vitro* (Arlorio *et al.*, 1992; Mauch *et al.*, 1988; Young and Pegg, 1982). Furthermore, recent

research has indicated that the breakdown products of fungal wall components, caused by hydrolytic activity, may act as the potential elicitors of secondary stress metabolites, which then elicit the active defense response of plants (Ham *et al.*, 1991; Keen and Yoshikawa, 1983; Takeuchi, 1990). This has been supported by evidence that increases in ß-1,3-glucanase and chitinase activities in tomato plants, following the infection by the pathogen of tomato leaf mould, *Cladosporium fulvum* (syn. *Fulvia fulva*), occurred earlier and to a higher extent in resistant than in susceptible tomato cultivars (Joosten and De Wit, 1989). Moreover, it has also been reported that transgenic tobacco seedlings constitutively expressing a bean chitinase gene show an enhancement in resistance to the fungal pathogen, *Rhizoctonia solani* (Boglie, 1991).

In an attempt to demonstrate the role of the hydrolytic enzymes in fungal disease resistance *in vivo*, Mauch and Staehelin (1989) and Mauch *et al.* (1992) investigated the subcellular localization of chitinase and ß-1,3-glucanase in ethylene-stressed bean leaves, and found that both enzymes accumulated mainly in intravacuolar aggregates, and that small amounts of ß-1,3-glucanase occurred in the middle lamellae of the plant cell walls. They proposed a model outlining the possible implication of these hydrolytic enzymes in defense and recognition events during host-parasite interactions. Benhamou *et al.* (1989) examined the spatial localization of ß-1,3-glucanase in fungal wilt-infected plants and found that ß-1,3-glucanase accumulation in resistant plants was an early event associated with the limitation of the fungal pathogens, and that ß-1,3-glucanase accumulated at the surface of walls of the invading fungus. Those authors concluded that ß-1,3-glucanase participates in resistance against fungal invasion. In the incompatible tomato-*Cladosporium fulvum* interaction, strong labelling for ß-1,3-glucanase activity was shwon on the degenerated materials of fungal origin and that very strong

labelling of ß-1,3-glucanase was present in the electron-dense structures of plant origin, which were only found in the incompatible interaction, in the extracellular space (Wubben *et al.*, 1992). The results indicated that ß-1,3-glucanase could play an important role in the active defense of tomato plants against *Cladosporium fulvum.*

For cereal diseases, Kemp *et al.* (1996a) reported that, in the wheat-*Puccinia recondita* Rob. ex Desm. f.sp. *tritici* Eriks. and Henn. interaction, at the adult plant stage, ß-1,3-glucanase activity in resistant wheat lines, which either show a hypersensitive reaction or a partial resistance reaction, is higher than that in a susceptible wheat line after inoculation. Those authors also described the role of ß-1,3-glucanase in the inhibition of germination of *Puccinia recondita* f.sp. *tritici* urediospores (Kemp *et al.*, 1996b). In a study of the ultrastructural localization of ß-1,3-glucanase in susceptible wheat leaves after infection by *Puccinia graminis* f.sp. *tritici*, Sock *et al.* (1990) found that ß-1,3-glucanase was mainly associated with the outer wall of host cell walls and fungal cell walls, and the extracellular matrix.

In this investigation, a detailed subcellular localization of extracellular ß-1,3-glucanase in compatible and incompatible interactions between wheat (*Triticum aestivum* L.) and *Puccinia recondita* f.sp. *tritici*, the pathogen of wheat leaf rust, is described. The possible role of ß-1,3-glucanase in the resistance reaction of wheat leaves against infection is discussed.

MATERIALS AND METHODS

Plant materials, inoculum and inoculation

Susceptible wheat line Thatcher, and resistant near-isogenic wheat line, RL 6078 (conferring resistant gene *Lr26*) were used in this study. The inoculum of *Puccinia recondita* f.sp. *tritici*, was the South African pathotype UVPrt 8 which has an avirulence/virulence combination of *3a,3bg,3ka,11,16,20,26,30/1,2a,2b,2c,10,14a,15,17,24*.Bothwheatseeds and inoculum were kindly provided by Professor Z.A, Pretorius, Department of Plant Pathology, University of the Orange Free State, South Africa. RL 6078 (*Lr26*) shows a hypersensitive reaction to UVPrt 8.

Freshly harvested urediospores of *P. recondita* f.sp. *tritici* from the plants of Agent, a susceptible wheat line used for the multiplication of the urediospores, were applied to inoculate the adaxial surface of the first leaf of 10-day-old plants at an inoculum dose of 45 mg urediospores per ml of Soltrol 130 (Phillips Chemical Co.), using a modified Andres and Wilcoxson (1984) inoculator. Inoculated plants were allowed to dry for about 1 hour before placement in a dark dew chamber at 20°C for 20 hours. The inoculated leaves were sampled 5 days after inoculation.

Tissue processing for electron microscopy

The harvested leaves were cut into 3×3 mm pieces and fixed in 3% glutaraldehyde in a 0.05 M sodium cacodylate buffer (pH 7.2) overnight, and washed twice in that buffer. The samples were dehydrated in serial ethanol and embedded in Epon-Araldite resin. Ultrathin sections were cut using a

diamond knife and collected on 200 or 300 mesh nickel grids for imunocytochemical processing.

Immunogold labelling

Antiserum raised in rabbit against the 33 kDa extracellular ß-1,3-glucanase purified from the intercellular washing fluid (IWF) was used for the subcellular localization of ß-1,3-glucanase in the wheat-*P. recondita* f.sp. *tritici* interaction in this study. The antibody was prepared by Dr X.M. Qian, Department of Botany, University of the Orange Free State, South Africa. Western blotting analysis indicated that the antiserum specifically recognizing both acidic and basic *ß-1,3-glucanase*s (Qian, personal communication).

Ultrathin sections on nickel grids were first treated with 5% aqueous sodium metaperiodate for 30 min to improve the immunolabelling and were then completely rinsed with double-distilled water, transferred to one drop of 0.01 M phosphate-buffered saline (PBS), pH 7.4, containing 0.2% (W/V) polyethylene glycol 20,000 (PEG 20,000) for 5 min at room temperature. Then the sections were incubated in a drop of block solution consisting of 0.01 M PBS, pH 7.4, 10% (V/V) fetal bovine serum, 1% (W/V) bovine serum albumin (BSA), 0.05% (V/V) Tween-20 and 0.2% (W/V) sodium azide for 30 min at room temperature. They were then incubated directly in a drop of 20 μl primary antibody (antiserum against ß-1,3-glucanase) at a 1:1200 dilution in 0.01 M PBS, pH 7.4, containing 1% BSA) in a moist chamber overnight at 4°C. After washing in a series of drops of washing solution (0.01 M PBS, pH 7.4, containing 1% BSA and 0.05% Tween-20), they were transferred into a drop of colloidal gold (10 nm)-conjugated goat antiserum to rabbit immunglobulins (GAR-gold antibody) diluted 1:20 in a PBS-BSA buffer for 1 hour at room temperature. Grids with sections were finally washed with 0.01

M PBS, pH 7.2, fixed in 1 % glutaraldehyde for 2 min, rinsed with double-distilled water and counterstained with uranyl acetate and lead citrate. The grids with sections were viewed with a JEOL 100 CX Transmission Electron Microscope at 80 kV.

Immunocytochemical controls

Controls for the specificity of the immunogold labelling were as follows: 1. incubation with PBS-BSA in the absence of the primary antibody; 2. substitution of the immune serum by the pre-immune serum; and 3. pre-absorption of antiserum with 20 μl purified wheat ß-1,3-glucanase. For pre-absorption, 20 μl ß-1,3-glucanase (120 $\mu g/ml^{-1}$) was added to 20 μl of a 1:50 dilution of antiserum and solutions were incubated at 4°C for 20 h.

RESULTS

Immunocytochemical controls

Immunocytochemical controls, either incubated with PBS-BSA in the absence of the primary antibody or after replacement of primary antibody with the pre-immune serum, were completely free of labelling (Figs. 1, 2). The sections treated with ß-1,3-glucanase, pre-absorbed with the purified antigen (ß-1,3-glucanase) showed a significant decrease in labelling intensity relative to the labelling of the sections (Fig. 3), indicating that the labelling with the antiserum is specific.

Immunogold localization of ß-1,3-glucanase in the compatible wheat-P. recondita f.sp. tritici interaction

The ultrastructural characteristics of the interaction between wheat and *P. recondita* f.sp. *tritici* have been described in more detail in Chapter 3. In the compatible interaction, little ß-1,3-glucanase labelling was found in the mesophyll cell plasmalemma and in the domain of the cell wall near the host plasmalemma (Fig. 4). Much labelling was observed on the cell walls of guard cells (Fig. 5), the secondary thickening of xylem vessels (Fig. 6), and the cell wall of phloem elements (Fig. 7). No or little labelling was displayed in the aggregates found in vacuoles, in the host cytoplasm and in the host organelles, such as nuclei, Golgi bodies, endoplasmic reticulum, mitochondria and choloroplasts. The fungal intercellular hyphae showed some labelling on the cell walls and in the hyphal cytoplasm (Fig. 8). Considerable labelling occurred in the hyphal wall where the fungal hypha was surrounded by mesophyll cells (Fig. 9).

A striking characteristic of labelling for ß-1,3-glucanase in the compatible interaction, was that labelling was observed to accumulate predominantly in the extrahaustorial wall and the extrahaustorial matrix (Fig. 10). On many occasions, labelling was only found in the extrahaustorial matrix (Fig. 11). The fungal haustorium of *P. recondita* f.sp. *tritici* is frequently observed to be closely associated with the host nucleus (Hu and Rijkenberg, unpublished; Chapter 3). Figs. 12 and 13 show a host nucleus invaginated by an invading haustorium with concentrated labelling in the extrahaustorial matrix. The haustorial neck remained free of labelling (Fig. 14).

PLATE 1

Fig. 1. Immunocytochemical control test. Ultrathin sections of wheat leaf tissues, infected by *Puccinia recondita* f.sp. *tritici* in the compatible interaction (Thatcher/UVPrt 8), obtained 5 days post-inoculation (dpi), were incubated with PBS-BSA to replace the primary antibody against ß-1,3-glucanase. No labelling is observed, neither in the host cytoplasm (HCy) nor in the wall of haustorial body (HB), extrahaustorial matrix (EHM) and haustorial cytoplasm. (Bar = 0.3 μm)

Fig. 2. Immunocytochemical control test. Ultrathin sections of wheat leaf tissues, infected by *Puccinia recondita* f.sp. *tritici* in the incompatible interaction (RL6078/UVPrt 8), sampled at 5 dpi, were incubated with pre-immune rabbit serum replacing the primary antibody. No labelling is found in the secondary thickening of xylem vessels. (Bar = 0.3 μm)

Fig. 3. Immunocytochemical control test. Ultrathin sections of wheat leaf tissues, infected by *Puccinia recondita* f.sp. *tritici* in the compatible interaction (Thatcher/UVPrt 8), obtained 5 days post-inoculation (dpi), were incubated with the antibody against ß-1,3-glucanase which was pre-absorbed with purified wheat ß-1,3-glucanase. No or little labelling is seen, neither in the host cytoplasm nor in the haustorial wall, extrahaustorial matrix (EHM) and haustorial cytoplasm. (Bar = 0.3 μm)

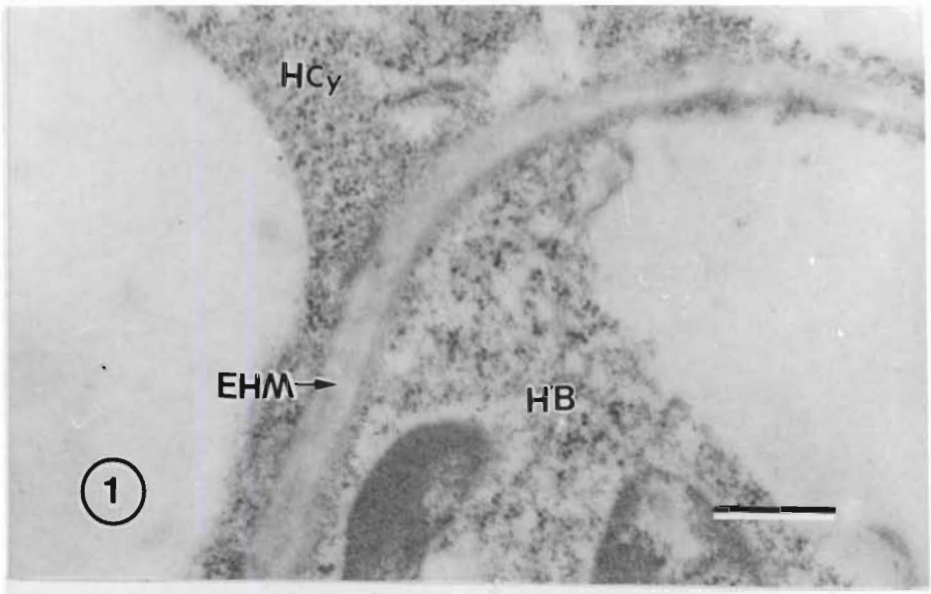
HCy
EHM
HB
1

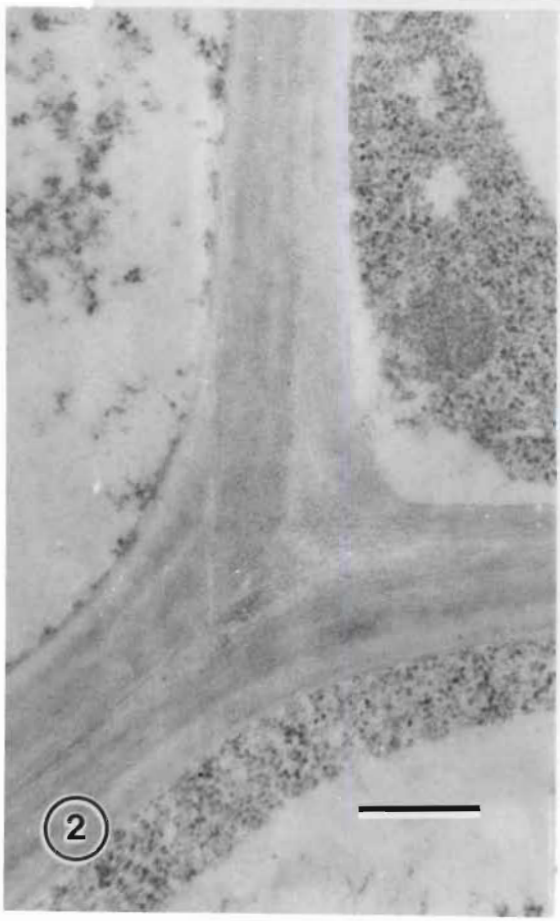
2

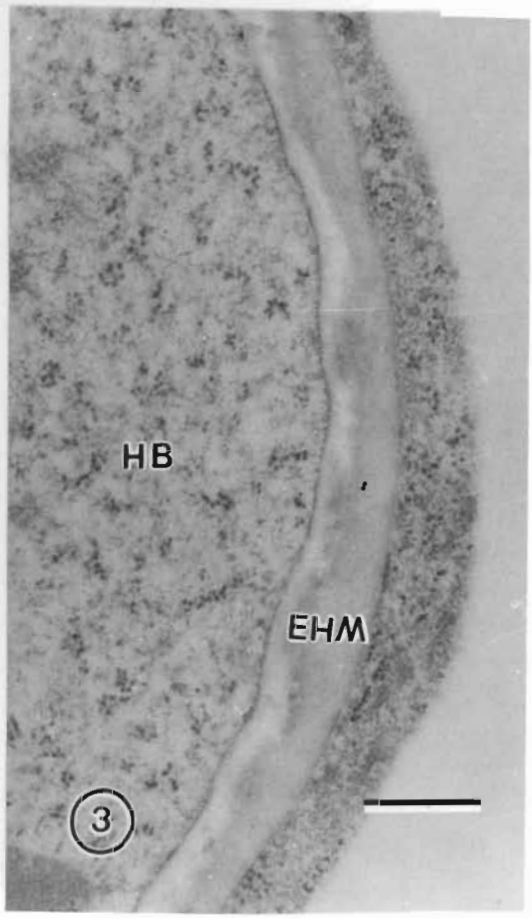
HB
EHM
3

PLATE 2

Fig. 4. Wheat leaf tissue of the compatible interaction (Thatcher/UVPrt 8), sampled at 5 dpi. Few gold particles sparsely located in the mesophyll (Mc) and epidermal cell (Ec) wall and plasmalemma. IS: Intercellular space. (Bar = 0.2 μm)

Fig. 5. Wheat leaf tissue of the compatible interaction (Thatcher/UVPrt 8), sampled at 5 dpi. Dense gold labelling is found in the cell walls of guard cells (Gc). (Bar = 1 μm)

Fig. 6. Wheat leaf tissue of the compatible interaction (Thatcher/UVPrt 8), sampled at 5 dpi. A clear deposition of gold particles is observed in the secondary thickening (Se) of xylem vessels. (Bar = 0.4 μm)

Fig. 7. Wheat leaf tissue of the compatible interaction (Thatcher/UVPrt 8), sampled at 5 dpi. Deposition of gold particles on the cell wall of phloem elements is shown. (Bar = 0.3 μm)

Fig. 8. Wheat leaf tissue of the compatible interaction (Thatcher/UVPrt 8), sampled at 5 dpi. A few gold particles occur sparsely in the cell wall of an intercellular hypha (IH) and a few gold particles are present in the hyphal cytoplasm. (Bar = 0.2 μm)

Fig. 9. Wheat leaf tissue of the compatible interaction (Thatcher/UVPrt 8), sampled at 5 dpi. Gold labelling is frequently found associated with the hyphal (IH) wall when the hypha is surrounded by the host mesophyll cells (Mc). No labelling is observed in the extracellular matrix. (Bar = 0.2 μm)

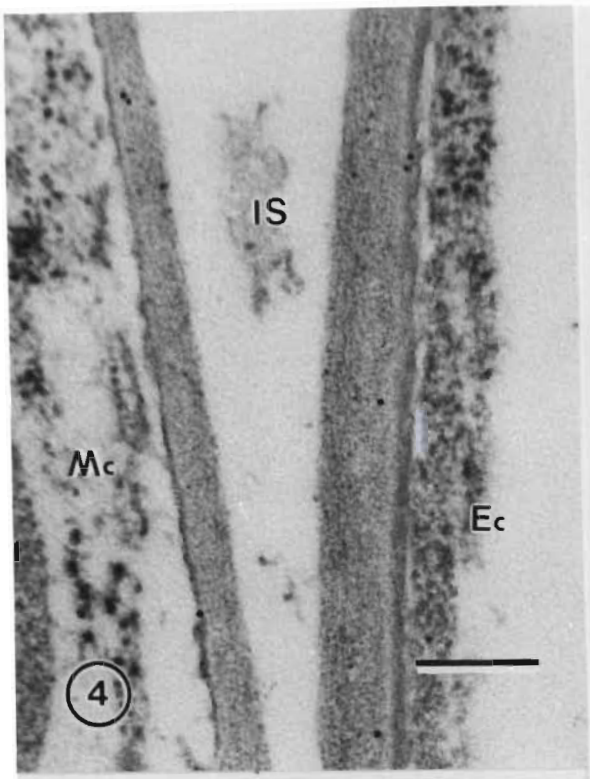
IS
Mc
Ec
4

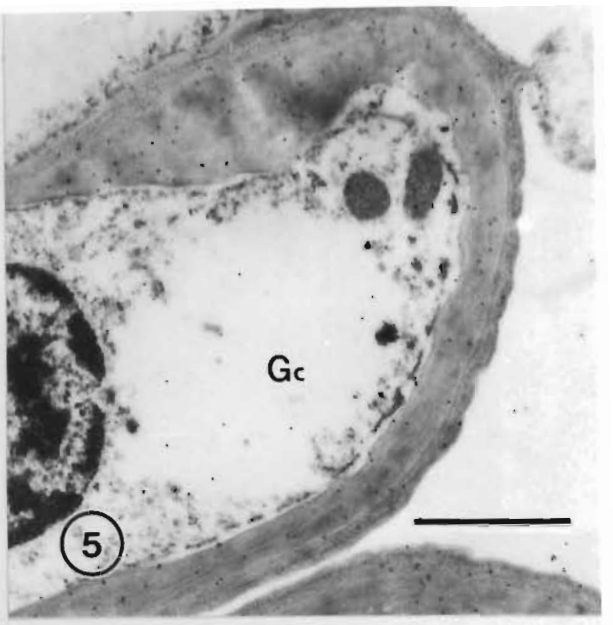
Gc
5

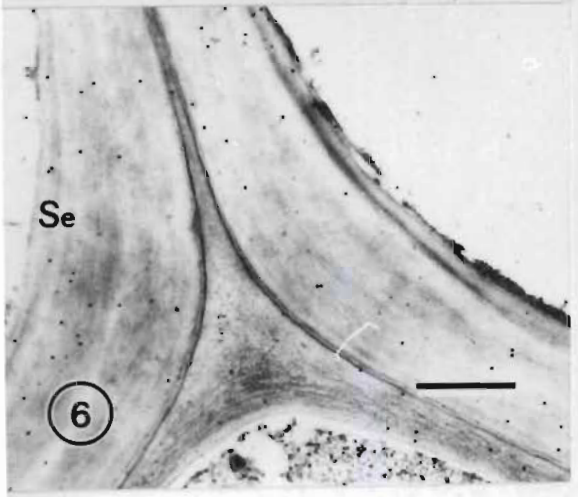
Se
6

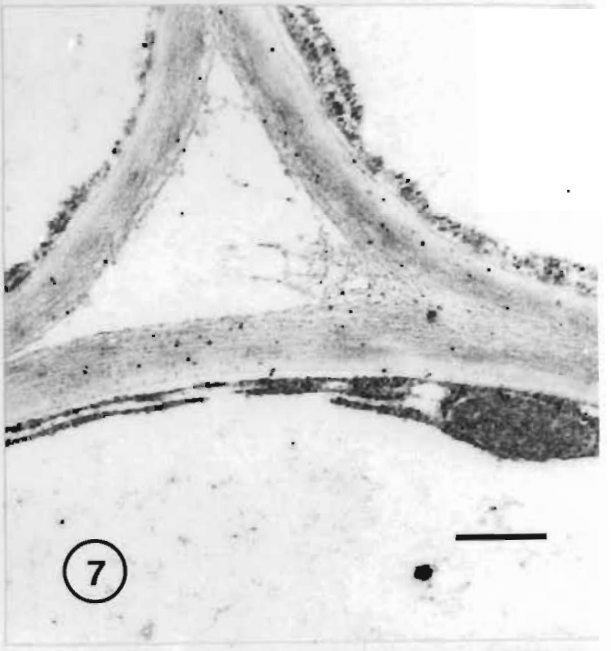
7

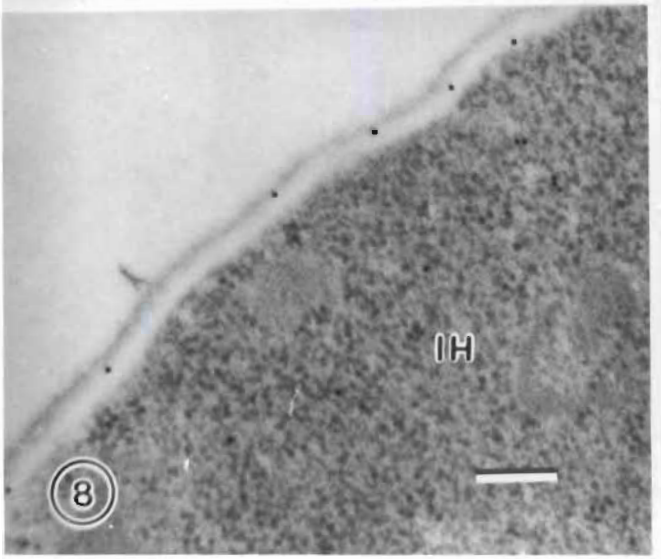
IH
8

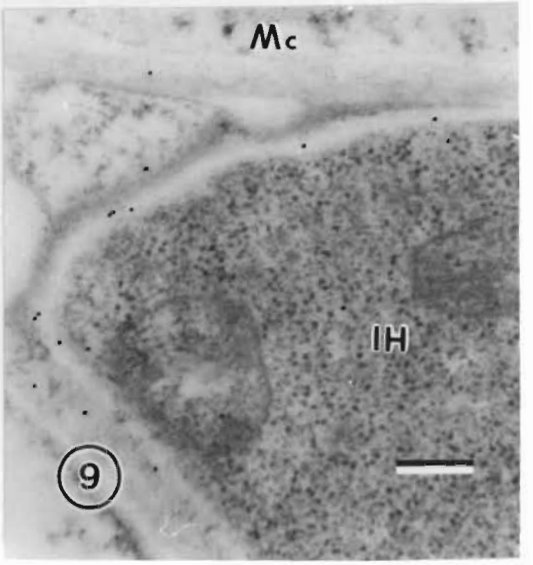
Mc
IH
9

PLATE 3

Fig. 10. Wheat leaf tissue of the compatible interaction (Thatcher/UVPrt 8), sampled at 5 dpi. A clear deposition of gold particles is shown in the haustorial wall and the extrahaustorial matrix. HB: Haustorial body. (Bar = 0.2 μm)

Fig. 11. Wheat leaf tissue of the compatible interaction (Thatcher/UVPrt 8), sampled at 5 dpi. Deposition of gold particles is mainly found in the extrahaustorial matrix. HB: Haustorial body. (Bar = 0.2 μm)

Fig. 12. Wheat leaf tissue of the compatible interaction (Thatcher/UVPrt 8), sampled at 5 dpi. Host nucleus (N) is invaginated by the invaded haustorium. HB: Haustorial body. (Bar = 2 μm)

Fig. 13. Enlargement of part of Fig. 12. Deposition of gold particles in the haustorial wall and extrahaustorial matrix, is evident. HB: Haustorial body; N: Host Nucleus. (Bar = 0.3 μm)

Fig. 14. Wheat leaf tissue of the compatible interaction (Thatcher/UVPrt 8), sampled at 5 dpi. Gold labelling is found in the extrahaustorial matrix in a host epidermal cell (Ec) while no ß-1,3-glucanase is detected in the walls of the haustorial neck (HN). HB: Haustorial body; HMC: Haustorial mother cell; V: Vacuole. (Bar = 0.5 μm)

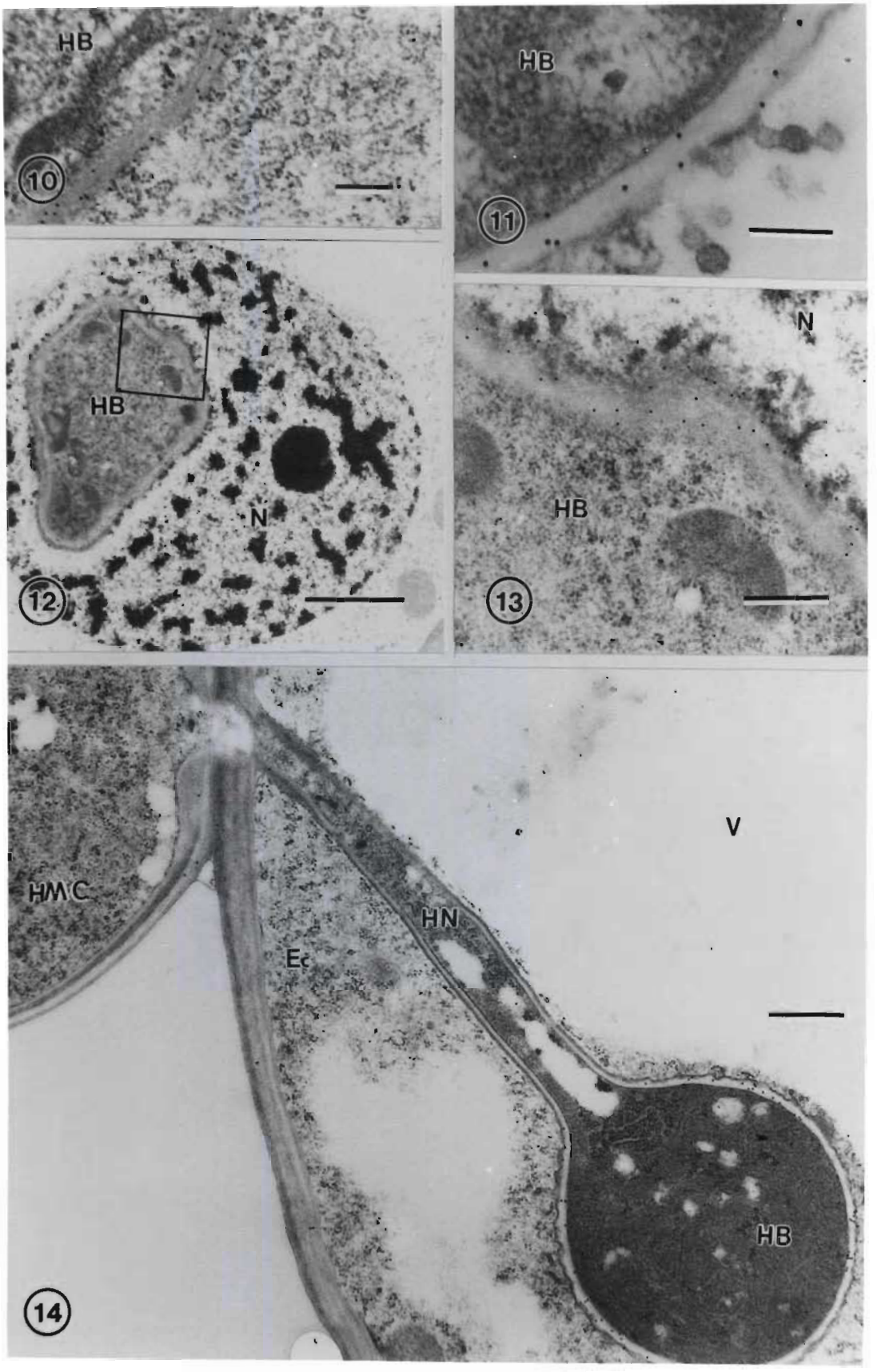
HB
10
HB
11
HB
N
12
N
HB
13
V
HMC
HN
Ec
HB
14

***Immunogold localization of ß-1,3-glucanase in the incompatible interaction between wheat and* P. recondita *f.sp.* tritici**

In the incompatible interaction, ß-1,3-glucanase accumulated in the host mesophyll cell plasmalemma near the fungus to a much higher extent (Fig. 15), than in the compatible interaction. The density of gold particles over the host mesophyll cell plasmalemma in the incompatible interactions measured 26 ± 2 (particles/μm^2), whereas a density of gold labelling (3 ± 1 particles/μm^2) was observed over a comparable area in compatible interactions. Strong labelling was also observed in the intercellular space at the juncture between mesophyll cells (Fig. 16) and in the extracellular matrix (Fig. 17). Similar to what was found in the compatible interaction, labelling was prevalent in the cell walls of guard cells and in the secondary thickening of xylem vessels.

In the incompatible interaction, the necrotic host cell, initiated after the fungal invasion, frequently gave rise to an amorphous, electron-dense substance which bound to the host cell wall in the intercellular space (Fig. 18). This type of electron-dense substance was strongly labelled for ß-1,3-glucanase (Fig. 19).

Cell wall apposition, formed between the host plasmalemma and cell wall, is considered a host resistance response to fungal attack in incompatible interactions in rusts. ß-1,3-Glucanase was found to be densely labelled in the cell wall apposition (Fig. 20) and in the membrane-like structures in the host cytoplasm adjacent to the cell wall apposition (Figs. 21, 22).

In many cases, the collapsed haustorium in necrotic cells (Figs. 23, 24) was also labelled by the antibody (see Fig. 24 which is an enlargement of part of

PLATE 4

Fig. 15. Wheat leaf tissue of the incompatible interaction (RL6078/UVPrt 8), sampled at 5 dpi. Gold particles are deposited in the plasmalemma of mesophyll cells (Mc) in greater quantities than in the compatible interaction. CW: Cell wall; M: Mitochondria. (Bar = 0.3 μm)

Fig. 16. Wheat leaf tissue of the incompatible interaction (RL6078/UVPrt 8), sampled at 5 dpi. Strong labelling is observed at the juncture of two mesophyll cells (Mc). No labelling is found in the host cytoplasm and in the Golgi body (Gb). (Bar = 0.2 μm)

Fig. 17. Wheat leaf tissue of the incompatible interaction (RL6078/UVPrt 8), sampled at 5 dpi. The extracellular matrix (Mx) between the mesophyll cells (Mc) is labelled. (Bar = 0.3 μm)

Fig. 18. Wheat leaf tissue of the incompatible interaction (RL6078/UVPrt 8), sampled at 5 dpi. An amorphous, electron-dense substance (D), bound to cell walls, is frequently found in the intercellular space. Nc: Necrotic cell. (Bar = 5 μm)

Fig. 19. Wheat leaf tissue of the incompatible interaction (RL6078/UVPrt 8), sampled at 5 dpi. The electron-dense substance (D), which only occurs on outer cell wall surface in the incompatible interaction, is strongly labelled with the antibody. Mc: Mesophyll cell; IS: Intercellular space. (Bar = 0.3 μm)

Fig. 20. Wheat leaf tissue of the incompatible interaction (RL6078/UVPrt 8), sampled at 5 dpi. Strong labelling is found in the cell wall apposition (CWP) on the inner cell wall surface. Mc: Mesophyll cell. (Bar = 0.3 μm)

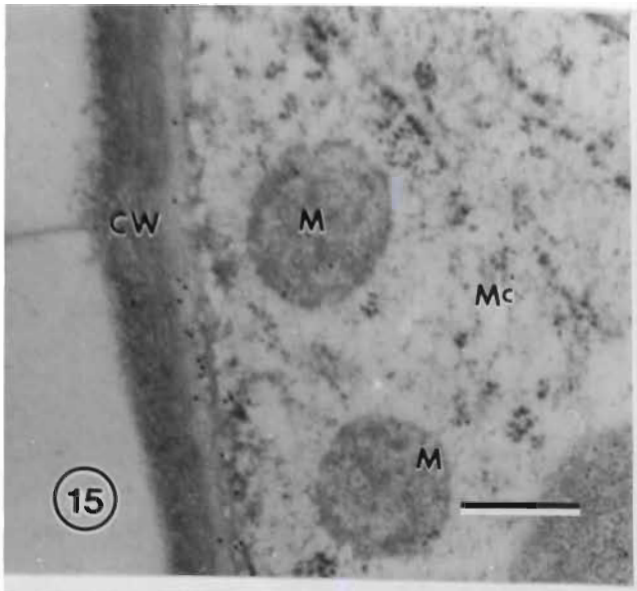
CW
M
Mc
M
15

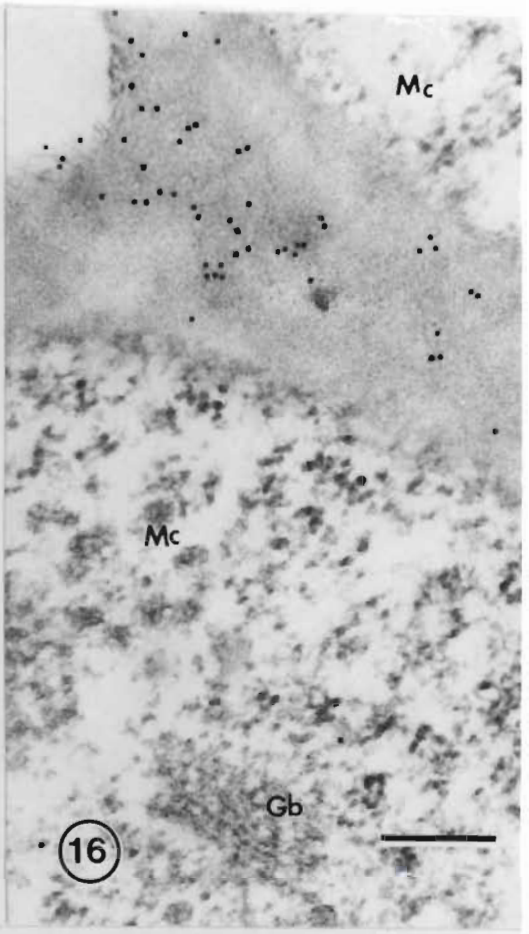
Mc
Mc
Gb
16

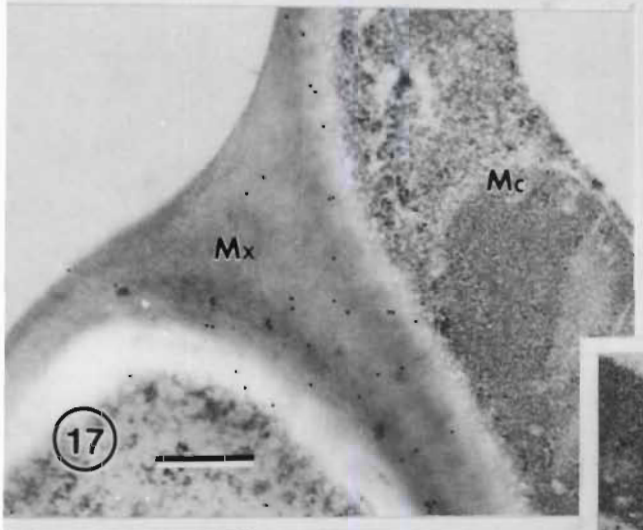
Mc
Mx
17

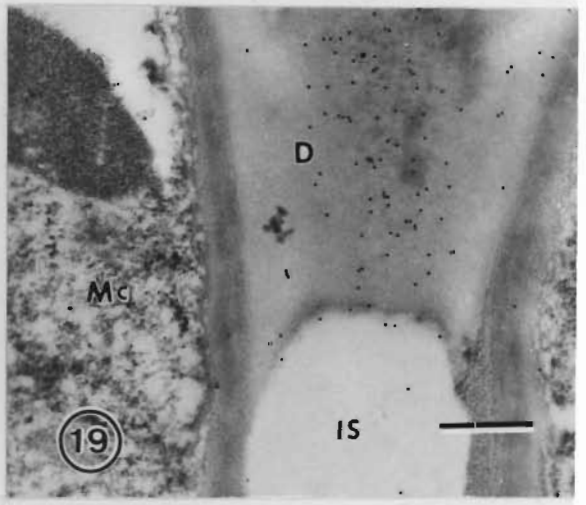
D
Mc
IS
19

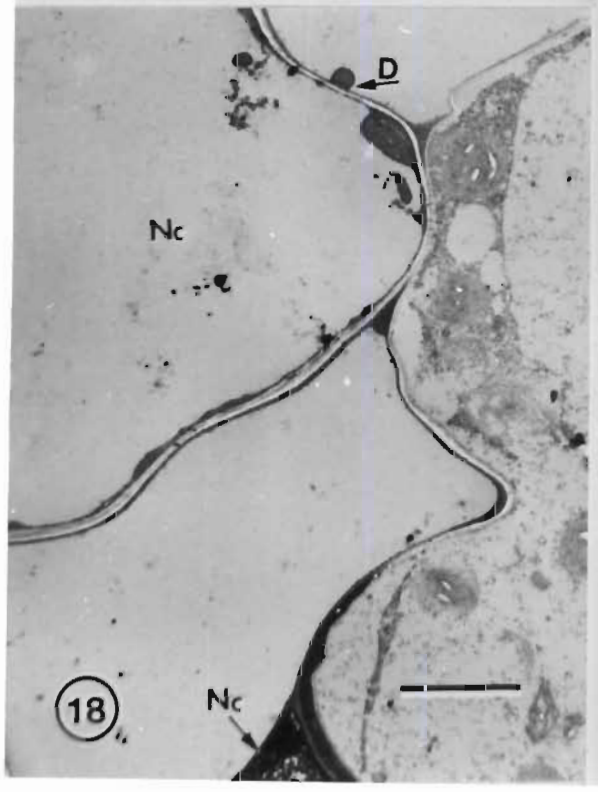
D
Nc
18
Nc

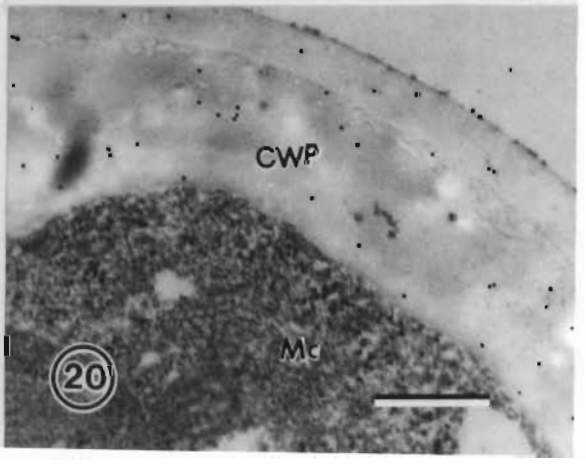
CWP
Mc
20

PLATE 5

Fig. 21. Wheat leaf tissue of the incompatible interaction (RL6078/UVPrt 8), sampled at 5 dpi. The membrane-like structure in host cytoplasm, which appears to be associated with the cell wall apposition. (Bar = 0.5 μm)

Fig. 22. Enlargement of part of Fig. 21. Gold labelling (arrow) is shown in the membrane-like structure in host cytoplasm. (Bar = 0.2 μm)

Fig. 23. Wheat leaf tissue of the incompatible interaction (RL6078/UVPrt 8), sampled at 5 dpi. Collapsed haustorium (HB) in a necrotic mesophyll cell is shown. The thick cell wall apposition is electron-opaque. An amorphous, electron-dense substance is also visible on the surface of mesophyll cell in the intercellular space. CWP: Cell wall apposition; CH: Chloroplast. (Bar = 1 μm)

Fig. 24. Enlargement of a lobe of the collapsed haustorium in mesophyll cell shown in Fig. 23. Gold particles (arrowhead) are associated with the collapsed haustorium. EHM: Extrahaustorial matrix. (Bar = 0.2 μm)

Fig. 25. Tissue of the incompatible interaction (RL6078/UVPrt 8), sampled at 5 dpi. A strong deposition of gold particles (arrow) is found in the cell wall and the septum of a possibly degenerating intercellular hypha (IH). (Bar = 1 μm)

Fig. 26. Wheat leaf tissue of the incompatible interaction (RL6078/UVPrt 8), sampled at 5 dpi. In mesophyll cells near necrotic host cells, a large number of aggregates, varying in size and shape, is found in vacuoles (V). CH: Chloroplast; CWP: Cell wall apposition. (Bar = 0.5 μm)

Fig. 27. High magnification of the aggregates in the host vacuoles, indicating the absence of gold particles. V: Vacuole. (Bar = 0.2 μm)

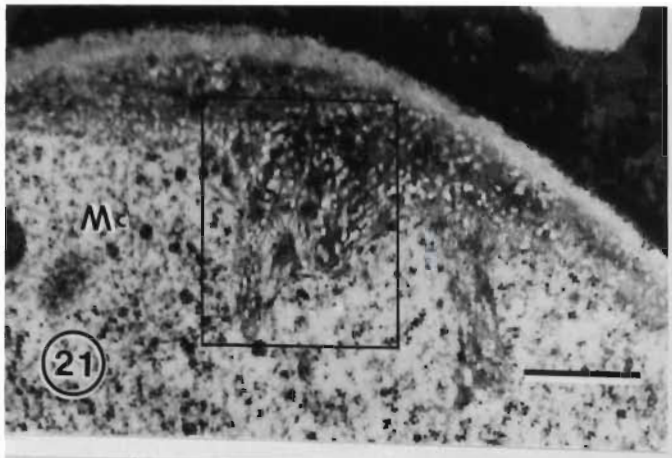
Mc
21

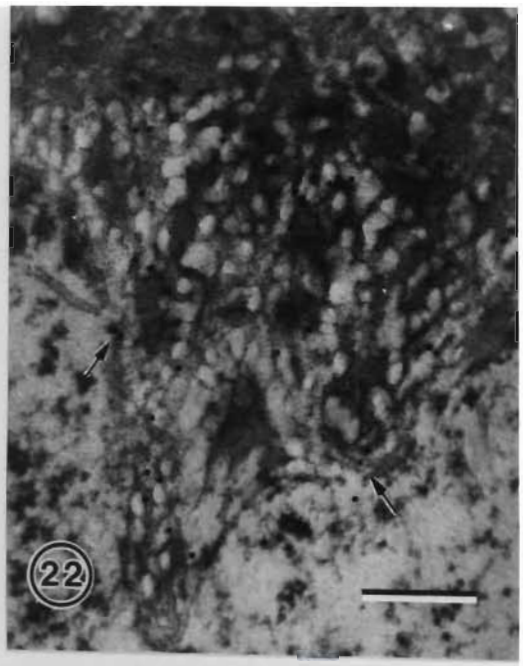
22


CH
HB
CWP
23

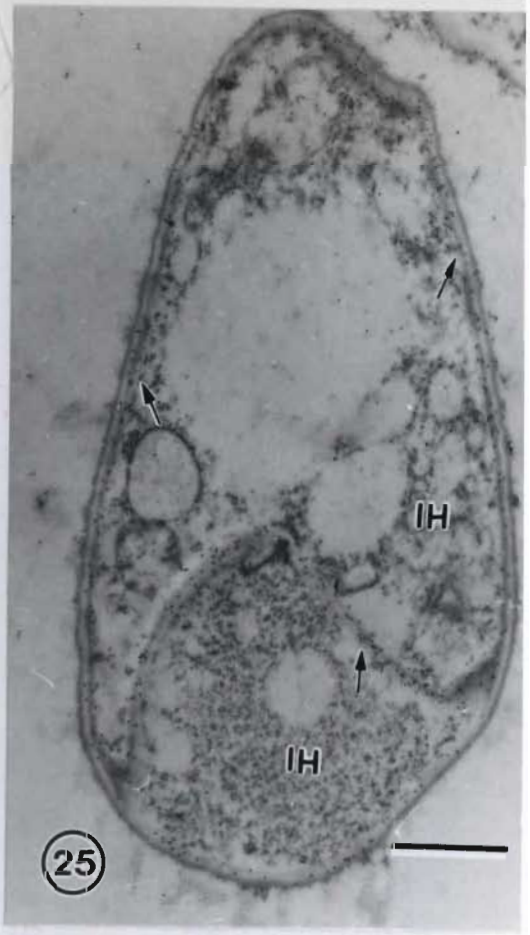
IH
IH
25

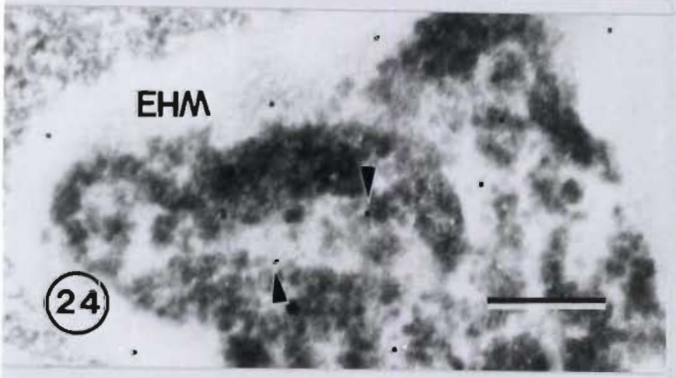
EHM
24

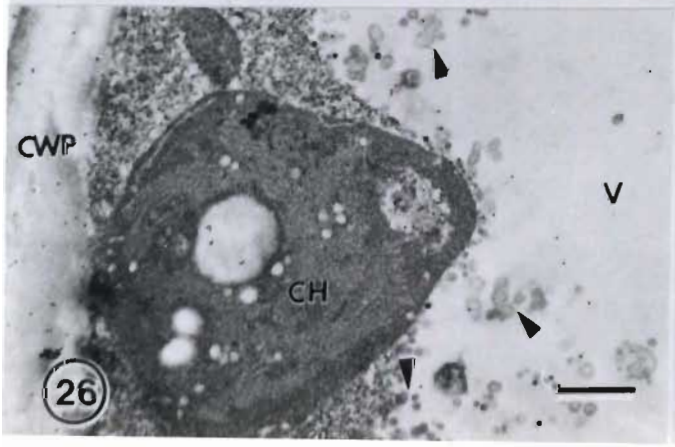
CWP
V
CH
26

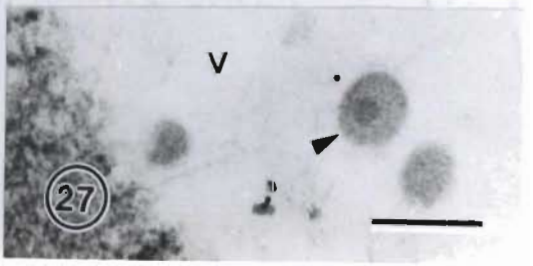
V
27

Fig. 23). In the incompatible interaction, strong labelling was also observed at the wall and septum of possibly degenerating hyphae (Fig. 25).

It was found that there were many aggregates in the host vacuoles in incompatible interaction (Fig. 26), however, no or little labelling was observed in association with such aggregates in the vacuoles (Fig. 27).

DISCUSSION

The ß-1,3-glucanase labelling in this investigation, in both compatible and incompatible interactions, shows that the enzyme occurs in the cell walls of host cells. This result is consistent with ß-1,3-glucanase labelling in the wheat-*Puccinia graminis* f.sp. *tritici* interaction (Sock *et al.*, 1990). The present observations showed that there is a much higher concentration of ß-1,3-glucanase in the host mesophyll cell plasmalemma and in the extracellular matrix of the intercellular space in infected resistant wheat leaves than in infected susceptible ones. It appears that higher labelling in the infected resistant wheat leaves is due to accumulation of ß-1,3-glucanase. However, it has been reported before that it is difficult to fix water-soluble proteins in the extracellular space with conventional fixation protocols (Dore *et al.*, 1991; Sock *et al.*, 1990; Wubben *et al.*, 1992). The high-pressure freezing technique could provide better antigen fixation and may circumvent the disadvantages of conventional fixation methods (Mendgen *et al.*, 1991).

In tomato infected by *Fusarium oxysporum* f.sp. *radici-lycopersici* and in eggplant infected by *Verticillium albo-atrum*, ß-1,3-glucanase was found mainly in host and fungal cell walls and in the fungal cytoplasm (Benhamou

et al., 1989). The authors assumed that the extensive labelling of fungal cytoplasm was possibly due to the enzyme redistribution resulting from the release of the enzyme by host cell damage caused by the fungal attacks. In the present study on the wheat-*P. recondita* f.sp. *tritici* interaction, the fungal cell wall and cytoplasm were sparsely labelled for ß-1,3-glucanase. This is similar to the description of the *Puccinia graminis* f.sp. *tritici*-wheat interaction provided by Sock *et al.*, (1990). Based on the dot blot assay and the Western blot technique, the latter authors suggested that the labelling of fungal cytoplasm is due to the cross-reaction between the anti-barley ß-1,3-glucanase antibody they used and the intracellular ß-1,3-glucanase of fungus. It will be interesting to determine if the anti-wheat ß-1,3-glucanase antibody we used cross-reacts with the fungal intracellular ß-1,3-glucanase of *P. graminis* f.sp. *tritici*.

The strong labelling of ß-1,3-glucanase of the haustorial wall and extrahaustorial matrix is striking. In many cases only the extrahaustorial matrix is strongly labelled in the compatible interaction. The extrahaustorial matrix is a complicated domain, which may play an important role in the recognition and interaction between the host and pathogen and it has being subjected to much attention in recent years (Harder and Chong, 1991). ß-1,3-Glucanase labelling was also found in the extrahaustorial matrix of the haustorium of *Puccinia graminis* f.sp. *tritici*. The occurrence of ß-1,3-glucanase in the extrahaustorial matrix in the wheat-*P. recondita* f.sp. *tritici* interface may indicate that the enzyme may play an important role in the interaction.

The biochemical characteristics of ß-1,3-glucanase have been extensively investigated (Boller, 1987). ß-1,3-Glucanases are encoded by small gene families (Broglie *et al.*,, 1989; Linthorst *et al.,* 1990) and typically occur as

basic and acidic isoforms that in their basic form are targeted to the vacuoles or in their acidic form are secreted into the intercellular space. Mauch and Staehelin (1989) and Mauch *et a*l. (1992) using antiserum against the basic forms of ß-1,3-glucanase found that the vacuolar aggregates were the major sites of accumulation of the ß-1,3-glucanase after the ethylene treatments, while only small amounts of ß-1,3-glucanase were found to be apoplastic, primarily in the middle lamella. Wubben *et al.* (1992), using an antibody which does not discriminate between the acidic and basic ß-1,3-glucanases to study the subcellular localization of ß-1,3-glucanases in the tomato-*Cladosporium fulvum* interaction, found that the protein aggregates in plant vacuoles in both compatible and incompatible interactions, were strongly labelled. Moreover, stronger labelling in the aggregates was found in the infected resistant tomato tissues than that in infected susceptible ones. They did not find labelling associated with the fungal cell walls. The occurrence of ß-1,3-glucanase in the protein aggregates of host vacuoles has also been described in various other plant tissues, following the treatment of ethylene or the attacks by microbes, such as fungi, bacteria, viruses and viroids (Dore *et al.*, 1991; Keefe *et al.*, 1990; Vera *et al.*, 1989). The antibody used in this study is against the 33 kDa acidic isoform of ß-1,3-glucanase purified from the intercellular washing fluid (IWF) of wheat but could recognize both the acidic and basic isoforms of the enzyme (Qian *et al.*, personal communication), however, it was not able to locate the antigen (ß-1,3-glucanase) in vacuoles in this study.

We observed an electron-dense substance of host origin in the intercellular space on cell wall surfaces which is strongly labelled with the ß-1,3-glucanase antibody. Such electron-dense structures were only found in the incompatible interaction. Similar structures were described to occur in virus-infected tobacco (Dore *et al.*, 1991). In tobacco, these structures, termed extracellular

pockets, were correlated with the hypersensitive response of tobacco plants. Similar electron-dense structures were also reported to occur in tomato leaves infected by the leaf mould pathogen, *Cladosporium fulvum* (Wubben *et al.,* 1992). The latter authors found that the appearance of electron-dense structures in the intercellular space was similar to that they observed in the protein aggregates in host vacuoles. Mauch and Staehelin (1989), on the basis of their observations, proposed a general model in which plant hydrolytic enzymes enter the extracellular space only after cell death accompanying the hypersensitive response. However, many investigations have shown that the regulation of the distribution of hydrolytic enzymes is much more complicated (Graham and Graham, 1990). In tobacco, both acidic and basic isoforms of ß-1,3-glucanases have been found (Vande Bulcke *et al.*, 1989). Infection with *Pseudomonas syringae*, or salicylic acid treatment, resulted in the accumulation of new acidic ß-1,3-glucanases in the extracellular space. The vacuolar isoforms of the enzyme were not secreted into the extracellular space following infection or chemical induction (Vande Bulcke *et al.,* 1989). Dore *et al.* (1991) also revealed that the extracellular pockets in tobacco contained mainly the acidic isoform of ß-1,3-glucanase, thus indicating there is no connection with the basic form of the enzyme in protein aggregates of the host vacuoles. In the present investigation, considering the fact that the antibody we used is against the wheat extracellular ß-1,3-glucanase while it could recognize both basic and acidic isoforms of the enzyme and that no labelling was associated with aggregates in the host vacuoles, we consider it likely that there is no connection between the ß-1,3-glucanase in the electron-dense substance in the intercellular space and that which may be present in the aggregates of the host vacuoles.

In the incompatible wheat-*P. recondita* f.sp. *tritici* interaction, dense labelling was found in the cell wall appositions. Cell wall appositions are believed to be

a product of the host cell in response to fungal attack (Jacobs, 1989a; 1989b). They are considered to be a structural or possibly a chemical barrier inhibiting the formation of a haustorium, by e.g. exerting a toxic effect on the haustorial mother cell (Jacobs, 1989a; 1989b), or preventing adherence of the haustorial mother cell to the host cell wall. Niks (1986) presumed that cell wall appositions probably cause the abortion of infection structures and delay the initial radial growth of rust colonies. Energy-Dispersive X-ray analysis (EDX) showed that the cell wall appositions are rich in silicon (Heath and Stumpf, 1986). Callose is also found in the cell wall apposition (Stumpf and Heath, 1985; Hu and Rijkenberg, unpublished). In this study, ß-1,3-glucanase is demonstrated to occur in the cell wall apposition which might indicate that the enzyme participates in the host resistance response to the fungal attack.

Although the intercellular hyphae were generally only sparsely labelled in this study, the walls and septa of some old, possibly degenerating fungal hyphae were occasionally shown to be strongly labelled with ß-1,3-glucanase antibody. Similar labelling was reported in tomato infected by *Cladosporium fulvum*. The accumulation of ß-1,3-glucanase in fungal hyphae during the hypersensitive response in the incompatible interaction may indicate that the ß-1,3-glucanase plays an important role in the active defense of wheat plants against *P. recondita* f.sp. *tritici.*

It has been reported that phenylalanine-ammonia-lyase (PAL), phenolic compounds and lignin-like components (Southerton and Deverall, 1990), callose (Southerton and Deverall, 1990) are associated with the resistance response in the wheat-*P. recondita* f.sp. *tritici* interaction, and histological observations have also indicated that some morphological modifications in wheat leaves can result in an increased resistance against *P. recondita* f.sp. *tritici* (Jacobs, 1989a; 1989b). These observations indicate that accumulation

of ß-1,3-glucanase in the incompatible wheat-*P. recondita* f.sp. *tritici* interaction may be only partly responsible for the active defense response of wheat against fungal invasion.

LITERATURE CITED

Andres, M.W. and Wilcoxson, R.D. (1984). A device for uniform deposition of liquid-suspended urediospores on seedling and adult cereal plants. *Phytopathology* **74,** 550-552.

Arlorio, M., Ludwig, A., Boller, T. and Bonfante, P. (1992). Inhibition of fungal growth by plant chitinases and ß-1,3-glucanases: A morphological study. *Protoplasma* **171,** 34-43.

Benhamou, N., Grenier, J. Asselin, A. and Legrand, M. (1989). Immunogold localization of ß-1,3-glucanase in two plants infected by vascular wilt fungi. *The Plant Cell* **1,** 1209-1221.

Benhamou, N., Joosten M.H.A.J. and De Wit, P.J.G.M. (1990). Subcellular localization of chitinase and of its potential substrate in tomato root tissues infected by *Fusarium oxysporum* f.sp. *radicis-lycopersici. Plant Physiology* **92,** 1108-1120.

Boller, T. (1987). Hydrolytic enzymes in plant disease resistance. In *Plant-Microbe Interactions. Molecular and Genetic Perspectives.* Vol 2. (Kosuge, T. and Nester, E. eds.) 385-413. Macmillan, New York.

Broglie, K., Chet, I., Holliday, M., Gressman, R., Biddle, P., Knowlton, S.,

Mauvais, C.J. and Broglie, R. (1991). Transgenic plants with enhanced resistance to the fungal pathogen *Rhizoctonia solani*. *Science* **254**, 1194-1197.

Dore, I., Legrand, M., Cornelissen, B.J.C. and Bol, J.F. (1991). Subcellular localization of acidic and basic PR proteins in tobacco mosaic virus-infected tobacco. *Archives of Virology* **120**, 97-107.

Graham, T.L. and Graham, M.Y. (1991). Cellular coordination of molecular response in plant defense. *Molecular Plant-Microbe Interactions* **4**, 415-422.

Ham, K.-S., Kauffman, S., Albersheim, P. and Darvill, A.G. (1991). Host-pathogen interactions XXXIX. A soybean pathogenesis-related protein with ß-1,3-glucanase activity releases phytoalexin elicitor-active heat-stable fragments from fungal walls. *Molecular Plant-Microbe Interactions* **4**, 5455-552.

Harder, D.E. and Chong, J. (1991). Rust haustoria. In: *Electron Microscopy of Plant Pathogens* (Mendgen, K. and Lesemann, D.-E. eds.) pp 235-250. Springer-Verlag. Berlin, Heidelberg.

Heath, M.C. and Stumpf, M.A. (1986). Ultrastructural observations of penetration sites of cowpea rust fungus in untreated and silicon-depleted French bean cells. *Physiological and Molecular Plant Pathology* **229**, 27-39.

Jacobs, Th. (1989a). The occurrence of cell wall appositions in flag leaves of spring wheats susceptible and partially resistant to wheat leaf rust. *Journal of Phytopathology* **127**, 239-249.

Jacobs, Th. (1989b). Haustorium formation and cell wall appositions in susceptible and partially resistant wheat and barley seedlings infection with

leaf rust. *Journal of Phytopathology* **127,** 250-261.

Joosten, M.H.A.J. and De Wit, P.J.G.M. (1989). Identification of several pathogenesis-related proteins in tomato leaves inoculated with *Cladosporium fulvum* (syn. *Fulvia fulva*) as 1,3-ß-glucanases and chitinases. *Plant Physiology* **89,** 945-951.

Keefe, D., Hinz, U. and Meins, F. Jr. (1990). the effect of ethylene on the cell type-specific and intracellular localization of ß-1,3-glucanase and chitinase in tobacco leaves. *Planta* **182,** 443-51.

Keen, N.T. and Yoshikawa, M. (1983). ß-1,3-Endoglucanases from soybean release elicitor-active carbohydrates from fungal cell walls. *Plant Physiology* **71,** 460-465.

Kemp, G., Botha, A.M. Pretorius, Z.A. and Kloppers, F.J. (1996a). The effect of *Puccinia recondita* f.sp. *tritici* infection on the expression of chitinase and ß-1,3-glucanase activity in wheat. *South African Journal of Science* **92,** xviii.

Kemp, G., Botha, A.M. Pretorius, Z.A. and Kloppers, F.J. (1996b). Effect of chitinase and ß-1,3-glucanase on the germination of *Puccinia recondita* f.sp. *tritici* urediospores. *Proceedings of the 9th European and Mediterranean Cereal Rusts and Powdery Mildews Conference*, Lunteren, the Netherlands. pp 64.

Linthorst, H.J.M. (1991). Pathogenesis-related proteins of plants. *Critical Reviews in Plant Sciences* **10,** 123-150.

Linthorst, H.J.M., Melchers, L.S., Mayer, A., Van Roekel., J.S.C., Cornelissen, B.J.C. and Bol, J. (1990). Analysis of gene families encoding acidic and basic ß-1,3-glucanases of tobacco. *Proceedings of the National Academy of Sciences U.S.A.* **87,** 8750-8760.

Mauch, F., Mauch-Mani, B. and Boller, T. (1988). Antifungal hydrolases in pea tissue. II. Inhibition of fungal growth by combinations of chitinase and ß-1,3-glucanase. *Plant Physiology* **88,** 936-942.

Mauch, F. and Staehelin, L.A. (1989). Functional implications of the subcellular localization of ethylene-induced chitinase and ß-1,3-glucanase in bean leaves. *The Plant Cell* **1,** 447-457.

Mauch, F., Meehl, J.B. and Staehelin, L.A. (1992). Ethylene-induced chitinase and ß-1,3-glucanase accumulate specifically in the lower epidermis and along vascular strands of bean leaves. *Planta* **186,** 367-375.

Mendgen, K., Welter, K., Scheffold, F. and Knauf-Beiter, G. (1991). High pressure freezing of rust infected plant leaves. In: *Electron Microscopy of Plant Pathogens* (Mendgen, K. and Lesemann, D.-E. eds.) pp 31-42. Springer-Verlag. Berlin, Heidelberg.

Niks, R.E. (1986). Failure of haustorial development as a factor in slow growth and development of partially resistant barley seedlings. *Physiological and Molecular Plant Pathology* **28,** 309-322.

Sock, J. Rohringer, R. and Kang, Z. (1990). Extracellular ß-1,3-glucanase in stem rust-affected and abiotically stressed wheat leaves. Immunocytochemical localization of the enzyme and detection of multiple forms in gels by activity staining with dye-labelled laminarin. *Plant Physiology* **94,** 1376-1389.

Southerton, S.G. annd Deverall, B.J. (1990). Histochemical and chemical evidence for lignin accumulation during the expression of resistance to leaf rust fungi in wheat. *Physiological and Molecular Plant Pathology* **36,** 483-494.

Stumpf, M.A. and Heath, M.C. (1985). Cytological studies of the interactions between the cowpea rust fungus and silicon-depleted French bean plants. *Physiological Plant Pathology* **27**, 369-385.

Takeuchi, Y., Yoshikawa, M., Takeba, G., Tanaka, K., Shibata, D. and Horino, O. (1990). Molecular cloning and ethylene induction of mRNA encoding a phytoalexin elicitor-releasing factor, ß-1,3-glucanase, in soybean. *Plant Physiology* **93**, 673-682.

Vande Bulcke, M., Bauw, G., Castesana, C., Van Montagu, M. and Vandekerckhove, J. (1989). Characterization of vacuolar and extracellular (1,3)-glucanases of tobacco: Evidence for a strictly compartmentalized plant defense system. *Proceedings of the National Academy of Sciences U.S.A.* **86**, 2673-2677.

Van Loon, L.C. (1989). Stress proteins in infected plants. In: *Plant-Microbe Interactions. Molecular and Genetic Perspectives*, Vol 3. (Kosuge, T. and Nester, E. eds.), 199-237. New York, McMillan.

Vera, P., Hernández-Yago, J. and Conejero, V. (1989). "Pathogenesis-related" PI(p14) protein..Vacuolar and apoplastic localization in leaf tissue from tomato plants infected with citrus exocortis viroid; *in vitro* synthesis and processing. *Journal of General Virology* **70**, 1933-1942.

Wessels, J.H.G. and Sietsma, J.H. (1981). Fungal cell walls: a survey. In: *Encyclopedia of Plant Physiology*, New Series, Vol. 13B, *Plant Carbohydrates II*. (Tanner, W. and Loewis, F.A. eds.). 352-394. Springer Verlag. New York.

Wubben, J.P., Joosten, M.H.A.J., Van Kan, J.A.L. and De Wit, P.J.G.M. (1992). Subcellular localization of plant chitinases and 1,3-ß-glucanases in *Cladosporium fulvum* (syn. *Fulvia fulva*)-infected tomato leaves. *Physiological*

and Molecular Plant Pathology **41,** 23-32.

Young, D.H. and Pegg, G.F. (1982). The action of tomato and *Verticillium albo-atrum* glycosidases on the hyphal wall of *V. albo-atrum*. *Physiological Plant Pathology* **21,** 411-423.

CHAPTER 7

ULTRASTRUCTURAL LOCALIZATION OF CYTOKININS IN *PUCCINIA RECONDITA* F.SP. *TRITICI*-INFECTED WHEAT LEAVES

INTRODUCTION

In the healthy plants, it is well established that cytokinins, one class of plant hormones, are involved in the mediation of cell division, in retarding of plant senescence, in the regulation of chloroplast development and in nutrient mobilization within plant tissues (Moore, 1978). A number of investigations have provided a wealth of evidence that cytokinin imbalances exist in the growth abnormalities associated with fasciation and gall-forming plant diseases (Ammon *et al.*, 1990; Surico and Iacobellis, 1992; Vizárová, 1979). In bacterium-infected plants, for instance, phytohormones produced by the invading bacteria alter the physiological hormone balance in the plant tissues and cause plant cells surrounding the infection sites to proliferate, inducing overgrowths, such as knots and galls (Surico and Iacobellis, 1992). Previous studies have also revealed that cytokinins, produced by the fungal pathogen, *Fusarium moniliforme* var. *subglutinans* Wollenw. and Rg., are associated with mango flower malformation (Van Staden *et al.*, 1989; Van Staden and Nicholson, 1989).

Many microorganisms, including plant pathogenic fungi and bacteria, are able

to produce cytokinins (Michniewicz *et al.*, 1986; Van Staden and Nicholson, 1989; Iacobellis *et al.* 1994; Lichter *et al.*, 1995; Morris, 1986). It has been suggested that the accumulation of cytokinins in the infection locus of biotrophic pathogens indicates that the normal pattern of translocation of photosynthetic metabolites in the host cells undergoes dramatic alteration (Dekhuizen, 1976).

A major reduction in the concentration of cytokinins in plants infected by some pathogens, especially the wilt-inducing *Verticillium* and *Phytophthora* fungi, has been reported (Cahill *et al.*, 1986; Patrick *et al.*, 1977). Some investigations have demonstrated that the reduction in cytokinins levels results in accelerated leaf senescence and increases susceptibility (Vidhyasekaran, 1988). On the other hand, work on rust diseases (Dekhuijzen and Staples, 1968; Király *et al.*, 1967; Vizárová *et al.*, 1986) and powdery mildew diseases (Mandahar and Garg, 1976; Vizárová, 1974, 1975, 1979, 1987) has frequently shown an increase in cytokinin activity with infection.

Considerable research has been conducted on the role of cytokinins in the formation of so-called green islands in response to infection by pathogens. Green islands are infected areas, generally of leaves, in which localized areas of chlorophyllous tissue, maintain their green appearance, while adjacent areas senescence and turn yellow. Both biotrophic and facultative microbial plant pathogens have been shown to produce green islands in nature (Bushnell and Allen, 1962). Bushnell and Allen (1962) mimicked the green-island effect with water-soluble components obtained from conidia of powdery mildew. Mothes *et al.* (1961) showed that local application of drops of cytokinin to the leaf can create a sink to which metabolites are transported from other part of the leaf or even other leaves. Cytokinins therefore appear to play a role in the formation of green islands.

Since the 1960s, it has been proposed that disease resistance may be modified by cytokinins (Beckman and Ingram, 1994; Dermastia and Ravnikar, 1996). Vidhyasekaran (1988) suggested that cytokinins counteract the senescence of plant tissues, and because senescence inducers increase susceptibility, it is possible that cytokinins induce resistance. Baláza *et al.* (1977) found that accumulation of cytokinins coincided with the time of development of systemic induced resistance in tobacco leaves against the virus attack. Many researchers, however, have indicated that cytokinins seem to reduce resistance by inhibiting the hypersensitive reaction in diseased plants and in tissue culture (Cole *et al.*, 1970; Dekker, 1963; Edwards, 1983; Liu and Bushnell, 1986). Beckman and Ingram (1994) found that cytokinins are able to inhibit the hypersensitive response and to induce susceptibility, and proposed the similarities between senescence and the plant defence response in the potato tuber slice-*Phytophthora infestans* (Mont.) de Bary interaction. Studies such as these corroborate the view that cytokinins may play an important role in the determination of disease susceptibility or resistance.

Although many biochemical studies have been conducted on the alteration of cytokinin levels associated with pathogen attack, no detailed research has thus far been reported on *in vivo* cytokinin localization in infected plants. Thus it remains unknown whether the plant or the pathogen, or both, is /are responsible for the cytokinin levels in plant tissues infected with pathogens. The lack of such information may be due to the low concentration of cytokinins in plant tissues, and/or the difficulty in the fixation of cytokinins during processing, because of their solubility and the absence of specific probes. There have been only a few reports of hormone localization, especially cytokinins, in literature. Zavala and Brandon (1983), using low-

temperature techniques, first localized dihydrozeatin riboside in maize roots. Eberle *et al.* (1987), using monoclonal antibodies, localized the isopentenyladenine and related cytokinins in a cytokinin-over-producing mutant of the moss, *Physcomitrella patens*. Sossountzov *et al.* (1988) detected cytokinins in Craigella tomato and a sideshootless mutant, by periodate coupling of isopentenyladenosine and zeatin riboside to cellular proteins, followed by post-embedding immunocytochemical procedures. Ivanova *et al.* (1994) showed the co-localized cytokinins and plant cell proliferation-associated nuclear proteins at the light microscopy level.

In the present investigation, the author describes the ultrastructural localization of cytokinins in *Puccinia recondita* Rob. ex Desm. f.sp. *tritici* Eriks. and Henn.-infected wheat leaves using anti-zeatin riboside (anti-ZR) and anti-isopentenyladenosine (anti-2iPA) antibodies. Post-embedding immunocytochemical procedures were employed in the this study.

MATERIALS AND METHODS

Plant materials, inocula and inoculation

The susceptible wheat line, Thatcher, and the resistant near-isogenic wheat line RL 6078 (conferring resistance gene *Lr26*) were used in this study. The South African pathotype UVPrt 8 of *Puccinia recondita* f.sp. *tritici*, which has an avirulence/virulence combination of *3a,3bg,3ka,11,16,20,26,30/1,2a,2b,2c,10,14a,15,17,24* was used as inoculum. Both wheat seeds and inoculum were kindly provided by Professor Z.A. Pretorius, Department of Plant Pathology, University of the Orange Free

State, South Africa. RL 6078 (*Lr26*) shows a hypersensitive reaction to UVPrt 8.

Freshly harvested urediospores of *P. recondita* f.sp. *tritici* from the plants of Agent, a susceptible wheat line, used for the multiplication of the urediospores, were applied to inoculate the adaxial surface of the first leaf of 10-day-old plants at an inoculum dose of 45 mg urediospores per ml of Soltrol 130 (Phillips Chemical Co.) using a modified Andres and Wilcoxson (1984) inoculator. Inoculated plants were allowed to dry for about 1 hour before placement in a dark dew chamber at 20°C for 20 hours. Inoculated and healthy leaves were sampled 5 days after inoculation.

Tissue-processing for electron microscopy

The harvested leaves were cut into 3×3 mm^2, fixed in 3% glutaraldehyde in a 0.05 M sodium cacodylate buffer (pH 7.2) overnight, and washed twice in that buffer. Then the samples were dehydrated in serial ethanol and embedded in Epon-Araldite resin. Some leaves sampled were submitted to the periodate-borohydride procedure, prior to fixation, to obtain the coupling of isopenyladenosine and zeatin riboside to cellular proteins (Sossountzov *et al.*, 1988; Sotta *et al.*, 1991), followed by the processing procedures mentioned above. Ultrathin sections were cut using a diamond knife and collected on 200 or 300 mesh uncoated nickel grids for further immunocytochemical processing.

Immunogold labelling

Antisera raised against zeatin riboside (ZR) and isopentenyladenosine (2iPA), respectively, were used for the subcellular localization of cytokinins in the *P.*

recondita f.sp. *tritici*-infected wheat leaf tissues in this study. The antibodies were kindly provided by Dr B. Sotta, Institut de Physiologie Végétale, CNRS, France. The sensitivity and specificity had been previously characterized and the antibodies have been used in the localization of cytokinins in Craigella tomato (Sossountzov *et al.*, 1988).

Ultrathin sections on nickel grids were first treated with 10% aqueous sodium metaperiodate for 30 min to improve the immunolabelling and completely rinsed with double-distilled water, then transferred to one drop of 0.01 M phosphate-buffered saline (PBS), pH 7.4, containing 0.2% (W/V) polyethylene glycol 20,000 (PEG 20,000) for 5 min at room temperature. Then sections were incubated in a drop of block solution consisting of 0.01 M PBS, pH 7.4, 10% (V/V) fetal bovine serum, 1% (W/V) bovine serum albumin (BSA), 0.05% (V/V) Tween-20 and 0.2% (W/V) sodium azide for 30 min at room temperature. They were then incubated directly in a drop of 20 μl primary antibody (antiserum against zeatin riboside, or against isopentenyladenosine) at a 1:200-500 dilution in 0.01 M PBS, pH 7.4, containing 1% BSA) in a moist chamber overnight at 4°C. After washing in a series of drops of washing solution (0.01 M PBS, pH 7.4, containing 1% BSA and 0.05% Tween-20), they were transferred onto a drop of colloidal gold (10 nm)-conjugated goat antiserum to rabbit immunoglobulins (GAR-gold antibody) diluted 1:20 in a PBS-BSA buffer for 1 hour at room temperature. Grids with sections were finally washed with 0.01 M PBS, pH 7.2, fixed in 1 % glutaraldehyde for 2 min, rinsed with double-distilled water and counterstained with uranyl acetate and lead citrate. The grids were then viewed with a JEOL 100 CX Transmission Electron Microscope at 80 kV.

Immunocytochemical controls

Controls for the specificity of the immunogold labelling were as follows: 1. incubation with PBS-BSA in the absence of the primary antibody; 2. substitution of the immune serum by the pre-immune serum; and 3. pre-absorption of antiserum with 20 μl purified zeatin riboside (ZR) or isopentenyladenosine (2iPA). For pre-absorption, 20 μl zeatin riboside or isopentenyladenosine (120 $\mu g/ml^{-1}$) was added to 20 μl of a 1:50 dilution of antiserum, and solutions were incubated at 4°C for 20 hours.

All chemicals used in this study were purchased from Sigma Chemical Co., St. Louis, MO. USA.

RESULTS

In the present investigation, no difference in the labelling pattern with antibodies was observed between the treatment of periodate-borohydride coupling and without the treatment. Thus, the results described here are mainly from the labelling without treatment of periodate-borohydride coupling. Moreover, the labelling pattern with anti-ZR or anti-2iPA appeared to be similar in this study.

Immunocytochemical controls

Immunocytochemical controls, either incubation with PBS-BSA in absence of the primary antibody or replacement of primary antibody with the pre-immune serum, were shown to be completely free of labelling (Figs. 1, 2). The sections treated with the antigens, zeatin riboside (ZR) or isopentenyladenosine (2iPA), showed a significant decrease in labelling

intensity (Figs. 3, 4), indicating that the labelling with antisera was specific.

Immunogold localization of cytokinins in healthy wheat leaf tissue

Labelling of leaves of non-inoculated wheat plants did not result in significant labelling either with anti-ZR or anti-2iPA antibodies. A few gold particles were present in the secondary thickening of xylem vessel walls (Fig. 5) and the wall of phloem cells (Fig. 6).

Immunogold localization of cytokinins in the compatible Puccinia recondita *f.sp.* tritici-*wheat interaction*

As was observed in healthy wheat leaves, some labelling with both anti-ZR and anti-2iPA antibodies occurred in the secondary wall of xylem vessels and in the wall of phloem elements in the compatible interaction. A few gold particles were deposited over the host chloroplasts when labelled with the anti-ZR antibody (Fig. 7). No significant labelling by the two antibodies was found with other host tissues or host organelles. However, strong labelling was found in the fungal cytoplasm and the inner cell wall of the intercellular hypha with both antibodies (Figs. 7, 8). In the older intercellular hyphae, labelling was only present in the inner cell wall (Fig. 9). Similar to that in the intercellular hypha, labelling in haustorial mother cells was mainly present in the fungal cytoplasm (Figs. 10, 11). No or very few gold particles were demonstrated in fungal vacuoles and mitochondria (Figs. 7, 8, 10, 11) whereas sparse labelling was observed in the fungal nucleus (Fig. 12). There was some labelling of that portion of the host cell wall which was in contact with the intercellular hypha (Figs. 7, 8).

PLATE 1

Figs. 1-4. Immunocytochemical control tests on ultrathin sections of wheat leaf tissue infected by *Puccinia recondita* f.sp. *tritici*.

Fig. 1. Wheat leaf tissue of the incompatible interaction (RL6078/race 8) was incubated with PBS-BSA in the absence of the primary antibody, followed by incubation with the colloidal gold-conjugated GAR-gold antibody. No gold deposition was observed in leaf tissue, nor in the hyphal cytoplasm. IH: Intercellular hypha; Mc: Mesophyll cell. (Bar = 0.3 μm)

Fig. 2. Wheat leaf tissue of the compatible interaction (Thatcher/race 8) was incubated with the pre-immune rabbit serum, followed by incubation with the colloidal gold-conjugated GAR-gold antibody. No labelling was found in the haustorial body (HB), extrahaustorial matrix and the host cytoplasm (HCy). (Bar = 0.1 μm)

Fig. 3. Wheat leaf tissue of the compatible interaction was incubated with the anti-zeatin riboside (anti-ZR) antibody, which was pre-absorbed with zeatin riboside (ZR). Both the intercellular hypha (IH) and the host cell (Mc) were free of gold labelling. (Bar = 0.3 μm)

Fig. 4. Wheat leaf tissue of a compatible interaction was incubated with the anti-isopentenyladenosine (anti-2iPA) antibody, which was pre-absorbed with isopentenyladenosine (2iPA). Almost no labelling was observed in the haustorial body (HB), the extrahaustorial matrix (EHM) and the host cytoplasm (HCy). (Bar = 0.3 μm)

Figs. 5-6. Cytokinin labelling of ultrathin sections of healthy wheat leaf tissue.

Fig. 5. Treatment of the thin sections of Thatcher leaf tissue with anti-ZR antibody. The secondary thickening (Se) of the xylem vessel was labelled with the antibody. (Bar = 0.2 μm)

Fig. 6. Application of anti-2iPA antibody to the ultrathin sections of RL6078 leaf tissue. A few gold particles were deposited over the cell wall of phloem elements. (Bar = 0.1 μm)

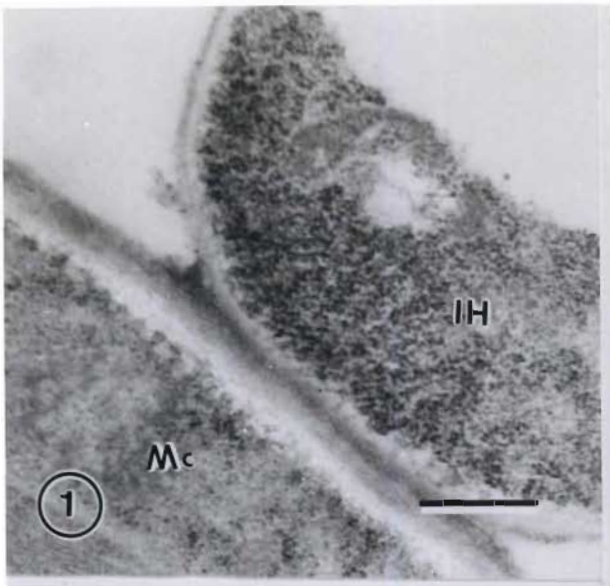
IH
Mc
1

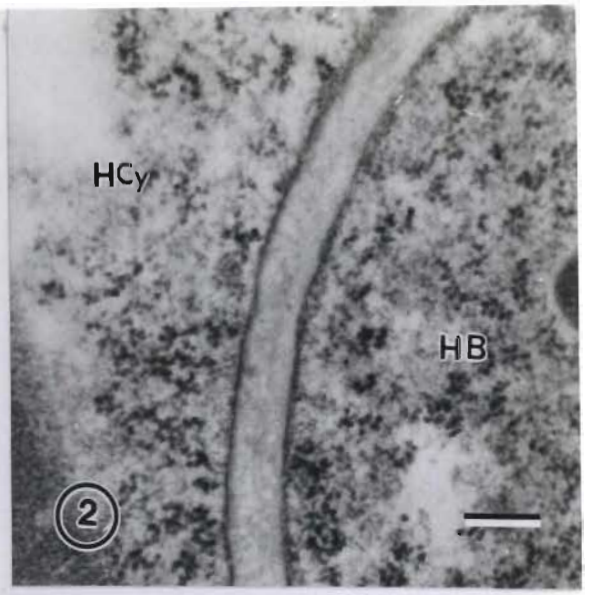
HCy
HB
2

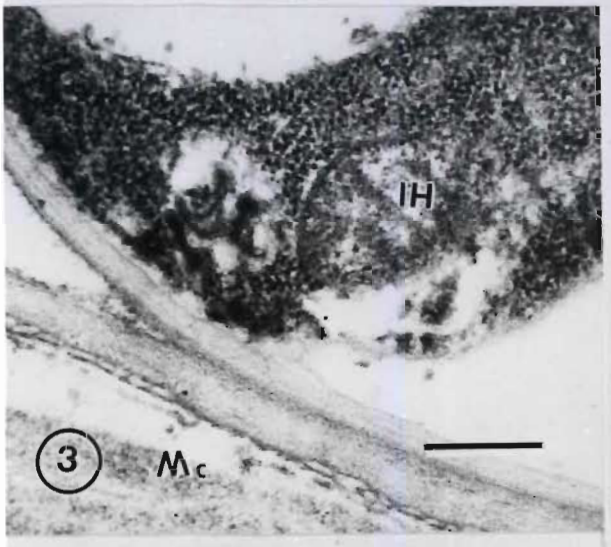
IH
3
Mc

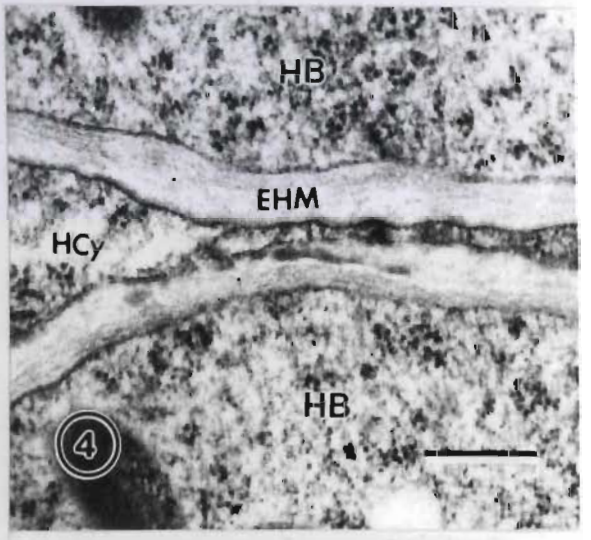
HB
EHM
HCy
HB
4

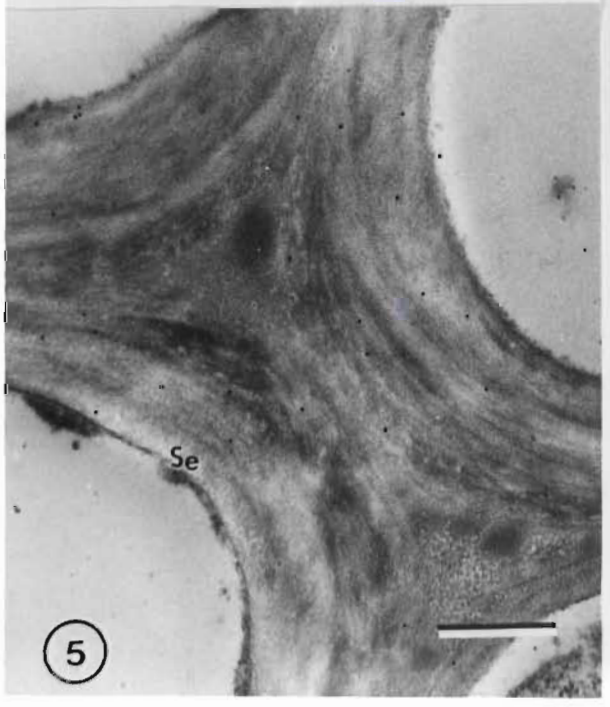
Se
5

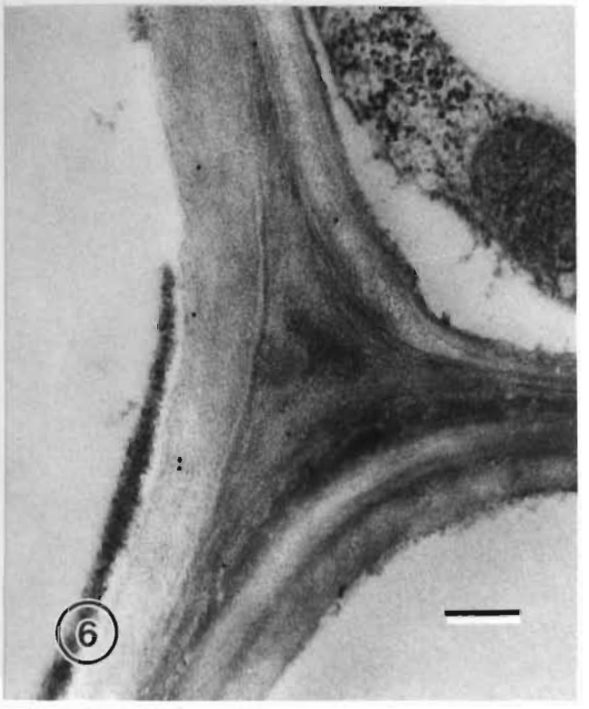
6

PLATE 2

Fig. 7. Ultrathin section of wheat leaf tissue in the compatible interaction (Thatcher/race 8), labelled with the anti-ZR antibody. The cytoplasm of the intercellular hypha (IH) and the inner wall layer of the hyphal cell wall were strongly labelled, while a few gold particles were seen over the host chloroplast (CH). Mc: Mesophyll cell; V: Vacuole. (Bar = 0.2 μm)

Fig. 8. Ultrathin section of wheat leaf tissue in the incompatible interaction (RL6078/race 8), labelled with anti-2iPA antibody. Gold particles accumulated in the hyphal cytoplasm (IH) and in the inner layer of hyphal cell wall (Mc). (Bar = 0.4 μm)

Fig. 9. Old intercellular hypha (IH) in the wheat leaf tissue of the compatible interaction (Thatcher/race 8), labelled with anti-ZR antibody. A few gold particles were visible over the inner layer of the hyphal cell wall. (Bar = 0.3 μm)

Fig. 10. Labelling of the ultrathin section of wheat leaf tissue in the compatible interaction (Thatcher/race 8) with anti-ZR antibody. The cytoplasm of the haustorial mother cell (HMC) was strongly labelled. Few gold particles were found in the extracellular matrix between the haustorial mother cell and the mesophyll cell (Mc), and none were observed in mitochondria and vacuoles in the hyphal cytoplasm. (Bar = 0.2 μm)

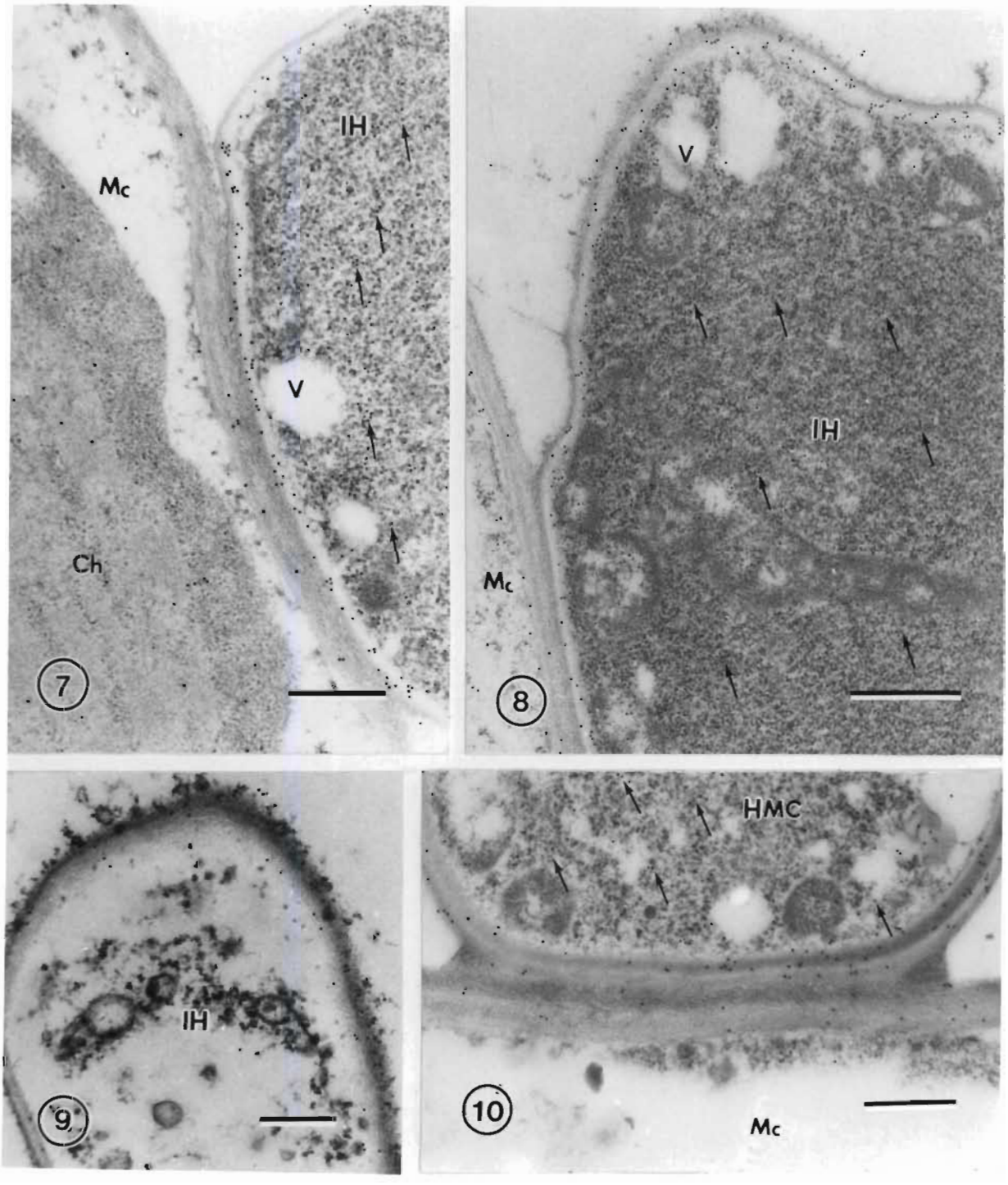
IH
Mc
V
Ch
7
V
IH
Mc
8
IH
9
HMC
10
Mc

PLATE 3

Fig. 11. Ultrathin sections of wheat leaf tissue in the compatible interaction, subjected to incubation with the anti-2iPA antibody. Labelling mainly occurred in the cytoplasm of the haustorial mother cell (HMC). The cytoplasm of the haustorial neck (HB) was also sparsely labelled. M: Mitochondria; Mc: Mesophyll cell; V: Vacuole. (Bar = 0.3 μm)

Fig. 12. Serial section of HMC shown in Fig. 11. The cytoplasm and nucleus of the haustorial mother cell (HMC) were labelled. The mitochondria (M) and vacuoles (V) were almost free of gold particles. Mc: Mesophyll cell; N: Nucleus. (Bar = 0.6 μm)

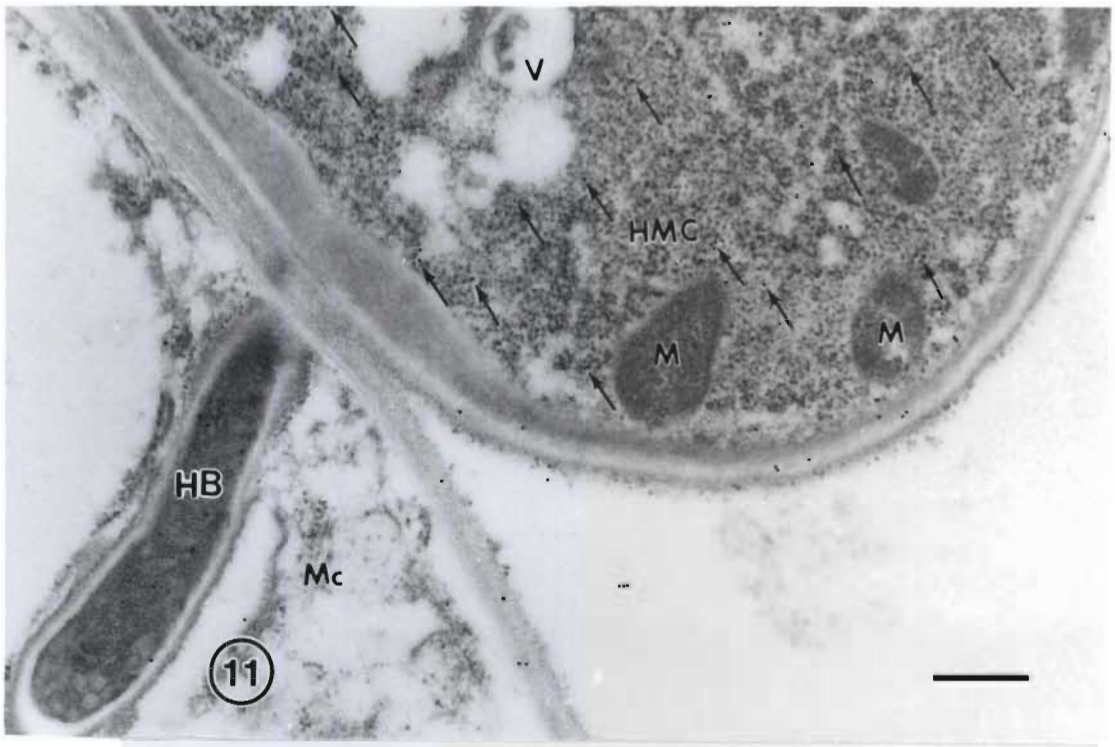
V
HMC
M
M
HB
Mc
11

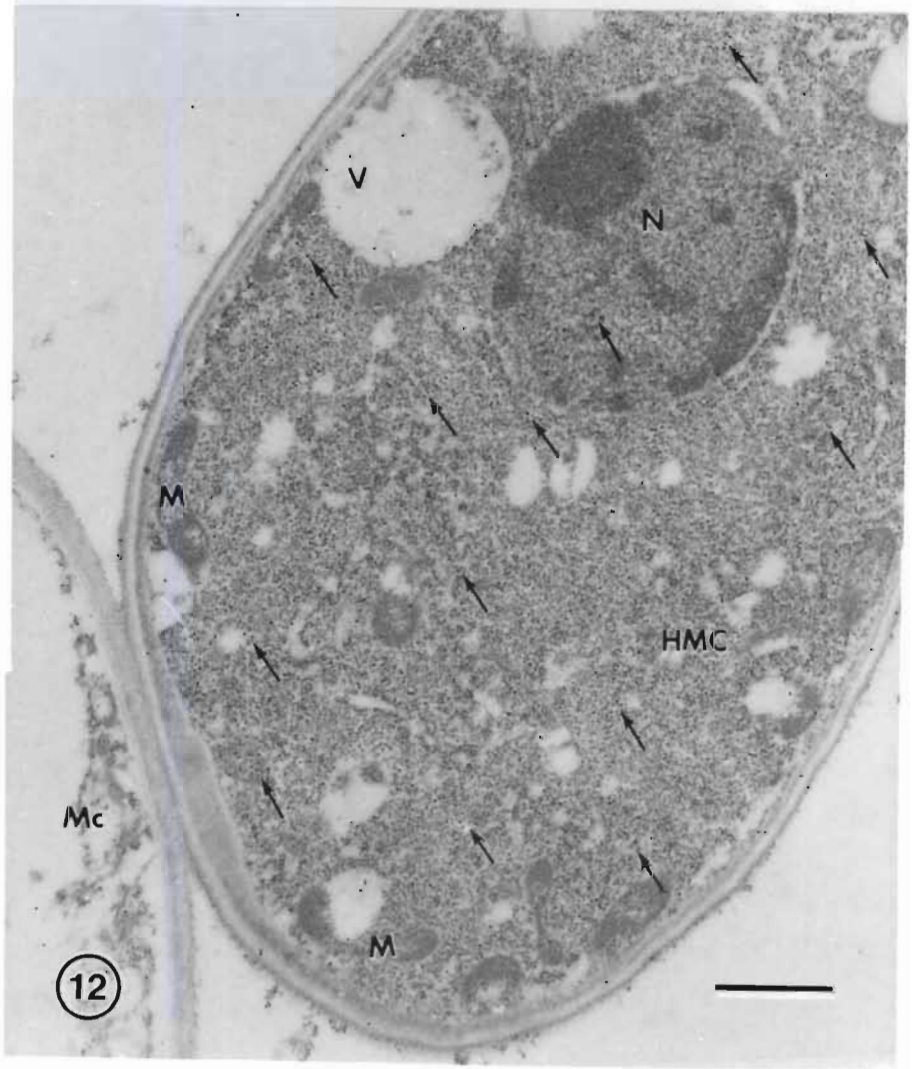
V
N
M
HMC
Mc
M
12

PLATE 4

Fig. 13. Section of a young haustorium in the compatible interaction (Thatcher/race 8), treated with the anti-ZR antibody. Gold particles were deposited over the haustorial cytoplasm and the extrahaustorial matrix (EHM) while some gold particles were observed in the host cytoplasm around the young haustorium. HB: Haustorial body. (Bar = 0.3 μm)

Fig. 14. Section of a young haustorium at the stage of expanding in the compatible interaction (Thatcher/race 8), treated with the anti-2iPA antibody. Labelling occurred in the cytoplasm of the young haustorium (HB) and in the extrahaustorial matrix. No labelling was observed over the vacuoles (V) in the haustorium. HCy: Host cytoplasm. (Bar = 0.3 μm)

Fig. 15. Mature haustorium in the compatible interaction (Thatcher/race 8), labelled with the anti-ZR antibody. Strong labelling was present in the extrahaustorial matrix (EHM). The cytoplasm of the mature haustorium (HB) was also labelled. The mitochondria (M) and vacuoles (V) in the haustorial cytoplasm were free of labelling. HCy: Host cytoplasm. (Bar = 0.1 μm)

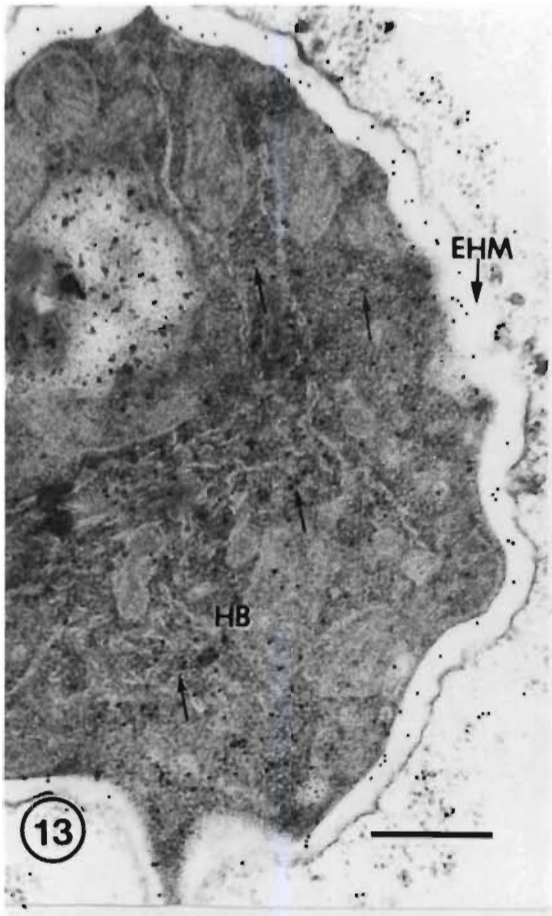
EHM
HB
13

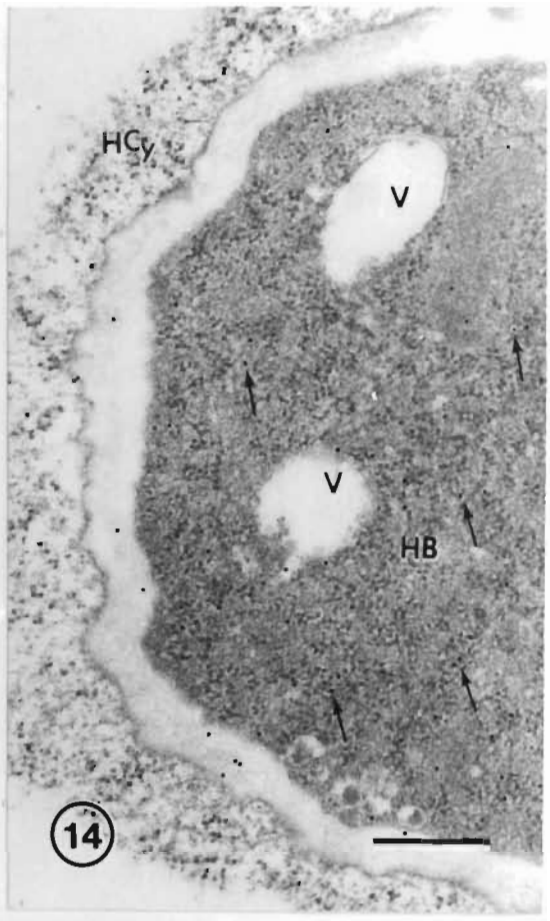
HCy
V
V
HB
14

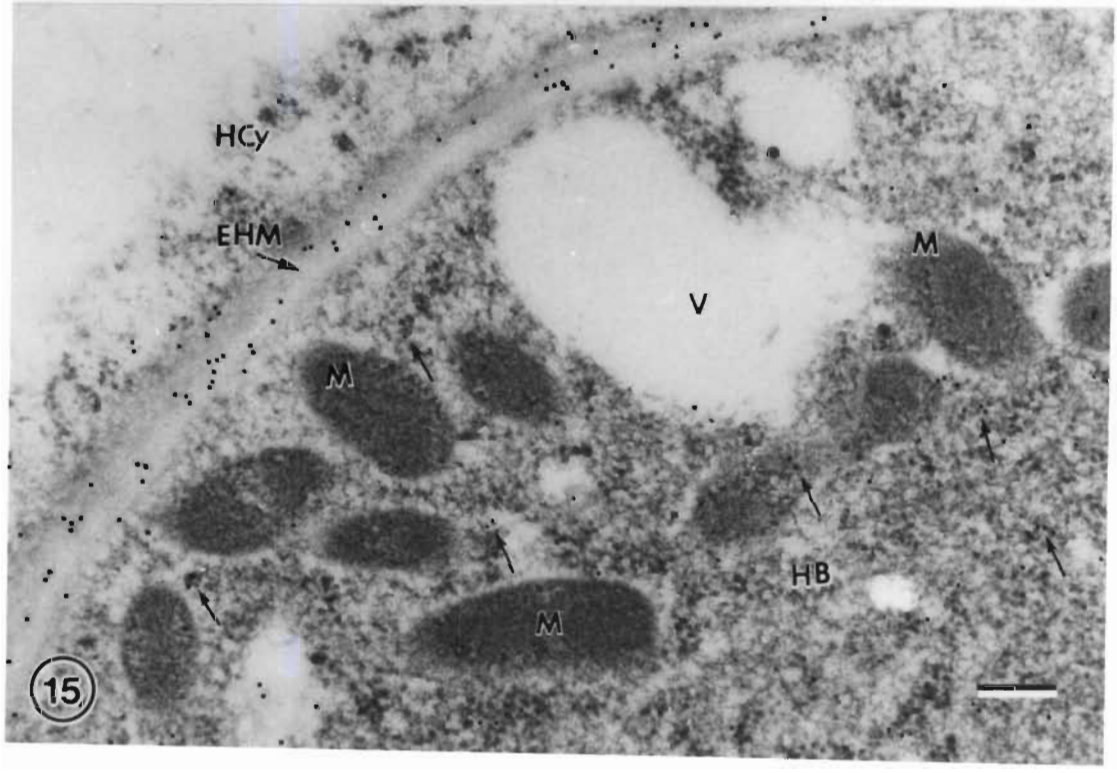
HCy
EHM
V
M
M
HB
M
15

PLATE 5

Fig. 16. Mature haustorium in the compatible interaction (Thatcher/race 8), labelled with the anti-2iPA antibody. Similar to anti-ZR labelling pattern in Fig. 15, gold particles were predominantly found in the extrahaustorial matrix (EHM). Some gold particles were present in the cytoplasm of the mature haustorium. HB: Haustorial body. (Bar = 0.1 μm)

Fig. 17. Ultrathin section of wheat leaf tissue in the incompatible interaction (RL6078/race 8), labelled with the anti-ZR antibody. The cytoplasm of the intercellular hypha (IH) was labelled with the probe while the mitochondria in the fungal cytoplasm were not labelled. (Bar = 0.1 μm)

Fig. 18. An oblique ultrathin section of wheat leaf tissue in the incompatible interaction (RL6078/race 8), labelled with the anti-2iPA antibody. The cytoplasm and intra penetration torus (IPT) of the haustorial mother cell (HMC) were labelled while the vacuoles (V) in the fungal cytoplasm were free of gold particle. The papilla-like structure in the host cell at the penetration cite was not labelled. A few gold particles were present in the host cytoplasm around the papilla-like structure (P). Mc: Mesophyll cell. (Bar = 0.3 μm)

Fig. 19. The extracellular matrix in the incompatible interaction (RL6078/race 8), treated with the anti-2iPA antibody. A few gold particles occurred in the matrix. Gi: Golgi body; Mc: Mesophyll cell. (Bar = 0.2 μm)

Fig. 20. The thickened wall (CWP) in the host cell (Mc) near a hypha (IH) in the incompatible interaction (RL6078/race 8) was strongly labelled with the anti-2iPA antibody. IS: Intercellular space. (Bar = 0.3 μm)

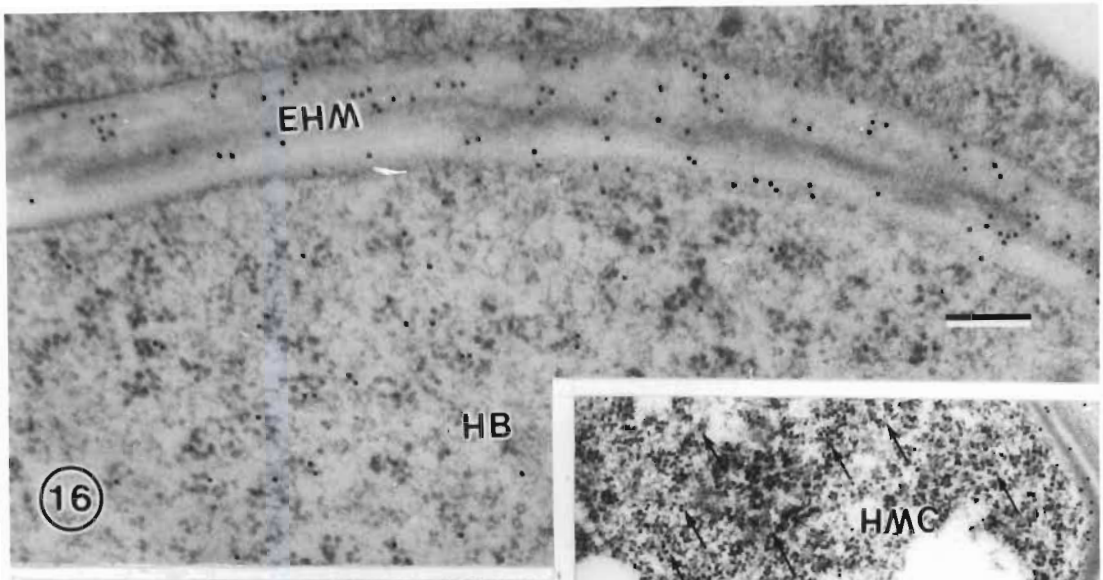
EHM
HB
16

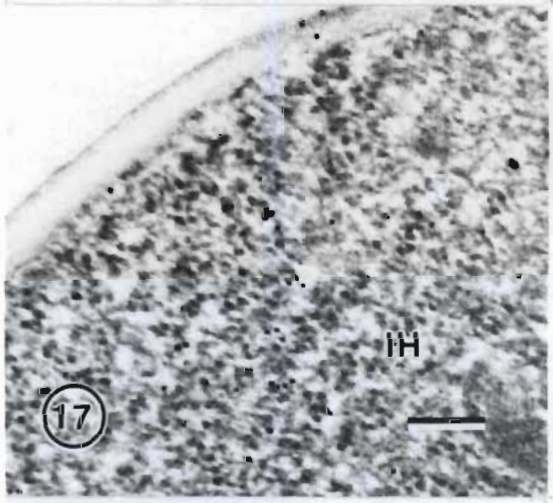
IH
17

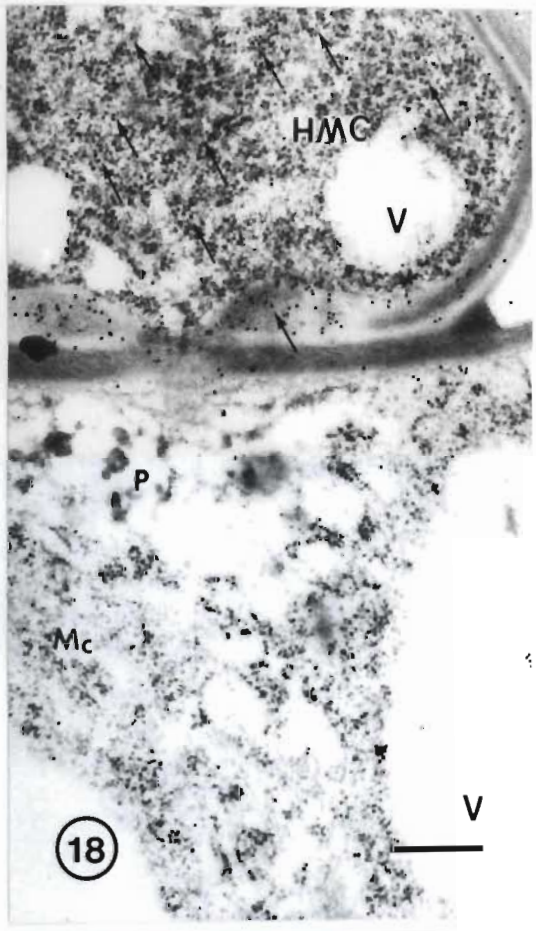
HMC
V
P
Mc
V
18

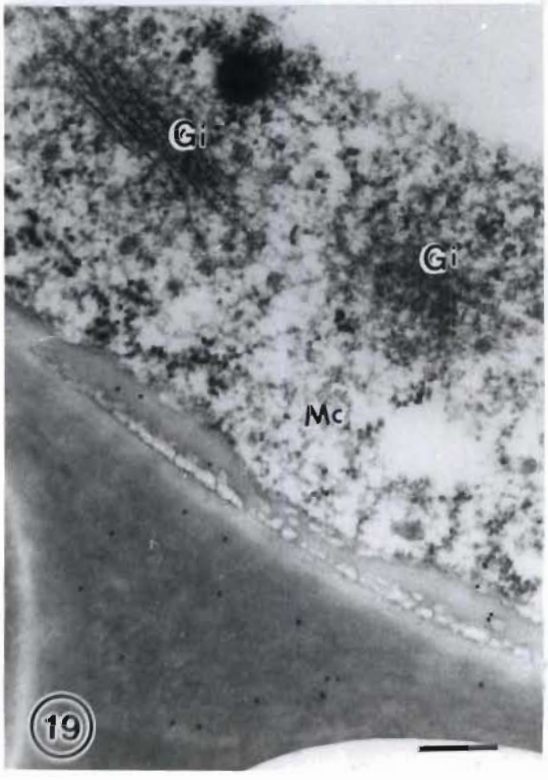
Gi
Gi
Mc
19

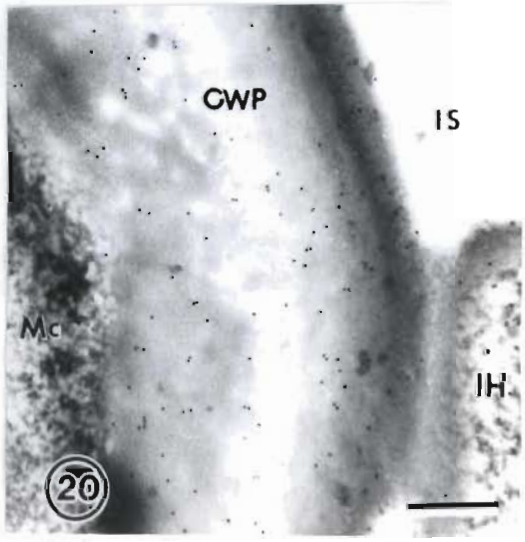
CWP
IS
Mc
IH
20

Labelling with anti-ZR and anti-2iPA antibodies indicated that gold particles were associated with both the young (Figs. 13, 14) and the mature haustorium (Figs. 15, 16). The haustorial cytoplasm and the extrahaustorial matrix were strongly labelled with both antibodies (Fig. 13, 14, 15, 16). The vacuoles and mitochondria in the haustorium were free of labelling.

Immunogold localization of cytokinins in the incompatible Puccinia recondita *f.sp.* tritici-*wheat interaction*

In the incompatible interaction, the secondary thickening of xylem vessel walls and the wall of phloem elements were also labelled with both antibodies. Cytokinins were also found in the fungal cytoplasm in both intercellular hyphal cells (Fig. 17) and haustorial mother cells (Fig. 18) with the treatment of anti-ZR and anti-2iPA antibodies. The papilla in the host cell at the point of penetration was free of gold particles (Fig. 18). However, the extracellular matrix between the mesophyll cells (Fig. 19) and the localized region of cell wall apposition in response to pathogenesis (Fig. 20), both frequently observed in the incompatible interactions, were labelled with the antibodies.

DISCUSSION

Many naturally occurring cytokinins have been found in diverse higher plant species, bacteria, fungi and algae, as well as some insects (Greene, 1980; Kende, 1971). Cytokinins can thus be regarded as being ubiquitous. The present study demonstrates that the rust fungus, *P. recondita* f.sp. *tritici* is also able to produce cytokinins.

The sites where cytokinins accumulate in the *P. recondita* f.sp. *tritici*-infected wheat leaves were not significantly different between the compatible and incompatible interactions. The cytokinins, demonstrated by the labelling with both anti-ZR and anti-2iPA antibodies, are mainly present in the cytoplasm of the cells of intercellular hyphae, haustorial mother cells, haustorial bodies and the extrahaustorial matrix.

A number of studies have reported that the mobilization of metabolites and the accumulation of substances in infected tissues (Allen, 1942; Dekhuijzen and Staples, 1968; Hwang *et al.*, 1986; Király *et al.*, 1967; Poszar and Király, 1966). It has been proposed that the accumulation of cytokinins might mediate nutrient translocation (Dekhuijzen, 1976). Ahmad *et al.* (1982) observed the accumulation of potassium and phosphorus in barley leaves infected with brown rust and this phenomenon was explained entirely by a relatively unaltered xylem import into diseased leaves and a reduced export of the phloem-mobile ions, but there was no confirmation of the production of cytokinin-like substances by the fungus directing transport to infection areas. The present investigation shows the cytokinins mainly distributed in the fungal cytoplasm. Little labelling of host cell wall which is in contact with the intercellular hypha possibly results from the diffussion of cytokinins from the fungus. Considering the ability of cytokinins to cause nutrient mobilization (Mothes *et al.*, 1961) and the subcellular localization of cytokinins in the rust infection, one may expect that cytokinins, of fungal origin, in rust infections, are powerful sinks and play a role in drawing and translocating nutrients from the host cell into the fungal cytoplasm.

An increase in cytokinin concentration with infection has been well documented for rust diseases (Ammon *et al.*, 1990; Dekhuijzen and Staples, 1968; Király *et al.*, 1967; Vizárová *et al.*, 1986) and powdery mildew

diseases (Mandahar and Garg, 1976; Vizárová, 1974, 1975, 1979, 1987). In the wheat-*Erysiphe graminis* DC. interaction (Vizárová, 1974, 1975, 1979, 1987), for instance, inoculated leaves had higher cytokinin activity than healthy leaves in both susceptible and resistant cultivars, however, the susceptible cultivars showed a much greater overall increase than resistant cultivars. There has been much debate as to the origin of the cytokinin increase in infected plants. The observation of cytokinin localization in rust infection presented in the present report supports the view (Yadav and Mandahar, 1981) that these increased cytokinin levels reflect secretion of cytokinin by the pathogen. Such cytokinins would create localized translocatory sinks towards which nutrients would move from the surrounding areas. However, Dekhuijzen (1976) suggested that infection stimulates the production of cytokinins by the plants. Dekhuijzen and Staples (1968) found that although the urediospore and mycelium of bean rust have cytokinin-like compounds, these are not the same as those found in infected tissues and they concluded that the cytokinin increase observed is strictly of host origin. This may reflect the difference between the different plant-pathogen combinations and the methods used.

The present investigation indicated that cytokinins occur in both xylem and phloem cells in healthy and infected wheat leaf tissues. Previous studies indicated that cytokinins are detected in both xylem extrudate (Cahill *et al.*, 1986; Gordon *et al.*, 1974; Hewett and Wareing, 1974) and in phloem sap (Phillips and Cleland, 1972). It is proposed that these growth hormones are probably transported through both living and non-living translocatory tissue (Davey and Van Staden, 1981). Zeatin and zeatin riboside are the major translocational forms of cytokinins in both xylem and phloem sap (Gordon *et al.*, 1974; Hewett and Wareing, 1974; Phillip and Cleland, 1972).

In the present study, in the incompatible interaction, the cytokinin labelling with anti-ZR and anti-2iPA antibodies occurs in the thickened area of the localized cell wall apposition and in the extracellular matrix. Similar to that found in the compatible interaction, labelling was also evident in the fungal cytoplasm and in the cell walls of vascular elements. It remains unresolved if the cytokinins in those areas are involved in the resistance mechanism against the fungal pathogen. To date, a number of investigations have been directed at elucidating the possible involvement of cytokinins in the expression of host resistance in response to fungal invasion. There is evidence that the production of phytoalexin, kievitone and phaseollin, in bean tissues or cell suspensions, is regulated by cytokinins and other growth hormones (Dixon and Fuller, 1978; Goossens and Vendrig, 1982). Kinetin, one of the cytokinins, has been reported to be able to render tissues resistant to powdery mildew (Cole and Fernandez, 1970; Dekker, 1963; Edwards, 1983). In the barley (*Hordeum vulgare* L.)-*Erysiphe graminis* (DC) Merat f.sp. *hordei* interaction, Liu and Bushnell (1986) revealed that the inhibitory effects of kinetin on fungus development are direct rather than through the activation of same or other defense mechanism in the host. Cytokinins, on the other hand, are also found to increase susceptibility or suppress host resistance to fungal pathogens. In tobacco, the production of a mRNA for a putative defence-related enzyme, chitinase, is blocked by auxin and cytokinin (Shinshi *et al.*, 1987), and cytokinin influences the levels of an additional three, presumably defence-related, mRNAs (Memelink *et al.*, 1987). Cytokinin, such as kinetin, was observed to inhibit the hypersensitive reaction in diseased plant (Balázs *et al.*, 1977; Novacky, 1972; Van Loon, 1979), and in tissue cultures (Helgeson, 1983). Helgeson (1983) and Beckman and Ingram (1994) suggested that the effects of cytokinins on preventing senescence and on inhibiting the hypersensitive response may be related. It has also been shown that systemic acquired resistance is accompanied by increased cytokinin

levels in plant tissues when resistance is induced by a necrosis-inducing fungus (Sarhan *et al.*, 1991). Beckman and Ingram (1994) hypothesized that cytokinins may interact with oxygen-free radicals, thereby inhibiting the formation of the superoxide (O_2) free radical. Previous reports have indicated that the generation of the superoxide anion, after infection, could be involved in the formation of necrotic symptoms in a few host-pathogen interactions (Doke, 1983; Adám *et al.*, 1989).

Thus far, only a few reports have appeared on the subcellular localization of growth hormones, especially the cytokinins. The lack of investigation in this area may be due to the technical problems of antigen loss or alteration during the processing for routine electron microscopy, and/or the existence of plant hormones in only small amounts in most tissues which makes their localization even less feasible. Zavala and Brandon (1983) first localized cytokinins in maize root tips with a freeze substitution technique. Eberle *et al.* (1987) used highly specific monoclonal antibody and low-temperature embedding to localize cytokinins in a cytokinin-over-producing mutant of the moss, *Physcomitrella patens*. Sossountzov *et al.* (1988) described a periodate-borohydride procedure to obtain the coupling of cytokinins to cellular proteins which improved the cytokinin labelling. In the present investigation, we have also used the periodate-borohydride procedure but found that the results are similar. Coupling cytokinin bases with aldehydes has been reported (Ivanova *et al.*, 1994; Sossountzov *et al.*, 1988; Zavala and Brandon, 1983). Recently developed high-pressure freezing techniques may be able to confer better antigen protection and may be an alternative to improved cytokinin labelling.

The anti-ZR antibody used in the present investigation, can recognize zeatin riboside and its base, zeatin (Z), whereas the anti-2iPA antibody reacts with isopentenyladenosine (2iPA) and isopentenyladenine (2iP) (Sossountzov *et al.*,

1988). Sossountzov *et al.*, (1988) and Sotta *et al.* (1992) have demonstrated that periodate coupling appears to be essential to tissue processing for demonstrating cytokinin ribosides, while aldehyde coupling permits the recognition of cytokinin bases by the antibodies. If this is true, the labelling described in this paper may indicate the distribution of cytokinin bases, viz. zeatin (Z) and isopentenyladenine (2iP), respectively, in the rust infection here studied. Moreover, since there was no demonstrable difference between results attained with or without periodate coupling, the cytokinins we labelled in this study are perhaps the cytokinin bases, zeatin and isopentenyladenine.

LITERATURE CITED

Adám, A., Farkas, T., Somlyai, G., Hevesi, M. and Király, Z. (1989). Consequence of O_2 generating during a bacterially induced hypersensitive reaction in tobacco: deterioration of membrane lipids. *Physiological and Molecular Plant Pathology* **34,** 13-26.

Ahmed, I. Owera, S.A.P., Farrar, J.F. and Whitbread, R. (1982). The distribution of five major nutrients in barley plants infected with brown rust. *Physiological Plant Pathology* **21,** 335-346.

Allen, P.J. (1942). Changes in the metabolism of wheat leaves induced by infection with powdery mildew. *American Journal of Botany* **29,** 425-435.

Ammon, V., Seifers, D. and Walkinshaw, C. (1990). Cytokinin activity in southern pines inoculated with *Cronartium quercuum* f.sp. *fusiforme*. *Canadian Journal of Plant Pathology* **12,** 170-174.

Andres, M.W. and Wilcoxson, R.D. (1984). A device for uniform deposition of liquid-suspended urediospores on seedling and adult cereal plants. *Phytopathology* **74,** 550-552.

Baláza, E., Sziraki, I. and Király, Z. (1977). The role of cytokinin in the systemic acquired resistance to tobacco hypersensitive to tobacco mosaic virus. *Physiological Plant Pathology* **11,** 29-37.

Beckman, K.B. and Ingram, D.S. (1994). The inhibition of the hypersensitive response of potato tuber tissues by cytokinins: similarities between senescence and plant defence responses. *Physiological and Molecular Plant Pathology* **44,** 33-50.

Bushnell, W.R. and Allen, P.J. (1962). Induction of disease symptoms in barley by powdery mildew. *Plant Physiology* **37,** 50-59.

Cahill, D.M., Weste, G.M. and Grant, B.R. (1986). Changes in cytokinin concentrations in xylem extrudate following infection of *Eucalyptus marginata* Donn ex Sm with *Phytophthora cinnamomi* Rands. *Plant Physiology* **81,** 1103-1109.

Cole, J.S. and Fernandes, D.L. (1970). Changes in the resistance of tobacco leaf to *Erysiphe cichoracearum* DC. induced by topping, cytokinins and antibiotics. *Annals of Applied Biology* **66,** 239-243.

Davey, J.E. and Van Staden, J. (1981). Cytokinin activity in *Lupinus albus*. V. Translocation and metabolism of (8- ^{14}C) zeatin applied to the xylem of fruiting plants. *Physiologia Plantarum* **51,** 45-48.

Dekhuijzen, H.M. (1976). Endogenous cytokinins in healthy and diseased plants. In: *Physiological Plant Pathology* (Eds. Heitefuss, R. and Williams,

P.H.), pp. 526-559. Springer-Verlag, Berlin.

Dekhuijzen, H.M. and Staples, R.C. (1968). Mobilization factors in urediospores and bean leaves infected with bean rust fungus. *Contributions from Boyce Thompson Institute for Plant Research* **24,** 39-52.

Dekker, J. (1963). Effect of kinetin on powdery mildew. *Nature* **197,** 1027-1028.

Dermastia, M. and Ravnikar, M. (1996). Altered cytokinin pattern and enhanced tolerance to potato virus Y^{NTN} in the susceptible potato cultivar (*Solanum tuberosum* cv. Igor) grown *in vitro*. *Physiological and Molecular Plant Pathology* **48,** 65-71.

Dixon, R.A. and Fuller, K.W. (1978). Effects of growth substances on non-induced and *Botrytis cinerea* culture filtrate-induced phaseollin production in *Phaseolus vulgaris* cell suspension cultures. *Physiological Plant Pathology* **12,** 279-288.

Doke, N. (1983). Involvement of superoxide anion generation in the hypersensitive response of potato tuber tissues to infection with an incompatible race of *Phytophthora infestans* and to the hyphal wall components. *Physiological Plant Pathology* **23,** 345-357.

Eberle, J., Wang, T.L., Cook, S., Wells, B. and Weiler, E.W. (1987). Immunoassay and ultrastructural localization of isopentenyladenine and related cytokinins using monoclonal antibodies. *Planta* **172,** 289-297.

Edwards, H.H. (1983). Effect of kinetin, abscisic acid, and cations on host-parasite relations of barley inoculated with *Erysiphe graminis* f.sp. *hordei*. *Phytopathologische Zeitschrift* **107,** 22-30.

Gordon, M.E., Letham, D.S. and Parker, C.W. (1974). The metabolism and translocation of zeatin in intact radish seedlings. *Annals of Botany* **38,** 809-825.

Goossens, J.F.V. and Nendrig, J.C. (1982). Effects of abscisic acid, cytokinins, and light on isoflavonoid-phytoalexin accumulation in *Phaseolus vulgaris* L.. *Planta* **154,** 441-446.

Greene, E.M. (1980). Cytokinin production by micro-organisms. *Botanical Review* **46,** 25-74.

Helgeson, J.P. (1983). Studies of host-pathogen interactions *in vitro*. In: *Use of Tissue Culture and Protoplasts in Plant Pathology* (Eds. Helgeson, J.P. and Deverall, B.J.), pp. 1-7. Academic Press, New York.

Hewett, E.W. and Wareing, P.F. (1974). Cytokinin changes during chilling and bud burst in woody plants. In: *Mechanisms of Regulation of Plant Growth* (Eds. Bieleski, R.L., Ferguson, A.R. and Creswell, M.M.), pp. 693-701. Bulletin 12, The Royal Society of New Zealand, Wellington.

Hwang, B.K., Ibenthal, W.-D. and Heitefuss, R. (1986). $^{14}CO_2$-assimilation, translocation of ^{14}C, and ^{14}C-carbonate uptake in different organs of spring barley plants in relation to adult-plant resistance to powdery mildew. *Annals of the Phytopathological Society of Japan* **52,** 201-208.

Iacobellis, N.S., Sisto, A., Surico, S., Evidente, A. and Dimaio, E. (1994). Pathogenicity of *Pseudomonas syringae* subsp. *savastanoi* mutants defective in phytohormone production. *Journal of Phytopathology* **140,** 238-248.

Ivanova, M.I., Todorov, I.T., Atanassova, L., Dewitte, W. and Van Onckelen, H.A. (1994). Co-localization of cytokinins with proteins related to cell

proliferation in developing somatic embryos of *Dactylis glomerata* L.. *Journal of Experimental Botany* **45,** 1009-1017.

Kende, H. (1971). The cytokinins. *International Review of Cytology* **31,** 301-338.

Király, Z., El Hammady, M. and Pozsár, B.I. (1967). Increased cytokinin activity of rust-infected bean and broad bean leaves. *Phytopathology* **57,** 93-94.

Lichter, A., Manulamit, S., Sagee, O., Gafni, Y., Gray, J., Meilan, R., Morris, R.O. and Barash, I. (1995). Production of cytokinins by *Erwinia herbicola* pv. *gypsophilae* and isolation of a locus conferring cytokinin biosynthesis. *Molecular Plant-Microbe Interactions* **8,** 114-121.

Liu, Z. and Bushnell, W.R. (1986). Effects of cytokinins on fungus development and host responses in powdery mildew of barley. *Physiological and Molecular Plant Pathology* **29,** 41-52.

Mandahar, C.L. and Garg, I.D. (1976). Cytokinin activity of powdery mildew infected leaves of *Abelmoschus esculentus*. *Phytopathologische Zeitschrift* **84,** 86-89.

Memelink, J., Hoge, J.H.C. and Schilperoort, R.A. (1987). Cytokinin stress changes the developmental regulation of several defence-related genes in tobacco. *The European Molecular Biology Organization Journal* **6,** 3579-3583.

Michniewicz, M., Rozej, B. and Bobkiewicz, W. (1986). The production of growth regulators by *Fusarium culmorum* (W.G.Sm.) Sacc. as related to the age of mycelium. *Acta Physiologiae Plantarum* 8, 85-91

Moore, T.C. (1978). *Biochemistry and Physiology of Plant Hormones*. pp. 147-180. Springer-Verlag. New York.

Morris, R.O. (1986). Genes specifying auxin and cytokinin biosynthesis in phytopathogens. *Annual Review of Plant Physiology* **37,** 509-538.

Mothes, K., Engelbrecht, L. and Schutte, H.R. (1961). Über die Akkumulation von α-Aminoisobuttersaure Blattgewebe unter dem Einfluss von Kinetin. *Physiologia Plantarum* **14,** 72-75.

Novacky, A. (1972). Suppression of the bacterially induced hypersensitive reaction by cytokinins. *Physiological Plant Pathology* **2,** 101-104.

Patrick, T.W., Hall, R. and Fletcher, R.A. (1977). Cytokinin levels in healthy and *Verticillium* infected tomato plants. *Canadian Journal of Botany* **55,** 377-382.

Phillips, D.A. and Cleland, C.F. (1972). Cytokinin activity from the phloem sap of *Xanthium strumarium* L.. *Planta* **102,** 173-178.

Pozsar, B.I. and Király, Z. (1966). Phloem transport in rust-infected plants and the cytokinin-directed long-distance movement of nutrients. *Phytopathologische Zeitschrift* **56,** 297-309.

Sarhan, A.R.T., Király, Z., Sziráki, I. and Smedegaard-Petersen, V. (1991). Increased levels of cytokinins in barley leaves having the systemic acquired resistance to *Bipolaris sorokiniana* (Sacc.) Shoemaker. *Journal of Phytopathology* **131,** 101-108.

Shinshi, H., Mohnen, D. and Meins, F. Jr. (1987). Regulation of a plant pathogenesis-related enzyme: Inhibition of chitinase and chitinase mRNA

accumulation in cultured tobacco tissues by auxin and cytokinin. *Proceedings of the National Academy of Sciences, U.S.A.* **84,** 89-93.

Sossountzov, L., Maldiney, R., Sotta, B., Sabbagh, I., Habricot, Y., Bonnet, M. and Miginiac, E. (1988). Immunocytochemical localization of cytokinins in Craigella tomato and a sideshootless mutant. *Planta* **175**, 291-304.

Sotta, B., Stroobants, C., Sossountzov, L., Maldiney, R. and Miginiac, E. (1992). Immunocytochemistry applied to cytokinins: Techniques and other validation. In: *Physiology and Biochemistry of Cytokinins in Plants* (Eds. Kaminek, M., Mok, D.W.S. and Zazimalová, E.). pp. 455-460. Academic Publishing bv. The Hague.

Surico, G. and Iacobellis, N.S. (1992). Phytohormones and olive knot disease. In: *Molecular Signals in Plant-Microbe Communications* (Ed. Verma, D.P.S.), pp. 209-227. CCR Press. Boca Raton.

Van Loon, L.C. (1979). Effect of auxin on the location of tobacco mosaic virus in hypersensitively reacting tobacco. *Physiological Plant Pathology* **14,** 213-226.

Van Staden, J., Bayley, A.D. and Macrae, S. (1989). Cytokinin and mango flower malformation III. The metabolism of (^{3}H)*iso*-pentenyladenine and (8-^{14}C) zeatin by *Fusarium moniliforme*. *Physiological and Molecular Plant Pathology* **35,** 433-438.

Van Staden, J. and Nicholson, R.I.D. (1989), Cytokinins and mango flower malformation II. The cytokinin complement produced by *Fusarium moniliforme* and the ability of the fungus to incorporate (8-^{14}C) adenine into cytokinins. *Physiological and Molecular Plant Pathology* **35,** 423-431.

Vidhyasekaran, P. (1988). *Physiology of Disease Resistance in Plants* (II). pp. 25-26. CRC Press. Boca Raton.

Vizárová, G. (1974). Level of free cytokinins in susceptible and resistant cultivars of barley infected by powdery mildew. *Phytopathologische Zeitschrift* **79,** 310-314.

Vizárová, G. (1975). Effect of powdery mildew on the level of endogenous cytokinins in barley with regard to resistance. *Phytopathologische Zeitschrift* **84,** 105-114.

Vizárová, G. (1979). Changes in the level of endogenous cytokinins of barley during the development of powdery mildew. *Phytopathologische Zeitschrift* **95,** 329-341.

Vizárová, G. (1987). Possible role of cytokinins in cereals with regard to the resistance to obligate fungus parasites. *Biologia Plantarum* (*Praha*) **29,** 230-233.

Vizárová, G., Shashkova, L.S., Mazin, V.V., Vozár, I. and Paulech, C. (1986). Free cytokinins in *Puccinia graminis* Pers. f.sp. *tritici* Eriks. & E. Henn. affected wheat leaves. *Mikologiya i Fitopatologiya* **20,** 281-285.

Yadav, B.S. and Mandahar, C.L. (1981). Secretion of cytokinin-like substances *in vivo* and *in vitro* by *Helminthosporium sativum* and their role in pathogenesis. *Zeitschrift fur Pflanzenkrankheiten und Pflanzenschutz* **88,** 726-733.

Zavala, M.E. and Brandon, D.L. (1983). Localization of a phytohormone using immunocytochemistry. *The Journal of Cell Biology* **97,** 1235-1239.